

TAXONOMY, PHYLOGENY, CULTIVATION, AND BIOLOGICALLY ACTIVE COMPOUNDS OF SELECTED AGARICUS AND BOLETE GENERA FROM NORTHERN THAILAND

BOONTIYA CHUANKID

DOCTOR OF PHILOSOPHY

IN

BIOSCIENCES

SCHOOL OF SCIENCE

MAE FAH LUANG UNIVERSITY

2021

©COPYRIGHT BY MAE FAH LUANG UNIVERSITY

TAXONOMY, PHYLOGENY, CULTIVATION, AND BIOLOGICALLY ACTIVE COMPOUNDS OF SELECTED AGARICUS AND BOLETE GENERA FROM NORTHERN THAILAND

BOONTIYA CHUANKID

THIS DISSERTATION IS A PARTIAL FULFILLMENT OF
THE REQUIREMENTS FOR THE DEGREE OF
DOCTOR OF PHILOSOPHY
IN
BIOSCIENCES

SCHOOL OF SCIENCE
MAE FAH LUANG UNIVERSITY
2021
©COPYRIGHT BY MAE FAH LUANG UNIVERSITY

TAXONOMY, PHYLOGENY, CULTIVATION, AND BIOLOGICALLY ACTIVE COMPOUNDS OF SELECTED AGARICUS AND BOLETE GENERA FROM NORTHERN THAILAND

BOONTIYA CHUANKID

THIS DISSERTATION HAS BEEN APPROVED
TO BE A PARTIAL FULFILLMENT OF THE REQUIREMENTS
FOR THE DEGREE OF DOCTOR OF PHILOSOPHY
IN
BIOSCIENCES
2021

EXAMINATION COMMITTEE

.....CHAIRPERSON
(Nakarin Suwannarach, Ph. D.)

.....ADVISOR
(Assoc. Prof. Kevin David Hyde, Ph. D.)

.....CO-ADVISOR
(Olivier Jean-Mari Raspé, Ph. D.)

.....CO-ADVISOR
(Asst. Prof. Sunita Chamyuang, Ph. D.)

.....EXAMINER
(Asst. Prof. Pattana Kakumyan, Ph. D.)

.....EXTERNAL EXAMINER
(Prof. Marc Stadler, Ph. D.)

Rui lin Zhao
.....EXTERNAL EXAMINER
(Prof. Rui-Lin Zhao, Ph. D.)

©COPYRIGHT BY MAE FAH LUANG UNIVERSITY

ACKNOWLEDGEMENTS

One day after dinner time, when I watch television with grandma
"Why that person has Dr. in front of their name?"
"Are they doctor? (Medical doctor in the thought of little child)"
She said: "No!"
and explained "They are the person who study PhD and expert on the field that they study. If you love to study, you can be like them one day"
and I said: Yes! Granny. I would like to be expert like them.

I remember the conversion still and now I am a PhD. I would say that the love of mushrooms and nature also from my grandmother. She is the one who inspired me and bring me into science.

I am extremely grateful to many people who I encountered which brought the new experiences and knowledge throughout the completion of my PhD. I would like to express special gratitude and respect to Emeritus Prof. Kevin David Hyde who gave me the opportunity to be his PhD student at Mae Fah Luang university. Without his support in research, patience, motivation, force and immense knowledge, my research will never turnout like this. Think outside the box! Blye. His connection opened my world into a huge world of mycology. I found a meaning of life that cannot be found only in books. Additionally, I am deeply grateful to all of my co-advisors. I would like to express my sincere appreciation to Dr. Olivier Raspé, for his scientific advice and consultation during my studies. Also, his help and support during my visiting at Botanic Garden Meise, Belgium. I always be grateful for his teaching on mushrooms collecting during the mushroom season which were so enlightening BUT SOME MUSHROOM WE NEED TO LET IT GROW AND GO! I learn a lot from his suggestion on mushrooms taxonomy and phylogeny. Thanks for allow me to study on his mushrooms collection, without this my work will not completed. I would like to express my sincere gratitude and appreciation to Assistant Professor Dr. Sunita Chamyuang, my co-advisor and teacher in the academic and the person who recommended me for this PhD. Working with her was a great experience for academic life. The things that I learn since my bachelor's degree have been a great learning experience. Thanks for helping me since I first started my PhD. My sincere appreciation goes to

Prof. Dr. Marc Stadler at Helmholtz Centre for Infection Research (HZI), Braunschweig, Germany for giving me an opportunity to work in his lab. He always supports me in any way he can. I so deeply appreciate him, for enriching my knowledge on chemistry and mycology, as well as his suggestions and discussions on publications. I would also like to deeply thank Dr. Naritsada Thongklang for her patience in guiding me during my research. I would like to express my sincere appreciation to Assistant Professor Dr. Pattana Kakumyan, who suggest and advise me during my PhD. Thanks to Dr. Santhiti Vadthanarat for teaching me how to work with microscope, descriptions and drawing as well as his suggestion for my publications.

I would like to express special gratitude to Prof. Dr. Eric H. McKenzie, Assoc. Prof. Dr. Rajesh Jeewon, and Dr. Shaun Pennycook, for their invaluable guidance, suggestions and great help during my study.

Many thanks to Wim Baert and Myriam de Haan for their help in the laboratory during my stay at Botanic Garden Meise, Belgium. Thanks to Dr. Hedda Schrey, who help me with chemical study at HZI, Germany. Thanks also go to Dr. Kathrin Wittstein, Dr. Frank Surup, and all for their warmest friendship and hospitality during my studies at HZI, Germany. In addition, I would like to thank the staff members of the Center of Excellence in Fungal Research, Mae Fah Luang University. Kasiphat Limsakul, Wilawan Punyaaboon, Waraporn Aiphuk, Sornram Sukpisit, Naruemon Huanraluek and staff in HZI Christiane Fritz-Braun, are thanked for their valuable support.

I also would like to sincerely give thanks to all my colleagues from Belgium, China, Germany, Laos, Mauritius, Philippines, Sri Lanka, Thailand and Vietnam for kind cooperation, being good friends and always having good teamwork, Dr. Mario Amalfi, Phongeun Sysouphanthong, Ishani Goonasekara, Chada Norphanphoun, Sirinapa Konta, Chanokned Senwanna, Didsanutda Gonkhom, Monthien phonemany, Kunthida Phutthacharoen, Napalai Chaiwan, Chuan-Gen Lin, Qiu-Ju Shang, Christopher Lambert, Sebastian Pfue, Kevin Becker, Pathompong Chailai Paomephan, Bhavesh Raghoonundon, Mark Calabon, Lê Quang Thái.

Thanks to our senior, Dr. Chayanard Phukhamsakda, Dr. Samantha Chandranath Karunarathna, Dr. Sinang Hongsanan, Dr. Saowaluck Tibpromma, Dr. Ruvishika S. Jayawardena, Dr. Benjarong Thongbai, Dr.

Rungtiwa Phookamsak, Dr. Jutamart Monkai, Dr. Saranyapat Boonmee, Dr. Milan C. Samarakoon, Assoc. Prof. Dr. Hiran Ariyawansa, Dr. Ausana Mapook, Dr. Yuan Pin Xiao, Dr. Komsit Wisitrassameewong, Dr. Jie Chen.

I am extremely grateful to the Thailand Research Fund for awarding me the Research and Researchers for Industries (RRi) grant (PHD57I0015), that financially supported me throughout my study in Thailand and abroad. The dissertation would not have happened without the support from these awards. I would also like to extend my warm thanks to laboratory facilities at MFLU, Botanic Garden Meise, and HZI.

My sincere thanks go to all of the defense committee members for their time and valuable advices. My dissertation would not be complete without their help and suggestion.

Last but not the least, I would like to express my uncountable thanks to my family who has provided me for the unconditional love and spiritual support. I would like to dedicate this piece of work to my late grandmother for her support, encouragement and for being my everything.

Boontiya Chuankid

Dissertation Title	Taxonomy, Phylogeny, Cultivation, and Biologically Active Compounds of Selected *Agaricus* and Bolete Genera from Northern Thailand
Author	Boontiya Chuankid
Degree	Doctor of Philosophy (Biosciences)
Advisor	Assoc. Prof. Kevin David Hyde, Ph. D.
Co-Advisor	Olivier Jean-Mari Raspé, Ph. D.
	Asst. Prof. Sunita Chamyuang, Ph. D.

ABSTRACT

Thailand, especially the northern part, has an amazingly high diversity of mushrooms. Those mushrooms can either be saprobic, ectomycorrhizal (EcM) or parasitic. All of these play important roles in ecosystems. Many species can be cultivated and studied for biotechnological applications such as the production of mushrooms for food or nutraceuticals, which may lead to drug development. This thesis included several aspects of basic and applied research on Thai Basidiomycota, focusing on their taxonomy, phylogeny, cultivation, and secondary metabolite production.

The Agaricomycetidae (Agaricomycetes) are the most morphologically diverse Basidiomycota and they comprise two well-known orders, Agaricales and Boletales. The taxonomy, phylogeny, diversity, and relationship of these two orders have been extensively studied. In this work, one genus from Agaricales, *Agaricus*, and five genera from Boletales, *Hourangia*, *Phlebopus*, *Phylloporus*, *Retiboletus*, and *Xerocomus* were studied. *Agaricus* (mainly *A. bisporus*) is widely consumed. Moreover, this genus

produces many biologically active compounds with antioxidant, antibacterial, anti-inflammatory, and antitumor properties. *Hourangia*, *Phlebopus*, *Phylloporus*, *Retiboletus*, and *Xerocomus* are ectomycorrhizal genera that contain small numbers of species compared to *Agaricus*. This study included multi-gene phylogenetic analysis of *Agaricus, Hourangia, Phlebopus, Phylloporus, Retiboletus, and Xerocomus* from diverse habitats in northern Thailand, using nuclear ribosomal (ITS), mitochondrial (ATP6) as well as nuclear protein-coding genes (RPB2, TEF1). New species were described and illustrated. For the utilization of Agaricomycetidae, *Agaricus* was selected for cultivation due to their life cycle and nutrition mode as saprotrophs can be mimicked. Also, morphological and phylogenetic evidence were used to classify the species (with a focus on edible sections of *Agaricus*). Mushrooms were collected, identified and isolated by tissue culture. The optimal condition of mycelia growth including medium, pH and temperature of new *Agaricus* species were investigated. After that, spawn was produced by inoculating optimal substrate with pure cultures. The inoculum was transferred to compost for mushrooms production. Further, the selected *Agaricus* and *Phlebopus* spp. (both on agar media and basidiomata) were extracted for biological assay. The bioactive compounds were analyzed by High-performance liquid chromatography technique (HPLC) and chemical structure elucidation by Nuclear magnetic resonance spectroscopy (NMR).

Morphological characters and multi-gene phylogenetic analyses were used to identify specimens collected in northern Thailand. Three new *Phylloporus* species, *P. pusillus, P. subbacillisporus* and *P. subrubeolus*, from southwestern China and northern Thailand were introduced with macro- and micro-descriptions and illustrations. They are found mostly in forests dominated by Fagaceae or Dipterocarpaceae trees. *Phylloporus pusillus* and *P. subrubeolus* are morphologically similar, but the former can be separated by very small basidiomata, lamellae becoming deeper yellow to reddish with age and less densely encrusted walls of pileipellis hyphae. *Phylloporus subbacillisporus* can be easily distinguished from other species by shallowly

intervenose lamellae and subbacilliform basidiospores. Two new geographical record of *Phylloporus*, *P*. *attenuatus* and *P*. *gajari* were also reported from Thailand.

Retiboletus brevibasidiatus was described as new to science, whereas *R*. *fuscus* and *R. nigrogriseus* were reported for the first time from Thailand. *Retiboletus brevibasidiatus* produces medium-sized basidiomes, with a dark blonde to clay pileus and densely reticulate stipe mostly on the upper part with pale yellow to chrome yellow basal mycelium. It is difficult to separate *R. brevibasidiatus* from other closely related species on the basis of macroscopic characters. However, the new species can be distinguished by microscopic characters, mostly the shorter basidia. The macro- and micro-morphology of the *R. fuscus* and *R. nigrogriseus* collections from Thailand fit well with the previous descriptions of materials from China and Japan.

Three novel species and two first records, *Hourangia microcarpa* and *H. nigropunctata*, were reported for *Hourangia* from Thailand. Moreover, two novel species and one first record, *Xerocomus microcarpoides*, were described from Thailand.

The genus *Agaricus* contains many edible and medicinal mushrooms and some of them are used for commercial purposes. Most *Agaricus* species have been described from temperate geographic areas, and their occurrence in the tropics is still underexplored. In this study, *Agaricus campestroides* and *A. flocculosipes* were selected for cultivation. *Agaricus campestroides* has been formally described as infrageneric taxon belongs to "Tropical clade b" and known as wild edible species from Ethiopia. *Agaricus flocculosipes* is also an edible species belonging to section *Arvenses*. The present study describes the successful cultivation of two wild strains of *A. flocculopsipes* and *A. campestroides* from Thailand, for the first time. The optimal conditions for mycelial growth have been evaluated for both strains, formation of basidiomata on compost could only be observed for *A. campestroides.* In the present study, mycelial growth and mushroom production conditions were optimized. The

temperature range of 25–30 °C with 80–90% humidity was assessed as preferred conditions for primordia and basidiomata formation in a compost rice straw medium with sandy-soil casing layer. Blazeispirols (blazeispirol A and D), a family of triterpenoids that is known to act as selective agonists of Liver X receptor alpha with beneficial effects in vivo in a murine model, were detected in crude extracts from submerged cultures of *A. campestroides* and *A. flocculosipes*.

Submerged cultures of the edible mushroom-forming species *Phlebopus portentosus* and *Phlebopus spongiosus* were screened for their secondary metabolites by HPLC-UV/Vis and HR-LC-ESI-MS. Two new compounds, 9′-hydroxyphenyl pulvinone (1), containing an unusual pulvinone structure, and phlebopyron (2), together with the seven known pigments, atromentic acid (3), xerocomic acid (4), variegatic acid (5), methyl atromentate (6), methyl isoxerocomate (7), methyl variegatate (8), and variegatorubin (9) were isolated from the cultures. Their structures were assigned on the basis of extensive 1D/2D NMR spectroscopic analyses, as well as HR-ESI-MS, and HR-ESI-MS/MS measurements. Furthermore, the isolated compounds were evaluated for their antimicrobial and cytotoxic properties. 9′-hydroxyphenyl pulvinone (1), xerocomic acid (4), and methyl variegatate (8) exhibited weak to moderate cytotoxic activities against several tumor cell lines. The present paper provides a comprehensive characterization of pigments from the class of pulvinic acids that are present in the basidiomes of many edible bolete species.

Keywords: Agaricales, Asia, Boletales, Edible Mushrooms, Systematics

TABLE OF CONTENTS

	Page
ACKNOWLEDGEMENTS	**(3)**
ABSTRACT	**(6)**
LIST OF TABLES	**(13)**
LIST OF FIGURES	**(14)**
ABBREVIATIONS AND SYMBOLS	**(17)**
CHAPTER	
1 INTRODUCTION	**1**
1.1 Introduction of Agaricomycetidae	1
1.2 Order Agaricales Underwood	4
1.3 Order Boletales	7
1.4 Mushroom Cultivation	14
1.5 Bioactive Compound Investigation of *Agaricus* and *Phlebopus*	16
1.6 Research Objectives	19
1.7 Research Outlines	19
2 RESEARCH METHODOLOGY	**21**
2.1 Taxonomy and Phylogeny Study	21
2.2 Cultivation and Identification of Blazeispirols from Wild *Agaricus campestroides* and *A. flocculosipes*	28
2.3 Secondary Metabolites of *Phlebopus* from Northern Thailand	32
3 RESEARCH RESULTS	**40**
3.1 Taxonomy and Phylogeny of *Phylloporus*	40
3.2 Taxonomy and Phylogeny of *Retiboletus*	59

TABLE OF CONTENTS (continued)

	Page
CHAPTER	
3.3 Taxonomy and Phylogeny of *Hourangia* and *Xerocomus*	74
3.4 Cultivation and Identification of Blazeispirols from Wild *Agaricus campestroides* and *A. flocculosipes*	110
3.5 Secondary Metabolites of *Phlebopus* from Northern Thailand	119
4 DISCUSSION	**127**
4.1 Taxonomy and Phylogeny of *Phylloporus*	127
4.2 Taxonomy and Phylogeny of *Retiboletus*	128
4.3 Taxonomy and Phylogeny of *Hourangia* and *Xerocomus*	129
4.4 Cultivation and Identification of Blazeispirols from Wild *Agaricus campestroides* and *A. flocculosipes*	130
4.5 Secondary Metabolites of *Phlebopus* from Northern Thailand	131
5 OVERALL CONCLUSIONS	**134**
5.1 Taxonomy and Phylogeny of *Agaricus* and Boletales	134
5.2 Secondary Metabolites of Selected *Agaricus* and Boletales species	135
5.3 Cultivation the Wild Strain of *Agaricus*	136
5.4 Research Advantages	137
5.5 Future Work	138
5.6 Publications	138
6 TAXONOMY AND PHYLOGENY OF OTHER AGARICOMYCETIDAE IN THE CONTRIBUTED PAPERS	**141**
6.1 *Agaricus* (Pseudochitonia) section *Cymbiformes* M.Q. He & R.L. Zhao, sect. nov.	141

TABLE OF CONTENTS (continued)

	Page
CHAPTER	
6.2 *Armillaria* (Fr.) Staude, Schwämme Mitteldeutschl. 28: xxviii, 130 (1857)	145
6.3 *Phylloporus* Quél., Fl. mycol. France (Paris): 409 (1888)	161
REFERENCES	**171**
APPENDICES	**198**
APPENDIX A CHEMICAL REAGENTS AND MEDIA	199
APPENDIX B HPLC-ESI-MS AND NMR DATA	203
APPENDIX C IDENTIFICATION OF PHLEBOPUS	235
APPENDIX D GROWTH CONDITION AND YIELD FOR SMALL SCALE LIQUID CULTIVATION OF PHLEBOPUS	243
APPENDIX E ANTIMICROBIAL ACTIVITY AND CYTOTOXICITY ASSAYS OF PHLEBOPUS	244
APPENDIX F LISTS OF CULTURES AND HERBARIUM	247
APPENDIX G ABSTRACT OF PUBLICATIONS	284
APPENDIX H PERMISSION TO INCLUDE AN ARTICLES INTO THESIS	293
CURRICULUM VITAE	**299**

LIST OF TABLES

Table	Page
3.1 List of collections used for DNA analyses with origin, GenBank accession numbers and references	41
3.2 GenBank BLAST searches results of ITS1+ITS2 sequences of *Phylloporus* species from this study	44
3.3 List of collections used for DNA analyses with origin, GenBank accession numbers and references	60
3.4 List of collections used for phylogenetic analyses, with origin, GenBank accession numbers, and references	75
3.5 Effect of different agar media, temperature, and pH on mycelia growth (biomass, mg) of *A. campestroides* and *A. flocculosipes*	114
3.6 Yields of crude extracts from the mycelia of *A. campestroides* and *A. flocculosipes* cultivated in different media	114
3.7 Occurrence of compounds 1 and 2 in the mycelia of *A. campestroides* and *A. flocculosipes* cultivated in different media	115
3.8 ^{1}H NMR and ^{13}C NMR Data (δ) for compounds 1 and 2 (700 MHz, 300 K) (δ in ppm, *J* in Hz)	123
3.9 Occurrence of compounds 1–9 in P. *spongiosus* and P. *portentosus* cultivated in different media	124
3.10 Antimicrobial activity of compounds 1, 7, and 8	125
3.11 Cytotoxic activity of compounds 1, 4, and 8	126
3.12 Nematicidal activitiy of compounds 3 and 4	126
6.1 DNA barcodes available for *Armillaria*	150

LIST OF FIGURES

Figure **Page**

1.1 Higher-level phylogenetic relationships of Agaricomycetidae 2
1.2 Agaricomycetidae 3
1.3 Agaricus subrufescens in the wild (MRC-29B) 6
1.4 *Hourangia microcarpa* in the wild (OR0138) 8
1.5 *Phlebopus portentosus from local market (BC001)* 10
1.6 *Phylloporus subrubeolus in the wild (BC022)* 11
1.7 *Retiboletus nigrogriseus* in the wild (OR049) 13
1.8 *Xerocomus microcarpoides* in the wild (OR0156) 14
1.9 Chemical structures of blazeispirol A (1) and D (2) found in *Agaricus* 17
1.10 Chemical structures of compounds 1–9 isolated from *Phlebopus portentosus* and *P. spongiosus* 18
3.1 Maximum likelihood phylogenetic tree inferred from the three-gene dataset (*atp*6, *rpb*2, *tef*1) of *Phylloporus* 45
3.2 Basidiomata of *Phylloporus pusillus* 48
3.3 Micro-morphological characters of *Phylloporus pusillus* 49
3.4 Basidiomata of *Phylloporus subbacillisporus* 52
3.5 Micro-morphological characters of *Phylloporus subbacillisporus* 53
3.6 Basidiomata of *Phylloporus subrubeolus* 56
3.7. Micro-morphological characters of *Phylloporus subrubeolus* 57
3.8 SEM micrograph of the basidiospores of the new *Phylloporus* species 58
3.10 Maximum likelihood phylogenetic tree inferred from the three-gene dataset (*atp*6, *rpb*2, *tef*1) of *Retiboletus* 62
3.11 Basidiomata of *Retiboletus brevibasidiatus* 65
3.12 Micro-morphological characters of *Retiboletus brevibasidiatus* 66

LIST OF FIGURES (continued)

Figure		Page
3.13	Basidiomata of *Retiboletus fuscus*	68
3.14	Micro-morphological characters of *Retiboletus fuscus*	69
3.15	Basidiomata of *Retiboletus nigrogriseus*	72
3.16	Micro-morphological characters of *Retiboletus nigrogriseus*	73
3.17	Xerocomoideae phylogenetic tree inferred from the three-gene dataset (*atp*6, *rpb*2, and *tef*1)	89
3.18	Basidiomata of *Hourangia* and *Xerocomus*	93
3.19	Micro-morphological characters of *Hourangia microcarpa*	94
3.20	Micro-morphological characters of *Hourangia nigropunctata*	97
3.21	Micro-morphological characters of *Hourangia* aff. *microcarpa*	99
3.22	Micro-morphological characters of *Hourangia* 1 sp. nov.	101
3.23	Micro-morphological characters of *Hourangia* 2 sp. nov.	103
3.24	Micro-morphological characters of *Xerocomus* 1 sp. nov.	105
3.25	Micro-morphological characters of *Xerocomus* 2 sp. nov.	107
3.26	Micro-morphological characters of *Xerocomus microcarpoides*	109
3.27	*Agaricus campestroides* (MFLU 14–0872) and *Agaricus flocculosipes* (MFLU 14–0874) in the wild and the mycelia growth	112
3.28	Microscopic characteristics of *Agaricus campestroides* (MFLU 14–0872)	113
3.29	Microscopic characteristics of *Agaricus flocculosipes* (MFLU 14–0874)	116
3.30	Mycelia growth of *Agaricus campestroides* on wheat grain spawn after 14 days	117
3.31	The basidiomata of *A. campestroides* (MFLU 14–0872) on compost medium	117
3.32	Chemical structures of blazeispirol A (1) and D (2)	118

LIST OF FIGURES (continued)

Figure	Page
3.33 HPLC-UV/Vis chromatogram of the crude extract of *A. flocculosipes* cultivated in YM-medium (190–600 nm)	119
3.34 Chemical structures of compounds 1–9 isolated from *P. portentosus* and *P. spongiosus* (liquid cultivation) and known compounds (10–16) isolated from air-dried basidiomes from *P. portentosus*	122
3.35 1H,1H COSY, 1H,13C HMBC, and key 1H,1H NOESY correlations for compounds 1 and 2	123
6.1 Phylogenetic tree of *Agaricus* subgenus *Pseudochitonia* generated from Bayesian analysis of ITS sequences	143
6.2 Maximium Clade Credibility tree of genus *Agaricus* based on ITS, LSU and *tef*1-α gene sequences with the outgroup *Heinemannomyces* sp.	144
6.3 Morphology of *Agaricus angusticystidiatus*	145
6.4 Phylogenetic tree generated by maximum likelihood analysis of combined ITS-IGS-*tef*1 sequence data of *Armillaria* species	147
6.5 Disease cycle of *Armillaria mellea* (redrawn from Agrios 2005)	161
6.6 Phylogram generated from maximum likelihood analysis based on combined ATP6, RPB2 and TEF1-α sequence data for selected *Phylloporus*	165
6.7 Basidiomata of *Phylloporus attenuatus* in the field	167
6.8 Microscopic characters of *Phylloporus attenuatus* (OR0914)	168
6.9 Basidiomata of *Phylloporus gajari* in the field	169
6.10 Microscopic characters of *Phylloporus gajari* (BC065)	170

ABBREVIATIONS AND SYMBOLS

cm	centimetre
dH2O	distilled water
diam.	Diameter
e.g.	for example
ESI	electrospray ionization
g	gram
HCl	hydrochloric acid
HPLC	high performance liquid chromatography
hr	hour
IC_{50}	half maximal inhibitory concentration
ITS	internal transcribed space
L	litre
LSU	large subunit of ribosomal RNA
M	Molar
M	meter
mg	milligram
MIC	minimal inhibitory concentration
min	minute
ml	milliliter
mm	millimeter

ABBREVIATIONA AND SYMBOLS (continued)

mM	millimolar
MS	mass spectrometry/mass spectrum
MW	molecular weight
NaOH	sodium hydroxide
nm	nanometre
NMR	nuclear magnetic resonance spectroscopy
nov.	novel things (species)
RP	reversed phase
RPB2	RNA polymerase II
rpm	rotation per minute
s	second
sp.	species
spp.	species (plural)
U	Unit
UV	ultraviolet
w/v	weight by volume
°C	degree Celsius
µg	microgram
µL	microliter
µm	micrometer

ABBREVIATIONA AND SYMBOLS (continued)

μmol	micromole
%	percent
≥	greater than or equal to

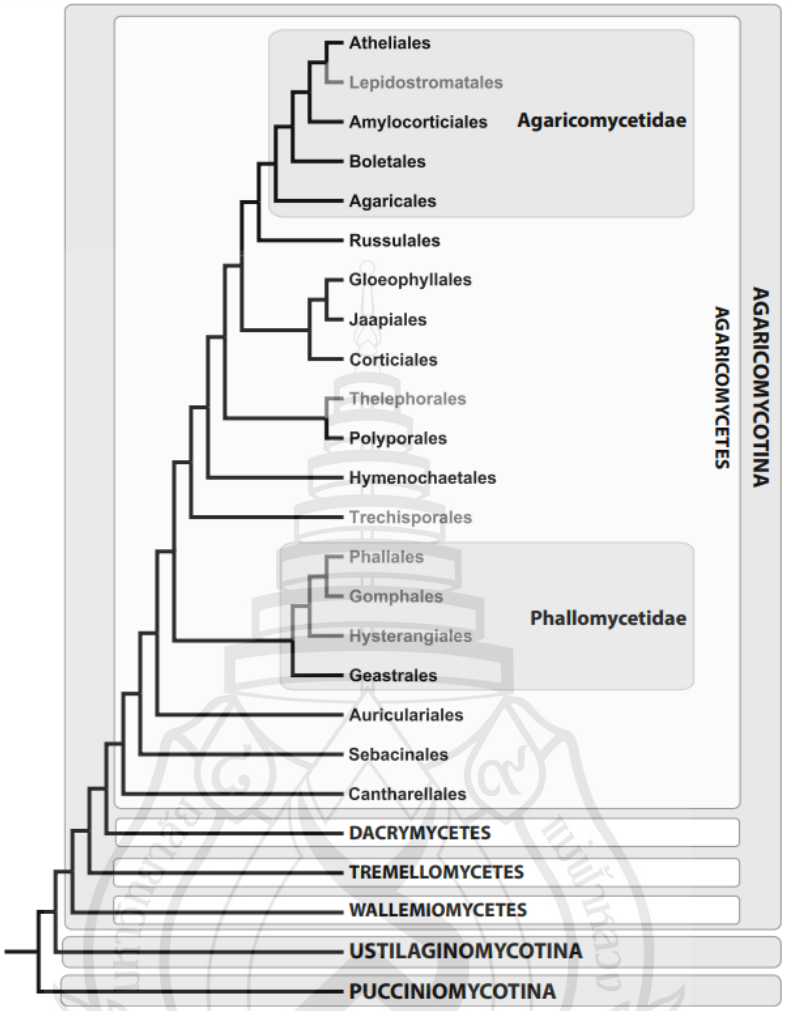


CHAPTER 1

INTRODUCTION

1.1 Introduction of Agaricomycetidae

Agaricomycetidae (Parmasto, 1986) is one of the most morphologically diverse subclasses of Agaricomycetes. The Agaricomycetidae are distributed worldwide and contain approximately 15,000 taxa in six orders. The subclass contains two large and well known orders, Agaricales and Boletales, as well as three small groups containing mostly corticioid forms, Amylocorticiales, Atheliales, Jaapiales, and Lepidostromatales (Hibbett et al., 2014)



Note Higher-level phylogenetic relationships of Agaricomycetidae with another Basidiomycota. The major topology phylogenomic analyses in black lines and text. Names in gray represent groups that have not been included in phylogenomic analyses; placements of these taxa are based on studies combining rRNA genes with 2–3 protein-coding genes

Source Adopted from Hibbett et al. (2014)

Figure 1.1 Higher-level phylogenetic relationships of Agaricomycetidae



Note Agaricomycetidae, including Agaricales (a, c), Amylocorticales (b), Atheliales (d), and Boletales (e, f). (a) *Lepiota lilacea*. (b) *Anomoporia bombycina*. (c) *Lycoperdon perlatum*. (d) *Athelia salicum*. (e) *Boletus lupinus*. (f) *Serpula lacrymans*. Photos by Guillermo Mun˜oz (a, c, e), Yu-Cheng Dai [b, reprinted from Binder et al. (2010), with permission of the Mycological Society of America], Paul Diederich (d), and Doris Haas (f)

Source Adopted from Hibbett et al. (2014)

Figure 1.2 Agaricomycetidae

1.2 Order Agaricales Underwood

The order Agaricales (Underwood, 1899) is the largest order of Agaricomycetes that dominated by pileate-stipitate forms with lamellate (e. g. *Agaricus*, *Amanita*, *Coprinus*, *Lepiota*) with wide variation on the fruiting body morphology such as the size of the basidiomata, the presence of veils (universal and partial), gills, and spore print color (white, brown, purple-brown, black, or pink). Microscopical characters are also diverse including spore size, shape, ornamentation, and chemical reactions; the arrangement of the pileipellis, stipitipellis, hymenophoral trama, and the presence of specialized structures (cystidia, setae) (Clémençon et al., 2004; Ginns et al., 1993; Singer, 1986). Even if pileate-stipitate gilled mushrooms are dominant in this order, secotioid or gasteroid (*Lycoperdon*), resupinate (*Cylindrobasidium*), coralloid (*Clavaria*), cyphelloid (*Henningsomyces*), pileate with poroid (*Favolaschia*), or tubular hymenophores (*Fistulina*) forms can also be found.

Agaricus

Classification

Kingdom Fungi
Division Basidiomycota
Class Agaricomycetes
Subclass Agaricomycetidae
Order Agaricales
Genus *Agaricus*

Agaricus (Linnaeus, 1753) belongs to kingdom Fungi, in Eumycota, Basidiomycota, class Agaricomycetes, subclass Agaricomycetidae and order Agaricales in the family Agaricaceae. This genus contains both edible and poisonous species, with more than 500 species worldwide (Bas, 1991; Chen et al., 2015; Chen et al., 2012; Gui et al., 2015; Lebel, 2013; Lebel & Syme, 2012; Parra, 2013; Wang et al., 2015; Zhao et al., 2011; Zhao et al., 2012; Zhao et al., 2016). The members of *Agaricus* are characterized by a fleshy pileus or cap, mostly free lamellae or gills with brown to dark brown spores and a partial veil, which protects the developing gills and

later forms a ring or annulus on the stipe. The macrochemical reactions: Schaeffer‘s cross-reaction, a chemical test with aniline and concentrated nitric acid and the alkali test (sodium or potassium hydroxide solutions), basidiomata color change when bruised or cut, odor (Heinemann, 1987), and the structure of the annulus, which can be superous or inferous, simple or double were recently been recognized as a importance characters. Many reports about the classification and phylogeny of *Agaricus* species are based on European and American taxa (Karunarathna et al., 2016). The monographs on tropical *Agaricus* mostly presented by Heinemann and *Agaricus* ranked species in subgenera and sections were established (Goossens-Fontana et al., 1957; Heinemann, 1953, 1956a, b, 1957; Heinemann, 1961; Heinemann, 1962a, b; Heinemann, 1962; Heinemann, 1962c; Heinemann, 1971, 1974, 1978, 1980, 1982, 1986, 1990a, b). According to Zhao et al. (2011), an eleven tropical clades were obtained, that aim to find appropriated system of classification for tropical *Agaricus* species. Further to Zhao et al. (2016), the divergence time were used as criteria for revised taxonomic ranks of *Agaricus*. *Agaricus* was proposed to segregated into five subgenera and 20 sections based on phylogenetic relationships and morphology. The new species or new records of *Agaricus* from Thailand are extensively studied (Chen et al., 2015; Chen et al., 2012; Karunarathna et al., 2014; Thongklang et al., 2016; Wisitrassameewong et al., 2012a; Wisitrassameewong et al., 2012; Zhao et al., 2013; Zhao et al., 2012). *Agaricus* is one of the most popular and potentially cultivatable genera as most species are edible, some are delicious, and widely consumed (*A. bisporus*). Most of *Agaricus* are saprotrophs that can be grown on soil, litter, or dung. *Agaricus bisporus* (button mushroom) is popular and commercially cultivated worldwide, belongs to *Agaricus* section *Bivelares* (Kerrigan et al., 2008; Parra, 2013). *A. subrufescens* is also cultivated mushroom with significant medicinal properties and belonging to the section *Arvenses* of the genus *Agaricus*. The popularity of this species is increasing rapidly, especially among Japanese, Brazilian and Chinese growers who are exporting dried fruiting bodies and fresh mushrooms (Geösel, 2011) and it has become an important export product of Brazil, reaching higher prices in comparison to other mushrooms (Dias et al., 2004). More from section *Arvenses, Agaricus arvensis, A. augustus,* and *A. silvicola* are collected from the wild for human consumption in Europe and America (Kalač, 2009; Wisitrassameewong et

al., 2012a). Several bioactive compounds that can be developed and used as therapeutic agents have been identified and characterized from this genus (Firenzuoli et al., 2008; Wisitrassameewong et al., 2012a; Wisitrassameewong et al., 2012b). The mushroom extracts shown many activities, such as anti-oxidant (Stojković et al., 2014; Wang, Wang et al., 2013; Wang & Xu, 2014), anti-genicity, anti-mutagenicity (Angeli et al., 2009) and anti-tumor (Gonzaga et al., 2009; Niu et al., 2009). For this genus, the high yields of mushroom production and good consumer attraction will be obtained by developed cultivation methods. As important as the agronomic performance, the final quality of mushrooms (physical, chemical and biological control of harvested mushroom) should also be taken into consideration. It can be defined by physical aspects: size, degree of maturation, absence of pests and diseases, etc.; chemical aspects: biologically active ingredients, no heavy metal, high presence of proteins and minerals, etc.; and finally, biological activities: bactericidal, antitumor and antioxidant activity. To identify and select the species for cultivation, the cultivated strains were selected from edible sections based on the taxonomic and phylogenetic evidence.



Figure 1.3 *Agaricus* subrufescens in the wild (MRC-29B)

1.3 Order Boletales

Classification

Kingdom Fungi
Division Basidiomycota
Class Agaricomycetes
Subclass Agaricomycetidae
Order Boletales
Genus *Hourangia*
Genus *Phlebopus*
Genus *Phylloporus*
Genus *Retiboletus*
Genus *Xerocomus*

Another group of Agaricomycetidae, Boletales (Gilbert, 1931) is one of the largest orders of fleshy mushrooms. Typically, basidiomes of boletes are pileate-stipitate with a tubular hymenophore (e.g., *Boletus, Suillus, Strobilomyces*), but sometimes gilled (*Phylloporus*) or gasteroid forms (e.g., *Astraeus, Mycoamaranthus, Scleroderma*) also occur. In addition, various forms of boletes basidiomes can be found such as resupinate forms with smooth or warted (*Coniophora*), merulioid (*Leucogyrophana*), and toothed (*Gyrodontium*) hymenophore. About 90% of species in Boletales form ectomycorrhizal symbioses (ECM) in association with, among others, *Acacia* (*s. stricto*), Arbutoideae, Betulaceae, Bossiaeeae, Caesalpinioideae, Casuarinacea, Cistaceae, *Coccoloba*, Dipterocarpaceae, Fagaceae, Leptospermoideae, Nothofagaceae, Pomaderreae, Pinaceae, Pisoniae, Salicaceae, and Uapacaceae (Newman & Reddell, 1987; Rinaldi et al., 2008; Tedersoo et al., 2010).

1.3.1 *Hourangia*

Hourangia (Zhu et al., 2015) is a recently described genus in the family Boletaceae. Based on molecular phylogenetic analyses of Boletaceae using multi-gene sequences, 22 new generic clades were revealed (Wu et al., 2014). Later, clade 8 which include of *Xerocomus* spp. was studied in more details. The additional specimens and

sequences shown five taxa is being distinct from *Xerocomus* spp. *Hourangia* is erected to accommodate *Xerocomus cheoi* and *Hourangia cheoi* is designed as type species (Zhu et al., 2015). This genus can be distinguished from other genera by the combination of the context becoming bluish and/or reddish to brownish red when cut or bruised. Most of the time bluing is only observed in the cap (sometimes only hymenophore) whereas reddening is observed also in the stipe. The thick hymenophore of the pileus context and the basidiospore surface with bacillate ornamentation shared with *Phylloporus* and *Xerocomus* sensu stricto, in which some *Hourangia* species were previously placed. The basidiomata are usually found on the ground in forests with *Castanopsis*, *Lithocarpus*, *Pinus* and *Quercus* spp. Currently, there are only four records of *Hourangia* spp. in Index Fungorum and MycoBank, *H. cheoi*, *H. microcarpa*, *H. nigropunctata*, and *H. pumila*. Those species have so far been reported only from China, Japan, Malaysia, and Indonesia. From this, the diversity and phylogeny of this genus from northern Thailand were studied.



Figure 1.4 *Hourangia microcarpa* in the wild (OR0138)

1.3.2 *Phlebopus*

Phlebopus was proposed as a subgenus of *Boletus* to accommodate *Boletus colossus* R. Heim by Heim (1936). Later, Singer (1936) elevated *Phlebopus* to genus with *P. colossus* (R. Heim) Singer as type species. Subsequently, Heinemann and Rammeloo (1982), Singer et al. (1983), and Singer (1986) emended the generic limits

to encompass all taxa of *Phaeogyroporus* (Singer, 1944). *Phlebopus* was classified in the Boletinellaceae (Boletales) by Binder and Bresinsky (2002). *Phlebopus* is a tropical or subtropical genus with boletoid basidiomata producing an olivaceous brown spore print, ellipsoidal smooth basidiospores (light microscope), and hyphae with clamp connections. Recently, there are 17 species were reported in database(IndexFungorum, http://www.indexfungorum.org/Names/Names.asp). Eight species (*P. braunii* (Bres.) Heinem., *P. bruchii bruchii* (Speg.) Heinem. & Rammeloo, *P. colossus* (R. Heim) Singer, *P. cystidiosus cystidiosus* Heinem. & Rammeloo, *P. harleyi* Heinem. & Rammeloo, *P. latiporus* Heinem. & Rammeloo, *P. silvaticus* Heinem., and *P. sudanicus* (Har. & Pat.) Heinem.) are known to be from Africa; four species (*P. marginatus* Watling & N.M. Greg., *P. spongiosus* Pham & Har. Takah., *P. viperinus* Singer, and *P. xanthopus* T.H. Li & Watling) are known to be from Asia and Australasia; three species (*P. brasiliensis* Singer, *P. maxicanus* Cappello, T.J. Baroni & B. Ortiz, and *P. tropicus* (Rick) Heinem. & Rammeloo) are known to be from the neotropics; *P. poretentosus* (Berk. & Broome) Boedijn is known to be from Asia, Africa and neotropics, and the last species; *P. beniensis* (Singer & Digilio) Heinem. & Rammeloo, is commonly found in Africa and the neotropics (Heinemann & Rammeloo, 1982; Ji et al., 2011; Pham et al., 2012a; Baroni et al., 2010; Pegler, 1977; Pegler, 1986; Halling, 1989; Palacio et al., 2014; Kumla et al., 2016; Calac et al., 2018). Typically, *Phlebopus* species are found around naturally growing or planted mycorrhizae plants (Pham et al. 2012a; Bougher et al., 1995; Watling, 2001; Watling, 2006; Mortimer et al., 2012). To date, *P. portentosus* is the only species in the genus *Phlebopus* that can be successfully cultivated without a host plant (Kumla et al., 2015; Zhang et al., 2017). A tropical bolete known as *P. spongiosus*, is an endemic edible mushroom that is indigenous to the southern part of Vietnam. Notably, it is priced higher than most other wild edible mushroom species (Pham et al., 2012a; Le et al., 2017). So far, only a few secondary metabolites have been reported from the genus of *Phlebopus*. For this, the secondary metabolites from *Phlebopus* were identified, to understand more about this genus.



Figure 1.5 *Phlebopus portentosus* from local market (BC001)

1.3.3 *Phylloporus*

Phylloporus (Quélet, 1888) is a Boletaceae genus which has a close relationship with *Xerocomus* (Neves et al., 2012; Zeng et al., 2013). The main difference between *Phylloporus* and *Xerocomus* is the lamellate hymenophore produced by *Phylloporus* species in contrast to the wide tubular hymenophore seen in *Xerocomus*. Typically, the lamellate hymenophore is one of characteristics that distinguishes *Phylloporus* from other genera in the Boletaceae. The phylogenetic analyses based on a multi-gene showed that the genera *Phylloporus*, *Hourangia*, and *Xerocomus* form a highly supported lineage in ML (100 %) and Bayesian (1.0) phylogenies, but are still separated from each other by large genetic distances (Wu et al., 2014). Most *Phylloporus* species are found in tropical or subtropical forests worldwide (Chantorn et al., 2007; Heinemann, 1971; Heinemann & Rammeloo, 1987; Hosen & Li, 2017; Montoya & Bandala, 1991; Neves & Halling, 2010; Singer & Gómez-Pignataro, 1984; Singer et al., 1990; Watling, 2008; Ye et al., 2014). However, the type species, *P. pelletieri*, is from Europe (Ladurner & Simonini, 2003). From Index Fungorum and MycoBank databases, this genus contains 114 species. The *Phylloporus* species are mycorrhizal with various trees, including species of Fabaceae (Caesalpinioideae, Mimosoideae), Casuarinaceae, Dipterocarpaceae, Fagaceae, Myrtaceae, and Pinaceae (Halling & Mueller, 2002; Heinemann & Rammeloo, 1987). However, most tropical regions have not been well studied and a few species were recorded from Thailand (4 species: *P.*

castanopsidis, *P. dimorphus*, *P. infuscatus*, and *P. rubiginosus*). In this study, the taxonomy, phylogenetic and relationships of *Phylloporus* species were investigated.



Figure 1.6 *Phylloporus subrubeolus* in the wild (BC022)

1.3.4 *Retiboletus*

Retiboletus was described by Binder and Bresinsky (2002), typified by *R. ornatipes* (Peck) Manfr. Binder & Bresinsky, a species native to North America. Retiboletus belongs in the Boletaceae, Boletales (He et al., 2019) and differs from other Boletaceae genera by its usually reticulate stipe with a base usually darker than the apical region. No part of the basidiomata stain blue after bruising like many other boletes, but rather yellow-orange to rusty brown. Moreover, the mushrooms often stain the fingers yellow on handling. This yellow staining is due to retipolides, a unique class of metabolites so far only found in Retiboletus (Justus et al., 2007). DNA phylogenetic analyses and the presence of retipolides prompted Binder and Bresinsky (2002) to erect *Retiboletus* as a new genus of Boletaceae. Retiboletus ornatipes and *R. retipes* (Berk. & M.A. Curtis) Manfr. Binder & Bresinsky, originally described in *Boletus*, are closely related species that are very difficult to separate in morphology. However, DNA analyses and chemotaxonomical characters, i.e. the structure of the unique metabolites named retipolides, allow separating the two species clearly (Binder & Bresinsky, 2002). *Retiboletus griseus* (Frost) Manfr. Binder & Bresinsky from Northern America and *R. nigerrimus* (R. Heim) Manfr. Binder & Bresinsky from Australia were also transferred

to *Retiboletus* based on morphological characters and sequence data (Binder & Bresinsky, 2002). However, the detection of retipolides in those two taxa remains to be established (Binder & Bresinsky, 2002; Gruber et al., 2013). As Binder and Bresinsky (2002) proposed the new bolete genus *Retiboletus* to accommodate *Boletus retipes* Berk. & M.A. Curtis, *B. ornatipes* Peck, *B. flavoniger* Halling, G.M. Muell. & L.D. Gómez, *B. griseus* Frost, and *B. nigerrimus* R. Heim. The first three species are characterized by the occurrence of retipolides (Binder & Bresinsky, 2002; Justus et al., 2007). Later, Gruber et al. (2013) studied the chemotaxonomy of the latter two species, and they detected a new pulvinic acid (retiboletic acid), and two phenylalaninol derivatives (nigerrimin A and B), but no retipolides. However, retiboletic acid and phenylalaninol derivatives could be other compounds characteristic of *Retiboletus*, especially *R. griseus*, and *R. nigerrimus*, because so far, they have been found only in *Retiboletus*. Thus, although intraspecific variation in secondary metabolites may occur, retipolides and other compounds have some chemotaxonomical value (Hellwig, 1998; Binder & Bresinsky, 2002; Gruber et al., 2013). Recently, *Retiboletus* collections from China were studied, and their molecular phylogenetic analyses confirmed the monophyly of *Retiboletus* (Wu et al., 2014; Zeng et al., 2016). To date, sixteen *Retiboletus* species (IndexFungorum (http://www.indexfungorum.org/Names/Names.asp) have been reported from temperate or tropical; Asia, *Retiboletus ater* Yan C. Li & T. Bau, *R. brevibasidiatus* Raspé & Chuankid, *R. brunneolus* Y.C. Li & Zhu L. Yang, *R. fuscus* (Hongo) N.K. Zeng & Zhu L. Yang, *R. kauffmanii* (Lohwag) N.K. Zeng & Zhu L. Yang, *R. nigrogriseus* N.K. Zeng, S. Jiang & Zhi Q. Liang, *R. pseudogriseus* N.K. Zeng & Zhu L. Yang, *R. sinensis* N.K. Zeng & Zhu L. Yang, *R. sinogriseus* Yan C. Li & T. Bau, *R. zhangfeii* N.K. Zeng & Zhu L. Yang; North America, *R. flavoniger* (Halling, G.M. Muell. & L.D. Gómez) Manfr. Binder & Halling, *R. griseus* (Frost) Manfr. Binder & Bresinsky, *R. ornatipes* (Peck) Manfr. Binder & Bresinsky, *R. retipes* (Berk. & M.A. Curtis) Manfr. Binder & Bresinsky, *R. vinaceipes* B. Ortiz, Lodge & T.J. Baroni; Oceania, *R. nigerrimus* (R. Heim) Manfr. Binder & Bresinsky.



Figure 1.7 *Retiboletus nigrogriseus* in the wild (OR049)

1.3.5 *Xerocomus*

Xerocomus Que´l. (1887) ~160 described species worldwide, many with tropical distributions (Heinemann & Goossens-Fontana, 1954; Heinemann, 1964; McNabb, 1968; Snell & Dick, 1970; Corner, 1972, 1974; Singer, 1986; Singer et al., 1983, 1991; Gomez, 1996; Ladurner & Simonini, 2003; Ortiz-Santana et al., 2007; Watling, 2008; Horak, 2011). *Xerocomus* has been differentiated from other boletes by its hymenophoral tubes that are sublamellate near the stipe and adnate to decurrent, subangular to angular, relatively large pores, cylindrical to subequal, thin, usually nonreticulate stipe, parallel to barely divergent (‘‘phylloporoid’’) tube trama and trichodermioid, dry pileipellis (e.g. Singer, 1986). While molecular delimitation of the Boletaceae genera remains elusive, diverse species complexes have been discovered within the north temperate *X. chrysenteron* s.l. and *X. subtomentosus* s.l. (Peintner et al. 2003; Taylor et al. 2006). S˘utara (2008) used detailed morphological analyses to erect the segregate genus *Xerocomellus* S˘utara. This group includes European *Xerocomus* s.l. species that are morphologically aligned with *X. chrysenteron* s.l. but has not been fully supported by molecular phylogenetic analyses (e.g., Binder and Hibbett 2006). According to Wu et al. (2014, 2016), multi-gene phylogeny of the family Boletaceae also accommodates the members of the genus *Xerocomus* can be placed as *Xerocomus* Quél. s. s. under subfamily Xerocomoideae. Although some progress has

been made in delimiting *Xerocomus* within the Boletaceae using molecular data, a full reassessment of *Xerocomus* were required much further study.



Figure 1.8 *Xerocomus microcarpoides* in the wild (OR0156)

1.4 Mushroom Cultivation

Since an ancient time, the consumption of mushrooms by humans was recorded. Historical data shown mushroom cultivation and consumption occurred in ancient civilizations of China, Rome, Greece, Egypt and Central America. In fact, Asian civilizations have been cultivating edible mushrooms for almost 1400 years (Chang & Miles, 1987). The first mushroom, *Auricularia auricula* (wood ear) was cultivated in China followed by *Flammulina velutipes* (enokitake), *Lentinula edodes* (shiitake), *Agaricus bisporus* (button), *Volvariella volvacea* (paddy straw), *Tremella fuciformis* (white jelly), and *Pleurotus ostreatus* (oyster). From the leading mushrooms that are being cultivated today, *Agaricus* is the only one that was not first grown in Asia (Miles & Chang, 2004). Nowadays, the market for mushrooms tends to increase due to interest in their nutritional, health benefits, and potential in waste management (Beetz & Greer, 1999). For this study, growing and storage of mycelium, as well as cultivation

conditions are described and compared to knowledge on *A. bisporus*. The important cultivated edible and medicinal mushrooms belong to the genus *Agaricus* are saprotrophic fungi acting as secondary decomposers in forest litters. The mushroom cultivation could be act as bioconversion of agricultural wastes which are cheap and easily available. Mushrooms compost is developed as the chemical nature of the raw ingredients is converted by the activity of microorganisms, heat, and some heat releasing by chemical reaction. The preparation of mushroom compost is usually done in two stages (Royse & Beelman, 2007), "Phase I composing involves the initial breakdown of the raw ingredients. Phase I composting is followed by a controlled conditioning stage (phase II) in which the compost is pasteurized at 60ºC and allowed to cool, before mushroom spawn is incorporated". It is well known that thermophilic fungi play important roles in the composting process by decomposing cellulose, aiding thermogenesis, and contributing to the destruction of pathogens. A large number of thermophilic fungi have been isolated from commercial mushroom compost. More specially, thermophilic fungi from the *Torula-Humicola* complex are considered to be highly significant in compost preparation and nutrition of *Agaricus*. Generally, composting is initiated by mixing and wetting the ingredients as they are stacked in a rectangular pile with tight sides and loose center. Normally, the bulk ingredients are put through a compost turner. Water is sprayed onto the manure or synthetic compost as these materials move through the turner. Nitrogen supplements and gypsum are spread over the top of the bulk ingredients and are thoroughly mixed by the turner. The pile is wetted and formed, aerobic fermentation (composting) started as a growth and reproduction of microorganisms, which occur naturally in the bulk ingredients. Heat, ammonia, and carbon dioxide are released as by products during this process (Wuest et al., 1979). To induced primordium, casing soil has an important to keep moisture and provided the air exchange. Peat is commonly used and recommended as a good casing in mushroom cultivation, even though several different casing materials instead of peat have been examined by many investigators (Largeteau et al., 2011).

However, some of the growers are still facing the problems about the low yield that occurred as followed: the preparations of substrates not suitable to mushrooms growth, the spawn used had not been well selected or bred, the origins of spawn were confused, and the growing houses were not well constructed. To overcome these

problems and increase mushrooms production, compost cultivation techniques were considered.

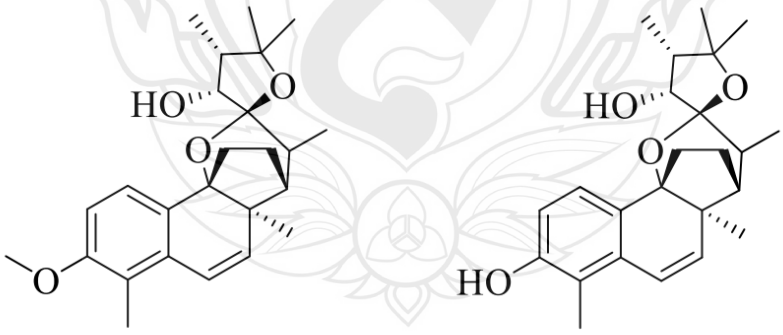
1.5 Bioactive Compound Investigation of *Agaricus* and *Phlebopus*

Due to the great economic importance, many species of *Agaricus* (e.g. *A. bisporus* and *A. subrufescens*) have been studied on their biologically active ingredients. This species were found both of toxins and metabolites benefits. Many basidiocarps of *Agaricus* contain agaritine (aromatic hydrazine), a secondary metabolite that is suspected to have toxic effects to the mammalian body but agaritin is readily destroyed by cooking and is not present in very high concentrations. That means, the risk is not very significant except eat the raw mushrooms. Based on this, a series of derivatives were generated by modifying agaritine which had markedly stronger binding interaction with the HIV protease than agaritine, suggesting that these derivatives might be good candidates for developing drugs for AIDS therapy (Gao et al., 2007). From Merdivan et al. (2016), agaritine was described and validated by solid phase extraction and measured by liquid chromatography with tandem mass spectrometry detection in positive ionization mode (LC-MS/MS). This method could be used for the quality control of cultivated mushrooms. Also, the *Agaricus* mycelia contain β-glucans that shown the similar activity as agaritine. The great example *A. subrufescens* extracts are rich in β-glucans that shown many activities, anti-oxidant (Stojković et al., 2014; Wang et al., 2013; Wang & Xu, 2014), anti-genicity, anti-mutagenicity (Angeli et al., 2009) and anti-tumor (Gonzaga et al., 2009; Niu et al., 2009). The chemical structures and some properties of the immuno-stimulating polysaccharide and glucan-protein complexes from *A. subrufescens* were studied (Hetland et al., 2008; Liu et al., 2008; Sorimachi et al., 2008). Blazein (triterpenoid) from fruiting bodies of *A. subrufescns* can induce apoptosis in lung cancer LU99 and stomach cancer KATO III cells (Itoh et al., 2008).

These mushrooms have many remarkable bioactive compounds to studied, different biological compounds that need to be isolated and characterized for their curative properties following evaluation of toxicological effects. For this study, the

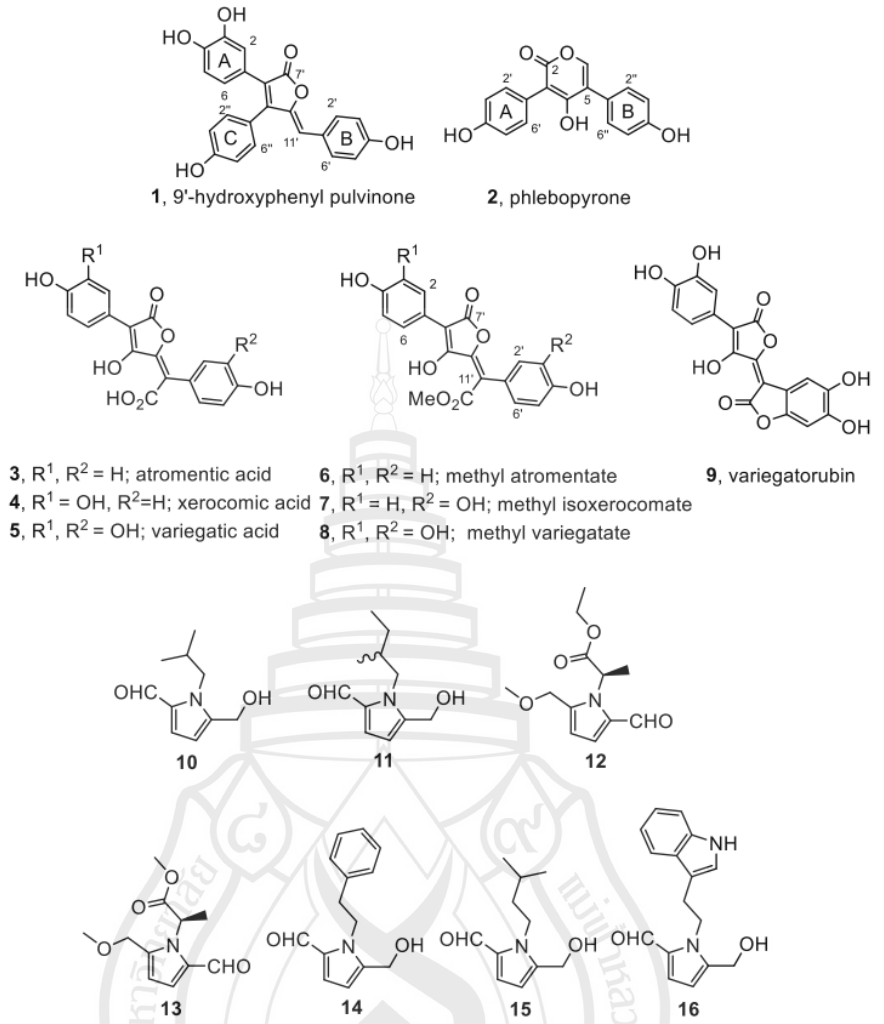
selected species were analyzed by liquid chromatography technique (HPLC-UV/Vis, LC/MS) and elucidated by Nuclear magnetic resonance spectroscopy (NMR). Further, the potential extracts were purified and used for another analyzed.

Another edible species from Boletales also presented here with the isolation and characterization of secondary metabolites from cultures of *P*. *portentosus* and *P*. *spongiosus*. The genus *Phlebopus* (R. Heim) Singer, classified in the Boletinellaceae (Boletales) and is widely distributed in tropical and subtropical areas (He et al., 2019). Some of them are highly important as local food source. For example, *Phlebopus portentosus* (Berk. and Broome) Boedijn is one of the most popular edible wild mushrooms in Northern Thailand and China. Due to their prized flavor, large size, and nutritional value, the basidiomes are harvested and sold at high prices on local markets in Yunnan, China and Thailand (Ji et al., 2011). Also, since 2018 cultivation of *P*. *spongiosus* started in Vietnam (Le Thi et al., 2018). Both *Phlebopus* species are the only species from the order Boletales that can be successfully cultivated under artificial conditions for commercial purpose (Zhang et al., 2017). So far, only a few secondary metabolites have been reported from the genus of *Phlebopus*. For instance, phlebopines A-C and other pyrrole alkaloids were isolated from dried basidiomes of *P*. *portentosus* (Fig. 1.10, Sun et al., 2018).



blazeispirol A (**1**) blazeispirol D (**2**)

Figure 1.9 Chemical structures of blazeispirol A (1) and D (2) found in *Agaricus*



Note Chemical structures of compounds 1–9 isolated from *Phlebopus portentosus* and *P. spongiosus* (liquid cultivation) and known compounds (10–16) isolated from air-dried basidiomes from *P. portentosus*

Source Sun et al. (2018)

Figure 1.10 Chemical structures of compounds 1–9 isolated from *Phlebopus portentosus* and *P. spongiosus*

1.6 Research Objectives

1.6.1 To document the diversity of selected Agaricomycetidae (*Agaricus*, *Hourangia*, *Phylloporus*, *Retiboletus*) from five provinces of northern Thailand (Chiang Rai, Chiang Mai, Mae Hong Son, Lampang and Phayao), with taxonomic and phylogenetic studies. Novel species or first records for Thailand will be reported.

1.6.2 To produce identification keys for *Hourangia*, *Phylloporus*, and *Retiboletus* from northern Thailand.

1.6.3 To use taxonomic and phylogenetic evidence to select the edible *Agaricus* sp. for cultivation.

1.6.4 To study biologically active compounds produced by the selected *Agaricus* sp. and *Phlebopus* sp.

1.7 Research Outlines

This thesis is comprised of eight chapters devoted to the study of selected Agaricomycetidae from northern Thailand. Each chapter includes two major sections, first on classification, and second on chemistry. A section on cultivation is also included in chapter five. The main focus of the theses is on mushrooms collected from Chiang Rai, Chiang Mai, Mae Hong Son, Lampang and Phayao provinces.

Chapter 1 – An introduction to the importance of the study of taxonomy, phylogeny, chemistry, and cultivation of selected Agaricomycetidae from Thailand. An overview of the genus *Agaricus*, *Hourangia*, *Phlebopus*, *Phylloporus*. This overview includes general characteristics used in identification, ecology, and distribution. Additionally, the history of natural products from Agaricomycetidae along with the history of cultivation of edible mushrooms in the country is discussed.

Chapter 2 – Research methodology.

Chapter 3 – Research results.

Chapter 4 – Discussion.

Chapter 5 – Provides overall conclusions and perspectives on this study.

Chapter 6 – Taxonomy and phylogeny of other genera in the contributed papers.

CHAPTER 2

RESEARCH METHODOLOGY

2.1 Taxonomy and Phylogeny Study

2.1.1 Morphological Study of *Phylloporus*

The *Phylloporus* collections were made from northern Thailand and southwestern China. Each collection was described from the field notes and photographs of fresh basidiomata. The macrochemical reactions on fresh basidiomata, habitat, altitude and localization of the collecting site were recorded. For each collection, a spore print was taken (if possible). Colour codes were given following Kornerup and Wanscher (1978). Finally, pieces of tissue were kept in CTAB for DNA isolation, and the mushrooms were dried with a hot air dryer at 40–50 °C and deposited in the Mae Fah Luang University herbarium (MFLU) or Herbarium of the Department of Biology, Faculty of Science, Chiang Mai University (CMUB), with duplicates deposited in the Botanic Garden Meise herbarium (BR). The dried specimens were used for microscopic observation. Micro-characters were studied and photographed using Nikon Eclipse Ni microscope. Tissues were observed in 5% potassium hydroxide (KOH) or 28–30% ammonium hydroxide (NH_4OH) solutions or stained with 1% ammoniacal Congo Red solution. The microscopic structures were observed at a magnification of × 400 or × 1000, photographed and measured using Image Frame Work program v. 0.9.7 (Tarosoft). At least 50 basidiospores were measured in side view, avoiding immature or abnormal ones. The notation '[*n*/*m*/*p*]' represents the number of basidiospores (*n*) measured from (*m*) basidiomata of (*p*) collections. At least 20 basidia, pleurocystidia, cheilocystidia, terminal cells and hyphae of pileipellis and stipitipellis were observed. The dimensions of microscopic structures are presented in the following format: (*a*–)*b*–*c*–*d*(−*e*), in which *c* represents the average, *b* the *5th*

percentile, *d* the *95th* percentile and minimum and maximum values *a* and *e* are shown in parentheses. *Q*, the length/width ratio, is presented in the same format. All microscopic features were drawn by free hand, using a drawing tube. For scanning electron microscopy (SEM), small fragments of dried hymenophore were mounted directly onto a SEM stub with double-sided carbon tape. The samples were coated with gold for 60 s using SPI-Module Sputter Coater, examined and photographed at 15.0 kV with a JSM-IT300 scanning electron microscope (JEOL, USA). Faces of Fungi (Jayasiri et al. 2015) and MycoBank numbers are provided for the new species.

2.1.2 PCR Amplification and Sequencing of *Phylloporus*

Genomic DNA was extracted from CTAB-preserved tissues or dry specimens (ca. 10 mg) using a CTAB isolation procedure adapted from Doyle and Doyle (1990). The ITS region and parts of the genes *atp6*, *tef1* and *rpb2* were amplified by polymerase chain reaction (PCR). For PCR amplification of the ITS1–5.8S-ITS2 region of rDNA, ITS1-F (Gardes & Bruns, 1993) and ITS4 (White et al., 1990) were used as primers. Amplifications were performed in 20 μL reactions containing 2 μL 10× polymerase buffer, 0.2 μM of each dNTP, 200 μg μL^{-1} bovine serum albumin (BSA), 0.25 μM of forward and reverse primers, 0.5 U Taq polymerase (DreamTaq, Thermo Scientific, St. Leon-Rot, Germany). Cycling was carried out using the following program: 3 min at 94 °C; 35 cycles of 30 s at 94 °C, 30 s at 52 °C, 60 s at 72 °C; 5 min at 72 °C. The PCR amplification, purification and sequencing of *atp6*, *rpb2* and *tef1* were used following the procedure from Raspé et al. (2016).

2.1.3 Sequence Data Analyses of *Phylloporus*

The sequences were assembled in Geneious Pro v. 5.0.4 (Biomatters). ITS1 and ITS2 sequences of *Phylloporus* from this study were extracted from the whole ITS amplicon sequence using ITSx (Bengtsson-Palme et al., 2013). Then, the ITS1 + ITS2 sequences were blasted against GenBank database to check the similarity with other *Phylloporus*. The *atp6*, *rpb2* and *tef1* sequences of 22 specimens were generated, which, along with sequences of 9 species retrieved from GenBank, were aligned using MAFFT version 7 (Katoh & Standley, 2013) on the server accessed at http://mafft.cbrc.jp/alignment/server/. Maximum likelihood (ML) phylogenetic tree inference was performed using RAxML version 8.2.10 (Stamatakis, 2014) on the

CIPRES web server (RAxMLHPC2 on XSEDE; Miller et al., 2010), using a mixed-model analysis, the GTRCAT model of substitution with 25 categories and four *Xerocomus* as outgroup (*X. subtomentosus* and three *X.* s.s. sp.). Four partitions were defined: *atp6*, *rpb2* exons, *tef1* exons and introns. Node support was obtained by rapid bootstrapping with 1000 replicates. Bayesian inference (BI) analysis was performed using the Markov Chain Monte Carlo (MCMC) method implemented in MrBayes 3.2.6 (Ronquist et al. 2012) with a mixed-model partition (partitions identical to the ones defined in the ML analysis). The best-fit nucleotide substitution model was separately determined for each partition with jModeltest version 2.1.10 (Darriba et al., 2012) on CIPRES, using the Bayesian Information Criterion. F81 + I + G, K80 + G, K80 + I + G and HKY + G were selected as best-fit models for *atp6*, *rpb2* exons, *tef1* exons and introns, respectively. Two MCMC runs with five chains were run for 500,000 generations and sampled every 200 generations. At the end of the runs, the average deviation of split frequencies was 0.001751. The burn-in phase (20%) was estimated by checking the stationarity in the plot generated by the sump command.

2.1.4 Morphological Study of *Retiboletus*

The *Retiboletus* collections were made from northern Thailand. Each collection was photographed and described based on field notes and photos of fresh basidiomata. Macro-chemical reactions on fresh basidiomata, habitat, elevation, and localization of the collecting site were recorded. Color codes were given following Kornerup and Wanscher (1978). Finally, the specimens were dried using a hot air dryer at ca. 50 °C and deposited in the Mae Fah Luang University herbarium (MFLU) or the Chiang Mai University herbarium (CMUB). The dried specimens were used for microscopic observations. Micro-characters were studied and photographed using Eclipse Ni (Nikon, Tokyo) microscope. Tissues were observed in 5% (w/v) potassium hydroxide (KOH) or 28–30% (w/v) ammonium hydroxide (NH_4OH) solutions or stained with 1% (w/v) ammoniacal congo red solution. The microscopic structures were observed at a magnification of 400× or 1,000×, and measured using Tarosoft (R) Image Frame Work program v. 0.9.7. At least 50 basidiospores, 20 basidia, pleurocystidia, cheilocystidia, terminal cells and hyphae of the pileipellis and stipitipellis were measured. The notation '[*n*/*m*/*p*]' represents the number of basidiospores *n* measured from *m* basidiomata of

p collections. The dimensions of microscopic structures are presented in the following format: (*a*–)*b*–*c*(–*d*), with the average, in which *b* represents the *5th* percentile, *c* the *95th* percentile and extreme values *a* and *d* are shown in parentheses. *Q*, the length/width ratio, is presented in the same format. All microscopic features were drawn by free hand, using a drawing tube. Faces of Fungi (Jayasiri et al., 2015) and MycoBank numbers (Westerdijk Fungal Biodiversity Institute) are provided for each species.

2.1.5 Molecular Phylogeny of *Retiboletus*

2.1.5.1 DNA extraction, amplification, sequencing and sequence alignment

Genomic DNA was extracted from CTAB-preserved tissues or dry specimen (OR0110) using a CTAB isolation procedure adapted from Doyle and Doyle (1990). Tissues were ground with a Retsch 300 mill with 0.2% .-mercaptoethanol was added to the CTAB lysis buffer just prior to extraction; samples were lysed for one hour at 60 °C; proteins and polysaccharides were removed by two consecutive extractions with chloroform: isoamylalcohol (24: 1), after which DNA was precipitated by the addition of 0.8 volume isopropanol to the aqueous phase; the pellet was washed once in 600 µL 70% (v/v) ethanol, air-dried and suspended in 100 µL TE pH 8.0; RNA was then digested with RNase A. The PCR amplification of *atp*6, *rpb*2 and *tef*1 were performed following the procedures described in Raspe et al. (2016). For amplification of *atp6*, we used ATP6-1M40F and ATP6-2M (Raspe et al., 2016). The primers EF1-983F and EF1-2218R (Rehner & Buckley, 2005) were used to amplify *tef*1. The primers bRPB2-6F and bRPB2-7.1R (Matheny, 2005) were used to amplify *rpb*2. PCR products were purified by adding 1 U of Exonuclease I and 0.5 U FastAP Alkaline Phosphatase (Thermo Scientific, St. Leon-Rot, Germany) and incubated at 37 °C for 1 h, followed by inactivation at 80 °C for 15 min. Sequencing was performed by Macrogen Inc. (The Netherlands) with PCR primers, except for *atp*6, for which universal primers M13F-pUC(-40) and M13F(-20) were used. For *tef*1, additional sequencing was performed with the two internal primers, EF1-1577F and EF1-1567R (Rehner & Buckley, 2005). Newly generated sequences were assembled in Geneious Prime ver. 2019.2.3 (Biomatters). The newly generated *atp*6, *rpb*2 and *tef*1 sequences, together with sequences of 17 specimens retrieved from GenBank were aligned using MAFFT

version 7 (Katoh & Standley, 2013) on the server accessed at http://mafft.cbrc.jp/alignment/server/.

2.1.5.2 Phylogenetic analyses

Maximum likelihood (ML) phylogenetic tree inference was performed using RAxML version 8.2.10 (Stamatakis, 2014) on the CIPRES web server (Miller et al., 2010), using a mixed-model analysis, and the GTRCAT model of substitution with 25 categories. Four species in the sub-family *Leccinoideae*, namely *Borofutus dhakanus* Hosen & Zhu L. Yang, *Ionosporus longipes* (Massee) Khmeln., Davoodian, Raspe, S.M.L. Lee & Halling, *Rhodactina rostratispora* Vadthanarat, Raspe & Lumyong, and *Spongiforma thailandica* Desjardin, Manfr. Binder, Roekring & Flegel were used as outgroup taxa. The partitions were defined as: *atp*6, *tef*1 exons, *rpb2* exons, and *tef1* introns plus *rpb2* intron. Node support was obtained by rapid bootstrapping with 1,000 replicates. Bayesian inference (BI) was performed using the Markov Chain Monte Carlo (MCMC) method implemented in MrBayes 3.2.6 (Ronquist et al., 2012) with a mixed-model partition (partitions identical to the ones defined in the ML analysis). The best-fit nucleotide substitution model was separately determined for each partition with jModeltest version 2.1.10 (Darriba et al., 2012) on CIPRES, using the Akaike Information Criterion. GTR+G, SYM+G, SYM+G and GTR+G were selected as best-fit models for *atp*6, *tef*1 exons, *rpb*2 exons, and introns, respectively. Two MCMC runs with five chains each were run for 2,000,000 generations and sampled every 200 generations. At the end of the runs, the average deviation of split frequencies was 0.00242. The burn-in phase was estimated by checking the stationarity in the log-likelihood plot generated by the sump command.

2.1.6 Morphological Study of *Hourangia* and *Xerocomus*

The collections were made from northern Thailand. Each collection was photographed and described based on field notes and photos of fresh basidiomata. Macro-chemical reactions on fresh basidiomata, habitat, elevation, and localization of the collecting site were recorded. Color codes were given following Kornerup and Wanscher (1978). Finally, the specimens were dried using a hot air dryer at ca. 50 °C and deposited in the Mae Fah Luang University herbarium (MFLU) or the Chiang Mai University herbarium (CMUB). The dried specimens were used for microscopic

observations. Micro-characters were studied and photographed using Eclipse Ni (Nikon, Tokyo) microscope. Tissues were observed in 5% (w/v) potassium hydroxide (KOH) or 28–30% (w/v) ammonium hydroxide (NH_4OH) solutions or stained with 1% (w/v) ammoniacal congo red solution. The microscopic structures were observed at a magnification of 400× or 1,000×, and measured using Tarosoft (R) Image Frame Work program v. 0.9.7. At least 50 basidiospores, 20 basidia, pleurocystidia, cheilocystidia, terminal cells and hyphae of the pileipellis and stipitipellis were measured. The notation '[*n*/*m*/*p*]' represents the number of basidiospores *n* measured from *m* basidiomata of *p* collections. The dimensions of microscopic structures are presented in the following format: (*a*–)*b*–*c*(–*d*), with the average, in which *b* represents the *5th* percentile, *c* the *95th* percentile and extreme values *a* and *d* are shown in parentheses. *Q*, the length/width ratio, is presented in the same format. All microscopic features were drawn by free hand, using a drawing tube. Faces of Fungi (Jayasiri et al., 2015) and MycoBank numbers (Westerdijk Fungal Biodiversity Institute) are provided for each species.

2.1.6 Molecular Phylogeny of *Hourangia* and *Xerocomus*

2.1.6.1 DNA extraction, amplification, sequencing and sequence alignment

Genomic DNA was extracted from CTAB-preserved tissues or dry specimen using a CTAB isolation procedure adapted from Doyle and Doyle (1990). Tissues were ground with a Retsch 300 mill with 0.2% .-mercaptoethanol was added to the CTAB lysis buffer just prior to extraction; samples were lysed for one hour at 60 °C; proteins and polysaccharides were removed by two consecutive extractions with chloroform: isoamylalcohol (24: 1), after which DNA was precipitated by the addition of 0.8 volume isopropanol to the aqueous phase; the pellet was washed once in 600 µL 70% (v/v) ethanol, air-dried and suspended in 100 µL TE pH 8.0; RNA was then digested with RNase A. The PCR amplification of *atp*6, *rpb*2 and *tef*1 were performed following the procedures described in Raspe et al. (2016). For amplification of *atp6*, we used ATP6-1M40F and ATP6-2M (Raspe et al., 2016). The primers EF1-983F and EF1-2218R (Rehner & Buckley, 2005) were used to amplify *tef*1. The primers bRPB2-6F and bRPB2-7.1R (Matheny, 2005) were used to amplify *rpb*2. PCR products were purified by adding 1 U of Exonuclease I and 0.5 U FastAP Alkaline Phosphatase

(Thermo Scientific, St. Leon-Rot, Germany) and incubated at 37 °C for 1 h, followed by inactivation at 80 °C for 15 min. Sequencing was performed by Macrogen Inc. (The Netherlands) with PCR primers, except for *atp*6, for which universal primers M13F-pUC(-40) and M13F(-20) were used. For *tef*1, additional sequencing was performed with the two internal primers, EF1-1577F and EF1-1567R (Rehner & Buckley, 2005). Newly generated sequences were assembled in Geneious Prime ver. 2019.2.3 (Biomatters). The newly generated *atp*6, *rpb*2 and *tef*1 sequences , together with sequences of 17 specimens retrieved from GenBank were aligned using MAFFT version 7 (Katoh & Standley, 2013) on the server accessed at http://mafft.cbrc.jp/alignment/server/.

2.1.6.2 Phylogenetic analyses

Before combining the data partitions, topological incongruence between the datasets was assessed using maximum likelihood (ML) and Bayesian inference (BI) separately on each of the four-character sets, *atp*6, *tef*1 exons, *rpb*2 exons, and the three introns of *tef*1 + the intron of *rpb*2. Paired trees were examined for conflicts involving only nodes with ML bootstrap (BS) > 70% and Bayesian posterior probabilities (PPs) > 0.90. For ML, phylogenetic inference was performed using RAxML (Stamatakis, 2006) on the CIPRES web portal (RAxML-HPC2 on XSEDE; Miller et al., 2009), using the GTRCAT model with 25 categories. Three *Boletellus* were used as outgroup. Statistical support of clades was obtained with 1,000 rapid BS replicates. For BI, the best-fit model of substitution among those implementable in MrBayes was estimated separately for each character set using jModeltest (Darriba et al., 2012) on the CIPRES portal, based on the Bayesian information criterion. The selected models were HKY+I+G for *atp*6, SYM+I+G for *tef*1 exons, and K80+I+G for *rpb*2 exons and GTR+I+G for intron partition. The Bayesian analysis was performed using the Markov Chain Monte Carlo (MCMC) method implemented in MrBayes 3.2.6 (Ronquist et al., 2012).

Then, phylogenetic inference of a combined, partitioned dataset was performed, using ML under the same model mentioned above. The phylogenetic tree was inferred from a single analysis with four-character sets: *atp*6, *tef*1 exons, *rpb*2 exons and the three introns of *tef*1 + the intron of *rpb*2. The same combined dataset was also analyzed by BI, based on the best-fit model mentioned previously. The two runs of five chains

were run for 5,000,000 generations and sampled every 500 generations. At the end of the run, the average deviation of split frequencies was 0.003712. The burn-in phase (25%) was estimated by checking the stationary in the plot generated by the sump command.

2.2 Cultivation and Identification of Blazeispirols from Wild *Agaricus campestroides* and *A. flocculosipes*

2.2.1 Sample Collection of *Agaricus* Strains

Two specimens of *A. campestroides* and *A. flocculosipes* were collected in Mae Fah Luang university campus, Chiang Rai province, Northern Thailand during the rainy season from June to August 2014. The specimens were dried at 45 °C by hot air dryer and kept in zip-lock plastic bags containing dehydrated silica gel as a desiccant to control humidity. The dried specimens were deposited in the herbarium of Mae Fah Luang University (MFLU herbarium), Chiang Rai, Thailand with the accession numbers: MFLU 14–0872 (*A. campestroides*) and MFLU 14–0874 (*A. flocculosipes*).

2.2.2 Isolation of Mycelia Cultures

Pure cultures were aseptically obtained by transferring sections of internal tissue from wild basidiomata of *Agaricus* onto potato dextrose agar (PDA) after incubation at 25 °C in a dark room for 14 days. The isolates were deposited in the culture collections of Mae Fah Luang University (MFLUCC) with the numbers MFLUCC 14–1024 (MFLU 14–0872) and MFLUCC 14–1026 (MFLU 14–0874). The cultures were kept at 4 °C, 25 °C, and -20 °C for further studies.

2.2.3 DNA Extraction, PCR, and Sequencing

Genomic DNA was extracted from dry specimens (ca. 10 mg) using a CTAB isolation procedure adapted from Doyle and Doyle (1990). The ITS region was amplified by polymerase chain reaction (PCR). For PCR amplification of the ITS1–5.8S–ITS2 region of rDNA, ITS1-F (Gardes & Bruns, 1993) and ITS4 (White et al., 1990) were used as primers. Raspé et al. (2016) and Chuankid et al. (2019) were followed for the PCR amplification, purification and sequencing of ITS region. The

sequences of Thai strains of *A. campestroides* and *A. flocculosipes* were deposited in the NCBI database under the accession numbers MZ596239 and MZ596240, respectively.

2.2.4 Optimization of Culture Conditions for Mycelia Growth

Four different media were used for optimized mycelia growth rates, included malt extract agar (MEA), malt yeast peptone agar (MYPA), potato dextrose agar (PDA), and potato dextrose yeast agar (PDYA), and pH of the media were adjusted to 6.3. After incubation for 10 days, the growing edge of each colony from pure cultures on PDA was cut out by used a cork-borer (8 mm in diameter) and placed on the centre of each optimization medium in 9 cm petri dishes. Three replicates of each medium were incubated in the dark at 25 °C for 30 days. Mycelia characteristics, such as colour, margin, and shape on the agar surface were recorded. Biomass of dry mycelium was measured by melting agar medium, drained away the liquid phase of medium, and dried the mycelia at 40 °C for 24 h. The mycelia dried weight was recorded using an electronic scale (gram). The biomass was measured every three days for 30 days. The day after mycelium fully colonised was selected for statistical analysis.

Mycelia disks (8 mm) from the colony edge of 10-day-old petri dish cultures of each strain were transferred to optimal medium. The optimal temperature for mycelia growth was determined by using four different temperatures: 20, 25, 30 and 35 °C. Three replicates of each strain were incubated in a dark room for 30 days. The biomass was measured as described above.

The medium exhibited the highest growth rate and optimal temperature was used to evaluate the optimal pH. The pH was adjusted to 5, 6, 7, and 8 with hydrochloric acid (HCl) and sodium hydroxide (NaOH). The pH range of the media were measured used a digital pH meter before autoclaved. The biomass of mycelium was measured for each pH value as described above.

2.2.5 Spawn Production

Spawn is the medium for mushroom mycelium that provides the backbone to any mushroom growing operation (seeds for cultivation). The preparation of spawn was adapted from Royse and Beelman (2016). Spawn was made by sterilized a mixture of wheat grain mixed with water, 1% calcium carbonate, and 0.5% calcium sulfate. The

spawn jars containing 100 g of wheat grain were inoculated with a 1/4 colony from actively growing mycelia of a 9 mm diameter petri dish and incubated at 25 °C until mycelium fully colonised.

2.2.6 Cultivation Substrate

The compost was prepared using the outdoor composting method, including 25 days of phase I and 7 days of phase II, totalling 32 days. The formulation used had a dry weight of 1,080 kg of *Oryza sativa*, 5.5% of rice bran, 1.1% of urea, 2.2% calcium oxide, and 2.2% gypsum. The bulk materials (*O. sativa* straw and rice bran) were moistened for 9 days and rotated every 2 days. The concentrated materials (urea, calcium oxide, and gypsum) were added after each turning operation throughout the composting phase I.

The casing mixture used contains 15% peat, 23% limestone, 37% fine sand, and 25% soil, as recommended by Zied et al. (2011a). When the mycelia were fully developed, the compost was pressed and levelled to facilitate the addition of the casing layer to a height of 5 cm. After casing, the trays were watered once a day. The mushroom production was carried out with four replicates trays (Royse, 2010; Llarena-Hernández et al., 2011).

2.2.7 Conditions for Fructification

Four trays filled with 5 kg of compost were inoculated with 5% spawn and incubated for 30 days in a grow room at 25 °C with 90% relative humidity. Then 5 cm of casing layer was added, and the trays were left under the same environmental conditions for a 7 day (post incubation period). The grow room was then set at 20 °C with 80% humidity. Time for mushroom forming was the number of days between casing and the first picking. The numbers and fresh weight of basidiomata were recorded until 65 days after casing. The experiments were performed according to a completely randomized design with four replicates per strain.

2.2.8 Investigation of the Secondary Metabolite Production

The production of secondary metabolites in submerged cultures was examined in strain *A. campestroides* (MFLUCC 14-1024) and *A. flocculosipes* (MFLUCC 14-1026) using four different media: yeast malt extract medium (YM), sugar malt extract

medium (ZM), cotton seed meal medium (Q6 ½), and mannitol salt medium (MMK). The mycelium was inoculated in 100 mL of each medium in 250-mL Erlenmeyer flasks at 24 °C and placed on a 140-rpm rotary shaker. After 5 days following the inoculation, the free glucose was measured with glucose test strips daily until the free glucose was consumed and the pH was checked with a pH meter (method adapted from Kuhnert et al. 2014). To qualitatively analyse the produced metabolites, an ethyl acetate extraction procedure was used for mycelia and submerged culture supernatant. Liquid media and biomass from liquid cultivation on different media were separated by filtration. Liquid media were discarded due to the lack of compounds. Each mycelium was extracted with acetone (200 mL) in an ultrasonic bath at room temperature for 30 min. After, the crude extract was filtered and redissolved in deionized water (100 mL), then partitioned with ethyl acetate (1 × 100 mL). The ethyl acetate layers were dried over anhydrous Na_2SO_4 and evaporated to dryness (for the yields see Table 2). All extracts were prepared to 1 mg/mL and subjected to analytical HPLC [Agilent 1260 Infinity with diode array detector and C18 Acquity UPLC BEH column (2.1 × 50 mm, 1.7 µm) from Waters; solvent A: deionized water (Milli-Q, Millipore, Schwalbach, Germany) + 0.1% formic acid, solvent B: acetonitrile + 0.1% formic acid, gradient system: 5% B for 0.5 min increasing to 100% B in 19.5 min, maintaining 100% B for 5 min, flow rate = 0.6 mL min^{-1}, UV detection [190−600 nm], coupled to an ion trap MS (amaZon speed™, Bruker). Mass spectrometry (MS) and ultraviolet (UV) data of the crude extracts were analysed and compared with the literature data using substance databases (CRC Dictionary of Natural Products, CAS SciFinder, Wiley-VCH Antibase).

Blazeispirols A (1) and D (2) were identified by HPLC-MS comparison (MS, UV/Vis, t_R) with an authentic sample (for detailed data see in supporting information; SI).

2.2.9 Statistical analysis

The optimum growth parameters and mushroom production data were subjected to statistical analysis. The mycelia growth values for growth rate, medium type, biomass, temperature, and pH optimization were compared to obtain a mean separation using Tukey's test ($p<0.05$), followed by post hoc tests. The results are expressed in a

one-way analysis of variance (ANOVA) analysis using the SPSS program version 19 (IBM Corp.).

2.3 Secondary Metabolites of *Phlebopus* from Northern Thailand

2.3.1 Fungal Material

Basidiomes of *Phlebopus portentosus* were bought from Pa Daet Market (Chiang Rai Province, Thailand) (22/05/2016, leg./det. B. Chuankid). A voucher specimen was deposited in the Herbarium of Mae Fah Luang University (MFLU16-2208). Basidiomes of *P. spongiosus* were collected around Mae Fah Luang University campus (Chiang Rai Province, Thailand) (30/04/2018, leg./det. B. Chuankid). A voucher specimen was deposited in the Herbarium of Mae Fah Luang University (MFLU18-1760).

2.3.2 Tissue Cultures of *P. portentosus* and *P. spongiosus*

Small tissue explants (about 3 × 3 × 3 mm) were cut with a scalpel from fracture planes made by band cleavage of clean basidiomes of *P. portentosus* and *P. spongiosus* and transferred to potato dextrose (PDA) and malt extract agar (MEA), respectively. The living cultures of *P. portentosus* (MFLUCC-T19–0088) and *P. spongiosus* (MFLUCC-T19-0091) were deposited in the Mae Fah Luang culture collection (MFLUCC) and periodically transferred.

2.3.3 Molecular Phylogenetic Analyses

Three DNA regions, ATP synthase subunit 6 (ATP6), DNA directed RNA polymerase II largest subunit (RPB2) and translation elongation factor 1-alpha (TEF1), were amplified for both isolates by polymerase chain reaction (PCR) following published protocols (Raspé et al., 2016; Chuankid et al., 2019). For the amplification of RPB2 and TEF1, the protocol was slightly modified with the use of JumpStart Taq ReadyMix (Sigma-Aldrich). Amplification of RPB2 was performed in 25-μL reactions containing 12.5-μL JumpStart Taq ReadyMix, 0.3 μM of forward and reverse primers, and 0.75 M betaine (B0300 Sigma-Aldrich, Germany). For TEF1, amplification was performed in 40-μL reactions containing 20-μL JumpStart Taq ReadyMix, 0.3 μM of

forward and reverse primers. The PCR products were purified by EZ-10 spin column purification kit (BIO BASIC) and sequenced by HZI in house sequencing service. The sequences were submitted to GenBank. A list of fungal strains studied and species descriptions are provided.

2.3.4 Investigation of the Secondary Metabolite Production

2.3.4.1 General experimental procedures

UV/Vis spectra were recorded using a Shimadzu UV−2450 UV/Vis spectrophotometer. NMR spectra were recorded on a Bruker Avance III 700 spectrometer with a 5-mm TXI cryoprobe ($^{1}H/^{13}C$ NMR: 700 MHz/176 MHz) and a Bruker Avance III 500 ($^{1}H/^{13}C$NMR: 500MHz/126MHz) spectrometer. Chemical shifts are reported in ppm using the solvent as an internal standard [$(CD_3)_2CO$ (^{1}H at 2.05 ppm; ^{13}C at 29.84 ppm), CD_3OD (^{1}Hat 3.31 ppm; ^{13}C at 49.0 ppm); CD_3CN (^{1}H at 1.94 ppm; ^{13}C at 1.32 ppm)] (Gottlieb et al., 1997).

HPLC-MS analyses (in both, the positive and negative ESI mode) were performed on an Agilent 1260 Infinity Systems instrument with a diode array detector and a Waters C18 Acquity UPLC BEH column (2.1 mm × 50 mm, 1.7 μm) using the following gradient system. Gradient A: Deionized water (Milli-Q, Millipore, Schwalbach, Germany) with 0.1% formic acid (FA; solvent A); acetonitrile with 0.1% FA (solvent B), gradient: 5% B for 0.5 min increasing to 100% in 19.5 min and then maintaining 100% B for 5 min, flow rate 0.6 mL/min. UV/Vis detection was conducted at λ = 200– 600 nm combined with an ion trap MS (Amazon Speed, Bruker).

HR-LC-ESI-MS and HR-ESI-MS/MS spectra were recorded with an Agilent 1200 series HPLC-UV system with a Waters C18 Acquity UPLC BEH column (2.1 mm× 50 mm, 1.7 μm) using gradient A. UV/Vis detection was conducted at λ = 200–600 nm combined with ESI-TOF-MS (Maxis, Bruker), scan range 100–2500 m/z, capillary voltage 4500 V, and dry temperature 200 °C.

Preparative RP HPLC was performed on a PLC 2020 from Gilson equipped with a Macherey-Nagel VP Nucleodur 100-5 C18 ec column (250 mm × 40 mm, 7 μm) used as a stationary phase with the following gradient programs. Gradient B: Deionized water (Milli-Q, Millipore, Schwalbach, Germany) with 0.1% TFA (Trifluoroacetic acid; solvent A) and acetonitrile with 0.1% TFA (solvent B) were used as mobile phase.

Elution gradient: 3% solvent B increased to 60% in 55 min, then 60 to 100% solvent B in 15 min, and finally isocratic conditions at 100% solvent B for 10 min. The flow rate was 40 mL/min, and UV detection was carried out at λ = 210 and 380 nm. Gradient C: Deionized water (Milli-Q, Millipore) with 0.1% formic acid (FA; solvent A) and acetonitrile with 0.1% FA (solvent B) were used as mobile phase. Elution gradient: 3% solvent B increased to 50% in 30 min, then 50 to 100% solvent B in 10 min, and finally isocratic conditions at 100% solvent B for 10 min. The flow rate was 40 mL/min and UV detection was carried out at λ = 250 and 300 nm. Gradient D: Deionized water (Milli-Q, Millipore) with 0.1% FA (solvent A) and acetonitrile with 0.1% FA (solvent B) were used as mobile phase. Elution gradient: 3% solvent B increased to 60% in 50 min and finally isocratic conditions at 100% solvent B for 10 min. The flow rate was 20 mL/min, and UV detection was carried out at λ = 250, 300, and 350 nm. Moreover, the separation was performed on a MZ Analysentechnik Kromasil 100–5 C18 column (20 × 250 mm, 7 μm) using the following gradient. Gradient E: Deionized water (Milli-Q, Millipore) with 0.1% FA (solvent A) and acetonitrile with 0.1% FA (solvent B) were used as mobile phase. Elution gradient: 3 to 45% solvent B in 60 min, then 45 to 100% solvent B in 5 min, and isocratic conditions at 100% solvent B for 5 min. The flow rate was 30 mL/min and UV detection was carried out at λ = 210 and 280 nm. Analytical TLC was performed on silica gel 60 F254 aluminum foils (Merck). Chemicals and solvents were obtained from AppliChem GmbH, Avantor Performance Materials, Carl Roth GmbH & Co. KG, and Merck KGaA in analytical and HPLC grades. Samples of atromentic acid (3), variegatic acid (5), and variegatorubin (9) originating from previous work in Steglich's group (LMUMunich), were kindly provided by the Department of Bioorganic Chemistry, Halle, and used as reference compounds for HR-LC-ESI-MS measurements and co-injection.

2.3.4.2 Small-scale liquid culture

Both *Phlebopus* were cultivated in five different liquid media: biotin medium (BAF), maltose medium (MGP), mannitol salt medium (MMK), yeast-malt medium (YM 5.5), and cotton seed medium (ZM 1/2); for the media compositions. For establishing the liquid cultivation of *P. portentosu*s and *P. spongiosus*, a well grown culture from a PDA was cut into small pieces using a cork borer (7 mm), and five pieces were transferred to 250-mL Erlenmeyer flasks containing 100-mL media. The cultures

were incubated on a rotary shaker (140 rpm) at 24 °C for 23–40 days. The growth of the mycelia was monitored by constantly checking the amount of free glucose using Medi-test Glucose (Macherey-Nagel). The liquid cultivations were terminated three days after glucose depletion. HR-LC-ESI-MS dereplication was carried out by comparing the masses of the detected peaks and their molecular formulas obtained from HR-ESI-MS measurements with those reported in the Dictionary of Natural Products (http://dnp.chemnetbase.com).

2.3.4.3 Scale-up of liquid culture

HR-LC-ESI-MS results indicated that similar metabolites were produced in all media since YM 5.5 medium produced the highest amounts of interesting secondary metabolites (compounds 1 and 2), it was used in the scale-up process. A well-grown PDA plate of mycelial culture from *P. spongiosus* was cut into small pieces using 7-mm cork borer and five pieces inoculated into 25 sterile flasks (500 mL) containing YM 5.5 medium (200 mL). The cultures were incubated on a rotary shaker (140 rpm) at 24 °C for 30 days.

2.3.4.4 Preparation of the extracts

Liquid media and biomass from small-scale liquid cultivation on different media were separated by filtration. Each liquid medium was partitioned with ethyl acetate (1 × 100 mL). The light-yellow organic layers were dried over anhydrous Na_2SO_4 and evaporated to dryness in vacuo. Each mycelium was extracted with acetone (200 mL) in an ultrasonic bath at room temperature for 30 min, filtered, redissolved in deionized water (100 mL), and partitioned with ethyl acetate (1 × 100 mL). The ethyl acetate layers were dried over anhydrous Na_2SO_4 and evaporated to dryness.

Liquid media and biomass from the large-scale liquid cultivation of *P. spongiosus* on YM 5.5 medium were separated by vacuum filtration. To the liquid medium 10% Amberlite XAD™ 16 N absorbent (Rohm & Haas Deutschland GmbH, Frankfurt am Main, Germany) was added and shaken for 4 h. The Amberlite resin was recovered by filtration and eluted with acetone (4 × 400 mL). The resulting extract was evaporated to dryness and redissolved in deionized water (100 mL) and partitioned with ethyl acetate (3 × 100 mL). The organic layer was dried over anhydrous Na_2SO_4, evaporated to dryness, and afforded 1.8-g crude extract. The mycelium was ultrasonicated for 30 min with acetone (4 × 400 mL). The extracts were combined,

evaporated to dryness, and redissolved in deionized water (200 mL). The water phase was partitioned with ethyl acetate (3 × 400 ml). The combined organic layers were filtered, dried over anhydrous Na_2SO_4, evaporated to dryness, and afforded 0.9 g of a brown crude extract.

2.3.4.5 Isolation of compounds 1–4 and 6

The lipophilic components of the extract from large-scale liquid cultivation of *P. spongiosus* mycelium in YM 5.5 were removed by MeOH/*n*-heptane (1:1) partition. The methanol layer (0.6 g) was fractionated on Sephadex LH-20 (Pharmacia) (solvent MeOH: dichloromethane 1:1; 33 × 820 mm; flow rate 3.4 mL/min). Sixty-seven fractions were collected according to the observed bands (F1–F67). Fractions F41–67 were combined and purified by preparative RP HPLC (gradient B) and provided compounds 1 (t_R 48.5 min, 2.7 mg), 3 (t_R 42.5 min, 20.3 mg), and 4 (t_R 38.5 min, 40.1 mg). Fractions F4–25 were combined and purified by preparative RP HPLC (gradient C) resulting in compound 2 (4.0 mg, t_R 28.5 min). Compound 6 (0.4 mg, t_R 43.5 min) was isolated from fractions F26–37 by preparative RP HPLC (gradient D).

2.3.4.6 Isolation of compounds 5, 7, and 8

HR-LC-ESI-MS measurements (in both positive and negative modes) of the crude extracts from small-scale cultivation indicated that *P. portentosus* in MMK medium produced the highest amounts of compounds 5, 7, and 8 (Table 2). Therefore, crude extract (0.09 g) from small-scale liquid cultivation of *P. portentosus* mycelium in MMK medium was dissolved in MeOH and purified with a SPME Strata-X 33 u Polymeric RP cartridge (Phenomenex, Aschaffenburg, Germany) by using H_2O (6 mL), H2O/acetonitrile (1:1, v/v, 6 mL) and acetonitrile (6 mL) as eluents. After combining the three fractions and evaporation of the solvents, the residue (0.05 g) was redissolved and separated by preparative RP HPLC (gradient E) and afforded compounds 5 (1.0 mg, t_R 25.5 min), 7 (7.5 mg, t_R 38.5 min), and 8 (3.6 mg, t_R 45.5 min), respectively.

9’-Hydroxyphenyl pulvinone (1) Yield 2.7 mg, orange-yellow solid, R_f = 0.44 (CH_2Cl_2: MeOH, 6: 4); UV/Vis (MeOH): λ_{max} (log ε) = 245 (4.09), 386 (4.22) nm; analytical HPLC (t_R) = 7.66 min; HR-ESI(+)-MS: *m*/*z* (%) = 799.1789 (6) $[2\ M+\ Na]^+$ ($C_{46}H_{32}NaO_{12}$ cald. for 799.1786), 777.1973 (0.6) $[2\ M+\ H]^+$ ($C_{46}H_{33}O_{12}$ cald. for 777.1967), 411.0841 (19) [M + Na] + ($C_{23}H_{16}NaO_6$, cald. for 411.0839), 389.1020 (100) $[M+\ H]^+$ ($C_{23}H_{17}O_6$, cald. for 389.1020); HR-ESI(+)-MS/MS (precursor ion *m*/*z*

389.1024, 34.6 eV): *m*/*z* (%) = 371.0921 (45) $[M + H–H_2O)]^+$ ($C_{23}H_{15}O_5$, cald. for 371.0921), 325.0864 (100) $[M + H–H_2O\text{-}CO]^+$ ($C_{22}H_{13}O_3$, cald. for 325.0859), 297.0915 (79) ($C_{21}H_{13}O_2$, cald. for 297.0910); ^1H and ^{13}C NMR data see Table 1.

Phlebopyrone (2) Yield 4.0 mg, colorless solid, R_f = 0.53 (CH_2Cl_2: MeOH, 6: 4); UV/Vis (MeOH): λ_{max} (log ε) = 245 (4.15), 328 (3.47) nm; analytical HPLC (t_R) = 5.03 min; HR-ESI(+)-MS: *m*/*z* (%) = 615.1264 (5) $[2 M + Na]^+$ ($C_{34}H_{24}NaO_{10}$, cald. for 615.1262), 593.1440 (1) $[2 M + H]^+$ ($C_{34}H_{25}O_{10}$, cald. for 593.1442), 319.0576 (20) $[M + Na]^+$ ($C_{17}H_{12}NaO_5$, cald. for 319.0577), 297.0754 (100) $[M + H]^+$ ($C_{17}H_{13}O_5$, cald. for 297.0758); HR-ESI(+)-MS/MS (precursor ion *m*/*z* 297.0775, 35.0 eV): *m*/*z* (%) = 251.0718 (12) $[M + H–H_2O–CO]^+$ ($C_{16}H_{11}O_3$, cald. for 251.0703), 223.0766 (100) $[M + H–CO–CO\text{-}H_2O]^+$ ($C_{15}H_{11}O_2$, cald. for 223.0754), 175.0399 (45) ($C_{10}H_7O_3$, cald. for 175.0390), 147.0446 (83) ($C_9H_7O_2$, cald. for 175.0390); ^1H and ^{13}C NMR data see Table 1.

Atromentic acid (3) Yield 20.3 mg; orange-yellow solid (for detailed data see SI). Identical in all aspects (NMR, MS, TLC, HPLC-coinjection) with an authentic sample.

Xerocomic acid (4) Yield 40.1 mg; orange-yellow solid (for detailed data see SI). NMR chemical shifts are comparable with those reported (Steglich et al., 1974; Ahmed & Langer, 2005).

Variegatic acid (5) Yield 1 mg; orange-yellow solid (for detailed data see SI). Identical in all aspects (NMR, MS, TLC, HPLC-coinjection) with an authentic sample.

Methyl atromentate (6) Yield 0.4 mg, orange-yellow solid. (for detailed data see SI). NMR chemical shift values are comparable with those reported (Murr et al., 2006).

Methyl isoxerocomate (7) Yield 7.5 mg, orange-yellow solid (for detailed data see SI). NMR chemical shifts are comparable with those reported (Gruber et al., 2014).

Methyl variegatate (8) Yield 3.6 mg, orange-yellow solid (for detailed data see SI). NMR chemical shifts are comparable with those reported (Edwards, 1977).

Variegatorubin (9) Identified by HR-LC-MS and HPLC coinjection with an authentic sample (for detailed data see SI).

2.3.5 Antimicrobial activity and cytotoxicity assays

2.3.5.1 Minimum inhibitory concentrations (MIC)

Compounds 1–4 and 6–8 were tested against several bacterial and fungal strains by using a 96-well serial dilution technique in Mueller-Hinton broth (MHB) media for bacteria and YMG media for filamentous fungi and yeasts as previously described (Becker et al., 2020). The selected organisms represent a broad spectrum of pathogens of clinical interest, as well as sensitive indicator strains, to discover new anti-infectives (bacteria): *Bacillus subtilis*, *Chromobacterium violaceum*, *Escherichia coli*, *Micrococcus luteus*, *Mycolicibacterium smegmatis*, *Pseudomonas aeruginosa*, *Staphylococcus aureus*; fungi: *Mucor hiemalis*, *Pichia anomala*, *Rhodotorula glutinis*, *Candida albicans*, and *Schizosaccharomyces pombe*). The compounds were redissolved in MeOH (1 mg/mL), diluted to a final concentration range of 66.7 to 0.52 µg/mL and incubated with the test organisms overnight. MeOH was used as negative control. Kanamycin (1.0 mg/mL; 2 µL), gentamicin (1.0 mg/mL; 2 µL), nystatin (1.0 mg/mL; 20 µL), and oxytetracycline (1.0 mg/mL; 2 µL [*C. violaceum*, *E. coli*, *M. luteus*, *S. aureus*] and 20 µL [*B. subtilis*]) were used as positive controls against tested organisms. Compound 5 was not tested because of the low yield.

2.3.5.2 In vitro cytotoxicity (IC_{50}) assays

The evaluation of in vitro cytotoxicity (IC_{50}) was performed with mouse fibroblast cell line L929 and mammalian HeLa KB3.1 cancer cells for compounds 1–4, and 6–8, as previously described (Becker et al., 2020). If an inhibition of cell viability with an IC50 < 50 µM was observed, further cell lines were tested: human ovarian carcinoma (SKOV-3 [compounds 4, 8]), human prostate cancer (PC-3 [compounds 4, 8]), human lung carcinoma tissue (A549 [compounds 4, 8]), human skin squamous cell carcinoma (A431 [compounds 4, 8]), and human breast adenocarcinoma (MCF-7 [compounds 1, 4, 8]). The compounds were dissolved in MeOH (1 mg/mL) which was used as negative control in this study; epothilone B (1 mg/mL) was used as positive control. After incubating the cell lines with a serial dilution of the test compounds (final range from 37 to 0.6×10^{-3} µg/mL) for five days, the cells were dyed using 3-(4,5-dimethyl-2-thiazolyl)-2,5-diphenyl-2H-tetrazolium bromide (MTT), which is only converted to its purple formazan derivative by living cells. The absorption at 595 nm was measured using a microplate reader to calculate the percentage of cell viability.

Results were expressed as IC_{50}, the half maximal inhibitory concentration (μM). Compound 5 was not tested because of the low yield.

2.3.5.3 Nematicidal assay

Caenorhabditis elegans AB1 was used for nematicidal activity of compounds 3 and 4. The nematodes were cultured on nematode agar [soypeptone 2 g, NaCl 1 g, agar 20 g, 1000 mL of deionized water; adding 0.5 mL of cholesterol (1 mg/mL EtOH), 1 mL of 1 M $CaCl_2$, 1 mL of 1 M $MgSO_4$, and 12.5 mL of 40 mM potassium phosphate buffer after autoclaving; pH adjusted to 6.8 with living *E. coli* DSM498, at 20 °C for a week, was assessed according to our previously reported protocol (Phukhamsakda et al., 2019). The compounds were dissolved in MeOH (1 mg/mL) of five different concentrations of each compound as 100, 50, 25, 12.5, and 6.25 μg/mL. Ivermectin (1.0 μg/mL) and methanol were used as positive and negative control, respectively. The plates were incubated at 20 °C in the dark, and nematicidal activity was recorded after 18 h of incubation and expressed as an LD_{50}.

2.3.5.4 Biofilm inhibition

Compounds 3 and 4 were evaluated in a biofilm inhibition assay against *Staphylococcus aureus* DSM 1104. *S. aureus* from −20 °C stock was incubated in 20 mL CASO (caseinpeptone soymeal-peptone medium) at 37 °C on a rotary shaker (100 rpm) for 16 h. The cell concentration was adjusted to match the turbidity of 0.5 McFarland standard. The assay was performed in 96-well flat bottom plates (Falcon™ Microplates, USA) as previously described (Chepkirui et al., 2018). The tested compounds were dissolved in MeOH (5mg/mL), diluted to a final range of 250 to 15.6 μg/mL and incubated with the *S. aureus* at 37 °C for 24 h. All experiments were carried out in duplicates and microporenic acid A (5 mg/ mL, 15 μL) was used as standard, MeOH was used as negative control (15 μL). The cells were dyed with crystal violet and the absorption was measured at $\lambda = 550$ nm using a microplate reader to calculate the percentage of inhibition.

CHAPTER 3

RESEARCH RESULTS

3.1 Taxonomy and Phylogeny of *Phylloporus*

3.1.1 DNA Sequence Analyses

A total of 62 new sequences were generated and deposited in GenBank (Table 3.1). The alignment contained 30 taxa and was 2632 characters long (TreeBase number 23073). From the BLAST results of ITS1 + ITS2 sequences, our new *Phylloporus* were identical or related to the undescribed *Phylloporus* that were reported by Zeng et al. (2013) (Table 3.2). The ITS sequences of *P. pusillus* showed relatively low similarity to *P.* sp. 6 (92.1–92.5%). The ITS sequences of *P. subbacillisporus* showed high similarity to *P.* sp. 4 (99.8–100%), indicating that *P.* sp. 4 is likely conspecific with *P. subbacillisporus*. The ITS sequence of *P. subrubeolus* showed high similarity to *P.* sp. 7 (99.8%) (Table 3.2), which also suggests conspecificity. In the phylogenetic tree obtained with the multi-gene DNA sequence dataset (*atp6*, *tef1* and *rpb2*), *P. pusillus* and *P. subrubeolus* are grouped together with 100% bootstrap support and posterior probability of 1. In our phylogenetic tree, those two species shared a sister relationship with *P. rubeolus*, although it is likely that the most closely related species is the recently described *P. pruinatus* (Zhao et al., 2018), for which only an ITS sequence was available to us and was, therefore, not included in the phylogeny. *P. subbacillisporus* grouped in a well-supported clade with *P.* sp. (OR0896), *P.* sp. (OR0989) and *P. pelletieri*, the type species of the genus (BS = 100, PP = 1).

Table 3.1 List of collections used for DNA analyses with origin, GenBank accession numbers and references.

Species	Voucher	Origin	*atp*6	*tef*1	*rpb*2	References
Phylloporus attenuatus	HKAS76168	Bangladesh	–	KR094791	KR094787	Hosen et al. 2017
Phylloporus aff. *bellus*	REH7733	Costa Rica	MH580777	–	–	This study
Phylloporus aff. *bellus*	OR0473	China	MH580778	MH580798	MH580818	This study
Phylloporus bellus	HKAS56763	China	MH671296	JQ967153	–	Zeng et al. 2013, This study
Phylloporus brunneiceps	OR0050	Thailand	KT823968	KT824034	KT824001	Raspé et al. 2016
Phylloporus castanopsidis	OR0052	Thailand	KT823969	KT824035	KT824002	Raspé et al. 2016
Phylloporus castanopsidis	BC074	Thailand	MH580779	MH580799	MH580819	This study
Phylloporus imbricatus	HKAS68642	China	–	KF112299	KF112786	Zeng et al. 2013
Phylloporus luxiensis	HKAS75077	China	–	KF112298	KF112785	Zang et al. 1978
Phylloporus maculatus	HKAS59730	China	–	JQ967194	JQ678700	Zeng et al. 2013
Phylloporus maculatus	OR0285	China	MH580780	MH580800	MH580820	This study

Table 3.1 (continued)

Species	Voucher	Origin	*atp*6	*tef*1	*rpb*2	References
Phylloporus pelletieri	WU18746	Austria	MH580781	MH580801	MH580821	This study
Phylloporus pusillus	OR0484	China	MH580782	MH580802	MH580822	This study
Phylloporus pusillus	OR1158	Thailand	MH580783	MH580803	MH580823	This study
Phylloporus pusillus	OR1310	Thailand	MH580784	MH580804	MH706703	This study
Phylloporus rhodoxanthus	WU17978	Austria	MH580785	MH580805	MH580824	This study
Phylloporus rubeolus	OR0251	China	MH580786	MH580806	MH580825	This study
Phylloporus rubiginosus	BC063	Thailand	MH580787	MH580807	MH580826	This study
Phylloporus rubiginosus	OR0169	China	MH580788	MH580808	MH580827	This study
Phylloporus subbacillisporus	OR0436	China	MH580792	MH580812	MH580831	This study
Phylloporus subrubeolus	BC022	Thailand	MH580793	MH580813	MH580832	This study
Phylloporus subrubeolus	OR0612	Thailand	MH580794	MH580814	MH580833	This study

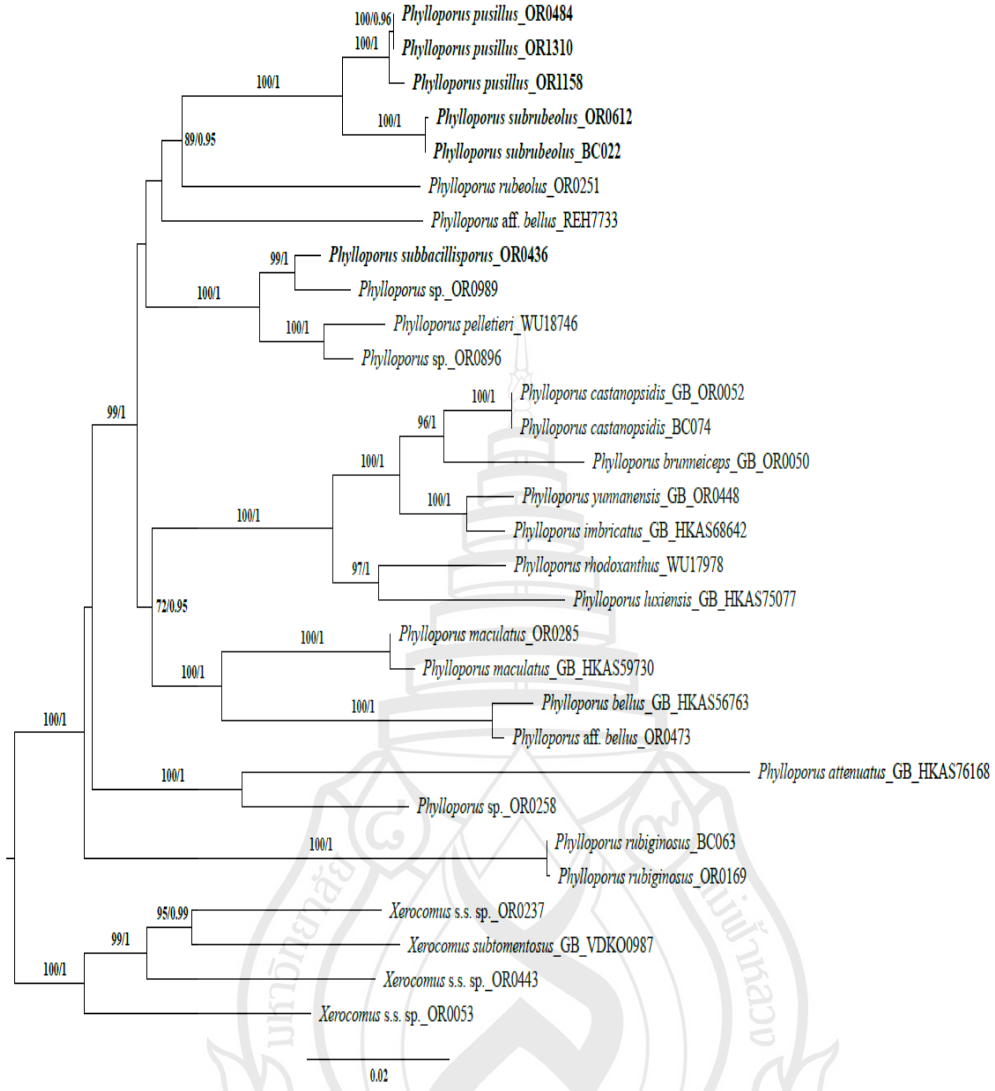
Table 3.1 (continued)

Species	Voucher	Origin	*atp*6	*tef*1	*rpb*2	References
Phylloporus yunnanensis	OR0448	China	MG212554	MG212598	MG212640	Vadthanarat et al. 2018
Phylloporus sp.	OR0258	China	MH580789	MH580809	MH580828	This study
Phylloporus sp.	OR0896	Thailand	MH580790	MH580810	MH580829	This study
Phylloporus sp.	OR0989	Thailand	MH580791	MH580811	MH580830	This study
Xerocomus subtomentosus	VDKO0987	Belgium	MG212572	MG212614	MG212657	Vadthanarat et al. 2018
Xerocomus s.s. sp.	OR0053	Thailand	MH580795	MH580815	MH580834	This study
Xerocomus s.s. sp.	OR0237	China	MH580796	MH580816	MH580835	This study
Xerocomus s.s. sp.	OR0443	China	MH580797	MH580817	MH580836	This study

Table 3.2 GenBank BLAST searches results of ITS1+ITS2 sequences of *Phylloporus* species from this study

Collections	Voucher, GB accession no.	Most similar ITS1+ITS2 sequences in GenBank	ITS1	ITS2	ITS1+ ITS2	Species name	Voucher	Locality	References
Phylloporus pusillus	OR0484, MH686275	JQ967278, I=92.5%, QC=95%	164/173	286/313	450/486	*Phylloporus* sp.6	HKAS 74687	Yunnan, China	Zeng et al. 2013
Phylloporus pusillus	OR1158, MH686278	JQ967278, I=92.5%, QC=95%	164/173	286/313	450/486	*Phylloporus* sp.6	HKAS 74687	Yunnan, China	Zeng et al. 2013
Phylloporus pusillus	OR1310, MH686279	JQ967278, I=92.1%, QC=95%	162/173	286/313	448/486	*Phylloporus* sp.6	HKAS 74687	Yunnan, China	Zeng et al. 2013
Phylloporus subbacillisporus	OR0436, MH686274	JQ967273, I=100%, QC=100%	213/213	304/304	517/517	*Phylloporus* sp.4	HKAS 74682	Yunnan, China	Zeng et al. 2013
Phylloporus subrubeolus	OR0612, MH686276	JQ967279, I=99.8%, QC=100%	175/175	326/327	501/502	*Phylloporus* sp.7	HKAS 74688	Yunnan, China	Zeng et al. 2013
Phylloporus sp.	OR0989, MH686277	JQ967273, I=98.2%, QC=100%	211/218	285/287	496/505	*Phylloporus* sp.4	HKAS 74682	Yunnan, China	Zeng et al. 2013

Note (I = Identity and QC = Query Cover).



Note Maximum likelihood phylogenetic tree inferred from the three-gene dataset (*atp*6, *rpb*2, *tef*1), including *Phylloporus pusillus*, *P. subbacillisporus*, and *P. subrubeolus* and selected *Phylloporus*. The three *Xerocomus* were used as outgroup taxa. Bootstrap frequencies ≥70% and posterior probabilities ≥0.95 are shown above supported branches. The prefix "GB" before voucher numbers indicates that sequences were retrieved from GenBank.

Figure 3.1 Maximum likelihood phylogenetic tree inferred from the three-gene dataset (*atp*6, *rpb*2, *tef*1) of *Phylloporus*

3.1.2 Taxonomy

Phylloporus pusillus Raspé, K.D. Hyde & Chuankid, Mycol. Progr. 18(5): 605, 2019
MycoBank number: MB 827266, Facesoffungi number: FoF 04842.
Etymology: *pusillus* refers to the (very) small size of the basidiomata.
Holotype: Thailand. Chiang Mai Province, Meuang District, Doi Suthep-Pui National Park, N18°48.6′–E98°53.5′, elev. 1450 m, 14/07/2016, O. Raspé, OR1310 (CMUB!, holotype; BR!, isotype).

Basidiomata small. *Pileus* 1–2 cm broad, convex to planoconvex, never depressed at centre; reddish brown (8E7) to dark brown (9F8) at centre, gradually paler towards margin; surface dry, tomentose to velutinous; context off-white to yellowish white, reddish brown under the pellis, unchanging. ***Hymenophore*** lamellate, decurrent; lamellae thick, distant, ventricose, some forking to intervenose, mostly near the margin, yellowish white (4A2) when young, in age deeper yellow, with a reddish tinge near the edge, sometimes with reddish dots, staining absent; lamellar edge even. ***Stipe*** 1.5–3 cm long, 0.2–0.3 cm wide, mostly equal; surface dry upper half finely pustulate, light brown (6D8) to cinnamon (6D6), consistently darker near apex; lower half glabrous to subglabrous, champagne (4A4) to yellowish white (4A2), staining absent; context solid, yellowish white (4A2), staining absent. ***Basal mycelium*** white, with fine white rhizoids. ***Macrochemical*** *reactions*: not recorded.

Basidiospores [150/3/3] (7.9–)8.3–*9.3*–10.3(–11) × (4.1–)4.2–*4.7*–5.2(–5.5) µm, *Q* = (1.65–)1.78–*1.99*–2.21(–2.47), variable in shape, elliptical to subovoid, sometimes more fusoid, greenish grey (1C2) in 5% KOH, smooth when examined with light microscope, but bacillate ornamentation when examined with SEM (Fig. 8a–b). ***Basidia*** (30–)30–*35.2*–42(–42) × (7.3–)7.3–*8.8*–10.7(–10.8) µm, clavate, hyaline, 4-spored. ***Cheilocystidia*** (57–)57–*68*–84(84) × (12.1–)12.1–*15*–18(–18) µm, utriform to sublageniform. ***Pleurocystidia*** (60.6–)60.6–*75.2*–93.1(–93.1) × (7.1–)7.2–*13.6*–18.2(18.2) µm, numerous, subclavate to broadly clavate or utriform to sublageniform, without encrusting pigments. ***Hymenophoral trama*** 100–170 µm thick, regular, composed of 7–15 µm wide cylindrical, smooth, hyaline hyphae. ***Pileipellis*** an interwoven trichoderm; hyphae slightly constricted at septa; terminal cells 25–55 × 7–16 µm, cylindrical, granular content present and sometimes with cell wall encrustations (mostly on terminal cells) visible in aqueous Congo Red. ***Pileus trama*** hyaline, smooth

hyphae 8–13 µm wide. ***Stipitipellis*** 75–100 µm thick, parallel hyphae and caulocystidia (18–)18–*24.6*–33(–33) × (7.1–)7.2–*9.2*–11.2(–11.4) µm, clavate to capitate, hyaline, smooth. ***Stipe trama*** composed of parallel, cylindrical, hyaline hyphae 7.5–15 µm wide. ***Clamp connections*** absent in all tissues.

Habit, habitat and distribution: Solitary on litter-poor soil (e.g. path or road verges) in forests dominated by Fagaceae. Thailand and Yunnan province, China.

Additional materials examined: China. Yunnan province, Cangyuan, Banhongxiang, N23°18.6′–E99°05.3′, elev. 1050 m, 10/07/2012, O. Raspé & R. Zhao, OR0484 (HMAS 279878). Thailand. Chiang Mai province, Mae-on District, Baan Mae Lai, N18°53.1′–E99°21.9′, elev. 1080 m, 18/08/2015, O. Raspé & S. Vadthanarat, OR1158 (CMUB, BR).

Notes: *Phylloporus pusillus* is macro-morphologically characterised by its small-sized, convex, reddish brown to dark brown pileus, stipe consistently darker near apex, white basal mycelium and somewhat forking to intervenose lamellae that get deeper yellow to reddish in age. The most striking microscopic characters of the species are variable shape of the basidiospores (elliptical to subovoid, sometimes more fusoid) and the encrustations on the walls of pileipellis hyphae.

Phylloporus pusillus is most similar to the recently described *P. pruinatus* (Zhao et al., 2018), both sharing small basidiome size, similar colours and incrusted pileipellis cell walls, but the basidiospores of the latter are characterised by a higher *Q* (2.23 against 1.99 for *P. pusillus*). Moreover, according to the phylogenetic tree in Zhao et al. (2018), *P. Pruinatus* is the *P.* sp. 6 of Zeng et al. (2013), of which the ITS sequence is the most closely related to *P. pusillus* ITS sequence (Table 3.2), but with only 92% similarity. *P. subrubeolus* is also macroscopically somewhat similar, but *P. pusillus* can be distinguished by smaller basidiomata and lamellae becoming deeper yellow to reddish with age. Those two species also can be separated microscopically, with *P. pusillus* having basidiospores of variable shape and scattered encrusting pigment on the terminal cells of the pileipellis, whereas *P. Subrubeolus* does not show variation in basidiospore shape and has abundant encrustations on the pileipellis cells, even in sub-terminal cells. When compared with other similar species, including *P. colligatus* Neves & T.W. Henkel, *P. Pachycystidiatus* Zeng, Z. L. Yang & L.P. Tang and *P. rubeolus* Zeng, Z. L. Yang & L.P. Tang, the hymenophore of those species changes

colour (blue, brighter yellow) when injured, but this character was not found in *P. pusillus*. Also, *P. pusillus* is smaller than *P. pachycystidiatus* and *P. rubeolus*.

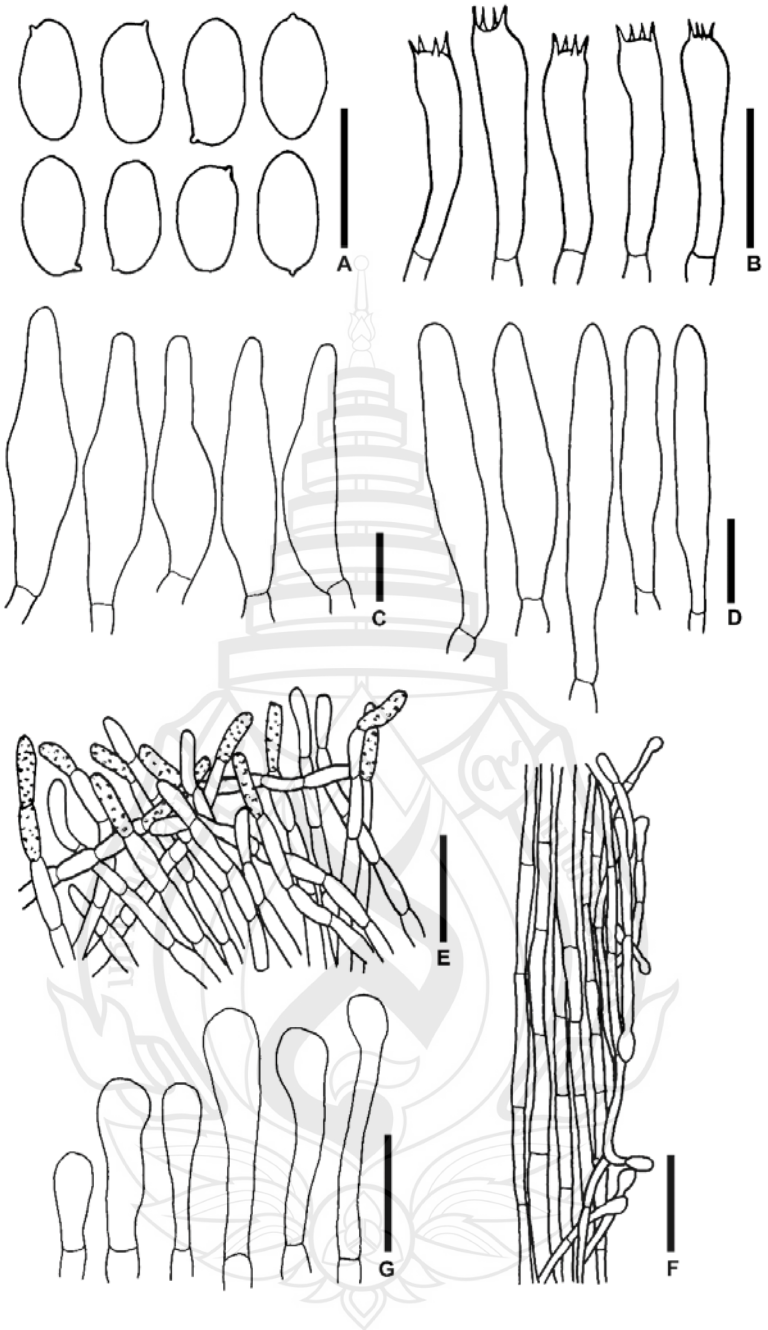
Spore shape is variable within a single basidiome of *P. pusillus*. Spores with two different shapes are also found in *P. bellus* (Massee) Corner and *P. dimorphus* Neves & R. E. Halling (Neves et al., 2012), but the encrustations on the pileipellis hyphae found in *P. pusillus* do not occur in either *P. bellus* or *P. dimorphus*.

The phylogenetic analyses showed a highly supported sister relationship with *P. subrubeolus* (BS = 100, PP = 1).



Note Basidiomata of *Phylloporus pusillus* (holotype, OR1310) in the field. a, b Photograph of basidiomata from upper and lower part. Scale bars = 1 cm.

Figure 3.2 Basidiomata of *Phylloporus pusillus*



Note Micro-morphological characters of *Phylloporus pusillus*. a Basidiospores. B Basidia. c Cheilocystidia. d Pleurocystidia. e Pileipellis. f Stipitipellis. g Caulocystidia. Scale bars: a = 10 μm; b–d, g = 20 μm; e, f = 50 μm. All drawings were made from the type (OR1310).

Figure 3.3 Micro-morphological characters of *Phylloporus pusillus*

Phylloporus subbacillisporus Raspé, K.D. Hyde & Chuankid, Mycol. Progr. 18(5): 608, 2019

MycoBank number: MB 827267; Facesoffungi number: FoF 04843.

Etymology: *subbacillisporus* refers to the very elongate, narrowly fusoid to subbacilliform basidiospores.

Holotype: China. Yunnan province, Nanjian County, Wuliangshan National Natural Reserve, N25°18.5′–E98°47.8′, elev. 1530 m, 03/07/2012, O. Raspé & R. Zhao, OR0436 (HMAS 279879).

Basidiomata small-sized. *Pileus* 2–4 cm broad, at first convex, with age plane or slightly depressed, when young brownish orange (5C6) to amber yellow near margin (4B6), with age brown (7E5); surface dry, tomentose sometimes cracking in age; context marmorate of greyish yellow (4B3) and white, slightly tough, inconstantly staining blue, then reddish with time. ***Hymenophore*** lamellate, adnate to slightly decurrent; lamellae subclose, ventricose, shallowly intervenose to somewhat anastomosing; lamellar edge entire; light yellow (3A4), staining blue, sometimes only weakly so, then reddish. ***Stipe*** 3.5–6.5 cm long, 0.5–1 cm wide, equal or somewhat tapering downward, dry; greyish to brownish orange (5B3 to 5C6), getting darker (7D5) with time when bruised; context solid, marmorate of greyish yellow (4B3) and white, unchanging when cut. ***Basal mycelium*** white. ***Odour*** fungoid, slightly rubbery. *Taste* fungoid, slightly astringent. ***Macrochemical reactions*** not recorded.

Basidiospores [60/1/1] (8.8–)9.2–*10.5*–11.9(–13.1) × (2.9–)3–*3.4*–3.7(–3.9) µm, *Q* = (2.70–)2.76–*3.12*–3.57(–3.89), narrowly fusoid to subbacilliform, greyish yellow (1B4) in 5% KOH, smooth when examined with light microscope, smooth or at most rugulose, never bacillate when examined with SEM (Fig. 8c–d). ***Basidia*** (30–)30–*34.5*–39(–39) × (8.5)8.6–*9.7*–11.1(–11.2) µm, clavate, hyaline in KOH, mostly 4-spored. ***Cheilocystidia*** (31–)31–*45.8*–60(–60) × (9.6–)9.7–*13.5*–18.3(–18.4) µm, subclavate to broadly clavate, hyaline when observed in 5% KOH. ***Pleurocystidia*** (26–)30–*58.7*–84(–84.5) × (11.7–)11.8–*15.1*–18.4(–18.5) µm, numerous on sides of lamellae, hyaline, subclavate to broadly clavate, some are septate. ***Hymenophoral trama*** 140–210 µm thick, subdivergent composed of 10–20 µm wide cylindrical hyphae. ***Pileipellis*** interwoven trichoderm, slightly constricted at septa, terminal cells

22–56 × 9–15 μm, cylindrical to slightly inflated, smooth, hyaline in KOH, granular content absent. ***Pileus trama*** smooth, hyaline hyphae 7–14 μm wide. ***Stipitipellis*** 75–150 μm thick, with parallel hyphae and caulocystidia (36.5–)36.5–*53.4*–73.3(–73.8) × (12.9–)12.9–*19*–26.3(–26.8) μm, clavate, hyaline, smooth. ***Stipe trama*** composed of parallel, cylindrical, hyaline hyphae, 7.5–15 μm wide. ***Clamp connections*** absent in all tissues.

Habit, habitat and distribution: Solitary to gregarious in forests dominated by Fagaceae. Yunnan province, China.

Notes: *Phylloporus subbacillisporus* is characterised by its small-sized basidiomata with a brown to brownish orange to amber yellow pileus, shallowly intervenose to somewhat anastomosing, adnate to only slightly decurrent lamellae that are variably bluing when injured and white basal mycelium. Microscopically, the most striking character is the elongate, narrowly fusoid to subbacilliform basidiospores, which are smooth to merely rugulose, never bacillate, under the SEM.

In the field, *P. subbacillisporus* is mostly similar to *P. catenulatus* Hosen & T.H. Li, with which it shares small to medium-sized basidiomata, intervenose to anastomosing, slightly decurrent lamellae that turn blue when injured and white basal mycelium (Hosen & Li, 2017). However, the pileus of *P. catenulatus* is dark red to reddish brown, whereas the pileus of *P. subbacillisporus* is paler, mostly brownish orange. Also, the basidiospores of *P. catenulatus* are not elongate like those of *P. subbacillisporus*.

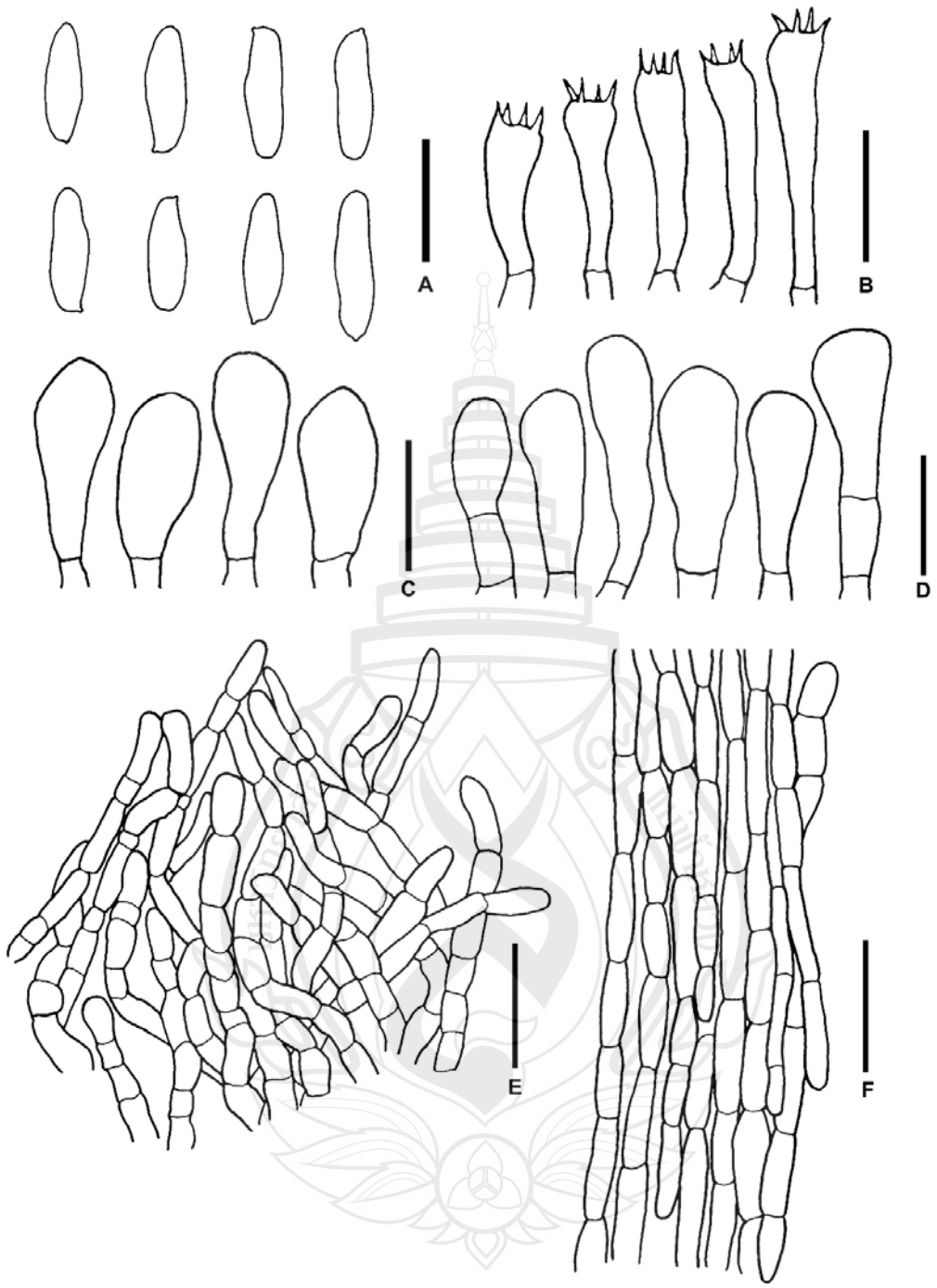
The basidiospores of *P. subbacillisporus* are distinct from all other species by their unusually high *Q* value and fusoid to subbacilliform shape and smooth or merely rugulose surface under the SEM. The latter character is shared with only few *Phylloporus* species, such as *P. alborufus* Neves & R. E. Halling and *P. centroamericanus* Singer & L.D. Gómez.

In the phylogenetic tree, *P. subbacillisporus* clustered with *P. pelletieri* and two yet undescribed species (OR0896 and OR0989) with high statistical supports (BS = 100, PP = 1). The ITS sequences of *P. subbacillisporus* showed 100% similarity to *P.* sp. 4 from China (Zeng et al., 2013), indicating that '*P.* sp. 4' is likely conspecific with *P. subbacillisporus*. Unfortunately, the specimens corresponding to those sequences were not made available to us for study.



Note Basidiomata of *Phylloporus subbacillisporus* (holotype, OR0436) in the field.

Figure 3.4 Basidiomata of *Phylloporus subbacillisporus*



Note Micro-morphological characters of *Phylloporus subbacillisporus*. A Basidiospores. b Basidia. c Cheilocystidia. d Pleurocystidia. e Pileipellis. F Caulocystidia. Scale bars: a = 10 μm; b–d = 20 μm; e, f = 50 μm. All drawings were made from the type (OR0436).

Figure 3.5 Micro-morphological characters of *Phylloporus subbacillisporus*

Phylloporus subrubeolus Chuankid, K.D. Hyde & Raspé, Mycol. Progr. 18(5): 609, 2019

MycoBank number: MB 827268, Facesoffungi number: FoF 04844.

Etymology: *subrubeolus* refers to the reddish brown pileus as well as to the close relationship with *P. rubeolus*.

Holotype: Thailand. Chiang Mai Province, Mae-on District, Mae Kam Pong, elev. 1300 m, 12/06/2016, Boontiya Chuankid, BC022 (MFLU16–2229).

Basidiomata small-sized. *Pileus* 2.5–3.5 cm broad, convex or plano-convex; lamellar edge entire; at centre brownish orange (6C8) abruptly paler to light orange (5A5) at margin; surface dry, velutinous or rimose, staining absent; context white, staining absent. ***Hymenophore*** lamellate, decurrent; lamellae subdistant with lamellulae, ventricose, intervenose to anastomosing, pastel yellow (1A4), staining absent. ***Stipe*** 3.5–5 cm long, 0.3–0.4 cm wide, mostly equal, dry; upper half finely pustulate, light orange (5A5); lower half venose light orange, staining absent; context solid, white, slightly blue at first, later become reddish orange (7A8). ***Basal mycelium*** white. ***Macrochemical reactions****:* with NH_4OH, browning on pileus and stipe.

Basidiospores [100/2/2] (6.9–)7.2–*8.4*–9.7(–10.8) × (4.2–)4.5–*5.2*–5.8(–6.2) µm, *Q* = (1.43–)1.49–*1.62*–1.81(–1.88), subovoid to elliptical, greyish yellow (1B3) in 5% KOH, smooth when examined with light microscope but with bacillate ornamentation when examined with SEM (Fig. 8e, f). ***Basidia*** (27.7–)27.8–*30.9*–33.8(–33.8) × (7.8–)7.9–*9.4*–10.5(–10.5) µm, clavate, hyaline, 4-spored. ***Cheilocystidia*** (47.5–)47.7–*66.4*–81(–81.1) × (12.1–)12.1–*15*–18.9(–18.9) µm, broadly clavate. ***Pleurocystidia*** (58.1–)58.8–*76*–91.7(–91.8) × (12.6–)12.7–*15.9*–19.3(–19.4) µm, utriform to sublageniform. ***Hymenophoral trama*** 125–250 µm thick, regular composed of 12–15 µm wide cylindrical, smooth, hyaline hyphae. ***Pileipellis*** interwoven trichoderm with terminal cells 24–52 × 9–13 µm, granular content present, with abundant cell wall encrustations pigment visible in aqueous Congo Red, also in sub-terminal cells. ***Pileus trama*** made of hyaline hyphae 10–25 µm wide. ***Stipitipellis*** 75–125 µm thick, with parallel hyphae and caulocystidia (27.0–)27.3–*49.6*–69.5(−69.7) × (12–)12–*16.1*–19.5(–19.5) µm, clavate, hyaline, smooth. ***Stipe trama*** parallel, cylindrical, hyaline hyphae 12.5–15 µm wide. ***Clamp connections*** absent in all tissues.

Habit, habitat and distribution: Solitary to gregarious on the ground in broad-leaved forest dominated by either Fagaceae or Dipterocarpaceae. Currently only known from Thailand.

Additionalmaterial examined: Thailand. Chiang Mai province, Meuang District, Doi Suthep-Pui National Park, N18°48.0′–E98°55.8′, elev. 720 m, 17/05/2015, O. Raspé, OR0612 (CMUB).

Notes: *Phylloporus subrubeolus* is characterised by its small-sized basidiomata, brownish orange to light orange pileus, intervenose to anastomosing lamellae and white basal mycelium. Microscopically, the abundant encrustations on the walls of the pileipellis hyphae and terminal cells, and the subovoid to elliptical basidiospores are the most important characters.

Phylloporus subrubeolus is most similar *P. pusillus*, based on macro-characters, but can be separated by the larger basidiomata, the stripe not darker near apex and the lamellae not getting reddish with age. Those two species also can be separated microscopically, with *P. subrubeolus* not showing variation in basidiospore shape. Moreover, the encrusted pigments in pileipellis of *P. subrubeolus* are abundant even in sub-terminal cells, but in *P. pusillus*, they are mostly found on the terminal cells. When compared with other similar species including *P. colligatus*, *P. pachycystidiatus* and *P. rubeolus*, the basidiomata of *P. subrubeolus* are larger than *P. colligatus* and the latter has pale yellow basal mycelium. Compared to *P. pachycystidiatus*, the hymenophore of *P. subrubeolus* does not stain when injured and has encrusted pigment in the pileipellis, but *P. pachycystidiatus* does not have those characters. For *P. rubeolus*, the pileus is larger than *P. subrubeolus*. Moreover, the hymenophore of *P. rubeolus* stains blue when injured, which was not seen in *P. subrubeolus*.

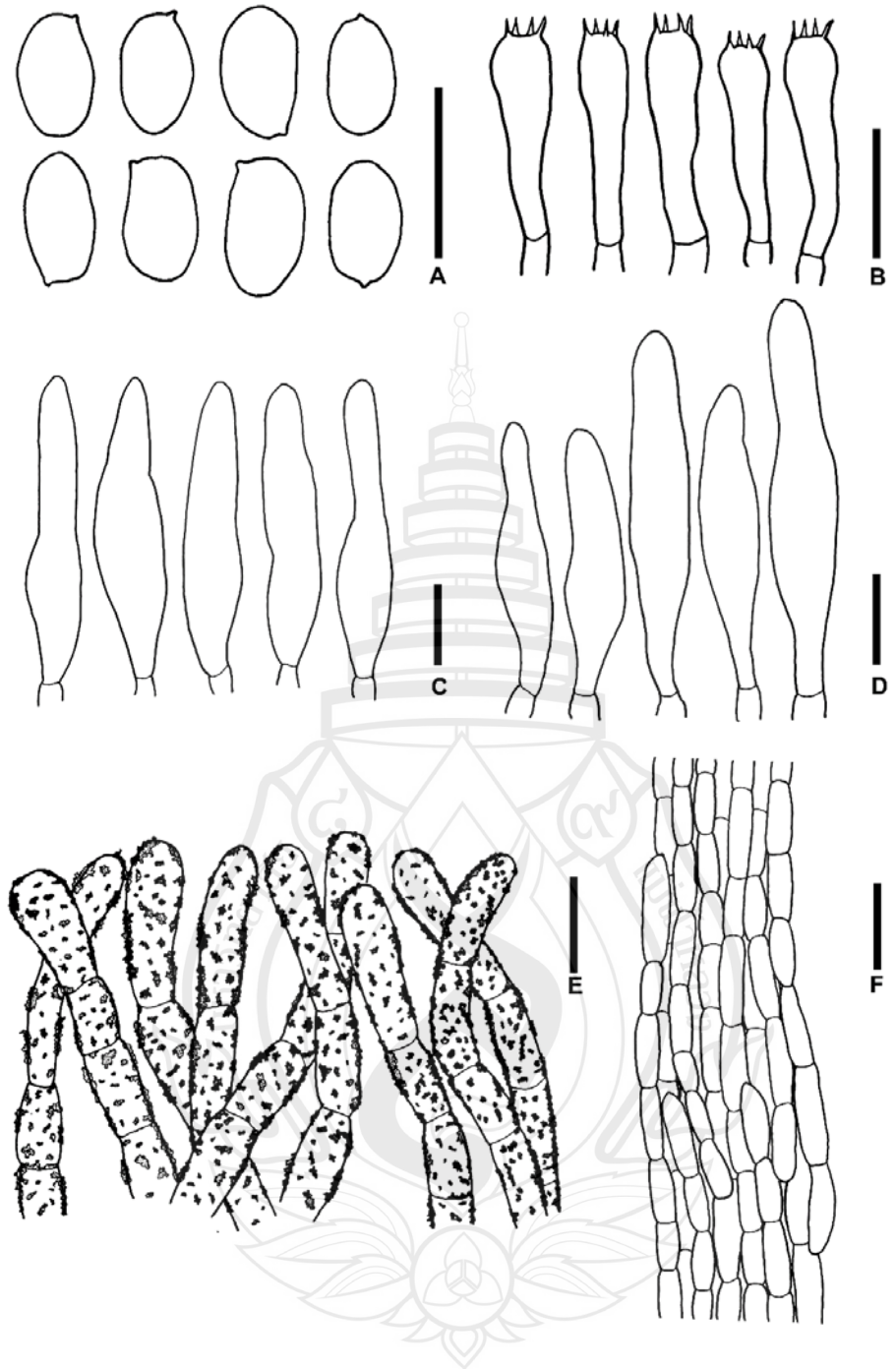
In the phylogenetic tree, *P. subrubeolus* appeared to be most closely related to *P. pusillus*, the two species forming a clade with high statistical support (BS = 100, PP = 1) Those two species together formed a well-supported clade with *P. subrubeolus*. The ITS sequence of *P. subrubeolus* is 99.8% similar to *P.* sp. 7 from China (Zeng et al., 2013), suggesting they are

conspecific. Unfortunately, the specimens corresponding to those sequences were not made available to us for study.



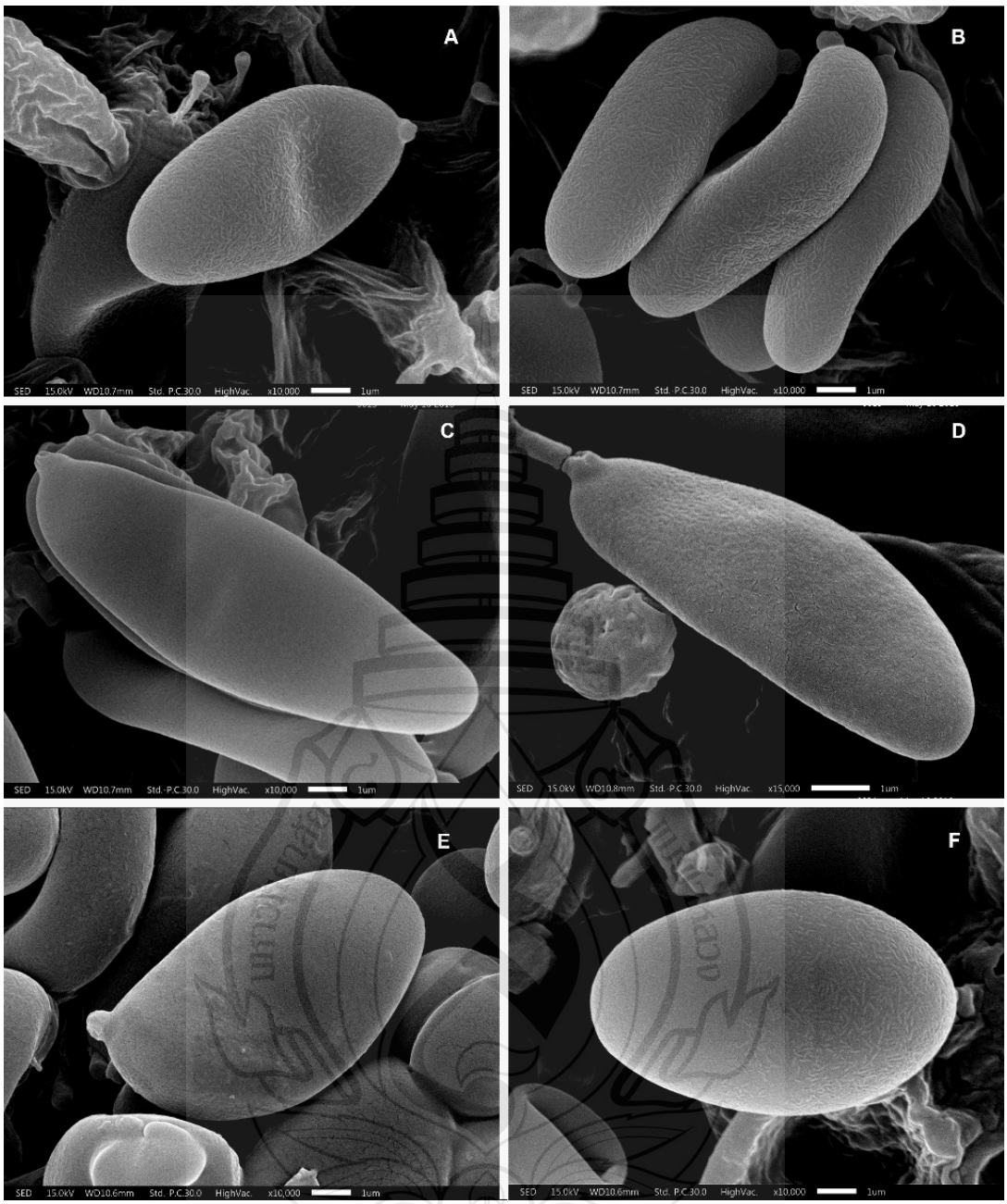
Note Basidiomata of *Phylloporus subrubeolus* (holotype, BC022) in the field. Scale bars = 1 cm.

Figure 3.6 Basidiomata of *Phylloporus subrubeolus*



Note Micro-morphological characters of *Phylloporus subrubeolus*. a Basidiospores. b Basidia. c Cheilocystidia. d Pleurocystidia. e Pileipellis. f Caulocystidia. Scale bars: a = 10 μm; b–d, f = 20 μm; e = 20 μm. All drawings were made from the type (BC022).

Figure 3.7 Micro-morphological characters of *Phylloporus subrubeolus*



Note SEM micrograph of the basidiospores of the new *Phylloporus* species. a, b *Phylloporus pusillus* (OR1310). c, d *Phylloporus subbacillisporus* (OR0436). e, f *Phylloporus subrubeolus* (BC022). Scale bars: 1 μm.

Figure 3.8 SEM micrograph of the basidiospores of the new *Phylloporus* species

3.2 Taxonomy and Phylogeny of *Retiboletus*

3.2.1 Molecular Analyses

A total of 22 new sequences were generated and deposited in GenBank (Table 3.3). The alignment contained 23 specimens and was 2642 characters long (TreeBase number S25985). The authors could not obtain *tef*1 and *rpb*2 sequences from the type OR0110 because its DNA was too degraded. However, the *atp*6 sequence obtained from this specimen was 100% identical to the other studied specimens of *R. brevibasidiatus*.

In the three-gene phylogeny, the new species was sister to *R. sinensis* with high statistical support (BS = 100%, PP = 1) (Fig. 1). Sequences from the other *Retibletus* specimens collected in Thailand grouped with either *R. fuscus* or *R. nigrogriseus* sequences with high support (BS = 100%, PP = 1).

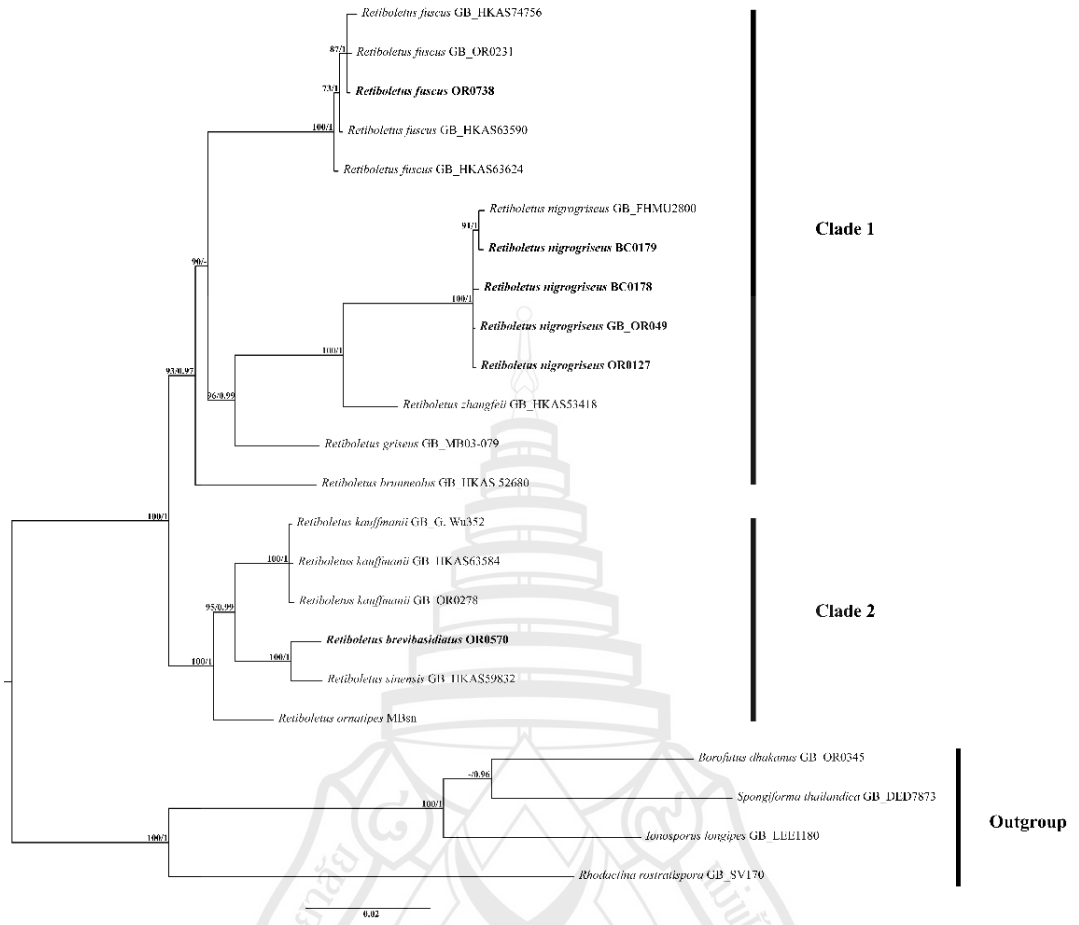
Table 3.3 List of collections used for DNA analyses with origin, GenBank accession numbers and references

Species	Voucher	Origin	*atp6*	*tef1*	*rpb2*	References
Borofutus dhakanus	OR345	Thailand	MG212533	MG212578	MG212620	Vadthanarat et al. 2018
Ionosporus longipes	LEE1180	Singapore	**MT085461**	**MT085471**	MH712031*	*Khmelnitsky et al. 2019, This study
Retiboletus brunneolus	HKAS 52680	China	–	KF112179	KF112690	Wu et al. 2014
Retiboletus fuscus	HKAS63590	China	–	KF112178	KF112691	Wu et al. 2016
Retiboletus fuscus	HKAS63624	China	–	KT990829	KT990466	Wu et al. 2016
Retiboletus fuscus	HKAS74756	China	–	KT990830	KT990467	Wu et al. 2016
Retiboletus fuscus	OR0231	China	MG212556	MG212600	MG212642	Vadthanarat et al. 2018
Retiboletus fuscus	OR0738	Thailand	**MT085462**	**MT085472**	**MT085477**	This study
Retiboletus griseus	MB03-079	U.S.A.	KT823964	KT824030	KT823997	Raspé et al. 2016
Retiboletus kauffmanii	G.Wu352	China	–	KP739301	KP739299	Zeng et al. 2016
Retiboletus kauffmanii	HKAS63584	China	–	KT990828	KT990465	Wu et al. 2016
Retiboletus kauffmanii	OR0278	China	MG212557	MG212601	MG212643	Vadthanarat et al. 2018
Retiboletus nigrogriseus	BC0178	Thailand	**MT085463**	**MT085473**	–	This study
Retiboletus nigrogriseus	BC0179	Thailand	**MT085464**	**MT085474**	**MT085478**	This study
Retiboletus nigrogriseus	OR049	Thailand	KT823967	KT824033	KT824000	Raspé et al. 2016

Table 3.3 (continued)

Species	Voucher	Origin	*atp6*	*tef1*	*rpb2*	References
Retiboletus nigrogriseus	OR0108	Thailand	**MT085465**	–	–	This study
Retiboletus nigrogriseus	OR0127	Thailand	**MT085466**	**MT085475**	–	This study
Retiboletus nigrogriseus	SV0218	Thailand	**MT085467**	–	–	This study
Retiboletus nigrogriseus	FHMU 2800	China	–	MH367488	–	Zeng et al. (2018)
Retiboletus ornatipes	MBsn	U.S.A.	**MT219514**	**MT219516**	**MT219515**	This study
Retiboletus sinensis	HKAS59832	China	–	KT990827	KT990464	Wu et al. 2016
Retiboletus sp.	OR0110	Thailand	**MT085468**	–	–	This study
Retiboletus sp.	OR0570	Thailand	**MT085469**	**MT085476**	**MT085479**	This study
Retiboletus sp.	OR0708	Thailand	**MT085470**	–	–	This study
Retiboletus zhangfeii	HKAS53418	China	–	KT990824	KT990462	Wu et al. 2016
Rhodactina rostratispora	SV170	Thailand	MG212560	MG212605	MG212645	Vadthanarat et al. 2018
Spongiforma thailandica	DED7873	Thailand	MG212563	KF030436*	MG212648	*Nuhn et al. 2013; Vadthanarat et al. 2018

Note Bold text indicates the sequences obtained in this study.



Note Maximum likelihood phylogenetic tree inferred from the three-gene dataset (*atp*6, *rpb*2, *tef*1), including *Retiboletus brevibasidiatus*, *R. fuscus*, *R. nigrogriseus* and selected *Retiboletus*. Four species were used as outgroup taxa: *Borofutus dhakanus*, *Ionosporus longipes*, *Rhodactina rostratispora*, *Spongiforma thailandica*. Bootstrap frequencies ≥ 70% and posterior probabilities ≥ 0.95 are shown above supported branches. The prefix "GB" before voucher numbers indicates that sequences were retrieved from GenBank.

Figure 3.10 Maximum likelihood phylogenetic tree inferred from the three-gene dataset (*atp*6, *rpb*2, *tef*1) of *Retiboletus*

3.2.2 Taxonomy

Retiboletus brevibasidiatus Raspe & Chuankid, Mycoscience 62: 299 (2021)

MycoBank no.: MB 835032, Faces of Fungi FoF 07863.

Holotype: THAILAND. Chiang Mai Province, Mae Taeng District, near Mushroom Research Center, 19°06’34’’N, 98°44’27’’E, elev. 1,090 m, 9 Jul 2010, O. Raspe, OR0110 (MFLU10-0942).

Etymology: the epithet *brevibasidiatus* refers to the shorter basidia as compared to the most closely related and resembling species *R. kauffmanii* and *R. sinensis*.

Macromorphology: ***Basidiomata*** medium-sized. *Pileus* 43–88 mm diam, convex when young, subhemispherical to convex when aged, densely subtomentose; surface dry, dark blonde to clay (5D4– 5) or hair brown to bronze (5E4–5) with brownish grey (6F8) patches; margin inflexed when young, then straight to slightly reflexed, abruptly paler than the rest of the pileus, at least in immature basidiomes; context 9–11 mm thick at center, 3–6 mm thick half-way between center and margin, pale yellow to light yellow (3A3–5), staining deeper chrome yellow (3A7) when bruised. ***Hymenophore*** poroid, sinuate-decurrent to decurrent; tubes 2–9 mm long, pale

yellow to light yellow (3A3–5), deeper chrome yellow when bruised; *pores* 0.3–1.5 mm in diam, angular, irregular surface, pale yellow to light yellow (3A3–5), staining pale orange (between 4A6 and 5A6) with time when bruised. ***Stipe*** 47–75 mm long, 9–19 mm wide, central, solid, equal or slightly enlarged at base, usually curved, densely reticulate over the upper 2/3; surface dry, background color yellow (1A5) on upper part, lower part golden blonde (4B4), staining vivid yellow (2A8) at first and changed to light brown (6D8) later when injured; reticulum light yellow to yellow (3A4–6) entirely, or only above, and then brownish-grey below (between 4B3 and 5C3); context white to yellow, staining deeper chrome yellow when cut, at least when young. ***Spore print*** not obtained. ***Basal mycelium*** pale yellow to chrome yellow, with some fine rhizoids. ***Odor*** fungoid, weak. ***Taste*** bitter. ***Macrochemical reactions***: Pileipellis reddish with violet tinge around the spot in KOH solution, pale orange in NH_4OH solution; pileus context pinkish white with KOH, yellow by reversal of the oxidation with an additional greenish tinge with NH_4OH solution.

Micromorphology: ***Basidiospores*** [55/1/1] (8–)9–11(–11.5) × (3.6–)3.7–4.3(–4.4) μm, 10.3 × 4.0 μm on average, *Q* = (1.9–)2.4–2.9(–3), 2.59 on average, subfusiform to ellipsoid, greenish grey to greyish green (1C2–3) in water and KOH, smooth. ***Basidia*** (17–)18–

25(–26) × 6–10 μm, 21.1 × 8.3 μm on average, clavate, four-spored, hyaline in KOH; sterigmata 2–4 μm long. ***Hymenophoral trama*** bilateral of the boletus-type, composed of hyphae 3–5 μm wide, hyaline in KOH. ***Cheilocystidia*** 34–46 × 7–13 μm, 40.7 × 9.9 μm on average, abundant, ventricose or subfusiform, usually with yellowish-brown (5E8) pigmented contents in water, but without cell wall encrustations. ***Pleurocystidia*** 24–40 × 7–11 μm, 32.1 × 9 μm on average, clavate or subfusiform, with yellowish-brown (5E8) pigmented contents in water, without cell wall encrustations. ***Pileipellis*** a trichoderm about 70–100 μm thick, composed of slightly interwoven hyphae 5–10 μm wide, brown (6E6) to blackish-brown in water and KOH; terminal cells 20–50 × 7–10 μm, narrowly clavate or subcylindrical. ***Pileal trama*** made of hyphae 6–10 μm, hyaline in KOH. ***Stipitipellis*** a disrupted hymeniderm about 60–90 μm thick, composed of emergent hyphae, hyaline in potassium, with 20–40 × 7–9 μm clavate or subfusiform terminal cells. ***Stipe trama*** composed of parallel hyphae, 5–8 μm wide, cylindrical, hyaline in KOH. ***Clamp connections*** not seen in any tissue.

Habitat: Solitary or in small groups on the leaves litter in forests dominated by *Fagaceae* (*Quercus*, *Lithocarpus*, *Castanopsis*) and/or *Dipterocarpaceae* (*Shorea*, *Dipterocarpus*).

Known distribution: Currently only known from northern Thailand.

Other materials examined: THAILAND. Lampang Province, Mueang Pan District, along Road 1252, 18°55’50’’N, 99°23’30’’E, elev. 1,420 m, Olivier Raspe & Komsit Wisitrassameewong, OR0570; Chiang Mai Province, Mae On District, Behind Tharnthong Lodges, 18°52’06’’N, 99°18’06’’E, elev. 760 m, 8 Aug 2013, O. Raspe & Benjarong Thongbai, OR0708 (MFLU13-0610).

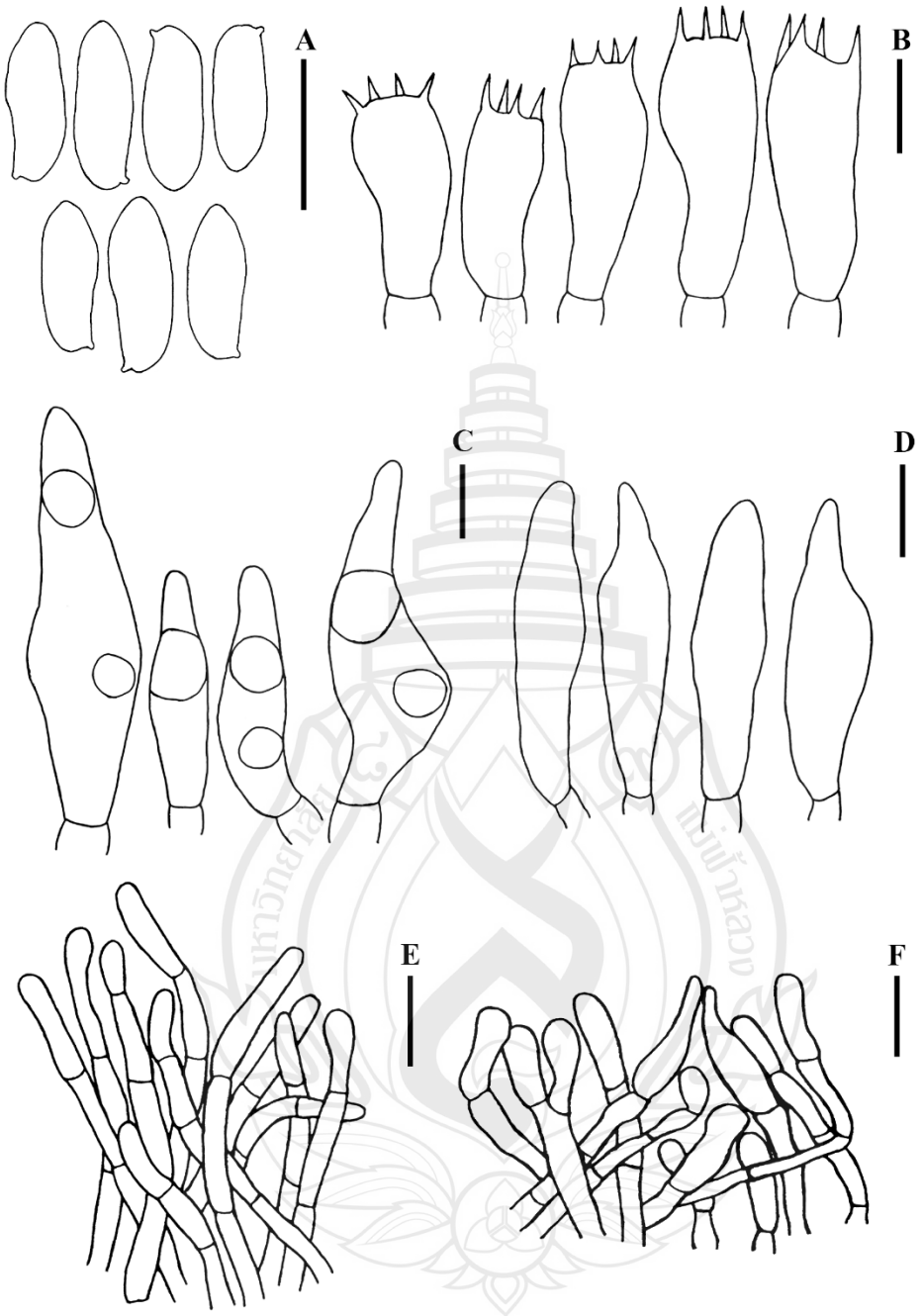
Note: *Retiboletus brevibasidiatus* is macro-morphologically characterized by its medium-sized basidiomes, dark blonde to clay or hair brown to bronze pileus, with brownish grey spots, context staining deeper yellow and pores changing to pale orange after bruising, stipe densely reticulate mostly on the upper part with pale yellow to chrome yellow basal mycelium. When compared to other *Retiboletus* species, *R. brevibasidiatus* is mostly similar to the two Chinese species *R. kauffmanii* and *R. sinensis* in pileus, hymenophore, and stipe colors. When cut, the context of *R. kauffmanii* does not change color, but it does in *R. brevibasidiatus* and *R. sinensis*. The most important discriminative character of *R. Brevibasidiatus* is the short basidia (18–26 μm long). The most closely related and resembling species *R. kauffmanii* and *R. sinensis* produce longer basidia (23–32 μm and 27–39 μm,

respectively). Also, the cheilocystidia and pleurocystidia of *R. brevibasidiatus* are broader (7–12 μm) than those of *R. sinensis* (4.5–7 μm), and tend to be broader than those of *R. kauffmanii* (6–10 μm). The new species also resembles *R. ornatipes* and *R. retipes* by the yellow tinge of the pileus and the strongly pigmented (yellowish brown) cystidia in KOH (Smith & Thiers, 1971; Binder & Bresinsky, 2002). However, upon closer examination, the pileus color of *R. brevibasidiatus* is more blonde than yellow. Based on the descriptions of *R. ornatipes* by Ortiz-Santana et al. (2007), the chemical reactions on pileus and pileus context are the most remarkable characters that could be used to difference *R. brevibasidiatus* from *R. ornatipes*. The pileus of *R. ornatipes* turns brown with KOH and shows no reaction to NH_4OH solution, whereas the pileus of *R. Brevibasidiatus* reddens with a violet tinge around the spot in KOH and turns pale orange with NH_4OH solution. The fresh pileus context of *R. Brevibasidiatus* turns pinkish white with KOH and changes to yellow with a greenish tinge with NH_4OH solution, but those characters were not found in pileus context of *R. ornatipes* (Ortiz-Santana et al., 2007). *Retiboletus retipes* mainly differs from *R. Brevibasidiatus* in its yellowish pulverulent pileus and stipe (Berkeley, 1872). Phylogenetically, *R. brevibasidiatus* groups with *R. sinensis* (BS=100% and PP=1), which together are sister to *R. kauffmanii* (BS=95% and PP=0.99).



Note Basidiomata of *Retiboletus brevibasidiatus* in the field. A: OR0570. B: OR0110 (holotype). *Bars*: 2 cm.

Figure 3.11 Basidiomata of *Retiboletus brevibasidiatus*



Notes Micro-morphological characters of *Retiboletus brevibasidiatus* (OR0110, holotype). A: Basidiospores. B: Basidia. C: Cheilocystidia. D: Pleurocystidia. E: Pileipellis. F: Stipitipellis. *Bars*: A–D 10 μm; E, F 20 μm.

Figure 3.12 Micro-morphological characters of *Retiboletus brevibasidiatus*

Retiboletus fuscus (Hongo) N.K. Zeng & Zhu L. Yang, Mycologia 108(2): 365, 2016 MycoBank no.: MB 811563, Faces of Fungi FoF 08036.

≡ *Boletus griseus* var. *fuscus* Hongo, J Jap Bot 4:301, 1974 (basionym)

Macromorphology: ***Basidiomata*** medium-sized. *Pileus* about 50 mm diam, broadly convex; surface dry, densely subtomentose, greyish brown (8F3) to black; margin straight; context 6–10 mm thick, dull yellowish white (4A2) or paler, slowly staining pale yellowish-grey (paler than 4B2) when cut. ***Hymenophore*** poroid, adnexed; tubes 2.5–6 mm long, dull yellowish white (4A2), inconsistently staining pale orange-grey (paler than 5B2) when bruised; *pores* 0.3–0.8 mm diam, angular, irregular surface, dull yellowish white (4A2). ***Stipe*** 80 mm long, 10–15 mm wide, central, cylindrical and tapering downward, solid, almost entirely reticulate; surface dry, background color cream (4A3) in the upper part, darker to the base; reticulum concolorous with the pileus; context fibrous, upper part yellowish white (4A2) unchanging or slightly yellowing when bruised, lower part yellow (3A6). ***Basal mycelium*** off-white to pale beige. ***Spore print*** not obtained. ***Odor*** rubbery. ***Taste*** acidulous. ***Macrochemical reactions***: Hymenophore orange in KOH solution; stipitipellis, pileus context and stipe context pink in KOH solution; pileipellis reaction subnull in KOH solution.

Micromorphology: ***Basidiospores*** [55/1/1] 9.5–12 × 4.0–5 μm, 10.69 × 4.48 μm on average, *Q* = (1.9–)2.1–2.7(–3), 2.39 on average, subfusiform to ellipsoid, greenish grey in water (1C2) and olive grey (1D2) in KOH, smooth. ***Basidia*** (25–)26–36(–37) × (7.5–)8–10 μm, 30.9 × 8.9 μm on average, clavate, four-spored, hyaline in KOH; sterigmata 2–4 μm long. ***Hymenophoral trama*** bilateral, of the boletus type; hyphae 5–7 μm diam. ***Cheilocystidia*** 31–43 × (5–)6–8 μm, 36.7 × 7 μm on average, subfusiform or narrowly fusiform, hyaline with some brown to yellowish-brown contents (5E5–8) when observed in water, no encrustations. ***Pleurocystidia*** 28–42 × 6–10 μm, abundant, 32.5 × 7.4 μm on average, subfusiform or narrowly fusiform, hyaline with some brown to yellowish-brown contents (5E5–8) when observed in water, no encrustations. ***Pileipellis*** a trichodermium about 70–120 μm thick, composed of more or less vertically arranged, interwoven, dark brown (7F8) to black hyphae in water, 4–10 μm wide; terminal cells 30–60 × 6–10 μm, narrowly clavate or subcylindrical, with some obtuse apex. ***Pileal trama*** composed of smooth hyphae 5–7 μm diam. ***Stipitipellis*** hymeniform, composed of smooth, hyaline hyphae, or dark blonde to honey yellow (5D4–6) hyphae in the reticulum, with clavate, subcylindrical, or subfusiform terminal cells; 25–30 × 10–13 μm and

occasionally with clavate, four-spored basidia. ***Stipe trama*** composed of cylindrical, smooth, parallel hyphae 4–6 μm diam. ***Clamp connections*** not seen in any tissue.

Habitat: Solitary on the forest ground, near *Pinus kesiya* Royle ex Gordon.

Known distribution: Japan (Hongo 1974), southwestern China, and northern Thailand.

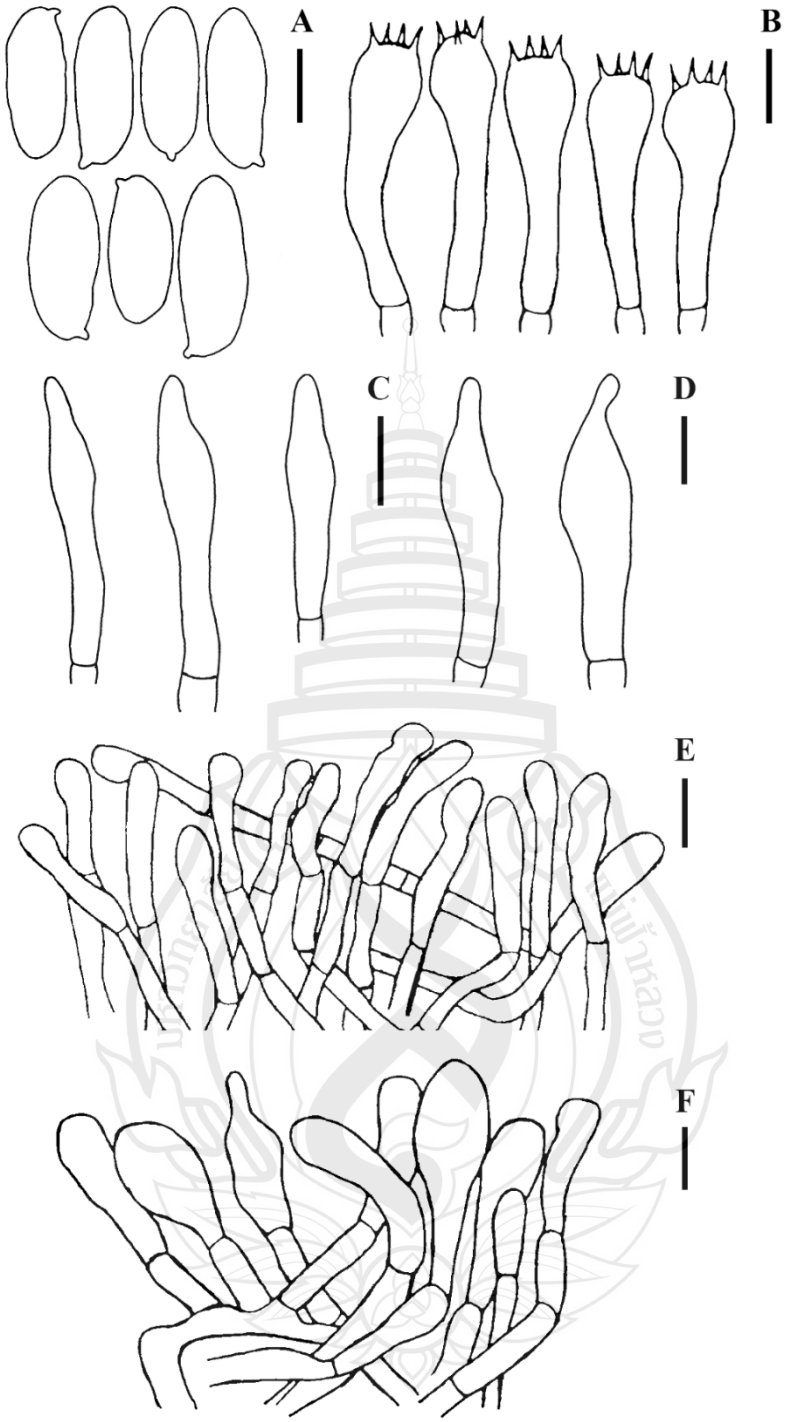
Material examined: THAILAND Chiang Rai Province, Mae Fah Luang District, 17 Jul 2014, Benjarong Thongbai, OR0738 (MFLU14-0460).

Notes: *Retiboletus fuscus* can be recognized by its greyish brown or dark grey pileus, dull yellowish white context sometimes slightly yellowing when bruised, concolorous stipe with darker reticulum on surface, and off-white mycelium at base. Zeng et al. (2016), elevated *Boletus griseus* var. *fuscus* Hongo to species rank based on a multi-gene (LSU, ITS, *tef*1) phylogeny. The macro- and micro-morphological characters of the specimen from Thailand were similar to *R. fuscus* from China and Japan. The combined phylogenetic analyses indicated the sequences from the Thai specimen clustered with those of *R. fuscus* from China with BS = 100%, PP = 1.0. Zeng et al. (2016) reported the species from *Fagaceae* forests. In Thailand, the specimen was collected in the vicinity of *P. kesiya* trees.



Note Basidiomata of *Retiboletus fuscus* (OR0738). A: Whole basidiome. B: Cut basidiome showing yellow tinge of context, especially in the lower half of the stipe. *Bars*: 2 cm.

Figure 3.13 Basidiomata of *Retiboletus fuscus*



Note Micro-morphological characters of *Retiboletus fuscus* (OR0738). A: Basidiospores. B: Basidia. C: Cheilocystidia. D: Pleurocystidia. E: Pileipellis. F: Stipitipellis. *Bars*: A 5 μm; B–D, F 10 μm; E 20 μm.

Figure 3.14 Micro-morphological characters of *Retiboletus fuscus*

Retiboletus nigrogriseus N.K. Zeng, S. Jiang & Zhi Q. Liang, Phytotaxa 367(1): 48, 2018

MycoBank no.: MB 825542, Faces of Fungi FoF 08037.

Macromorphology: ***Basidiomata*** medium to large-sized. *Pileus* 60–115 mm diam, convex when young, applanate to slightly plano-concave in age; surface dry, finely tomentose, brownish grey (5C2) to black with patches of light brown (6D7) or white; margin straight to slightly reflexed; context 10–20 mm thick at center, 5–7 mm thick half-way between center and margin, white to yellowish white, bruising greyish (1B1) then slowly violaceous grey (15D2), with a yellowish to greenish tinge above stipe. ***Hymenophore*** poroid, adnate at first, then sinuate to sinuate and narrowly decurrent; tubes 3–7 mm long, white to yellowish white, bruising greyish (1B1) then slowly violaceous grey (15D2); *pores* 0.1–0.4 mm diam, angular, irregular surface, white, bruising dark grey (1F1). ***Stipe*** 65–85 mm long, 10–29 mm wide, central, solid, equal or tapering upwards to clavate or sub-bulbous, sometimes curved, densely reticulate over the upper 2/3; surface dry, background color cream (4A3) or white around the apex, darker towards the base, with more or less pronounced yellow to pale orange stains; reticulum pale grey (1B2), dark brown (6F7) or black; context fleshy fibrous, marbled white to yellowish white bruising greyish white (1B1) or olive green (3D7) tinged with silver white to greyish yellow (2B3–5), with some yellow or orange-yellow stains on the sides and base of stipe. ***Basal mycelium*** white. ***Spore print*** not obtained. ***Odor*** fungoid-sclerodermatoid. ***Taste*** slightly bitter. ***Macrochemical reactions***. pileipellis and stipitipellis yellow to orange-yellow in KOH solution, unchanging to yellowish in NH_4OH solution; pileus context and stipe context pale yellow in KOH solution, unchanging to yellowish in NH_4OH solution.

Micromorphology: ***Basidiospores*** [285/5/5] (9–)10–12(–13.5) × 4–5 μm, 10.95 × 4.52 μm on average, *Q* = (1.9–)2.1–2.7(–3), 2.42 on average, elliptical to subfusiform, greenish grey (1C2) in water and KOH, smooth. ***Basidia*** 26–40(–41) × (8–)9–11(–12) μm, 33.2 × 10 μm on average, clavate, four-spored, hyaline in KOH; sterigmata 3–5 μm long. ***Hymenophoral trama*** bilateral of the boletus type, composed of hyphae 4–10 μm in wide, hyaline with some rustbrown (6E8) hyphae in KOH. ***Cheilocystidia*** (35–)36–63 × (7–)8–13 μm, 50.9 × 11.4 μm on average, abundant, ventricose or subfusiform, usually with reddish brown to dark brown (7E–F8) intracellular pigments, without encrustations. ***Pleurocystidia*** same as cheilocystidia. *Pileipellis* a trichodermium about 100–150 μm thick, composed of hyphae 6–10 μm wide,

greyish yellow (4C5) to reddish brown (8E8) in KOH; terminal cells 17–50 × 5–10 µm, subfusiform, clavate, or subcylindrical, with obtuse apex. ***Pileal trama*** made up of hyphae 5–9 µm wide, hyaline in KOH. ***Stipitipellis*** hymeniform, about 70–140 µm thick, composed of emergent hyphae, golden (4C6) to raw umber (5F8), or blackish in water and KOH, with 25–60 × 7–17 µm, clavate, ventricose, or subfusiform terminal cells. ***Stipe trama*** composed of longitudinally arranged, parallel hyphae, 4–10 µm wide, cylindrical, almost hyaline in KOH, brown to mustard brown (5E5–6) in water and ammonium solution. ***Clamp connections*** not seen in any tissue.

Habitat: Solitary to gregarious on the ground in forests with *Lithocarpus* spp., *Castanopsis* spp., *Shorea* spp., and *Dipterocarpus* spp.

Known distribution: Southern China and Thailand.

Material examined: THAILAND. Chiang Mai Province, Mae Taeng District, 30 Jun 2010, O. Raspe & S.C. Karunarathna, OR0049 (MFLU10-0881); —Pa Pae, 9 Jul 2010, O. Raspe & S.C. Karunarathna, OR0108 (MFLU10-0940); —, 12 Jul 2010, O. Raspe & S.C. Karunarathna, OR0127 (MFLU10-0959); —, 22 Jun 2018, B. Chuankid, BC0178 (MFLU18-1772) and BC0179 (MFLU18-1773); —, Mueang District, Doi Suthep-Pui National Park, 18°47’16’’N, 98°55’25’’E, elev. 860 m, 14 Aug 2015, S. Vadthanarat, SV0218 (BKF, SDBR-CMU).

Note: Macro- and micro-morphology of *R. Nigrogriseus* specimens from Thailand match the description of the specimens from China (holotype, FHMU 2800), except for the pileipellis structure, which was reported to be a subcutis by Zeng et al. (2018), whereas we observed a trichodermium. This discrepancy may be due to observations being made on basidiomes at different stages of development. It is indeed common in boletes to have a trichodermium in young basidiomes which more or less collapses and may look like a subcutis with age. In addition, *R. nigrogriseus* is characterized by its pileus and stipe context changing brownish to fuliginous when injured, stipe with grey to black reticulum and white basal mycelium. When observed in KOH, greyish yellow to reddish brown pigments were found in terminal cells of the pileipellis. The hymeniform stipitipellis is composed of emergent hyphae, golden to raw umber, or blackish pigments in water and KOH.

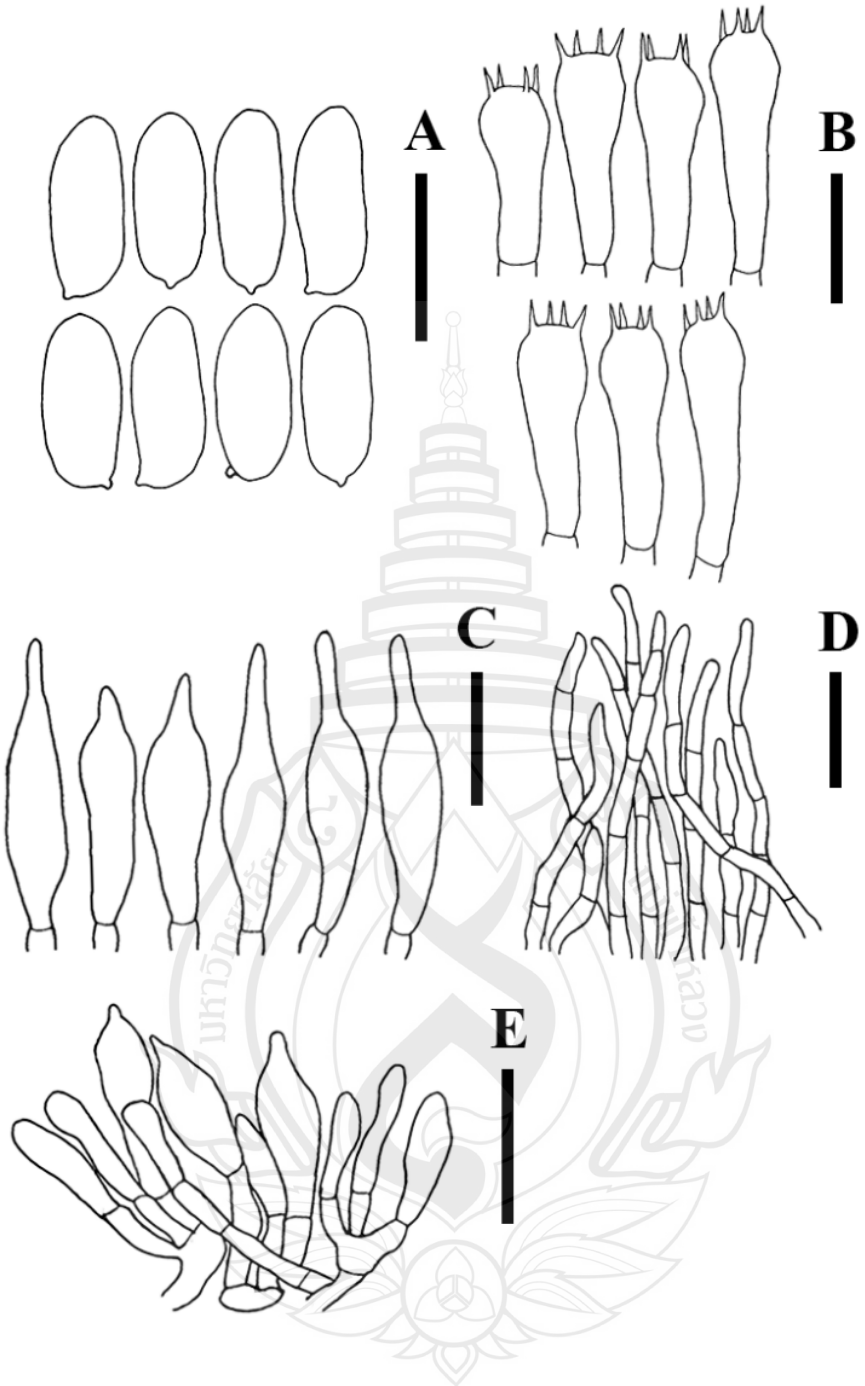
In the phylogenetic analyses of Zeng et al. (2018), a collection from Thailand (OR049) was included, which seemed to be related to *R. nigrogriseus*, but they did not study the morphology of this collection. The sequences of OR049 were first published in Raspe et al.

(2016), who also did not give a morphological description of the material. Here, we provide both three-gene phylogenetic evidence and morphological evidence to support the identification of the original material from Thailand as *R. nigrogriseus*.



Note Basidiomata of *Retiboletus nigrogriseus* in the field. A: OR049. B, C: OR0108. D: OR0127. *Bars*: 2 cm.

Figure 3.15 Basidiomata of *Retiboletus nigrogriseus*



Note Micro-morphological characters of *Retiboletus nigrogriseus* (OR049). A: Basidiospores. B: Basidia. C: Cheilocystidia and pleurocystidia. D: Pileipellis. E: Stipitipellis. *Bars*: A 10 μm; B, C 20 μm; D, E 50 μm.

Figure 3.16 Micro-morphological characters of *Retiboletus nigrogriseus*

3.3 Taxonomy and Phylogeny of *Hourangia* and *Xerocomus*

3.3.1 Phylogenetic Analyses

A total of 68 sequences were newly generated in this study and deposited in GenBank (Table 3.4). For the Xerocomoideae tree, the alignment contained 284 sequences comprising three genes (83 for *atp*6, 98 for *rpb*2, 103 for *tef*1) from 149 voucher specimens corresponding to 102 taxa, and was 2658 characters long. Maximum likelihood and BI trees of the combined three-gene dataset were similar in topology, without any supported conflict (BS ≥70% and PP ≥0.90). The phylogram of RAxML bipartition retrieved the ten genera from subfamily Xerocomoideae. The statistical support of *Rubinosporus* was not monophyly (with low support), like in previously published phylogenies (Vadthanarat et al., 2022). However, the monophyly of another genus in this group was highly supported.

Table 3.4 List of collections used for phylogenetic analyses, with origin, GenBank accession numbers, and references

Species	Voucher	Origin	*atp*6	*rpb*2	*tef*1	Reference(s)	Note
Alessioporus ichnusanus	AMB12756	Italy	–	–	KJ729513	Gelardi et al. (2014)	Epitype
Aureoboletus auriflammeus	CFMR:BOS-699	USA	–	MK766269	MK721060	Kuo & Ortiz-Santana (2020)	
Aureoboletus catenarius	HKAS54467	China	–	KT990349	KT990711	Wu et al. (2016)	Holotype
Aureoboletus duplicatoporus	HKAS50498	China	–	KF112754	KF112230	Wu et al. (2014)	
Aureoboletus formosus	GDGM44441	China	–	KT291751	KT291744	Zhang et al. (2015)	
Aureoboletus gentilis	ADK4865	Belgium	KT823961	KT823994	KT824027	Raspé et al. (2016); Vadthanarat et al. (2019b)*	
Aureoboletus glutinosus	GDGM44477	China	–	MH700229	MH700205	Zhang et al. (2019)	
Aureoboletus innixus	CFMR:BOS-544	USA	–	MK766270	MK721061	Kuo & Ortiz-Santana (2020)	
Aureoboletus mirabilis	HKAS57776	Chia	–	KF112743	KF112229	Wu et al. (2016)	
Aureoboletus moravicus	VDKO1120	Belgium	MG212528	MG212615	MG212573	Vadthanarat et al. (2018); Vadthanarat et al. (2019b)*	

Table 3.4 (continued)

Species	Voucher	Origin	*atp*6	*rpb*2	*tef*1	Reference(s)	Note
Aureoboletus nephrosporus	HKAS74929	China	–	KT990358	KT990721	Wu et al. (2016)	Holotype
Aureoboletus projectellus	AFTOL-ID-713	USA	DQ534604*	AY787218	AY879116	Binder & Hibbett (2006)*; Binder, Matheny & Hibbett, Unpublished	
Aureoboletus raphanaceus	GDGM 53127		–	MN549706	MN549676	Zhang et al. (2019)	
Aureoboletus roxanae	CFMR:BOS-698	USA	–	MK766272	MK721063	Kuo & Ortiz-Santana (2020)	
Aureoboletus russellii	CFMR:BOS-716	USA	–	MK766273	MK721064	Kuo & Ortiz-Santana (2020)	
Aureoboletus shichianus	HKAS76852	China	–	KF112756	KF112237	Wu et al. (2016)	
Aureoboletus singeri	CFMR:BOS-468	Belize	–	MK766274	MK721065	Kuo & Ortiz-Santana (2020)	
Aureoboletus sp.	OR0245	China	MH614653	MH614749	MH614702	Vadthanarat et al. (2019b)	
Aureoboletus sp.	OR0369	Thailand	MH614654	MH614750	MH614703	Vadthanarat et al. (2019b)	
Aureoboletus tenuis	GDGM42601	China	–	KT291754	KT291745	*Aureoboletus formosus*, a new bolete species from Hunan province	Holotype

Table 3.4 (continued)

Species	Voucher	Origin	*atp*6	*rpb*2	*tef*1	Reference(s)	Note
Aureoboletus thibetanus	AFTOL-ID-450	China	DQ534600*	DQ366279	DQ029199	Binder and Hibbett (2006)*; Unpublished	
Aureoboletus tomentosus	HKAS90216	China	–	KT990355	KT990717	Wu et al. (2016)	
Aureoboletus viscidipes	HKAS77103	China	–	KT990360	KT990723	Wu et al. (2016)	
Aureoboletus viscosus	OR0361	Thailand	MH614655	MH614751	MH614704	Vadthanarat et al. (2019b)	
Aureoboletus yunnanensis	HKAS75050	China	–	KT990361	KT990724	Wu et al. (2016)	
Aureoboletus zangii	HKAS74751	China	–	KT990362	KT990725	Wu et al. (2016)	
Boletellus aff. *ananas*	NY815459	Costa Rica	–	KF112760	KF112308	Wu et al. (2014)	
Boletellus aff. *emodensis*	OR0061	Thailand	KT823970	KT824003	KT824036	Raspé et al. (2016); Vadthanarat et al. (2019b)*	
Boletellus ananas	K(M)123769	Belize	MH614658	MH614754	MH614707	Vadthanarat et al. (2019b)	
Boletellus areolatus	TNS-F-61444 or BLT-7	Japan	–	AB999754	–	Sata & Hattori (2015)	

Table 3.4 (continued)

Species	Voucher	Origin	*atp*6	*rpb*2	*tef*1	Reference(s)	Note
Boletellus aurocontextus	TNS-F-61501 or BLT-65	Japan	–	AB999770	–	Sata & Hattori (2015)	
Boletellus emodensis	TNS-F-61564 or BLT-128	Japan	–	AB999782	–	Sata & Hattori (2015)	
Boletellus sp.	OR0621	Thailand	MG212529	MG212616	MG212574	Vadthanarat et al. (2018); Vadthanarat et al. (2019b)*	
Hemileccinum depilatum	AF2845	Belgium	MG212547	MG212633	MG212591	Vadthanarat et al. (2018); Vadthanarat et al. (2019b)*	
Hemileccinum hortonii	MICH:KUO-07050706	USA	–	MK766377	MK721175	Kuo & Ortiz-Santana (2020)	
Hemileccinum impolitum	ADK4078	Belgium	MG212548	MG212634	MG212592	Vadthanarat et al. (2018); Vadthanarat et al. (2019b)*	
Hemileccinum indecorum	OR0863	Thailand	MH614677	MH614772	MH614726	Vadthanarat et al. (2019b)	
Hemileccinum rubropunctum	REH-8501	USA	–	MK766327	MK721122	Kuo & Ortiz-Santana (2020)	
Hemileccinum rugosum	HKAS84355	China	–	KT990413	KT990774	Wu et al. (2016)	Holotype

Table 3.4 (continued)

Species	Voucher	Origin	*atp*6	*rpb*2	*tef*1	Reference(s)	Note
Hemileccinum subglabripes	MICH:KUO-07230802	USA	–	MK766300	MK721092	Kuo & Ortiz-Santana (2020)	
Heimioporus australis	REH9288	Australia	–	–	KP327703	Halling et al. 2015	
Heimioporus conicus	HKAS53451	China	–	KF112805	KF112226	Wu et al. (2016)	
Heimioporus cooloolae	REH9817	Australia	–	–	KP327710	Halling et al. 2015	
Heimioporus fruticicola	REH8962	Australia	–	–	KP327696	Halling et al. 2015	
Heimioporus gaojiaocong	HKAS80582	China	–	KT990409	KT990770	Wu et al. (2016)	
Heimioporus ivoryi	REH8620	Costa Rica	–	–	KP327683	Halling et al. 2015	
Heimioporus japonicus	OR0114	Thailand	KT823971	KT824004	KT824037	Raspé et al. 2016	
Heimioporus japonicus	SV0016	Thailand	MT136776	MT136766	MT136771	Vadthanarat et al. (2020)	
Heimioporus mandarinus	OR0218	Thailand	MG212546	MG212632	MG212590	Vadthanarat et al. (2018)	

Table 3.4 (continued)

Species	Voucher	Origin	*atp*6	*rpb*2	*tef*1	Reference(s)	Note
Heimioporus retisporus	HKAS52237	China	–	KF112806	KF112228	Wu et al. (2016)	
Heimioporus subcostatus	SV0235	Thailand	MT136780	MT136770	MT136775	Vadthanarat et al. (2020)	
Heimioporus subretisporus	HKAS80581	China	–	KT990407	KT990769	Wu et al. (2016)	
Hourangia cheoi	HKAS52269	China	–	KF112773	KF112286	Zhu et al. (2015)	
Hourangia dilatata	FHMU2979	China	–	–	MT650116	Wang et al. (2020)	Holotype
Hourangia microcarpa	HKAS53378	China	–	KF112775	KF112300	Wu et al. (2016)	
Hourangia nigropunctata	HKAS 57427	China	–	KP136978	KP136927	Zhu et al. (2015)	
Hourangia cf. *pumila*	OR0762	Thailand	MH614680	MH614775	MH614728	Vadthanarat et al. (2019b)	
Hourangia sp.	HKAS68178	China	–	KF112776	KF112301	Wu et al. (2016)	
Hourangia cf. *microcarpa*	BC0189	–	–	–	–	–	–
Hourangia cf. *microcarpa*	OR0102	–	–	–	–	–	–

Table 3.4 (continued)

Species	Voucher	Origin	*atp*6	*rpb*2	*tef*1	Reference(s)	Note
Hourangia cf. *microcarpa*	OR0106	–	–	–	–	–	–
Hourangia cf. *microcarpa*	OR0138	–	–	–	–	–	–
Hourangia cf. *microcarpa*	OR1029	–	–	–	–	–	–
Hourangia cf. *microcarpa*	OR1156	–	–	–	–	–	–
Hourangia cf. *microcarpa*	OR1266	–	–	–	–	–	–
Hourangia cf. *microcarpa*	OR1275	–	–	–	–	–	–
Hourangia cf. *nigropunctata*	BC024	–	–	–	–	–	–
Hourangia cf. *nigropunctata*	OR0042	–	–	–	–	–	–
Hourangia cf. *nigropunctata*	OR0046	–	–	–	–	–	–
Hourangia cf. *nigropunctata*	OR0077	–	–	–	–	–	–
Hourangia cf. *nigropunctata*	OR0078	–	–	–	–	–	–
Hourangia cf. *nigropunctata*	OR0485	–	–	–	–	–	–
Hourangia cf. *nigropunctata*	OR0506	–	–	–	–	–	–

Table 3.4 (continued)

Species	Voucher	Origin	*atp*6	*rpb*2	*tef*1	Reference(s)	Note
Hourangia cf. *nigropunctata*	OR1130	–	–	–	–	–	–
Hourangia cf. *nigropunctata*	OR1239	–	–	–	–	–	–
Hourangia cf. *nigropunctata*	OR1247	–	–	–	–	–	–
Hourangia cf. *nigropunctata*	OR1249	–	–	–	–	–	–
Hourangia cf. *nigropunctata*	OR1271	–	–	–	–	–	–
Hourangia cf. *nigropunctata*	OR1280	–	–	–	–	–	–
Hourangia cf. *nigropunctata*	OR1281	–	–	–	–	–	–
Hourangia cf. *nigropunctata*	OR1284	–	–	–	–	–	–
Hourangia cf. *nigropunctata*	OR1309	–	–	–	–	–	–
Hourangia cf. *nigropunctata*	OR1320	–	–	–	–	–	–

Table 3.4 (continued)

Species	Voucher	Origin	*atp*6	*rpb*2	*tef*1	Reference(s)	Note
Hourangia cf. *pumila*	OR0762	–	–	–	–	–	–
Hourangia sp. (aff *microcarpa*)	OR0429	–	–	–	–	–	–
Hourangia sp. 1	OR0348	–	–	–	–	–	–
Hourangia sp. 1	OR0353	–	–	–	–	–	–
Hourangia sp. 2	OR0669	–	–	–	–	–	–
Phylloporus bellus	OR0473	China	MH580778	MH580818	MH580798	Chuankid et al. (2018); Vadthanarat et al. (2019b)*	
Phylloporus brunneiceps	OR0050	Thailand	KT823968	KT824001	KT824034	Raspé et al. (2016); Vadthanarat et al. (2019b)*	
Phylloporus castanopsidis	OR0052	Thailand	KT823969	KT824002	KT824035	Raspé et al. (2016); Vadthanarat et al. (2019b)*	
Phylloporus grossus		China	-	-	MW574462		
Phylloporus maculatus	OR0285	China	MH580780	MH580820	MH580800	Chuankid et al. (2018)	
Phylloporus microsquamus		China	–	–	MW574471		
Phylloporus nigrobrunneus		China	–	–	JQ967186		

Table 3.4 (continued)

Species	Voucher	Origin	*atp*6	*rpb*2	*tef*1	Reference(s)	Note
Phylloporus pachycystidiatus	HKAS53422	China	–	KF112777	KF112288	Wu et al. (2016)	
Phylloporus pelletieri	WU18746	Austria	MH580781	MH580821	MH580801	Chuankid et al. (2018); Vadthanarat et al. (2019b)*	
Phylloporus pusillus	OR1158	Thailand	MH580783	MH580823	MH580803	Chuankid et al. (2018); Vadthanarat et al. (2019b)*	
Phylloporus rhodoxanthus	WU17978	Austria	MH580785	MH580824	MH580805	Chuankid et al. (2018); Vadthanarat et al. (2019b)*	
Phylloporus rubeolus	OR0251	China	MH580786	MH580825	MH580806	Chuankid et al. (2018); Vadthanarat et al. (2019b)*	
Phylloporus rubiginosus	OR0169	China	MH580788	MH580827	MH580808	Chuankid et al. (2018); Vadthanarat et al. (2019b)*	
Phylloporus rubrosquamosus	HKAS52552	China	–	KF112780	KF112289	Wu et al. (2016)	
Phylloporus scabripes	CFMR:BOS-621	Belize	–	MK766359	MK721156	Kuo & Ortiz-Santana (2020)	
Phylloporus sp.	OR0896	Thailand	MH580790	MH580829	MH580810	Chuankid et al. (2018); Vadthanarat et al. (2019b)*	
Phylloporus subbacillisporus	OR0436	China	MH580792	MH580831	MH580812	Chuankid et al. (2018); Vadthanarat et al. (2019b)*	

Table 3.4 (continued)

Species	Voucher	Origin	*atp*6	*rpb*2	*tef*1	Reference(s)	Note
Phylloporus tenuissimus		China	-	-	MW574452		
Phylloporus yunnanensis	OR0448	China	MG212554	MG212640	MG212598	Vadthanarat et al. (2018); Vadthanarat et al. (2019b)*	
Pulchroboletus roseoalbidus	AMB 12757	France	–	–	KJ729512	Gelardi et al. (2014)	Epitype
Pulchroboletus sclerotiorum	FLAS F 60333	USA	–	MF614169	MF614167	Crous et al. (2019)	
Pulchroboletus sclerotiorum	FLAS F 60334	USA	–	MF614164	MF614165	Crous et al. (2019)	
Rubinosporus auriporus	SV0090	Thailand	MZ355896	MZ355901	MZ355903	Vadthanarat et al. (2022)	Holotype
Xerocomus ferrugineus	CFMR:BOS-545	USA	–	MK766375	MK721173	Kuo & Ortiz-Santana (2020)	
Xerocomus ferrugineus	MICH:KUO-08100701	USA	–	MK766376	MK721174	Kuo & Ortiz-Santana (2020)	
Xerocomus fraternus	HKAS55328	China	–	KT990497	KT990869	Wu et al. (2016)	Holotype
Xerocomus fulvipes	HKAS76666	China	–	KF112789	KF112292	Wu et al. (2016)	

Table 3.4 (continued)

Species	Voucher	Origin	*atp*6	*rpb*2	*tef*1	Reference(s)	Note
Xerocomus magniporus	HKAS58000	China	–	KF112781	KF112293	Wu et al. (2016)	
Xerocomus microcapoides	HKAS54753	China	–	–	KT990868	Wu et al. (2016)	
Xerocomus microcapoides	HKAS53374	China	–	–	KT990867	Wu et al. (2016)	
Xerocomus piceicola	HKAS76492	China	–	–	KT990872	Wu et al. (2016)	Epitype
Xerocomus puniceiporus	HKAS80683	China	–	KU974146	KU974138	Wu et al. (2016)	
Xerocomus rugosellus	HKAS58865	China	–	KF112784	KF112294	Wu et al. (2016)	
Xerocomus s.s. sp.	OR0237	China	MH580796	MH580835	MH580816	Chuankid et al. (2018)	
Xerocomus s.s. sp.	OR0443	China	MH580797	MH580836	MH580817	Chuankid et al. (2018); Vadthanarat et al. (2019b)*	
Xerocomus sp.	OR0053	Thailand	MH580795	MH580834	MH580815	Chuankid et al. (2018); Vadthanarat et al. (2019b)*	
Xerocomus spadiceus var. *gracilis*	MICH:KUO-07080702	USA	–	MK766378	MK721176	Kuo & Ortiz-Santana (2020)	

Table 3.4 (continued)

Species	Voucher	Origin	*atp*6	*rpb*2	*tef*1	Reference(s)	Note
Xerocomus subparvus	LE315595	Viet Nam	–	–	MW033315	Pham & Morozova (2020)	
Xerocomus subparvus	HKAS50295	China	–	KT990491	-	Wu et al. (2016)	
Xerocomus subtomentosus	VDKO0987	Belgium	MG212572	MG212657	MG212614	Vadthanarat et al. (2018); Vadthanarat et al. (2019b)*	
Xerocomus tenax	MICH:KUO-08241404	USA	–	MK766379	MK721177	Kuo & Ortiz-Santana (2020)	
Xerocomus tenax	REH6871	USA	–	–	KF030437	Nuhn et al. (2013)	
Xerocomus velutinus	HKAS68135	China	–	–	KT990861	Wu et al. (2016)	
Xerocomus sp. 1	OR0200	–	–	–	–	–	–
Xerocomus sp. 1	OR0639	–	–	–	–	–	–
Xerocomus sp. 1	OR0997	–	–	–	–	–	–
Xerocomus sp. 1	OR0998	–	–	–	–	–	–
Xerocomus sp. 1	OR1134	–	–	–	–	–	–
Xerocomus sp. 1	OR1311	–	–	–	–	–	–
Xerocomus sp. 1	OR1324	–	–	–	–	–	–
Xerocomus sp. 1	OR1327	–	–	–	–	–	–

Table 3.4 (continued)

Species	Voucher	Origin	*atp*6	*rpb*2	*tef*1	Reference(s)	Note
Xerocomus sp. 2	OR0179	–	–	–	–	–	–
Xerocomus sp. 2	OR0503	–	–	–	–	–	–
Xerocomus sp. 2	OR0531	–	–	–	–	–	–
Xerocomus sp. 2	OR1201	–	–	–	–	–	–
Xerocomus sp. 2	OR1209	–	–	–	–	–	–
Xerocomus sp. 2	OR1283	–	–	–	–	–	–
Xerocomus sp. 3	OR0156	–	–	–	–	–	–
Xerocomus sp. 3	BC0220	–	–	–	–	–	–
Xerocomus sp. 3	OR0490	–	–	–	–	–	–

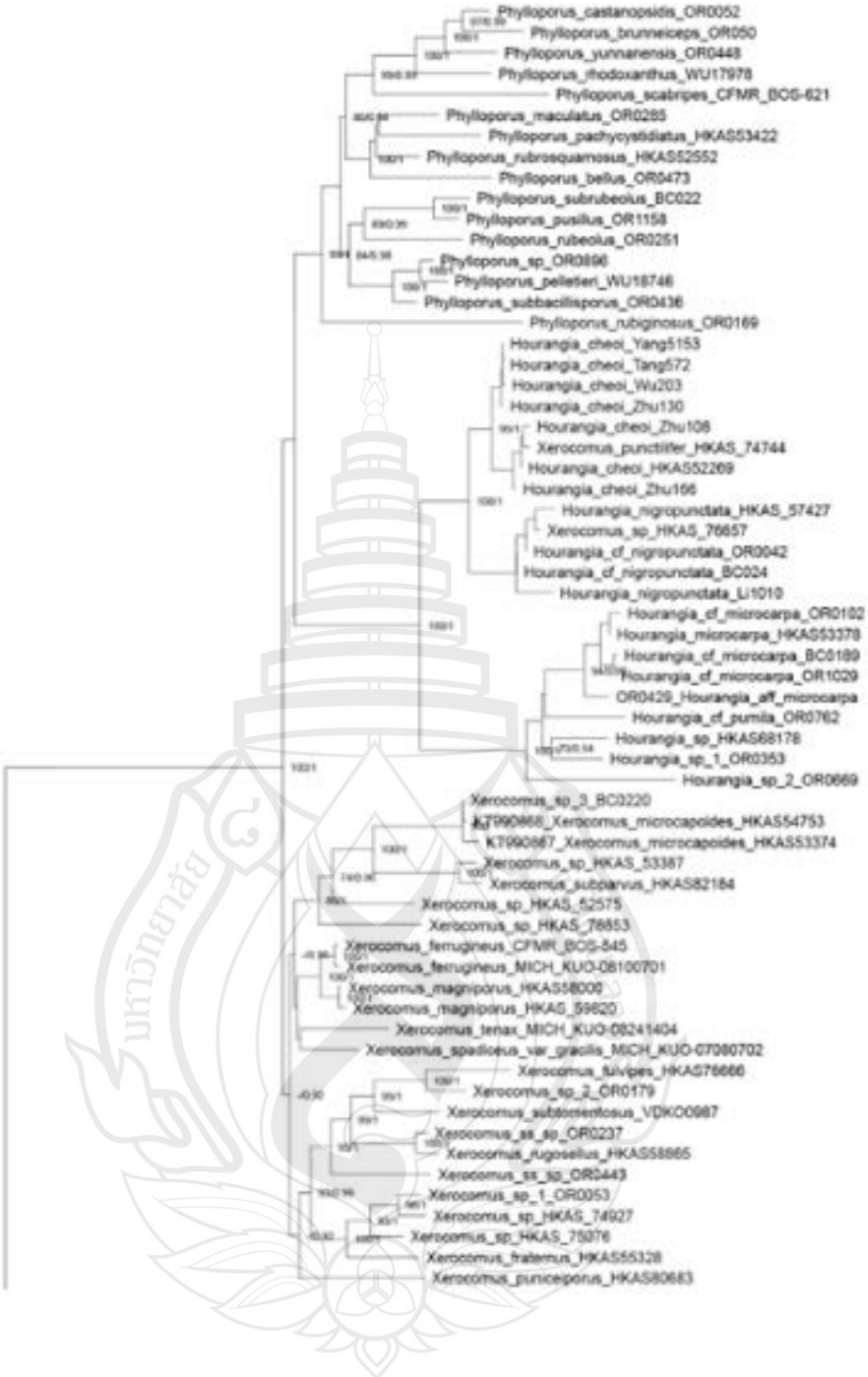
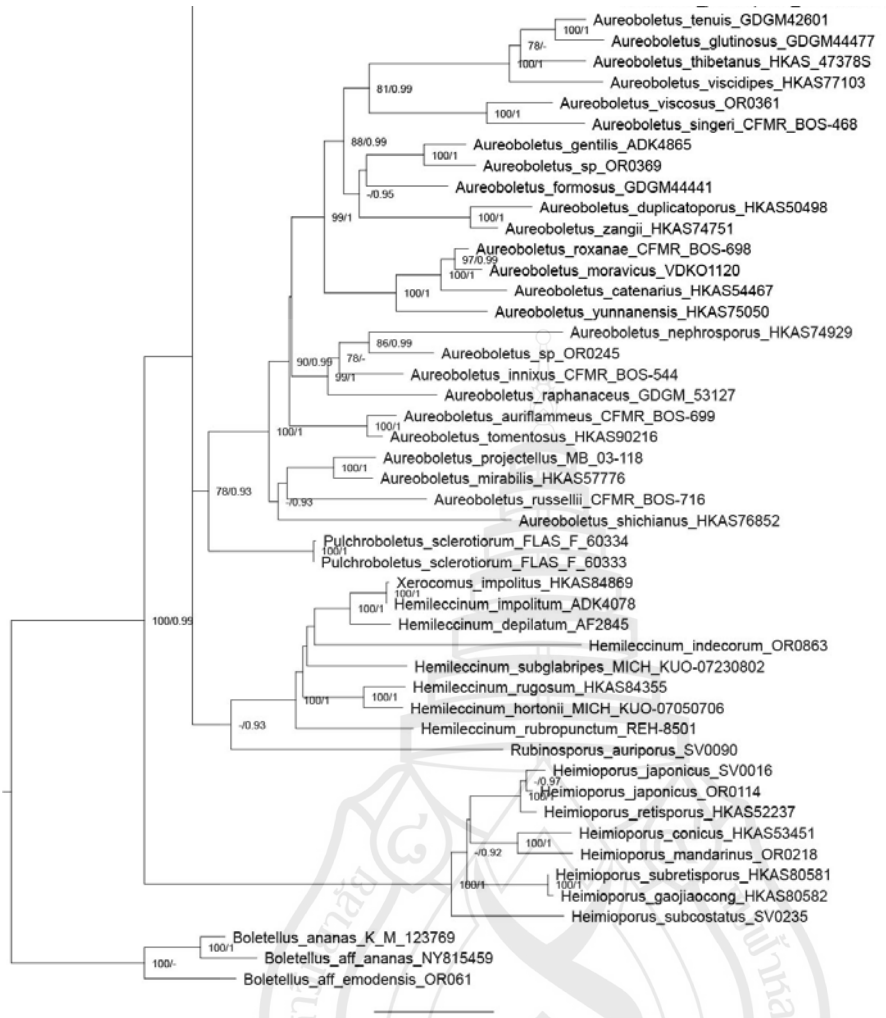


Figure 3.17 (continued)



Note Xerocomoideae phylogenetic tree inferred from the three-gene dataset (*atp*6, *rpb*2, and *tef*1), including new genus, new records of *Hourangia* and *Xerocomus*, with selected Xerocomoideae using Maximum Likelihood and Bayesian Inference methods. The three *Boletellus* were used as the outgroup. Bootstrap support values (BS ≥70%) and posterior probabilities (PP ≥0.90) are shown above the supported nodes.

Figure 3.17 Xerocomoideae phylogenetic tree inferred from the three-gene dataset (*atp*6, *rpb*2, and *tef*1)

3.3.2 Taxonomy

Hourangia microcarpa (Corner) G. Wu, Xue T. Zhu & Zhu L. Yang, Mycol Progress 14: 37 (2015), ***new geological record***

Index Fungorum number: IF 810795; MycoBank: MB 810795

≡ *Boletus microcarpus* Corner, Boletus in Malaysia (Singapore): 209 (1972)

Basdiomata small-sized, solitary, stipitate, boletoid. *Pileus* 13–33 mm in diam., circular, hemispherical to applanate; surface minutely furfurraceous-subtomentose, dark reddish brown (8F8); *margin* straight or slightly appendiculate, with sterile marginal veil; *context* 1–3 mm thick, whitish to yellowish white (4A1–2), staining dull blue very slowly when cut. *Hymenophore* tubular, adnate with decurrent tooth; *pores* 0.7–1 mm wide, radial, angular, light yellow to yellow (1A4–8), staining dull blue when bruised; *tubes* 1–7 mm long, concolorous with pores, staining dull blue when cut. *Stipe* 35–53 × 4–6 mm, central, cylindrical to tapering upwards, subpruinose, concolorous with pileus; context solid, fleshy, whitish to cream (4A1–2), staining blue when cut. *Basal mycelia* white.

Basidiospores [300/6/6] (6.8–)7.9–*8.8*–9.7(–10.5) × (3.4–)3.7–*4*–4.4(–5.6) µm, *Q* = (1.75–)1.95–*2.18*–2.42(–2.54), oblong to subcylindrical or subfusiform, with apical papilla, greyish green (1C3) in water, ammonium and potassium hydroxide solution, smooth under compound microscope, strongly bacillate under SEM. *Basidia* 25–36 × 7–11 µm, 4-spored, sterigmata 7–10 µm long, narrowly cylindrical to cylindrical or narrowly clavate to clavate, hyaline. *Hymenophoral trama* divergent; hyphae subcylindrical to cylindrical, 7–15 µm wide, hyaline. *Cheilocystidia* 33–61 × 7–12 µm, narrowly ventricose or narrowly fusiform to fusiform with some obtuse apex, hyaline. *Pleurocystidia* 38–86×8–14 µm, fusoid-ventricose, often with subacute apex, hyaline. *Pileipellis* 100–200 µm thick, a trichodermium to intricate trichodermium composed of inflated hyphae with terminal cells 20–75 × 6–16 µm, which are cylindrical to subcylindrical or sometimes subacute towards the apex, greyish yellow (1B3). *Pileal trama* composed of interwoven hyphae 7–15 µm wide, hyaline. *Stipitipellis* 60–100 µm thick, 12–32 × 5–9 µm of cylindrical or clavate terminal cells, greyish yellow (1B3), 39–89 × 9–14 µm of caulocystidia, conical, greyish yellow (1B3). *Stipe trama* composed of parallel hyphae 3–7 µm wide, hyaline. *Clamp connections* absent in all tissues.

Notes – Macro- and micro-morphology of *H. micocacrpa* specimens from Thailand match the description of Corner RSNB 8073 (holotype) the specimens from Malaysia and HKAS 83763 (epitype) from China. *Hourangia microcarpa* was originally described as

Boletus microcarpus by Corner (1972), and is characterized by its small basidioma, thick hymenophore with bluing reaction when bruised, thin context with very slow bluing reaction when bruised, and small basidiospores.

Phylogenetically, *H. microcarpa* is close to *H.* aff. *microcarpa* (OR0429), BS = 94%, PP = 0.99, but *H.* aff. *microcarpa* has a strongly crack at center of pileus with wider hymenophore (1–3 mm wide). The stipe of *H. microcarpa* is tapering upwards, while the stipe of *H.* aff. *microcarpa* is tapering downwards. Caulocystidia of *H. microcarpa* also distinct from other *Hourangia*. The previously described specimen of *H. microcarpa* from China (HKAS 53378) also grouped with our specimens with highly support.



Note Basidiomata of *Hourangia* and *Xerocomus* in the field (Scale bar = 1 cm).

Fig. 3.18 Basidiomata of *Hourangia* and *Xerocomus*

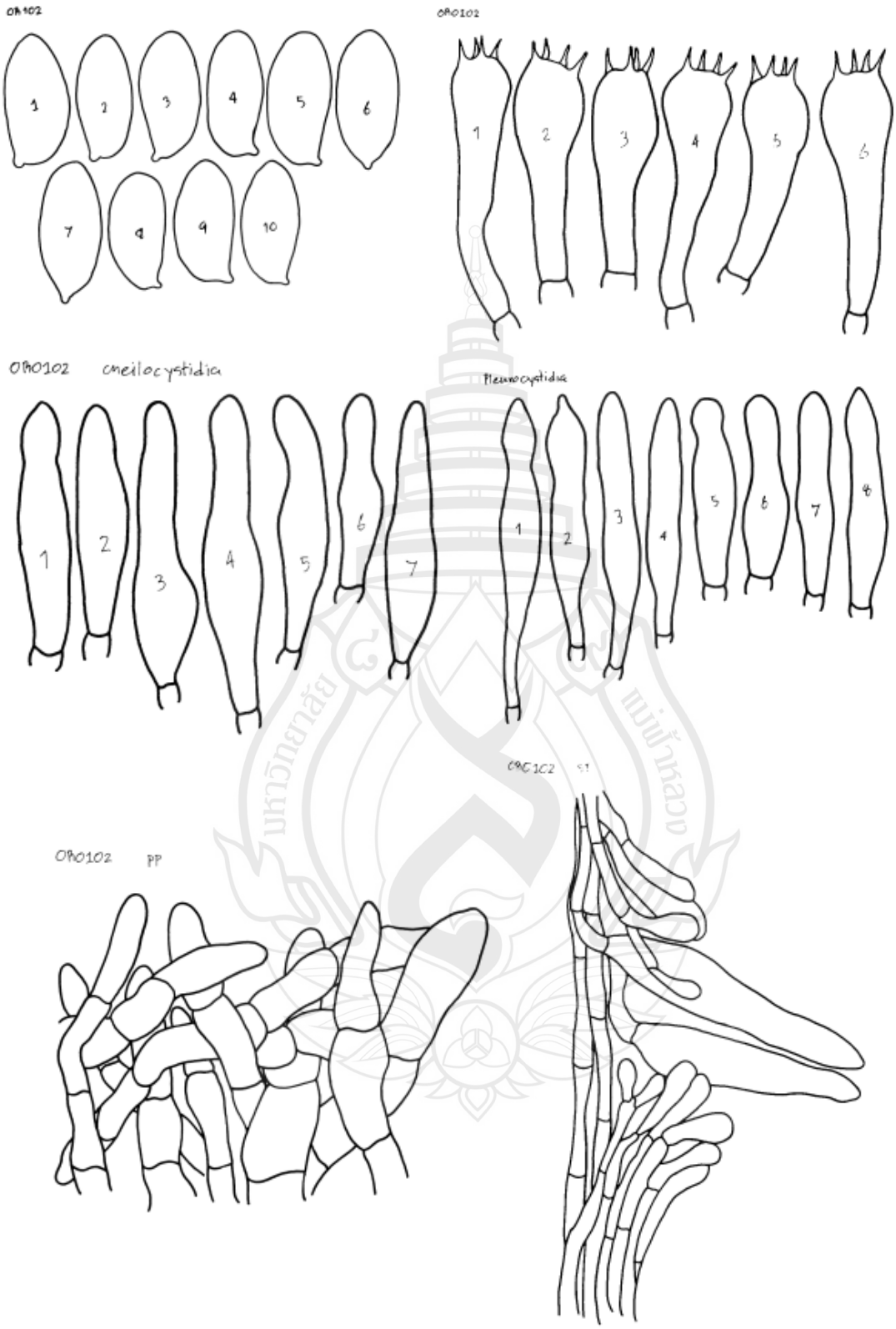


Figure 3.19 Micro-morphological characters of *Hourangia microcarpa*

Hourangia nigropunctata (W.F. Chiu) Xue T. Zhu & Zhu L. Yang, Mycol Progress 14: 37 (2015), ***new geological record***

Index Fungorum number: IF 810697; MycoBank: MB 810697

≡ *Boletus nigropunctatus* W.F. Chiu, Mycologia 40 (2): 214 (1948) [≡ *Xerocomus nigropunctatus* (W.F. Chiu) F.L. Tai, Syll. fung. sinicorum: 813 (1979)]

Basdiomata small to medium-sized, gregarious to fasciculate, stipitate, boletoid. *Pileus* 27–60 mm in diam., circular, at first hemispherical, then convex to plano-convex; surface tomentose when young, densely covered by reddish brown (8F8) and melon (5A6) squamules gradually paler to margin, becoming rimose with some granulose when aged, staining blue when bruised; margin straight; context 1–4 mm thick, yellowish white (1A2), turning blue at first, then reddening and finally blackish when cut. *Hymenophore* tubular, adanate with decurrent tooth; *pores* 1–5 mm wide, radial, subregular to irregular, angular, yellow (2A7), bluing immediately when bruised; *tubes* 4–10 mm long, concolorous with pores, staining blue when cut. *Stipe* 40–67 × 4–9 mm, central, cylindrical to clavate, melon (5A6) or cocoa (6E6); context yellowish white (1A2), bluing at first, then reddening to brownish red in a few minutes after exposed and darkening after long time. *Basal mycelia* white. *Macrochemical reactions*: Pileus, stipe, pileus, and stipe context turning brown with KOH and NH_4OH.

Basidiospores [150/4/4] (5.4–)6.3–*8.1*–9.6(–10.6) × (3–)3.4–*4*–4.5(–5) µm, *Q* = (1.39–)1.61–*2.01*–2.28(–2.5), ellipsoid to oblong with apical papilla, greyish yellow (2C3) in water, ammonium and potassium hydroxide solution, smooth under compound microscope, bacillate under SEM. *Basidia* 22–43 × 8–15 µm, 4-spored, sterigmata 3–5 µm long, clavate or cylindrical, clay (5D5) in ammonium and potassium hydroxide solution. *Hymenophoral trama* regular; hyphae cylindrical, 6–12 µm wide, light brown (5D6) to hyaline. *Cheilocystidia* 35–74 × 9–14 µm, narrowly ventricose with some obtuse apex, sunburn (6D5) in ammonium and potassium hydroxide solution. *Pleurocystidia* 34–71 × 10–17 µm, shapes same as cheilocystidia, sunburn (6D5) or hyaline in ammonium and potassium hydroxide solution. *Pileipellis* 100–200 µm thick, a trichoderm composed of short elements with 28–73 × 10–27 µm of terminal cells, short cylindrical or clavate, sunburn (6D5) in ammonium and potassium hydroxide solution. *Pileal trama* composed of interwoven hyphae 8–15 µm wide, hyaline. *Stipitipellis* 50–100 µm thick, 17–43 × 9–15 µm of caulocystidia, clavate, gloden yellow (5B7) to golden brown in ammonium and potassium hydroxide solution, with 21–52 × 6–11 µm

terminal cells, cylindrical, colour same as caulocystidia. *Stipe trama* composed of parallel hyphae 25–50 μm wide, colour same as caulocystidia. *Clamp connections* absent in all tissues.

Notes – *Hourangia nigropunctata* (≡ *Boletus nigropunctatus* W.F. Chiu) is characterized by its small to medium-sized basidioma and small spores (7.5–9×3.5–4.0 μm). The size and color of *H. nigropunctata* pileus are very similar to *H. cheoi*. However, the spores of *H. nigropunctata* (Q_m = 2.01) is longer than those from *H. cheoi* (Q_m = 2.48). The HKAS 76657 was designated as the epitype of this species after re-combination.

Also, the combined phylogenetic analyses indicated the sequences from the Thai specimens clustered with those of *H. nigropunctata* from China (HKAS 57427, 76657, Li1010) with BS = 100%, PP = 0.99.

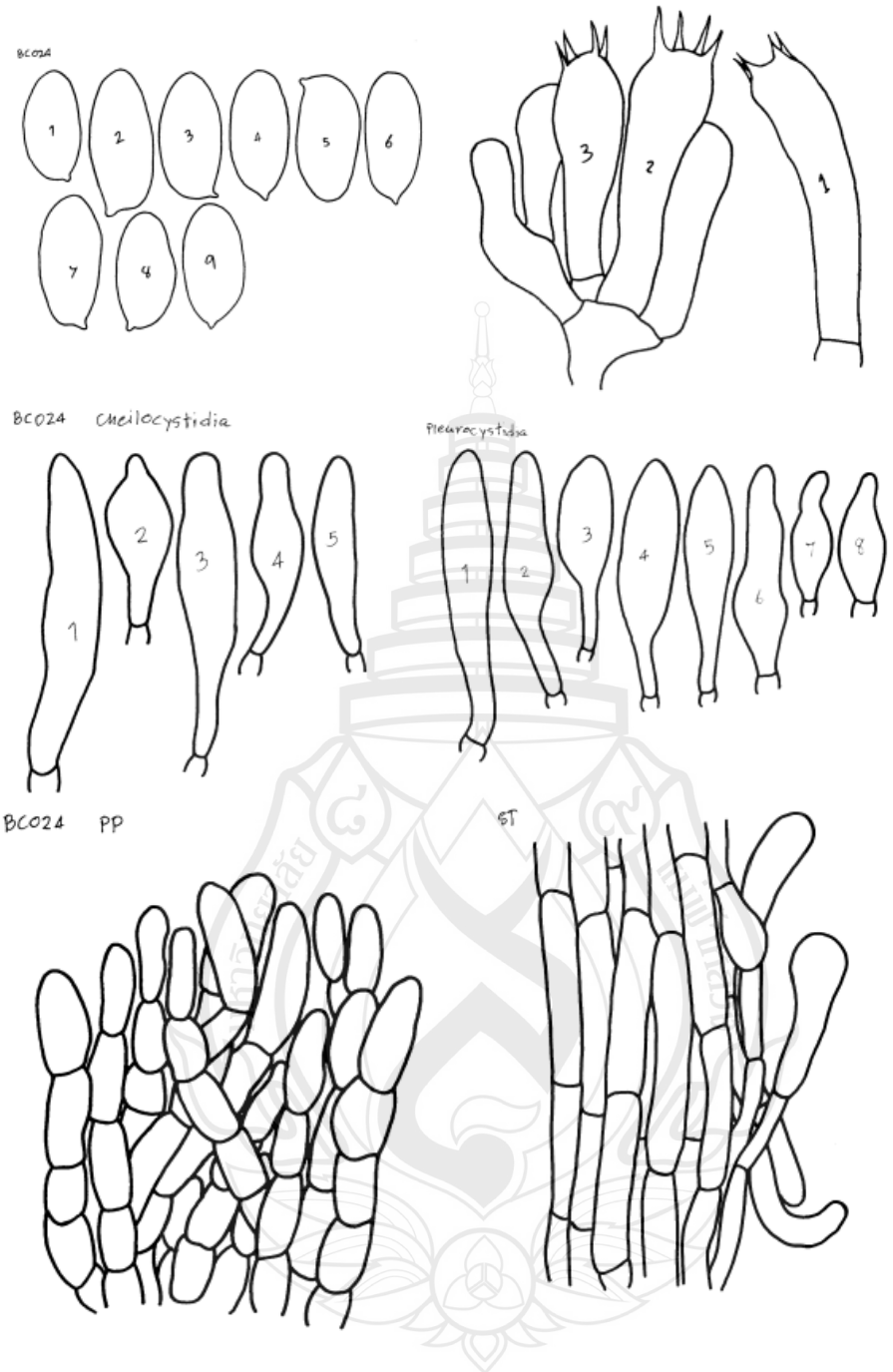


Figure 3.20 Micro-morphological characters of *Hourangia nigropunctata*

Hourangia* aff. *microcarpa

Basdiomata small-sized, caespitose, stipitate, boletoid. *Pileus* 33–34 mm in diam., circular, applanate; surface rimose with cracks on the center and regularly with crevices toward to the margin, subtomentose, rust brown (6E8) at the center then gradually paler to margin;

margin straight; context 1–5 mm thick, white (1A1). *Hymenophore* tubular, adanate with decurrent tooth; *pores* 1–3 mm wide, radial, subregular to irregular, angular, sun yellow (2A5), strongly cyanescent on bruising; *tubes* 6–7 mm long, concolorous with pores strongly cyanescent on bruising. *Stipe* 29–33 × 4–6 mm, central, tapering downwards, subpruinose, concolorous with pileus; context light brown (7D5). *Basal mycelia* white.

Basidiospores [100/2/1] (8.1–)8.4–*9.4*–10.4(–11.1) × (3.6–)3.6–*4*–4.3(–4.6) µm, *Q* = (1.97–)2.15–*2.33*–2.54(–2.83), fusiform with apical papilla, greyish green (1C3) in water, ammonium and potassium hydroxide solution, smooth under compound microscope, bacillate under SEM. *Basidia* 21–37 × 10–14 µm, 4-spored, sterigmata 2–4 µm long, clavate, hyaline. *Hymenophoral trama* regular; hyphae cylindrical, 6–9 µm wide, hyaline. *Cheilocystidia* 43–79 × 10–15 µm, fusiform to ventricose, sometimes constricted at the base, hyaline. *Pleurocystidia* 43–70 × 7–13 µm, fusiform to ventricose, with some subacute apex, sometimes constricted at the base, hyaline. *Pileipellis* 120–200 µm thick, a trichoderm composed of inflated hyphae with terminal cells 27–70 × 11–21 µm, subcylindrical or sometimes subacute towards the apex, ivory (4B3) in ammonium and potassium hydroxide solution. *Pileal trama* composed of interwoven hyphae 10–15 µm wide. *Stipitipellis* 50–100 µm thick, with 23–44 × 5–9 µm terminal cell, cylindrical, golden wheat (4B5) in ammonium and potassium hydroxide solution. *Stipe trama* composed of parallel hyphae 7–14 µm wide, colour same as terminal cells. *Clamp connections* absent in all tissues.

Notes – Morphology of *Hourangia* aff. *microcarpa* quite similar to *H. microcarpa.* In contrast, *H.* aff. *microcarpa* has a strongly crack at center of pileus with wider hymenophore (1–3 mm wide). The stipe of *H. microcarpa* is tapering upwards, while the stipe of *H.* aff. *microcarpa* is tapering downwards. *Hourangia* aff. *microcarpa* (OR0429) is close to *H. microcarpa* with BS = 94%, PP = 0.99. Here, the voucher OR0429 was designed as *H.* aff. *microcarpa*, multiple collection needs to be investigated to confirm their novelty.

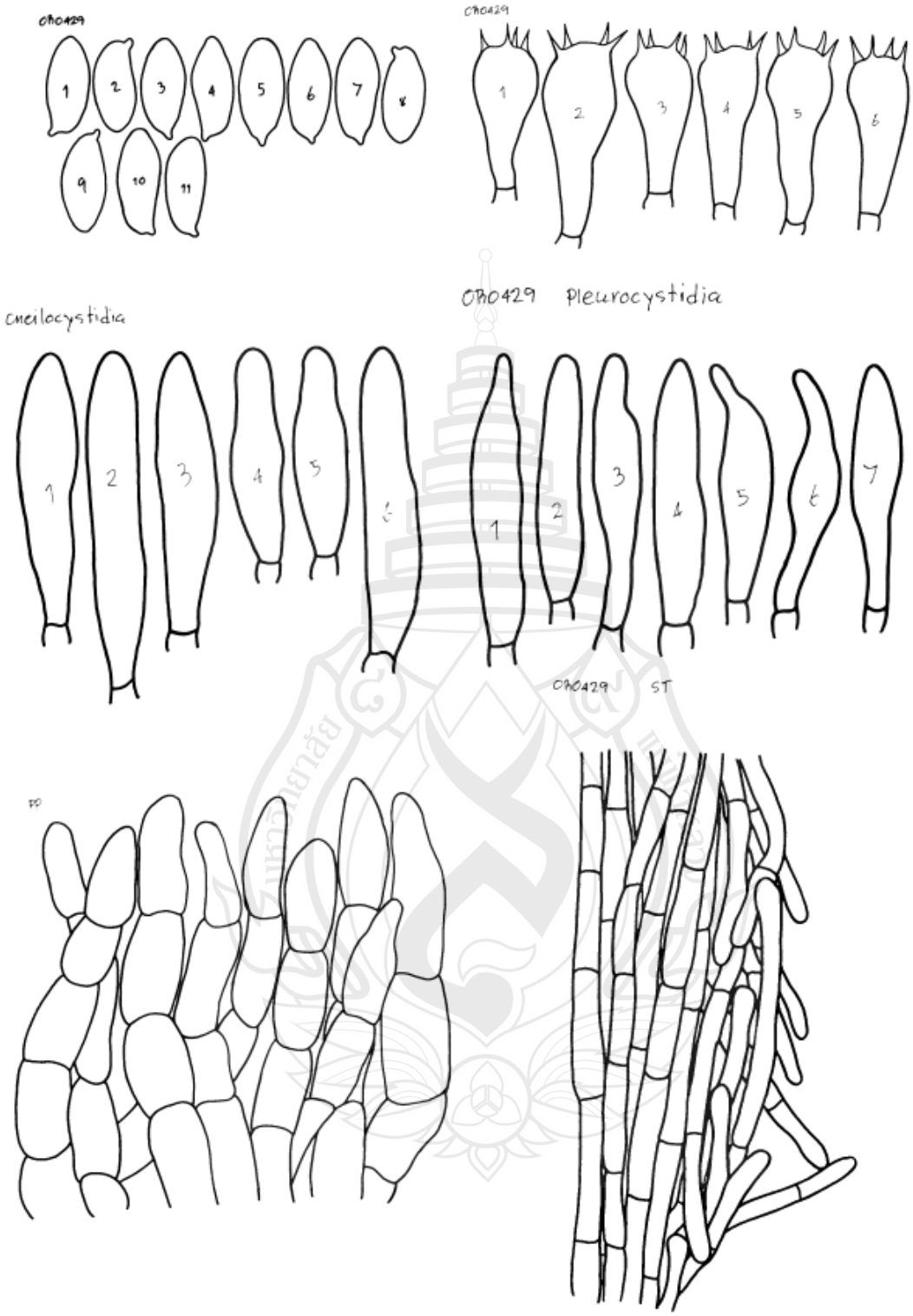


Figure 3.21 Micro-morphological characters of *Hourangia aff. microcarpa*

***Hourangia* 1** sp. nov.

Basdiomata small-sized, caespitose, stipitate, boletoid. *Pileus* 22–33 mm in diam., circular, hemispherical when young, convex to plano-convex with aged, velutinous, yolk yellow (4B8); margin straight; context 4–7 mm thick, white (1A1), staining pale blue when cut. *Hymenophore* tubular, adanate with decurrent tooth; *pores* 0.4–3 mm wide, regular, angular, yellow (2A6), cyanescent on bruising; *tubes* 3–5 mm long, concolorous with pores, cyanescent on bruising. *Stipe* 34–51 × 7–13 mm, central, cylindrical to tapering upwards, slightly curved, subpruinose, concolorous with pileus; context fleshy, light brown (6D7). *Basal mycelia* white.

Basidiospores [100/2/2] (7.3–)7.8–*8.7*–9.5(–9.8) × (3.9–)4–*4.3*–4.7(–5) µm, *Q* = (1.58–)1.83–*2.04*–2.25(–2.34), ellipsoid to subcylindrical with apical papilla, greyish yellow (2C3) in water, ammonium and potassium hydroxide solution, smooth under compound microscope, bacillate under SEM. *Basidia* 27–39 × 8–12 µm, 4-spored, sterigmata 3–5 µm long, clavate, golden wheat (4B5) or hyaline in water, ammonium and potassium hydroxide solution. *Hymenophoral trama* regular; hyphae subcylindrical to cylindrical, 6–15 µm wide. *Cheilocystidia* 42–94 × 11–16 µm, ventricose, hyaline. *Pleurocystidia* 36–78 × 9–15 µm, ventricose, hyaline. *Pileipellis* 120–180 µm thick, a palisade composed of inflated hyphae with terminal cells 30–78 × 10–21 µm, subcylindrical or sometimes subacute towards the apex, hyaline. *Pileal trama* composed of interwoven hyphae 9–17 µm wide, hyaline. *Stipitipellis* 60–100 µm thick, caulocystidia 37–85 × 7–14 µm, clavate, sun burn (6D5) or hyaline. *Stipe trama* composed of parallel hyphae 7–12 µm wide, hyaline. *Clamp connections* absent in all tissues.

Notes – *Hourangia* sp. 1 is mostly resembled to *H. densisquamata* N.K. Zeng, Yi Wang & Zhi Q. Liang and *H. dilatata* N.K. Zeng, Yi Wang, S. Jiang & Zhi Q. Liang based on morphology. Both species were described from China by Wang et al. (2020). *Hourangia densisquamata* is characterized by a pileus densely covered with pale brown to brown squamules, a bluish color change of hymenophore and context, a stipe covered with brown squamules and a layer of white pruina, more or less inflated hyphae in the pileipellis. *Hourangia dilatata* is characterized by relatively small basidiomata, a pileus densely covered with pale brown to brown squamules, a bluish color change of hymenophore and context, basidiospores smaller than those of *H. densisquamata*, thick-walled cystidia (up to 1.5 µm), and inflated hyphae in the pileipellis. The characters mention before are matched with our descriptions, except, the pileus surface of *H.* sp. 1 is more likely a dotted of velutinous granules.

Hourangia microcarpa is more closely related to *H*. sp. 1 (BS = 70, PP = 0.94), but the pileus of *H*. *microcarpa* is usually cracked on the surface with some reddish tinge.

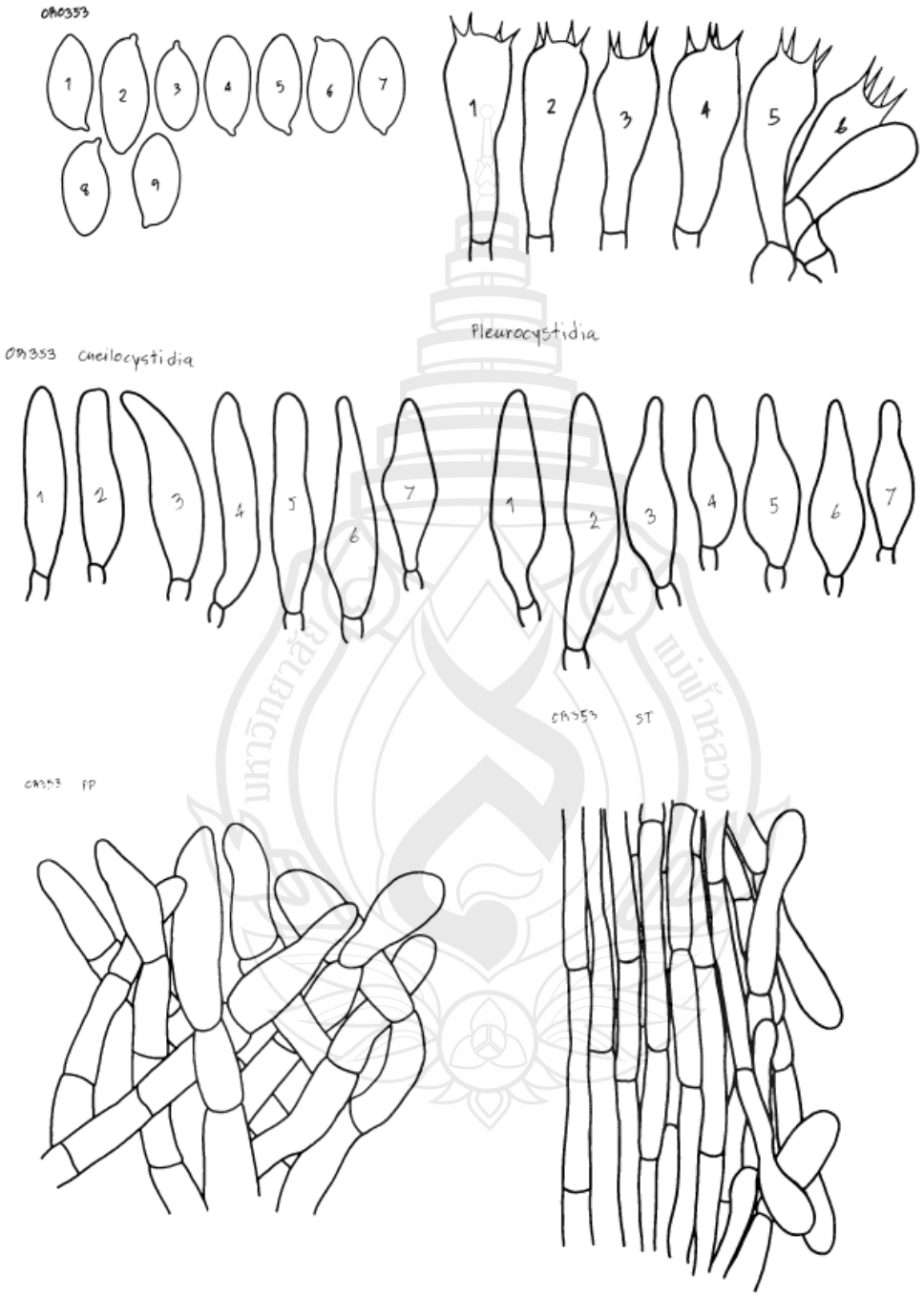


Figure 3.22 Micro-morphological characters of *Hourangia* 1 sp. nov.

***Hourangia* 2** sp. nov.

Basdiomata small-sized, solitary, stipitate, boletoid. *Pileus* 20 mm in diam., circular, plano-convex, densely tomentose at center, coarsely rimose with cracked towards to the margin, dark brown (6F8) at the center with light brown (6D7) cracked part; margin straight; context 0.5–1 mm thick, beige (4A3). *Hymenophore* tubular, adanate with decurrent tooth; *pores* 0.5–1 mm wide, radial, roundish to slightly angular, yellow (3A6), cyanescent then blackened on bruising; *tubes* 1–3 mm long, concolorous with pores, cyanescent on bruising. *Stipe* 35 × 2 mm, central, cylindrical, subpruinose, sunburn (5D5); context sunburn (5D5). *Basal mycelia* white.

Basidiospores [50/1/1] (9–)9.1–*10*–11.3(–11.8) × (3.9–)4–*4.6*–5(–5.2) µm, *Q* = (1.9–)1.93–*2.17*–2.44(–2.67), subcylindrical with apical papilla, greyish green (1C3) in water, ammonium and potassium hydroxide solution, smooth under compound microscope, bacillate under SEM. *Basidia* 25–42 × 8–12 µm, 4-spored, sterigmata 2–4 µm long, narrowly clavate to clavate, pale yellow (3A3) or hyaline in water, ammonium and potassium hydroxide solution. *Hymenophoral trama* regular to subregular; hyphae subcylindrical to cylindrical, 6–11 µm wide, pale yellow (3A3) or hyaline in water, ammonium and potassium hydroxide solution. *Cheilocystidia* and *pleurocystidia* absent. *Pileipellis* 50–100 µm thick, a palisade composed of inflated hyphae with terminal cells 20–37 × 8–14 µm, subcylindrical, hyaline. *Pileal trama* composed of interwoven hyphae 6–10 µm wide, hyaline. *Stipitipellis* up to 80 µm thick, with 16–29 × 5–8 µm terminal cells, light brown (5D5). *Stipe trama* composed of parallel hyphae 6–10 µm wide, hyaline. *Clamp connections* absent in all tissues.

Notes – From the descriptions of young basidiomes of OR0669, the pileus surface and hymenophore are the most remarkable characteristics among other *Hourangia*. The statistical support is high (BS = 100, PP = 1). Due to the specimen condition, some morphological characters still lack. The fully developed specimen with multiple collection is required. For this, the voucher OR0669 is designed as *Hourangia* sp.

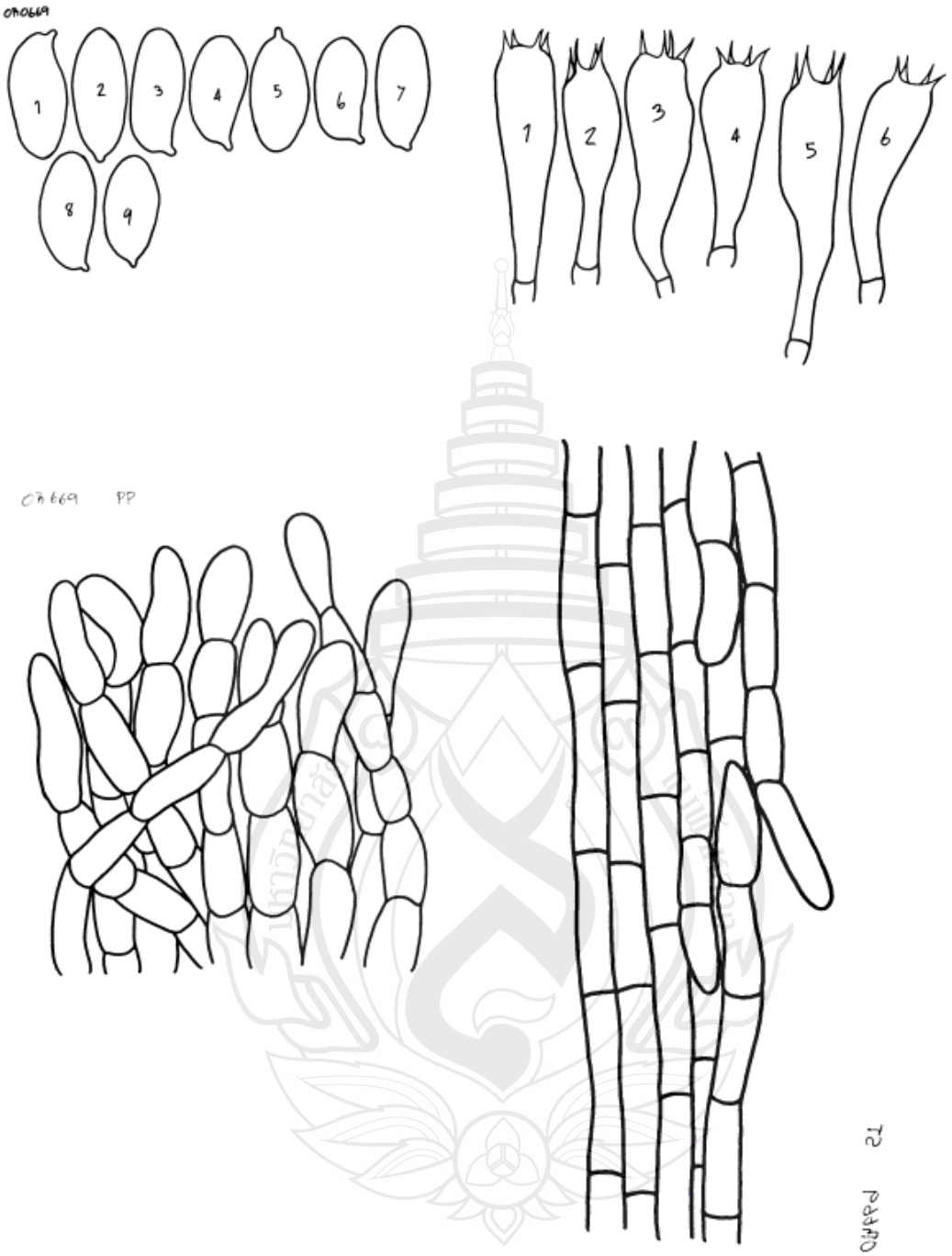


Figure 3.23 Micro-morphological characters of *Hourangia* 2 sp. nov.

***Xerocomus* 1** sp. nov.

Basidioma small to medium-sized, solitary, stipitate, boletoid. *Pileus* 23–63 mm in diam., hemispherical to clavate or applanate to slightly plano-concave; surface densely tomentose, oak brown (5D6), golden brown (4B5) or dark brown (6F8); context 1–17 mm thick, white (1A1), orange white (5A2) or light yellow (3A4). *Hymenophore* tubular, adnate, sinuate or adnate with decurrent tooth; *pores* 0.2–4 mm in diam., compound, angular, regular to subregular, pale yellow (3A3) to yellow (3A7), staining blue when bruised; *tubes* 1–7 mm long, concolorous with pores, staining blue when cut. *Stipe* 31–60 × 3–16 mm, central, subcylindrical to tapering upwards, slightly curved, sunburn (6D5) light brown (7D5), with fine longitudinal striations; context concolorous with pileus context. *Basal mycelium* white.

Basidiospores [350/7/5] (6.7–)7.8–*8.9*–9.9(–10.8) × (3.2–)4–*4.4*–4.9(–5.5) µm, *Q* = (1.61–)1.75–*2.01*–2.27(–2.48), ellipsoid to subcylindrical with apical papilla, greyish green (1C3) in water, ammonium and potassium hydroxide solution, smooth under compound microscope, bacillate under SEM. *Basidia* 24–36 × 8–12 µm, 4-spored, sterigmata 2–4 µm long, clavate, hyaline. *Hymenophoral trama* subregular, hyphae subcylindrical to cylindrical, 6–10 µm wide, hyaline. *Cheilocystidia* 30–53 × 9–14 µm, scattered, lanceolate to ventricose, hyaline. *Pleurocystidia* scattered, 31–41 × 7–12 µm, lanceolate to ventricose, hyaline. *Pileipellis* 100–200 µm thick, a trichoderm composed of hyaline hyphae; 26–77 × 7–15 µm terminal cells, subcylindrical tocylindrical, hyaline. *Pileal trama* composed of interwoven hyphae 7–12 µm wide, hyaline. *Stipitipellis* up to 60–120 µm thick, 17–30 × 8–13 µm terminal cells, clavate, hyaline. *Stipe trama* composed of parallel hyphae 7–11 µm wide, hyaline. *Clamp connections* absent in all tissues.

Notes – Based on multi-genes phylogeny, *Xerocomus* sp. 1 allied to *Xerocomus fraternus* Xue T. Zhu & Zhu L. Yang and undescribed species from China (BS = 98, PP = 100). *Xerocomus* sp. 1 can be differentiated from *X. fraternus* by pores turn bluing when injured, and white context of stipe. While, *X. fraternus* pores is turning red-brown tinge with red-brown context of stipe near the stipe surface. The pileipellis which are yellow-brown in water for *X. fraternus* but hyaline in all solutions for *X.* sp. 1.

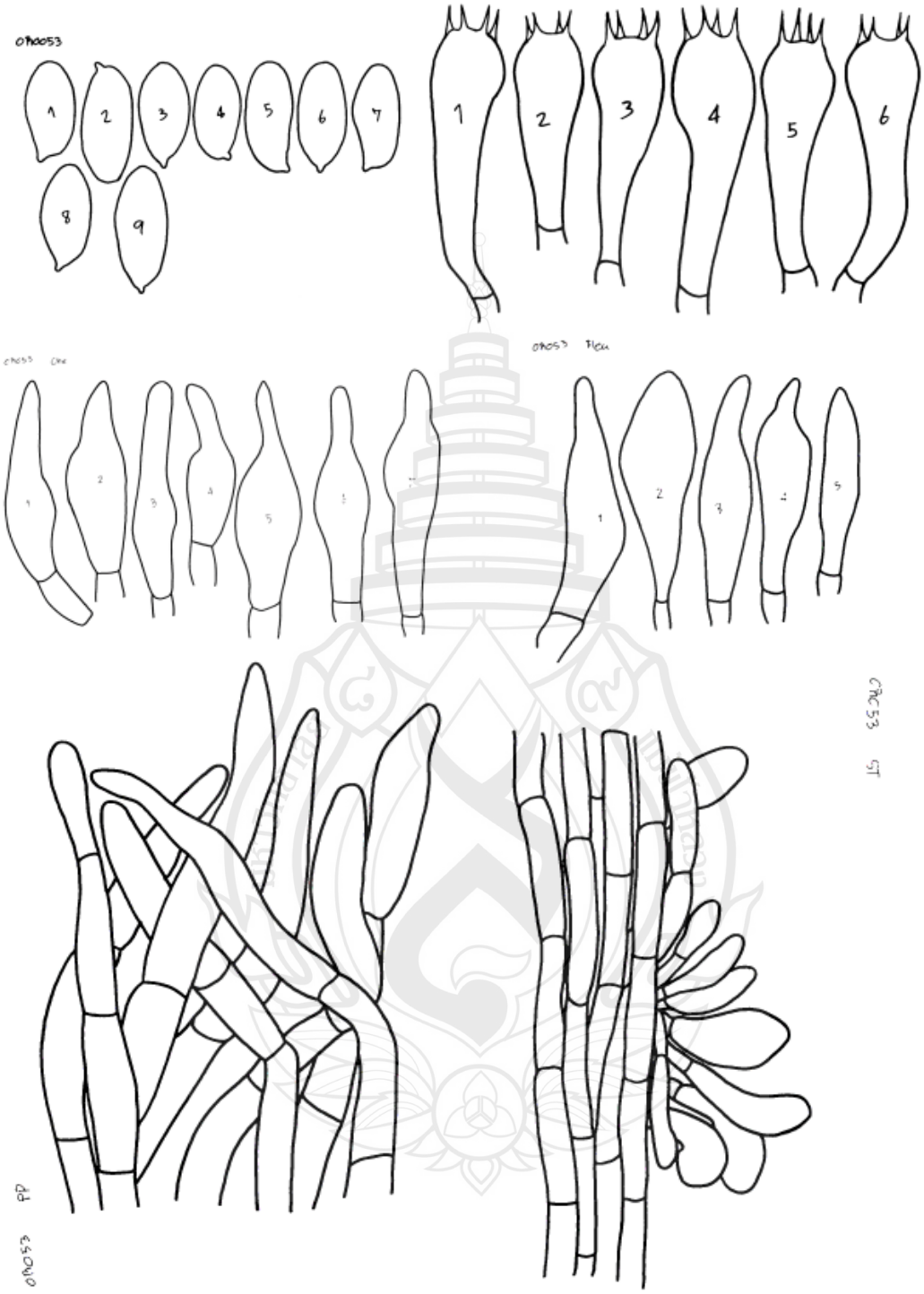


Figure 3.24 Micro-morphological characters of *Xerocomus* 1, sp. nov.

***Xerocomus* 2** sp. nov.

Basidioma small to medium-sized, solitary, stipitate, boletoid. *Pileus* 34–78 mm in diam., convex to applanate, densely tomentose, dark brown (6F8), becoming light brown (6D5) when age; context 3–9 mm thick, white (1A1) to light yellow (1A5), staining bluish slowly or faintly bluish when injured. *Hymenophore* tubular, adnate to sinuate with decurrent tooth; *pores* 0.5–3 mm in diam., compound, angular, regular, light yellow (3A4) when young, greenish yellow (1A8) to vivid yellow (2A8) with age, staining blue slowly or indistinctly when bruised; *tubes* 3–7 mm long, concolorous with pores, bluing slowly when injured. *Stipe* 30–59 × 5–11 mm, central, cylindrical to subcylindrical, with some slightly tapering upwards, yellow (2A7) around apical part, rust brown (6E8) in other part, fine longitudinal striations half from apical, with some cracked scaly at the base when aged; context white (1A1) to light yellow (2A4) on the upper part, cinnamon (6D6) on the lower part, staining bluish slowly or indistinctly when injured. *Basal mycelium* white.

Basidiospores [250/5/5] (8.8–)9.7–*11.4*–13(–13.8) × (4.2–)4.4–*4.8*–5.3(–6) µm, *Q* = (1.77–)2.03–*2.35*–2.68(–2.96), fusiform to broadly fusiform with apical papilla, greyish yellow (3C3) in water, ammonium and potassium hydroxide solution, smooth under compound microscope, bacillate under SEM. *Basidia* 26–36 × 9–12 µm, 4-spored, sterigmata 3–4 µm long clavate, dull yellow (3B3) in water, ammonium and potassium hydroxide solution. *Hymenophoral trama* regular to sunregular, hyphae subcylindrical to cylindrical, 6–10 µm wide, hyaline. *Cheilocystidia* 31–61 × 8–14 µm, scattered, ventricose, colour same as basidia. *Pleurocystidia* 31–44 × 9–12 µm, scattered, ventricose with some mucronate apex, colour same as basidia and cheilocystidia. *Pileipellis* 60–160 µm thick, an ixotrichoderm composed of 26–46 × 8–14 µm terminal cells, subcylindrical with some subobtuse apex, hyaline. *Pileal trama* composed of interwoven hyphae 7–14 µm wide, hyaline. *Stipitipellis* 60–100 µm thick, composed of 18–38 × 6–13 µm terminal cells, clavate or cylindrical, wax yellow (3B5) in water, ammonium and potassium hydroxide solution. *Stipe trama* composed of parallel hyphae 6–10 µm wide, hyaline. *Clamp connections* absent in all tissues.

Notes – The new species could be distinguished from other by their stipe that yellow around apical part, rust brown in other part, fine longitudinal striations half from apical, with some cracked scaly at the base when aged. Microscopically, the ixotrichoderm pileipellis were found in the pileus. *Xerocomus fulvipes* Xue T. Zhu & Zhu L. Yang is closely related to our new species except the pileipellis is not the same. Phylogenetically, *X. fulvipes* (BS = 100, PP

= 1) and *X. subtomentosus* (BS = 99, PP = 1) is closely related to new species. However, *X. subtomentosus* differs from new species in its dirty white to yellowish stipe. Also, the trichoderm pileipellis that was not found in novel species as mention above.

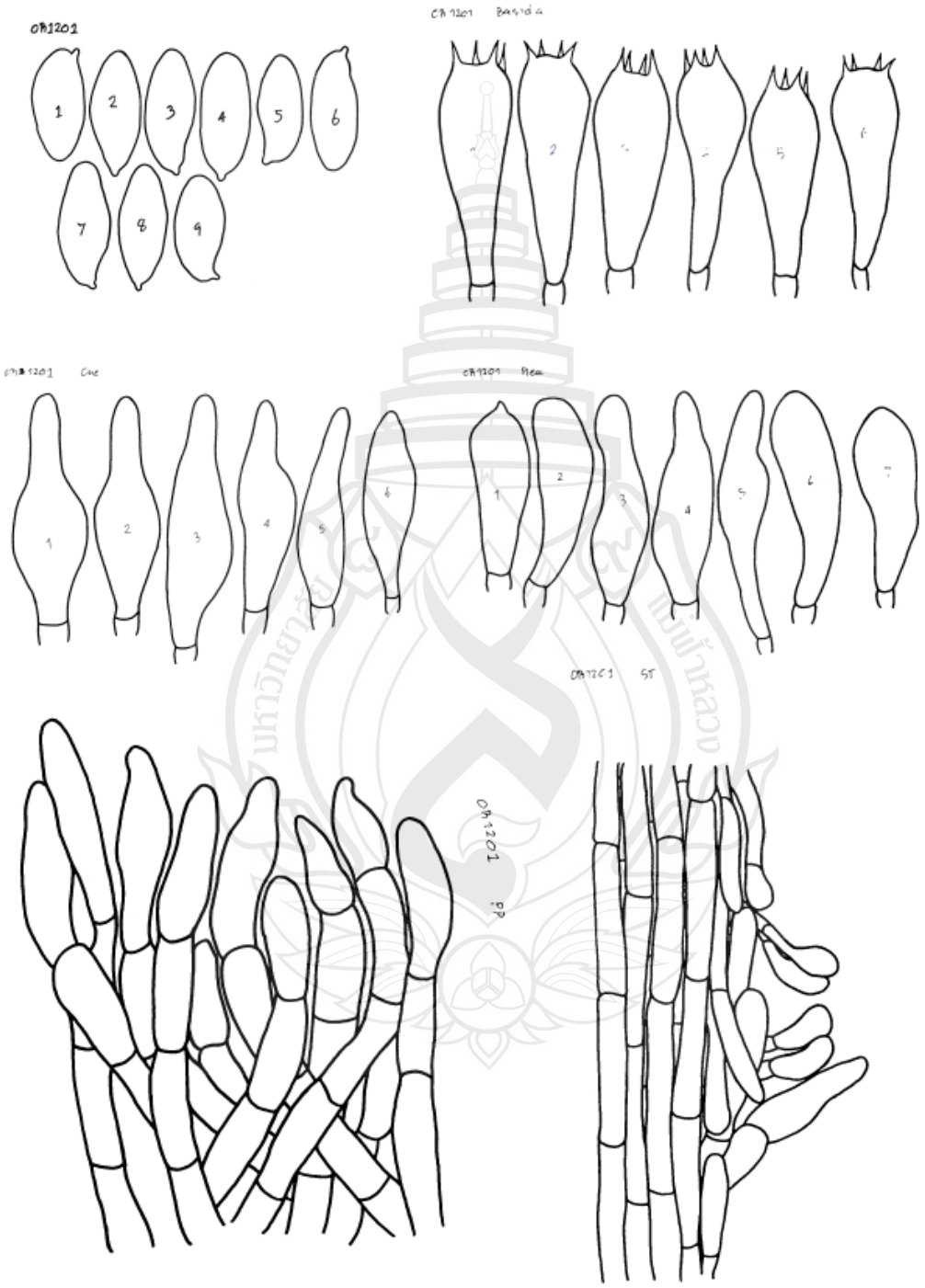


Figure 3.25 Micro-morphological characters of *Xerocomus* 2 sp. nov.

Xerocomus microcarpoides

Basidioma small to medium-sized, solitary, stipitate, boletoid. *Pileus* 25–56 mm in diam., circular, convex to applanate, densely tomentose, camel (6D4) to cinnamon (6D6); context 3–9 mm thick, white (1A1) to pale yellow (1A3), staining bluish slowly or indistinctly when injured. *Hymenophore* tubular, adnate with decurrent tooth; *pores* 0.3–2 mm in diam., compound, angular, greenish yellow (1A7) to yellow (2A7), staining blue, then reddening and blackened with time when bruised; *tubes* concolorous with pores, staining blue when cut. *Stipe* 20–72 × 3–14 mm, subcylindrical, slightly tapering upwards, light yellow (2A5) around the apical, with brown mahogany (8E7) fine granular on upper part, lower part brown mahogany (8E7) with fine longitudinal striations; context pale yellow (3A3). *Basal mycelium* white.

Basidiospores [100/2/2] (7.9–)9–*10.3*–11.5(–12.6) × (3.7–)3.8–*4.3*–4.7(–5.1) µm, *Q* = (1.81–)2.09–*2.42*–2.66(–2.71), fusiform with apical papilla, greyish yellow (3C3) in water, ammonium and potassium hydroxide solution, smooth under compound microscope, bacillate under SEM. *Basidia* 23–37 × 8–11 µm, 4-spored, sterigmata 3–4 µm long, clavate, with small granules, hyaline. *Hymenophoral trama* regular, hyphae subcylindrical to cylindrical, 6–11 µm wide, hyaline. *Cheilocystidia* 33–61 × 7–12 µm, abundant, lanceolate, clavate to ventricose, some obtuse apex, with small granules, hyaline. *Pleurocystidia* 35–67 × 9–16 µm, abundant, lanceolate to ventricose, with small granules, hyaline. *Pileipellis* up to 100 µm thick, an irregular trichoderm, composed of 28–60 × 7–13 µm terminal cells, subcylindrical, with small granules, hyaline. *Pileal trama* composed of interwoven hyphae 6–12 µm wide, hyaline. *Stipitipellis* up to 100 µm thick, 32–57 × 6–12 µm caulocystidia, clavate to narrowly conical, with small granules and incrusted pigments in ammonium, potassium hydroxide with/without congo red solution, composed of 16–35 × 5–8 µm terminal cells, cylindrical or clavate, with small granules and incrusted pigments in ammonium, potassium hydroxide with/without congo red solution. *Stipe trama* composed of parallel hyphae 6–14 µm wide, with incrusted pigments in ammonium, potassium hydroxide with/without congo red solution. *Clamp connections* absent in all tissues.

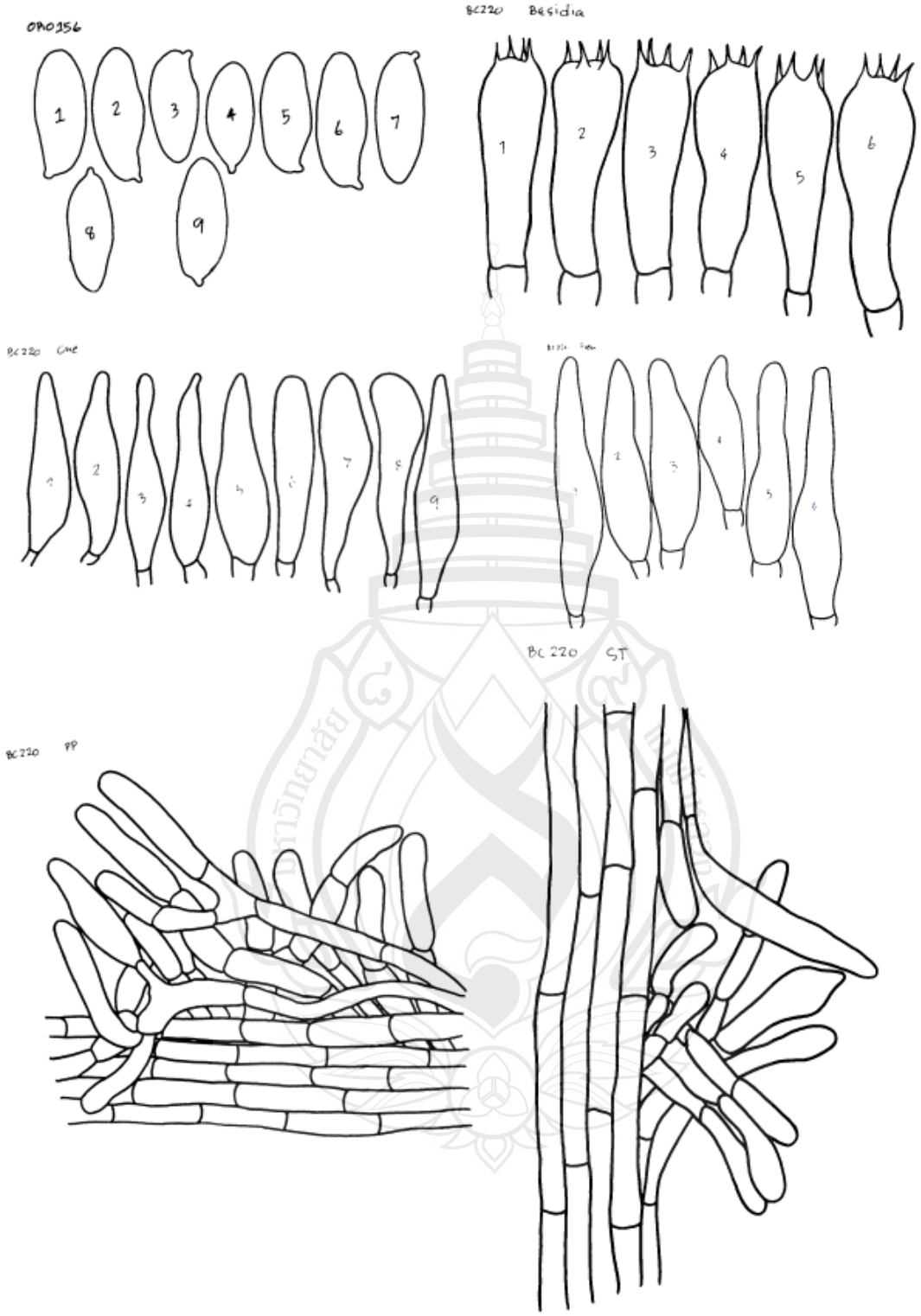


Figure 3.26 Micro-morphological characters of *Xerocomus microcarpoides*

3.4 Cultivation and Identification of Blazeispirols from Wild *Agaricus campestroides* and *A. flocculosipes*

3.4.1 Confirmation of the Identity of the Cultivated Species

Agaricus campestroides Heinem. & Gooss.-Font., Bull. Jard. bot. Brux. 26: 20 (1956), ***new geological record***

Index Fungorum number: IF292252

Pileus at first hemispherical, becoming convex, broadly convex to plano-convex; surface white to cream-colour, ochraceous, with greyish to pale ochraceous fibrils darker to margin, dry; margin incurved at first, finally expanding to decurved. ***Lamellae*** free, dark brown, crowded, with lamellulae**.** ***Stipe*** central, cylindrical; surface white and silky, white appressed fibrils. ***Spores print*** dark brown, anise-like smell.

Basidiospores 6.0–8.0 × 4.0–4.5 µm, *Q* = 1.71, ellipsoid, inamyloid, dark brown, with apical endosporium. ***Basidia*** 14–17 × 6–7 µm, clavate, 4-spored. ***Cystidia*** 9–18 × 7–13 µm, subspherical or clavate, hyaline, smooth. ***Pileipellis*** a trichoderm; hyphae 9–11 µm in diameter, cylindrical, hyaline. ***Stipitipellis*** a cutis of hyphae 6–10 µm in diameter, cylindrical, smooth, hyaline. ***Clamp connections*** absent in all tissues.

Culture characters: After 21 days of incubation in PDYA medium, the agar surface was fully colonized with a white mycelium. The mycelium is linear to thread-like hyphae.

Material examined: Thailand, Chiang Rai, Muang Chiang Rai, Mae Fah University, on grassland, 20 June 2014, B. Chuankid, BC079 (MFLU 14–0872); living culture, MFLUCC 14–1024.

Hosts: On grassland soil—(Dejene et al., 2017; this study).

Distribution: Ethiopia, Thailand—(Dejene et al., 2017; this study).

GenBank accession numbers: ITS: MZ596239.

Notes: The nrITS nucleotide sequences of MFLU 14–0872 revealed that the most similar sequences were from *A. campestroides* JF727842 from Togo (Zhao et al., 2011), at 99.03% similarity with 96% query cover. From Index Fungorum, this species was listed in *Micropsalliota campestroides* (Heinem. & Gooss.-Font.) Heinem. The comparison between the type specimen and our specimen were not similar. The shapes of basidia and cystidia of our specimens were subspherical or clavate, while the type specimen is another shape (claviforms

basidia and inconspicuous cystidia). Pileipellis also not incrusted with pigments like other *Micropsalliota*. From this, our specimen fits to the descriptions of *Agaricus*.

Agaricus flocculosipes R.L. Zhao, Desjardin, Guinb. & K.D. Hyde, Mycoscience 53: 302 (2012)

Index Fungorum number: IF561690

The basidiomata of MFLU 14–0874 that grew in the wild was confirmed as the same species as *A. flocculosipes*. The floccose stipe, almond odour, well-developed squamules on the pileus, two-layered annulus, and catenulate cheilocystidia were typical of the species (Thongklang et al., 2014).

Basidiospores 5.0–6.5 × (3.5–4.0) µm, *Q* = 1.61, ellipsoid, with apical endosporium, smooth, reddish brown, thick walled. ***Basidia*** 10–13 × 4–6 µm, clavate, 4-spored. ***Cystidia*** 40–46 × 8–12 µm, narrowly conical or fusiform to narrowly utriform, hyaline, smooth. ***Pileipellis*** a cutis; hyphae 6–8 µm in diameter, cylindrical, straight or curved, with brown pigments. ***Stipitipellis*** a cutis of hyphae 5–8 µm in diameter, cylindrical, smooth, hyaline. ***Clamp connections*** absent in all tissues.

Culture characters: After 21 days of incubation in MYPA medium, the agar surface was colonized with a white mycelium. The mycelium is circular with smooth hyphae.

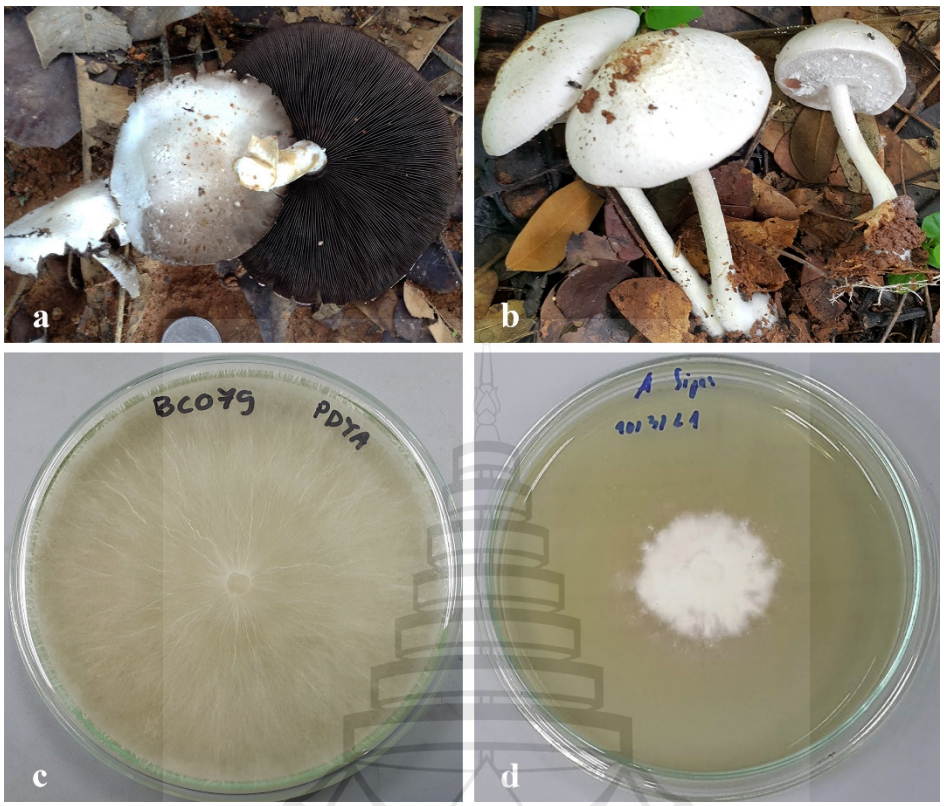
Material examined: Thailand, Chiang Rai, Muang Chiang Rai, Mae Fah University, on grassland, 9 Jul 2014, B. Chuankid, MFLU 14–0874.

Hosts: on rich soil or over heavily rotted wood in forests or grassland soil—(Zhao et al. 2012; Gui et al. 2015; this study).

Distribution: Thailand and China—(Zhao et al., 2012; Gui et al., 2015; this study).

GenBank accession numbers: ITS: MZ596240.

Notes: The collection has identical morphology with *A. flocculosipes*, nrITS nucleotide sequence was subjected to a BLAST search against the NCBI database. The nrITS nucleotide sequences in the NCBI database revealed that the most similar sequences were from *A. flocculosipes* KP705076 from Thailand (Thongklang et al., 2016), at 100% similarity with 96% query cover.



Note a: *Agaricus campestroides* (MFLU 14–0872) and b: *Agaricus flocculosipes* (MFLU 14–0874) in the wild. c: the mycelia growth of *A. campestroides* on PDYA medium and d: *Agaricus flocculosipes* on MYPA medium after 30 days.

Figure 3.27 *Agaricus campestroides* (MFLU 14–0872) and *Agaricus flocculosipes* (MFLU 14–0874) in the wild and the mycelia growth

3.4.2 Effect of Media on Mycelia Growth

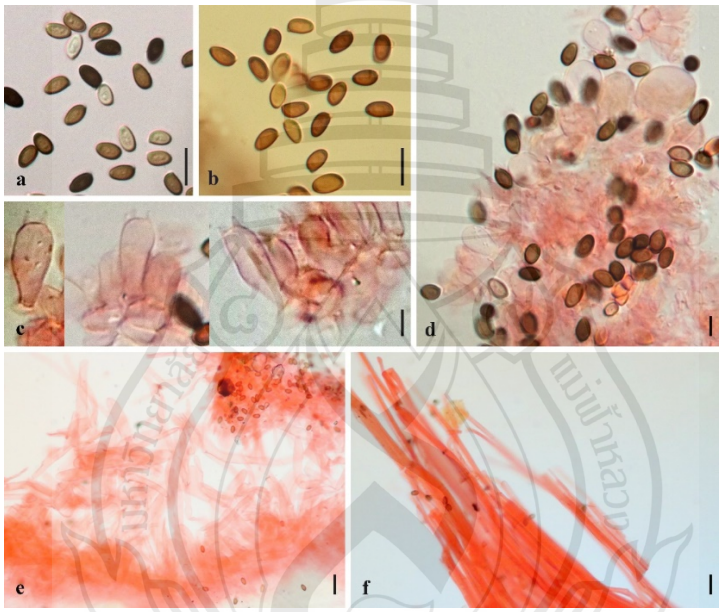
In *A. campestroides*, the largest radial mycelial growth was observed on PDYA, MEA, PDA, and MYPA, respectively. The colour characteristics of the surface mycelium were not different for the four media types. The morphology of the colony was filamentous on all media. The maximum yield by dry weight mycelium occurred on PDYA, followed by MEA, PDA, and MYPA. The same mycelia character was found on *A. flocculosipes* (MFLU 14–0874). The maximum yield by dry weight mycelium occurred on MYPA, followed by PDYA, PDA, and MEA but the data were not significantly different among four media. The effect of four agar media on mycelia growth (biomass, mg) are given in Table 3.5.

3.4.3 Effect of Temperature on Mycelia Growth

The optimal temperature for mycelia growth of *A. campestroides* is between 20 to 30 °C and *A. flocculosipes* was growing well at 25 °C. (Table 3.5).

3.4.4 Effect of pH on Mycelia Growth

The optimal pH of *A. campestroides* was pH 5 with the optimal medium and temperature. The result form this study showed that optimal pH range for mycelia growth of *A. flocculosipes* (MFLU 14–0874) was pH 5–8. The effects of pH on mycelia growth (biomass, mg) are given in Table 3.5.



Note Microscopic characteristics of *Agaricus campestroides* (MFLU 14–0872). a: Basidiospores in KOH. b: Basidiospores in Melzer's reagent. c: Basidia. d: Cystidia. e: Pileipellis. f: Stipitipellis. Bars: a, b = 10 µm; c, d, f = 5 µm; e = 20 µm.

Figure 3.28 Microscopic characteristics of *Agaricus campestroides* (MFLU 14–0872)

Table 3.5 Effect of different agar media, temperature, and pH on mycelia growth (biomass, mg) of *A. campestroides* and *A. flocculosipes*

Medium name	Biomass (mg)	
	A. campestroides	***A. flocculosipes***
MEA	109.99±0.07898^{ab}	11.23±0.00250^{a}
PDA	23.58±0.01838^{c}	13.47±0.00347^{a}
MYPA	96.12±0.06923^{b}	21.07±0.00196^{a}
PDYA	115.51±0.08054^{a}	19.17±0.00151^{a}
Temperature (°C)		
20	50.30±0.05030^{b}	4.90±0.00490^{b}
25	73.53±0.07353^{a}	10.83±0.01083^{a}
30	80.67±0.08067^{a}	3.20±0.00320^{b}
35	6.63±0.00663^{c}	3.10±0.00310^{b}
pH		
5	37.33±0.03733^{a}	18.17±0.002^{a}
6	1.77±0.00177^{b}	15.67±0.009^{a}
7	2.47±0.00247^{b}	15.36±0.002^{a}
8	0.63±0.00063^{b}	17.87±0.001^{a}

Note Biomass data = mean weight of dried mycelium± standard deviation. Values with the same letter are not significantly different (p<0.05) by Tukey's test.

Table 3.6 Yields of crude extracts from the mycelia of *A. campestroides* and *A. flocculosipes* cultivated in different media

Strains	Yields (mg)			
	MMK	**Q6 ½**	**YM**	**ZM**
A. campestroides	3.2	10.6	1.9	1.8
A. flocculosipes	3.3	NG	4.5	4.5

Note (NG): not growth.

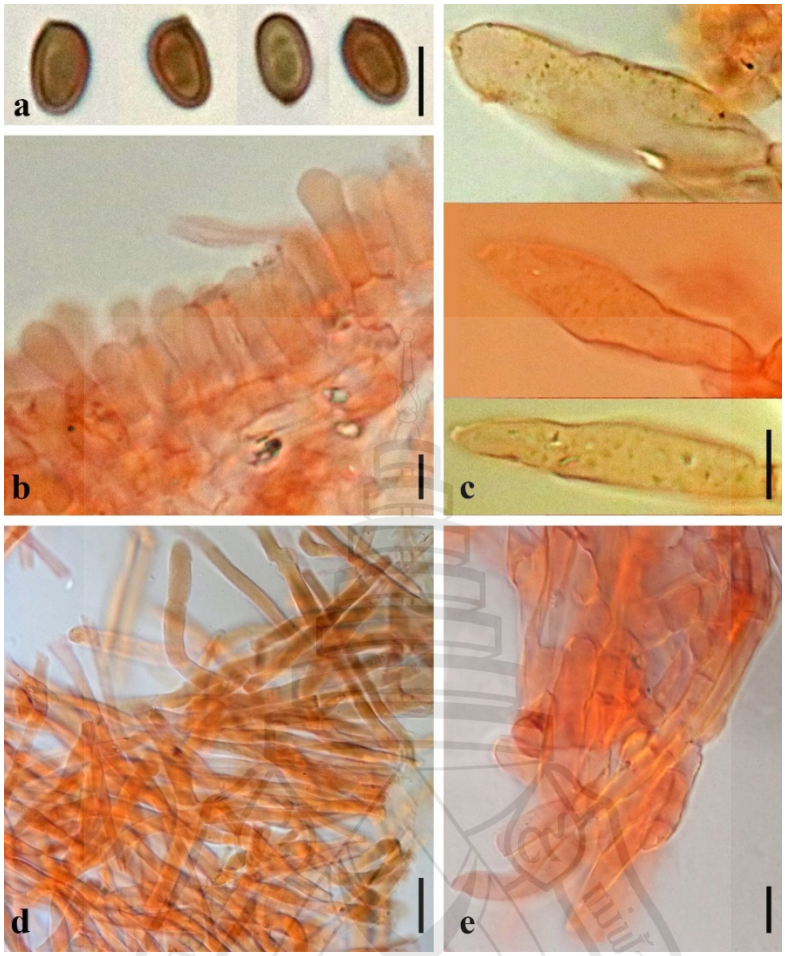
Table 3.7 Occurrence of compounds 1 and 2 in the mycelia of *A. campestroides* and *A. flocculosipes* cultivated in different media

	A. campestroides				***A. flocculosipes***			
	MMK	**Q6 ½**	**YM**	**ZM**	**MMK**	**Q6 ½**	**YM**	**ZM**
Blazeispirol A (**1**)	+++	++	++	-	+++	NG	+++	++
Blazeispirol D (**2**)	+	-	-	-	++	NG	++	-

Note (-): not observed, (+): observed in traces, (++): observed in small amounts, (+++); observed in high amounts, (NG): not growth.

3.4.5 Spawn Production

Mycelium started to colonize the substrates after five days of incubation, and fully grown within two weeks (Figure 3.30). Interestingly, the primordial started to form in three or four weeks of incubation. After one week, the pinning and mushrooms formed in wheat grain spawn.

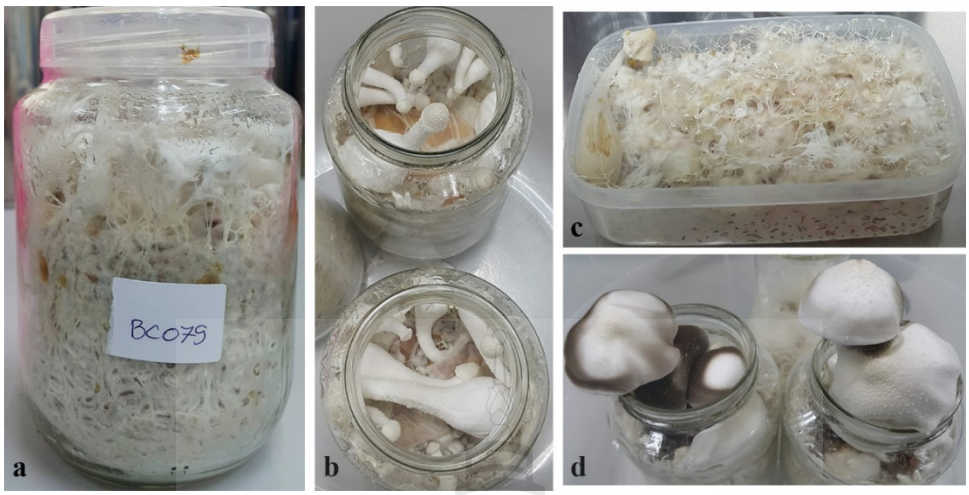


Note Microscopic characteristics of *Agaricus flocculosipes* (MFLU 14–0874). a: Basidiospores in KOH. b: Basidia. c: Cystidia. d: Pileipellis. e: Stipitipellis. Bars: a, b = 5 µm; c, e = 10 µm; d = 20 µm.

Figure 3.29 Microscopic characteristics of *Agaricus flocculosipes* (MFLU 14–0874)

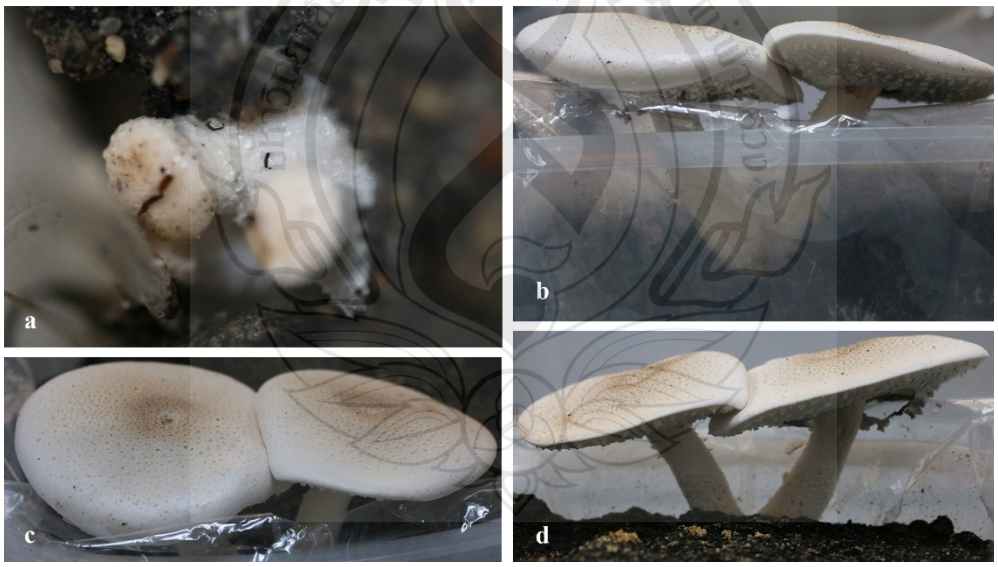
3.4.6 Harvesting/Production

Approximately 30 days, mycelium colonized the entire compost. Pre-primordial and mature basidiomata formed on the surface of the casing layer after 20 days at 25 °C. Dense hyphae growth always formed on the edge of casing where basidiomata produced. Successfully cultivated Thai strain of *A. campestroides* is shown in Figure 3.31, but the yields were still very low. Unfortunately, the Thai strain of *A. flocculosipes* could not be cultivated.



Note Mycelia growth of *Agaricus campestroides* on wheat grain spawn after 14 days. a and c: Mycelium fully colonised on substrate in different container. b and d: A week after mycelium fully colonised, the primordial and mushrooms formed in spawn.

Figure 3.30 Mycelia growth of *Agaricus campestroides* on wheat grain spawn after 14 days



Note The basidiomata of *A. campestroides* (MFLU 14–0872) on compost medium after 20 days of casing at 20 °C with 80% humidity.

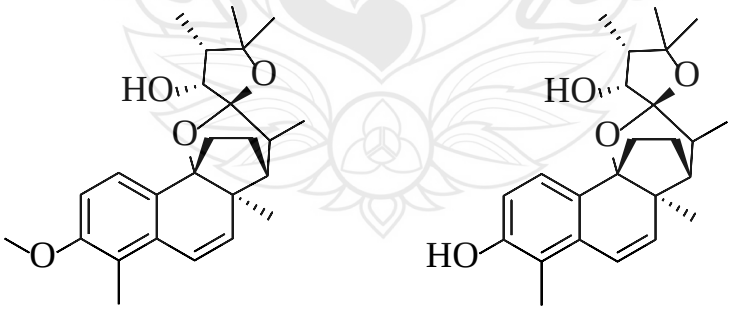
Figure 3.31 The basidiomata of *A. campestroides* (MFLU 14–0872) on compost medium

3.4.7 HPLC Profiling and Detection of Blazeispirol

The crude extracts of *A. campestroides* and *A. flocculosipes* were screened for their secondary metabolites in four different liquid media by HPLC-UV/Vis and HPLC-MS. Investigation on the crude extracts indicated the presence of the triterpenoids blazeispirol A (1) and D (2) (Figure 3.32), which could be detected from the mycelia of both strains. The compounds were identified based on their spectral data [UV/Vis, ESI(+)-MS] and HPLC comparison with an authentic sample. Herein, blazeispirol A (1) was observed as the main component of the crude extracts, while blazeispirol D (2) could only detected in small amounts (Figure 3.33). Although blazeispirol A (1) could be identified in both mycelium and supernatant of the crude extracts, but the larger amounts were significantly present in mycelium. Comparison of the metabolic profiles of different liquid media demonstrated that the highest production of the compounds (1 and 2) was found in mannitol salts medium (MMK) for both strains and YM in case of *A. flocculosipes*.

Whereas blazeispirol 1 has not yet been detected in the basidiomata, it is produced in large quantities by liquid mycelium fermentation of *A. blazei* (Grothe et al., 2016). Further investigations hypothesized that blazeispirol D (2) and Z seemed to be the actual intermediates of the blazeispirol A biosynthesis, which might be derived from ergosterol (Hirotani et al., 2001).

According to the MS spectra of the observed compounds, the chlorinated triglycerides could not be detected in any extract.



blazeispirol A (**1**) blazeispirol D (**2**)

Figure 3.32 Chemical structures of blazeispirol A (1) and D (2)

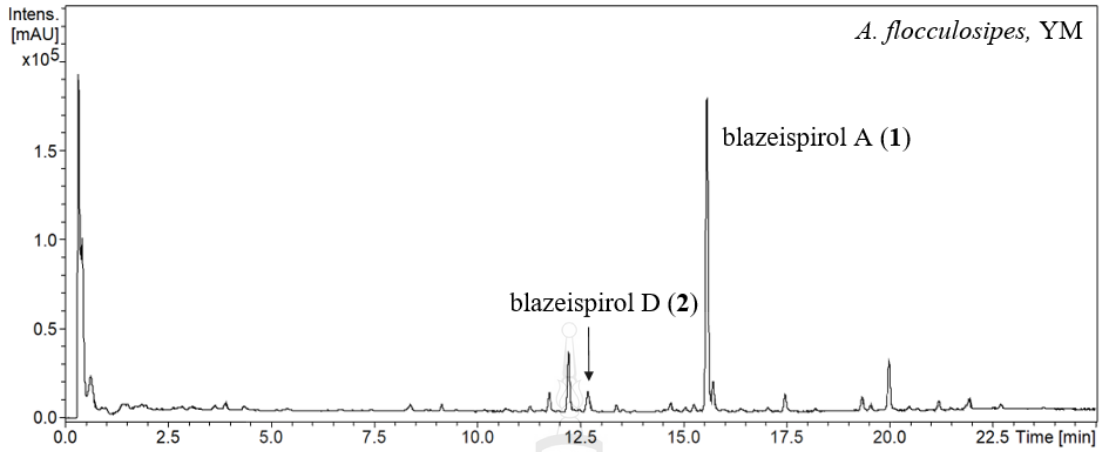


Figure 3.33 HPLC-UV/Vis chromatogram of the crude extract of *A. flocculosipes* cultivated in YM-medium (190–600 nm)

3.5 Secondary Metabolites of *Phlebopus* from Northern Thailand

The analyses of the secondary metabolite profiles from small-scale extraction of *P. portentosus* and *P. spongiosus* by HPLC-UV/Vis and HR-LC-ESI-MS indicated the presence of interesting pigments with absorption maxima between λ = 300–550 nm. Therefore, extensive chromatographic studies of the crude extracts were conducted. These finally led to the isolation of two new compounds, named 9′-hydroxyphenyl pulvinone (1) and phlebopyrone (2).

Compound 1 was isolated as a yellow amorphous solid and exhibited absorption maxima at λ = 245 and 386 nm suggesting the existence of an extended conjugated π system in the molecule. The molecular formula was determined to be $C_{23}H_{16}O_6$, based on HR-(+)-ESI-MS measurements of the molecular ion *m/z* 389.1020 ($[M+ H]^+$, cald. for 389.1020), corresponding to 16 degrees of unsaturation. The ^1H NMR spectrum, recorded at 300 K in CD_3OD, exhibited 12 nonexchangeable protons (Table 1). Consequently, 1 contains four exchangeable protons. Furthermore, the ^{13}C NMR spectrum revealed the presence of 23 carbons. According to the molecular formula and the ^1H,^{13}C HSQC spectrum, the carbon signals could further be classified into 12 methine groups showing eight signals, four of which are assigned to a pair of equivalent carbons each in two paradisubstituted aromatic rings, and 11-nonprotonated carbons including six oxygenated ones. Analysis of the NMR spectra for 1 indicates the presence of a 1,3,4-trisubstituted benzene ring [benzene ring A: H-2 (δ_H 6.91 ppm,

d, J = 2.2 Hz), H-5 (δ_H 6.64 ppm, d, J = 8.3 Hz), H-6 (δ_H 6.77 ppm, dd, J = 8.3, 2.2 Hz)], and two 1,4-disubstituted benzene rings [benzene ring B: H-2′/6′ (δ_H 7.62 ppm, d, J = 8.7 Hz), H-3′/5’(δ_H 6.77 ppm, d, J = 8.7 Hz); benzene ring C: H-2″/6″ (δ_H 7.16 ppm, d, J = 8.5 Hz), H-3″/5″ (δ_H 6.87 ppm, d, J = 8.5 Hz)], as well as an isolated methine proton C-11′ (δ_H 5.97 ppm, s). Moreover, the 1D NMR data of pigment 1 resembled those of pulvinone analogues (Gao et al., 2013). The 1,3,4-trisubstituted benzene ring exhibits deshielded chemical shift values for C-3 (δ_C 148.3 ppm) and C-4 (δ_C 146.7 ppm) requiring substitution by oxygen. According to a strong ^3J(H,C) HMBC correlation of H-2 (δ_H 6.91 ppm) and H-6 (δ_H 6.77 ppm) with C-8′ (δ_C 123.2 ppm), the trisubstituted benzene group is connected to the butenolide unit at C-8′ through C-1 (δ_C 122.55 ppm). Furthermore, the strong ^3J(H,C) HMBC correlation of H-2’/H-6′ (δ_H 7.62 ppm) to C-11′ (δ_C 114.7 ppm) indicates that the substituted benzene ring B is connected via C-1′ (δ_C 125.6 ppm) to the methine carbon C-11′. On account of its chemical shift value C-4′ (δ_C 162.4 ppm) is substituted by a phenol group. Due to the ^{1}H,^{13}C HMBC correlation from H-2″/6″ (δ_H 7.16 ppm) to C-9′ (δ_C 151.0 ppm), benzene ring C has to be connected at C-9′ in the butanolide unit via C-1″ (δ_C 122.4 ppm) forming the pulvinone derivative 1, named 9′-hydroxyphenyl pulvinone. The configuration of the double bond between C-10′ and C-11′ was assigned by NOE experiments as Z configured according to a NOE correlation between H-11′ (δ_H 5.97 ppm) and H-2”/H-6″ (δ_H 7.16 ppm). Pulvinones, characterized by a 4-hydroxy-2(5*H*)-furanone ring, are known as a key structural element in many natural products (Georgiadis, 2013). Prominent representatives are the trihydroxypulvinones (Edwards & Gill, 1973) isolated from *Suillus grevillei* or the group of aspulvinones from *Aspergillus* spp. (Ojima et al., 1973; Golding & Rickards, 1975; Pang et al., 2017). However, substitution of the butenolide unit by a third phenyl group at C-9′ has not been found in nature so far and provides a new subclass of pulvinones. A synthetic derivative was only described in the one-step synthesis of α- phenyl-γ-benzylidene-α,β-unsaturated-butenolide in 1975 (Rao, 1975).

The UV/Vis spectrum of compound 2 exhibits absorption maxima at λ = 245 and 328 nm suggesting the presence of a conjugated π system in the molecule. The HR(+)-ESI-MS spectra of 2 shows an $[M + H]^+$ ion at *m/z* 297.0754 (cald. for 297.0758) consistent with the molecular formula $C_{17}H_{12}O_5$ and 12 degrees of unsaturation. The ^{1}H NMR spectrum of 2, recorded at 300 K in CD_3CN, exhibits nine nonexchangeable protons which can further be classified as one isolated methine C-5 (δ_H 7.48 ppm) and four pairs of aromatic methines. According to the molecular formula, compound 2 contains three exchangeable protons.

Furthermore, the NMR spectra suggested two parasubstituted benzene rings [benzene ring A: H-2′/6′ (δ_H 7.25 ppm, d, J = 8.7 Hz), H-3′/5′ (δ_H 6.91 ppm, d, J = 8.7 Hz); benzene ring B: H-2″/6″ (δ_H 7.29 ppm, d, J = 8.6 Hz),H-3″/5″ (δ_H 6.89 ppm, d, J = 8.6 Hz)] with deshielded resonances for C-4′ (δ_C 157.7 ppm) and C-4″ (δ_C 158.2 ppm) requiring substitution by oxygen. The ^{1}H,^{13}C HMBC spectrum exhibits correlations of methine proton H-6 (δ_H 7.48 ppm) with C-2 (δ_C 164.5 ppm), C-3 (δ_C 106.4 ppm), C-4 (δ_C 164.1 ppm), and C-5 (δ_C 118.4 ppm). Consideration of the number of oxygen atoms and the characteristic chemical shifts of C-3-C-6 and H-6 indicates compound 2 contains a 4-hydroxy-α-pyrone moiety. The substituted benzene ring A is connected to the α-pyrone moiety at C-3 (δ_C 106.4 ppm) through C-1′ (δ_C 123.6 ppm), since ^{1}H,^{13}C HMBC correlations of the aromatic protons H-2′/6′ (δ_H 7.25 ppm) to C-3 (δ_C 106.4 ppm) can be observed. Furthermore, protons H-2″/6″ (δ_H 7.29 ppm) show a strong ^3J(H,C) HMBC correlation to C-5 (δ_C 118.4 ppm) of the α-pyrone moiety. Therefore, substituted benzene ring B has to be connected to C-5 through C-1″ (δ_C 123.6 ppm) forming the bis(hydroxyphenyl)-α-pyrone derivative 2, named phlebopyrone.

Furthermore, seven known pigments were isolated from the crude extracts [large-scale cultivation (YM 5.5 medium) from *P. spongiosus* and small-scale (MMK medium) from *P. portentosus*]. The structures were identified based on their spectral data [UV/Vis, 1D/2D NMR, MS (3–8)] as atromentic acid (3), xerocomic acid (4), variegatic acid (5), methyl atromentate (6), methyl isoxerocomate (7), and methyl variegatate (8) and by HPLC comparison with authentic samples (3 and 5). Variegatorubin (9) was identified by UV/Vis spectra, HR-LC-ESI(+)-MS, HR-ESI(+)-MS/MS, and HPLC comparison with an authentic sample. The red pigment variegatorubin (9) could only be detected in traces in the crude extracts of *P. portentosus* and was probably formed during isolation process by oxidation of variegatic acid (5) (Steglich et al., 1970).

To investigate the antimicrobial, cytotoxic, biofilm inhibition, and nematicidal effects, the isolated compounds 1–4 and 6–8 were tested against selected microorganisms. Thus, xerocomic acid (4) and methyl variegatate (8) showed weak to moderate cytotoxic activities against several tumor mammalian cell lines except for human prostate cancer PC-3. Weak cytotoxic activity against Hela KB3.1 cells and MCF-7 cells could be observed for 9′-hydroxypulvinone (1). Moreover, methyl isoxerocomate (7) and methyl variegatate (8) showed weak effects against several microorganisms, e.g. *S. aureus*, *M. hiemalis*, *S. pombe*. In former studies, antibacterial activities were already observed from the acetone extracts of *P.*

sulphureus and *P. lignicola* cultures against *B. subtilis* and *E. coli* (Madhosingh, 1966). In addition, atromentic acid (3) and xerocomic acid (4) showed weak activity against *C. elegans*. Phlebopyrone (2), atromentic acid (3), and methyl atromentate (6) showed neither antimicrobial nor cytotoxic activities, and no inhibition could be observed for compounds 3 and 4 for biofilm formation.

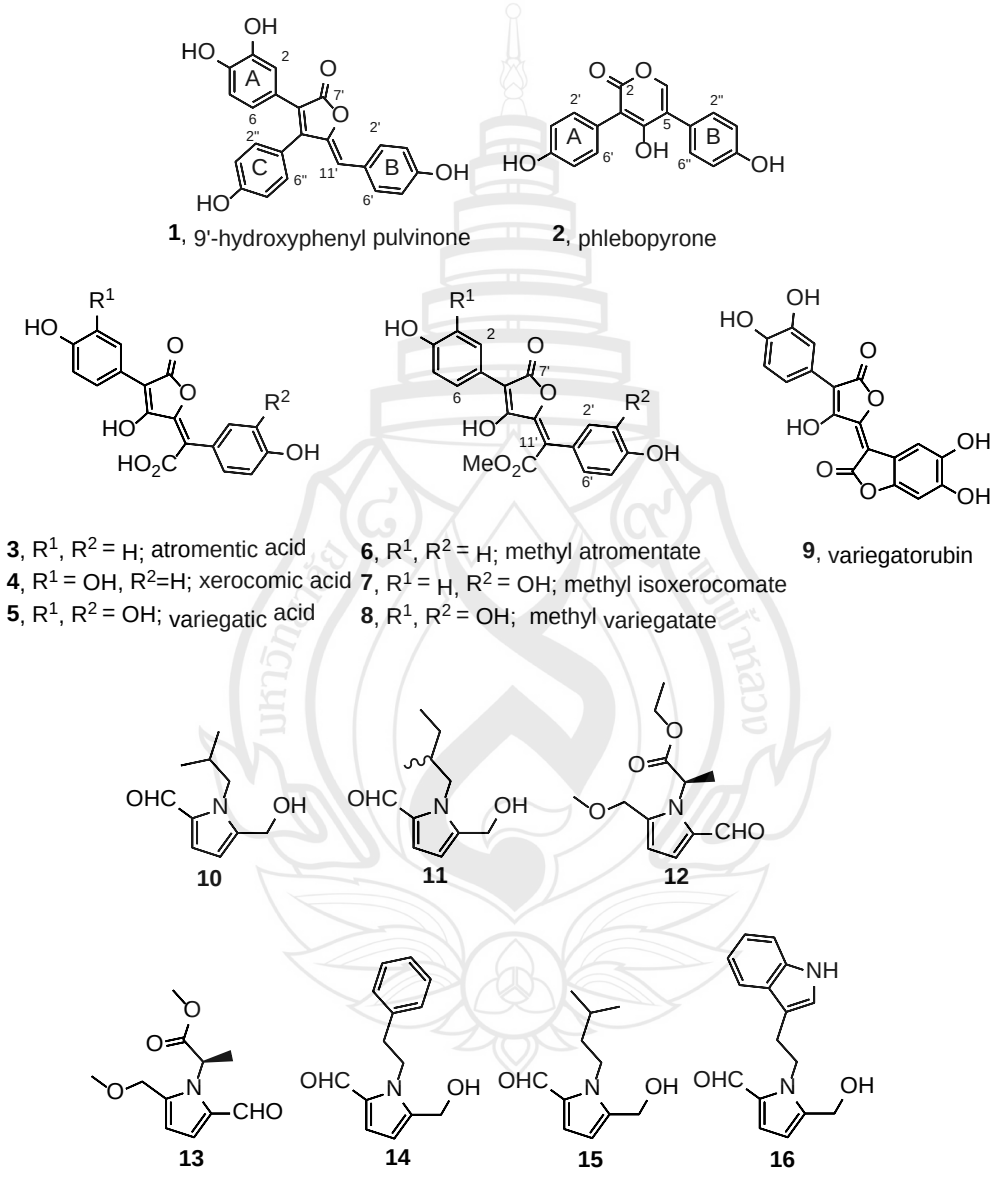


Figure 3.34 Chemical structures of compounds 1–9 isolated from *P. portentosus* and *P. spongiosus* (liquid cultivation) and known compounds (10–16) isolated from air-dried basidiomes from *P. portentosus*

Source Sun et al. (2018)

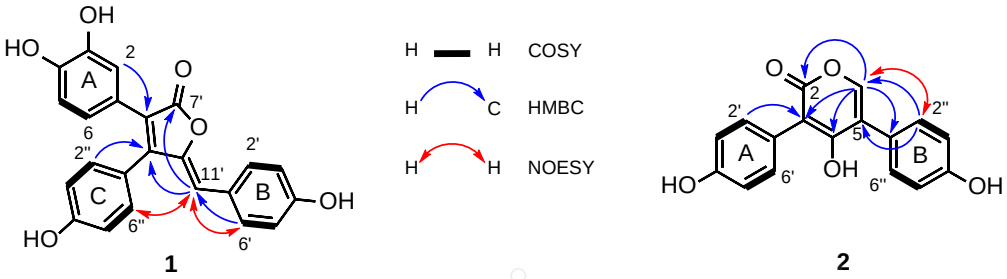


Figure 3.35 $^{1}H,^{1}H$ COSY, $^{1}H,^{13}C$ HMBC, and key $^{1}H,^{1}H$ NOESY correlations for compounds 1 and 2

Table 3.8 ^{1}H NMR and ^{13}C NMR Data (δ) for compounds 1 and 2 (700 MHz, 300 K) (δ in ppm, J in Hz)

	1[a]		**2**[b]	
No.	**δ_C**	**δ_H (mult., J)**	**δ_C**	**δ_H (mult., J)**
1	122.55, C	-	-	-
2	117.2, CH	6.91 (d, 2.2)	164.5, C	-
3	148.3, C	-	106.4, C	-
4	146.7, C	-	164.1, C	-
5	116.2, CH	6.64 (d, 8.3)	118.4, C	-
6	122.6, CH	6.77 (dd, 8.3; 2.2)[c]	149.2, CH	7.48 (s)
1’	125.6, C	-	123.6, C	-
2’	133.7, CH	7.62 (d, 8.7)	133.4, CH	7.25 (d, 8.7)
3’	117.8, CH	6.77 (d, 8.7)[c]	116.5, CH	6.91 (d, 8.7)
4’	162.4, C	-	157.7, C	-
5’	117.8, CH	6.77 (d, 8.7)[c]	116.5, CH	6.91 (d, 8.7)
6’	133.7, CH	7.62 (d, 8.7)	133.4, CH	7.25 (d, 8.7)
7’	171.8, C	-	-	-
8’	123.2, C	-	-	-
9’	151.0, C	-	-	-
10’	147.8, C	-	-	-

Table 3.8 (continued)

		1[a]		**2**[b]
No.	**δ_C**	**δ_H (mult., *J*)**	**δ_C**	**δ_H (mult., *J*)**
11’	114.7, CH	5.97 (s)	-	-
1’’	122.4, C	-	123.6, C	-
2’’	132.0, CH	7.16 (d, 8.5)	131.9, CH	7.29 (d, 8.6)
3’’	117.5, CH	6.87 (d, 8.5)	116.4, CH	6.89 (d, 8.6)
4’’	161.6, C	-	158.2, C	-
5’’	117.5, CH	6.87 (d, 8.5)	116.4, CH	6.89 (d, 8.6)
6’’	132.0, CH	7.16 (d, 8.5)	131.9, CH	7.29 (d, 8.6)

Note [a]CD_3OD. [b] CD_3CN, the carbon chemical shift values were obtained from the ^1H,^{13}C HSQC and ^1H,^{13}C HMBC spectra. [c] Overlapping signals.

Table 3.9 Occurrence of compounds 1–9 in *P. spongiosus* and *P. portentosus* cultivated in different media

			1	**2**	**3**	**4**	**5**	**6**	**7**	**8**	**9**
P. portentosus	BAF	m	++	+	+++	+++	+++	-	++	-	+
		l	++	++	+++	+++	+++	-	+	-	+
	MGP	m	+	++	+++	+++	++	+	+++	++	+
		l	+	++	+++	+++	++	-	+	-	+
	MMK	m	+	+	++	+++	+++	-	+++	+++	-
		l	-	++	-	+++	-	-	+++	-	-
	YM	m	+	++	+++	-	-	+	+	-	-
	5.5	l	-	+	+++	-	-	+	+	-	-
P. spongiosus	BAF	m	+	++	+++	+++	+++	-	+	-	+
		l	+	++	++	++	++	-	+	-	+
	MGP	m	+	++	+++	+++	+++	+	++	-	+
		l	+	++	+++	+++	+++	-	+	-	-

Table 3.9 (continued)

			1	2	3	4	5	6	7	8	9
P. spongiosus	MMK	m	-	++	-	+++	+++	-	-	-	-
		l	-	++	-	+++	++	-	-	-	-
	YM	m	++	++	+++	+++	-	+	-	-	-
	5.5	l	++	++	+++	++	-	-	++	-	-

Note m = mycelium, l = liquid media. (-) = not observed, (+) = observed in traces, (++) = observed in small amounts, (+++) = observed in high amounts.

Table 3.10 Antimicrobial activity of compounds 1, 7, and 8

Tested organisms	**Strain No.**	**Minimum inhibitory concentration (MIC) [µg/mL]**			
Bacteria		**1**	**7**	**8**	**Reference**
Bacillus subtilis	DSM 10	-	-	-	8.3[a]
Chromobacterium violaceum	DSM 30191	-	-	-	0.8[a]
Escherichia coli	DSM 1116	-	-	-	6.7[a]
Micrococcus luteus	DSM 1790	-	-	33.3	0.8[a]
Mycobacterium smegmatis	ATCC 700084	-	-	-	1.7[b]
Pseudomonas aeruginosa	PA14	-	-	-	0.4[c]
Staphylococcus aureus	DSM 346	66.7	66.7	66.7	0.8[a]
Fungi					
Mucor hiemalis	DSM 2656	-	66.7	66.7	33.3[d]
Pichia anomala	DSM 6766	-	66.7	66.7	16.7[d]
Rhodoturula glutinis	DSM 10134	-	-	-	8.3[d]
Yeast					
Candida albicans	DSM 1665	-	-	-	66.7[d]
Schizosaccharomyces pombe	DSM 70572	-	66.7	66.7	8.3[d]

Note [a] oxytetracycline hydrochloride, [b] kanamycin, [c] gentamicin, [d] nystatin.

Table 3.11 Cytotoxic activity of compounds 1, 4, and 8

Cell Lines	**IC_{50} [µM]**			
	1	**4**	**8**	**Epothilone B**
Epidermoid carcinoma A431	nt	9.0	16.8	0.000028
Adenocarcinomic human alveolar basal epithelial A549	nt	8.7	16.0	0.000019
HeLa KB3.1	18.5	17.4	17.6	0.000024
Fibroblasts L929	-	16.5	17.8	0.00061
MCF-7	46.4	3.9	6.5	0.000025
Human prostate cancer PC-3	nt	-	-	0.000028
Ovarian cancer SKOV-3	nt	25.6	49.2	0.00009

Note (-) = no inhibition, (nt) = not tested.

Table 3.12 Nematicidal activity of compounds 3 and 4

Tested organisms	**Strain No.**	**LD_{50} [µg/mL]**		
		3	**4**	**ivermectin**
Caenorhabditis elegans	AB1	100.0	100.0	1.0

CHAPTER 4

DISCUSSION

4.1 Taxonomy and Phylogeny of *Phylloporus*

Morphological characters and the molecular analyses support *P. pusillus*, *P. subbacillisporus* and *P. subrubeolus* as new *Phylloporus*. In addition to these three newly described species, new species from China and Thailand such as OR0258, OR0896 and OR0989 were sequenced but not formally described because of insufficient material. Similarly, a number of species from China were not formally described because of the lack of collections and differences in morphology or ecology (Zeng et al., 2013).

ATPase subunit 6 (*atp6*), RNA polymerase II (*rpb2*) and elongation factor 1-alpha (*tef1*) sequence data seem to be useful for delimitation of *Phylloporus*, although many species are missing in our phylogeny because *atp6, rpb2* or *tef1* sequences were unavailable from GenBank. From this study, the pileus and stipe colour did not show much variation among species; in only some species can those characters be used for identification, i.e. *P. pusillus* and *P. subbacillisporus*. Some other macroscopic characters are also useful to identify the species, such as colour of basal mycelium, hymenophore structure and the staining of context and hymenophore (Corner, 1970; Neves & Halling, 2010; Neves et al., 2012). The microscopical characters sometimes are necessary to discriminate *Phylloporus*. For example, the form and size of stipitipellis terminal cells are useful characters to discriminate *P. pusillus*. Also, pigmentation and encrustations of cystidia (Corner, 1970), hyphae of pileipellis and stipitipellis should be carefully observed in water, ammonium hydroxide and potassium hydroxide. Sometimes, the presence of encrusted pigments will vary when observed in different solutions. In *P. pusillus* and *P. subrubeolus*, numerous encrusted pigments can

be observed on the pileipellis hyphae when mounted in water or ammonium hydroxide, but less in potassium hydroxide.

Interestingly, *P. pusillus* showed variability in spore shape, which has been found only in one other *Phylloporus*, *P. dimorphus* (two forms of spores) described from northern Thailand by Neves et al. (2012). The lack of spore ornamentation (smooth even under SEM) in *P. subbacillisporus* has only rarely been found in *Phylloporus* (*P. alborufus* and *P. centroamericanus*), in which spores normally show bacillate ornamentation when examined with SEM, albeit sometimes only in parts of the spores. Smooth spores have been observed in some other Xerocomoideae Singer as well, namely *Hourangia pumila* (Neves & Halling) Zhu, R. E. Halling & Z. L. Yang and *Xerocomus piceicola* M. Zang&M. S. Yuan (Wu et al., 2016).

4.2 Taxonomy and Phylogeny of *Retiboletus*

The combined sequences data supported *R. brevibasidiatus* as distinct from other *Retiboletus*. Our molecular data also allowed identification of other collections from Thailand as *R. fuscus* and *R. nigrogriseus*, which were previously described from Japan and China, respectively. The collection labelled as "OR049_*R. nigerrimus*" in Raspe et al. (2016) from Thailand is here confirmed as *R. nigrogriseus*. *Retiboletus brevibasidiatus*, *R. kauffmanii*, and *R. sinensis* formed a highly supported clade (BS = 95%, PP = 0.99).

Zeng et al. (2016) stated that the species with dark grey to black pileus and white basal mycelium were grouped in the same clade (*R. nigerrimus* and *R. zhangfeii*, clade I), whereas the species with brown pileus and white basal mycelium were grouped in another clade (*R. griseus*, *R. fuscus* and *R. pseudogriseus*, clade II). The species with yellow basal mycelium, including the type species of the genus, were in the third clade (*R. kauffmanii*, *R. ornatipes*, *R. retipes*, and *R. sinensis*, clade III). In our phylogenetic tree, however, *R. griseus* was part of a well-supported clade (BS = 96%, PP = 0.99) with *R. nigrogriseus* and *R. zhangfeii*. The claim by Zeng et al. (2016) that clades I and II are characterized by 'black' and brown pileus, respectively, seems artificial to us. Indeed, *R. fuscus R. griseus*, and *R. pseudogriseus*, which belonged to clade II, were

said to have greyish (*R. griseus*) or greyish brown to greyish black (*R. pseudogriseus* and *R. fuscus*) pileus in the key (Zeng et al., 2016). Therefore, all the species in that clade may have grey or dark grey (blackish) pileus. Also, because clade II of Zeng et al. (2016) was relatively weakly supported (BS = 84%, PP < 0.9) and most nodes within it also not or weakly supported, we prefer to lump clade I and II of Zeng et al. (2016) in a single clade (clade 1) characterized by white basal mycelium. Our clade 2, which includes the type species *R. ornatipes*, has the following morphological synapomorphies: yellow basal mycelium and deep yellow context, at least in the stipe. The color of basal mycelium, stipe context, and to a lesser extent of the pileus, are therefore useful for separating *Retiboletus*. *Retiboletus ornatipes*/*retipes* were described from Central and North America (Binder & Bresinsky, 2002; Ortiz-Santana et al., 2007; Zeng et al., 2016) while *R. kauffmanii* and *R. sinensis* were both described from China, and *R. brevibasidiatus* from Thailand. As previously found in a number of ectomycorrhizal mushroom genera, including bolete genera, specimens from different continents that were previously thought to be conspecific were frequently shown to belong to different species (e.g., Feng et al., 2012; Badou et al., 2018; Davoodian et al., 2018; Delgat et al., 2019). Biogeographical evidence could, therefore, also be useful to separate species when morphological differences are limited. Ecological evidence such as elevation could also be used to separate species, since *R. Kauffmanii* was found at high elevations (over 2,000 m), whereas *R. brevibasidiatus* was found between 700 and 1,500 m. However, more data are needed to confirm the specificity of this ecological character and its usefulness for species identification.

4.3 Taxonomy and Phylogeny of *Hourangia* and *Xerocomus*

The combined sequences data supported the identification of *Hourangia* and *Xerocomus* collections from Thailand. The collections from Thailand were resembled to *Hourangia microcarpa* and *H. nigropunctata,* which were previously described from Malaysia and China, respectively. Also, one novel species and undescribed species were found from our collections. Two novel species with one new record of *Xerocomus* also reported in this study.

From the Xerocomoideae phylogeny, the monophyly of all genera were highly supported except *Rubinosporus*. The relationship of *Rubinosporus* to the other genera within Xerocomoideae remains unclear. It formed a clade close to *Hemileccinum* with low support. In addition, the three genera *Hourangia*, *Phylloporus*, and *Xerocomus* formed a highly supported clade. *Phylloporus* formed a clade sister to *Hourangia*, and both genera are sisters to *Xerocomus*. The result is similar to Wu et al. (2016) phylogeny (based on 28S, *tef*1, *rpb*1, and *rpb*2), but slightly different from Vadthanarat et al. (2022), which *Phylloporus* was sister to *Xerocomus*, not *Hourangia*.

4.4 Cultivation and Identification of Blazeispirols from Wild *Agaricus campestroides* and *A. flocculosipes*

This study demonstrates the successful cultivation and domestication of *A. campestroides*, collected in northern Thailand. The optimal culture medium, pH, temperature, and yield were investigated for the best mycelia growth. For the two strains, used in this study, the best growth rates were obtained using PDYA for *A. campestroides* and all media were suitable for *A. flocculosipes*. The two strains of *Agaricus* showed optimal temperature between 25–30 °C for mycelia growth which is consistent with the previous study by Zied et al. (2011b). *Agaricus campestroides* was growing well at pH 5 while *A. flocculosipes* was able to grow at pH 5–8. Park (2001) reported the optimal pH for the substrate reaction range between 6–7, high acid or basic condition inhibited mycelia growth. Kopytowski et al. (2008) reported that the optimal pH range for compost substrate and casing layer is pH 7.0–7.5. It is suggested that neutral pH was the suitable pH for this mushroom.

The two strains of *Agaricus* were cultivated by using rice straw as the main substrate mixed with the ingredients. Only *A. campestroides* were produced at the temperature of 20 °C with 80% relative humidity 14 days after the casing layer was applied. The mushroom requires high temperature and high humidity to produce mushrooms like *A. subrufescens* (Dias et al., 2004; Mantovani et al., 2007; Dias, 2010). The humidity during the formation of primordial was at 80–90%, while 75–80% relative humidity was maintained during the development of mushrooms (Iwade &

Mizuno, 1997; Stamets, 2000). According to Chang (2008), humidity of 70–85% was the optimum for mushroom formation. The wild strains of *A. campestroides* showed a potential to grow in northern Thailand since the optimal conditions for growing these stains were temperature range from 25–30 °C with 80–90% relative humidity that is related with the weather in northern Thailand (Thai Meteorological Department, 2015). Moreover, the study of secondary metabolites of *A. campestroides* and *A. flocculosipes* has led to the identification of blazeispirols A (1) and D (2) in cultured mycelia of both species.

So far, blazeispirols (A, B, C, D, E, F, G, X, Y, Z) are a class of unique spiro-triterpenoids, isolated from cultured mycelia of *Agaricus blazei* (=*A. subrufescens*) (Hirotani et al., 1999, 2000, 2001, 2002) Therefore, the detection of blazeispirols in other species of *Agaricus* extends the natural occurrence of these type of compounds. Since it was assumed that their occurrence is restricted to *A. subrufescens*, blazeispirol A (1) was constituted as a phylogenetic and chemotaxonomical marker for this taxon (Thongklang et al., 2017).

4.5 Secondary Metabolites of *Phlebopus* from Northern Thailand

HR-LC-ESI(+)-MS comparison of the crude extracts of *P. portentosus* and *P. spongiosus* growing on different media indicated that atromentic acid (3), xerocomic acid (4), and variegatic acid (5) are the major pigments in both species. The compounds belong to the pulvinic acids, a group of impressive pigments which are responsible for the yellow and red colors of most boletes. They have been detected in over 100 species of the Boletales (Gill & Steglich, 1987; Nelsen, 2010). Mainly variegatic acid is responsible for the bluing reaction of most boletoid basidiomata due to the oxidation to the corresponding blue quinone methide anion (Velíšek & Cejpek, 2011). Pulvinic acids are chemotaxonomic marker compounds of Boletales sensu lato and successfully used to reorder the systematics of this order (Gill & Steglich, 1987; Bresinsky, 2014). Therefore, the isolation of pulvinic acids 3–5 and 9 from *P. portentosus* and *P. spongiosus* underlines the taxonomic position of *Phlebopus* in the Boletales and even the Boletaceae. Remarkably, the new compounds 9′-hydroxyphenyl pulvinone (1) and

phlebopyrone (2) could be isolated for the first time. Both compounds may act as chemotaxonomic marker compounds for the genus *Phlebopus*. HR-LC-ESI(+)-MS comparison of the crude extracts from different media indicated that compounds 1–9 appear in both species. Furthermore, depending of the liquid media, differences could be observed in the occurrence of compounds 1–9 between mycelium and liquid media. A metabolite profile of the crude extracts of dried basidiomata of *P. portentosus* and *P. spongiosus* indicated dimer forms of pulvinic acids as the major compounds of the fruiting bodies. HR-LC-ESI(+)-MS measurements of *P. portentosus* revealed the presence of ions at m/z: 651.0775, 679.0722, and 695.0671, consistent with the molecular formulae of bisnorbadiochinone A (Steffan & Steglich, 1984), norbadione A (Steffan & Steglich, 1984), and pisoquinone (Gill & Kiefel, 1994). In *P. spongiosus*, HR-LC-ESI(+)-MS comparison indicated small amounts of atromentic acid (3) and xerocomic acid (4) together with large amounts of tentatively identified bisnorbadiochinone A (Steffan & Steglich, 1984) (*m/z*: 651.0774) and norbadione A (*m/z*: 679.0726) (Steffan & Steglich, 1984). Norbadione A, which was isolated from the cap skin of *Boletus badius*, is biosynthetically derived from two molecules of xerocomic acid (4) via [4 + 2]cycloaddition (Winner et al., 2004). The orange-brown pigment can complex K or Cs ions (Aumann et al., 1989).

Mushrooms that contain this type of pigment can strongly concentrate radioactive ^{137}Cs in their basidiomata, which is absorbed from the environment by their mycelia and transported to the basidiomata (Aumann et al., 1989). To investigate whether the basidiomata of *Phlebopus* species show high values for radionuklides, further investigations are needed. Interestingly, phlebopyrone (2) could be detected as a minor compound in the basidiomata of both *Phlebopus* species. Pulvinic acids and the pulvinones exhibit an impressive structural variety, but less is known about their biological activities. Xerocomic acid (4) showed weak antiviral effects and inhibited swarming and colony biofilm spreading of *Bacillus subtilis* (Gordon et al., 2007; Tauber et al., 2018). Moreover, xerocomic acid (4) and variegatic acid (5) are inhibitors of cytochrome P450 enzymes (Huang et al., 2009). Significant antibacterial activities were observed for synthetic biphenyl-substituted pulvinones against Gram-positive bacteria (Antane et al., 2006).

In conclusion, from the liquid cultivation of the edible mushrooms *P. portentosus* and *P. spongiosus*, a series of pulvinic acid derivatives (3–9) could be recognized, some of them with significant antimicrobial and cytotoxic activities. Interestingly, alkaloids (10–16) as reported from the basidiomes could not be observed from liquid cultures (Sun et al., 2018).

CHAPTER 5

OVERALL CONCLUSIONS

This dissertation focused on the biodiversity of mushrooms from Agaricaceae (*Agaricus*) and Boletales (*Hourangia*, *Phlebopus*, *Phylloporus*, *Retiboletus*, and *Xerocomus*). The mushroom specimens were described using morphological observation and phylogenetic analyses. The taxonomy of mushrooms was addressed along with their ability to produce secondary metabolites and to be cultivated. The species selected for investigations of the ability to produce novel bioactive compounds were *Agaricus campestroides*, *Agaricus flocculosipes*, *Phlebopus portentosus*, and *Phlebopus spongiosus*.

5.1 Taxonomy and Phylogeny of *Agaricus* and Boletales

Morphological and phylogenetic evidence were used for introducing and identifying mushroom taxa. From 270 specimens, 33 cultures were obtained, focusing on *Agaricus* and *Phlebopus* species (Appendix F). In this study, mushrooms were identified from 85 specimens collected from northern Thailand. Sixty-one specimens were described and illustrated based on the multi-gene phylogeny (ATP6, ITS, RPB2, and TEF1). The study revealed nine new species and ten new geographical records.

Morphological characters and the combined sequences (ATP6, RPB2, TEF1) supported *Phylloporus pusillus*, *P. subbacillisporus* and *P. subrubeolus* as new species. In addition, three new *Phylloporus* species from China and Thailand each represented by one specimen (OR0258, OR0896 and OR0989) were sequenced but not formally described because of insufficient material. A total of 62 new sequences from *Phylloporus* were generated and deposited in GenBank.

Based on morphology and phylogeny, using the same methods as for *Phylloporus*, *Retiboletus brevibasidiatus* was described as new species. Our molecular

data also allowed identification of other collections from Thailand as *R. fuscus* and *R. nigrogriseus*, which were previously described from Japan and China, respectively. The collection labelled as "OR049_*R. nigerrimus*" in Raspé et al. (2016) from Thailand is here confirmed as *R. nigrogriseus*. A total of 22 new sequences were generated from *Retiboletus* and deposited in GenBank.

The identification of *Hourangia* and *Xerocomus* collections from Thailand were performed with morphology and phylogeny. Some collections from Thailand were similar to *Hourangia microcarpa* and *H. nigropunctata*, which were previously described from Malaysia and China, respectively. Also, one novel species and undescribed species were found from our collections. Two novel species with one new record, *Xerocomus microcarpoides* are also reported in this study. A total of 68 sequences of *Xerocomus* and *Hourangia* were newly generated in this study and deposited in GenBank.

For cultivation and secondary metabolites investigation, the specimens used in those analyses were also identified to species level based on morphological observations and molecular analyses.

ATPase subunit 6 (*atp*6), RNA polymerase II (*rpb*2) and elongation factor 1-alpha (*tef*1) sequence data seem to be useful for delimitation of *Hourangia*, *Phlebopus*, *Phylloporus*, *Retiboletus*, and *Xerocomus* species, although many species are missing in our phylogeny because *atp*6, *rpb*2 or *tef*1 sequences were unavailable from GenBank.

Most taxonomic research in our study has focused on northern Thailand. The discovery of novel species suggests that additional research is still needed to explore more diversity in other parts of the country with different hosts and ecology.

5.2 Secondary Metabolites of Selected *Agaricus* and Boletales Species

The species novelty in northern Thailand is amazing, ranging between 55 and96% depending on the taxonomic group (Hyde et al., 2018), which illustrates the challenge of exploring the high fungal diversity in Thailand and inspired the portion of this dissertation on secondary metabolites of selected strains. Recently, bioactive compounds from mushrooms such as *Agaricus campestroides*, *A. flocculosipes*,

Phlebopus portentosus, and *P. spongiosus* discovered in Thailand were extensively studied (Chuankid et al., 2020, 2021). The study of Thai mushrooms biodiversity, including basidiomata and cultured mycelium, provides an opportunity to discover new antibiotics and other active substances for use in foods, supplements, pharmaceutical and agrochemical applications. Most saprotrophic species can be brought into culture, opening up the possibility for studying mycelia cultures to find out their potential to produce secondary metabolites with interesting bioactivities.

This study shows that selected strains can produce unique compounds such as blazeispirol derivative from *Agaricus* spp., which showed selective agonist activity against Liver X receptor alpha with beneficial effects in vivo in a murine model. Also, novel natural products produced by *Phlebopus* spp. in liquid fermentation were found to exhibit weak to moderate cytotoxic activities against several tumor cell lines. All the strains from this study have been deposited in MFLU culture collection and can be further studied for production of antibiotics and other beneficial secondary metabolites. Moreover, the biosynthesis pathways could be also studied to enhance the production of new natural products.

5.3 Cultivation the Wild Strain of *Agaricus*

In this part of the dissertation, several mycelia cultures were isolated, studied and preserved for further discovery of potential bioactive compounds, as well as cultivation of edible wild mushrooms from Thailand. This study reported the first successful cultivation of a wild strain of *Agaricus campestroides* from Thailand. The morphological description and molecular examination of the mushroom was included, in order to confirm the identification of *A. campestroides*. Optimization was carried out for mycelium growth and mushroom production. Potato dextrose yeast agar (PDYA) at pH 5.0 and a temperature of 20–30 °C on a sorghum spawn was used for up-scaling of the mycelium to be used for mushroom production. Optimal conditions for the mushroom production phase were 25–30 °C with 80–90% humidity in the compost with casing soil. Additionally, the secondary metabolites from basidiomes and cultured mycelium were investigated. Blazeispirols (blazeispirol A and D), a family of

triterpenoids that is known to act as selective agonists against Liver X receptor alpha with beneficial effects in vivo in a murine model, were detected in crude extracts from submerged cultures of *A. campestroides* and *A. flocculosipes*. The mating studies should be done with the aim of finding the best strains to increase mushroom production and the content in usable bioactive compounds. A reliable method for cultivation that is cost-efficient and easy for mushrooms growers to follow need to be considered.

5.4 Research Advantages

This dissertation implemented an interdisciplinary approach for mushroom identification and cultivation. A combined approach was applied based on morphological species concept, secondary metabolite profiles, and phylogenetic species concepts among taxa.

5.4.1 This research contributed ten novel taxa to science with illustration and molecular data. Newly generated sequences of four loci including *atp*6, ITS, *rpb*2, and *tef*1, were deposited in GenBank. Also, the secondary metabolites of *A. campestroides*, *A. flocculosipes*, and *P. spongiosus* were studied for the first time. Two blazeispirols were obtained from *Agaricus* which might give rise to the development of a new anti-hypercholesterolemia and anti-diabetic medicines or food supplements. The 9′-hydroxyphenyl pulvinone from *Phlebopus* exhibited weak to moderate cytotoxic activities against several tumor cell lines. It could be developed in the future to a drug that acts in combination with other compounds to combat the tumor cells.

5.4.2 The mushroom classification and review of important bioactive compounds and their application is expected to inspire further research on secondary metabolites in Thai mushrooms.

5.4.3 This is the first study on successfully cultivation of *A. campestroides* for Thailand with included detection of secondary metabolites from mycelia cultures. The results will be useful for researchers who study on mushrooms cultivation and to develop production methods for *A. campestroides* on the industrial scale. Cultivable mushrooms are a promising source of income for local populations in Thailand and other countries.

5.5 Future work

5.5.1 Thailand is a hotspot to explore mushroom biodiversity as many of the collections which are collected there are new to science. More collections are needed, to confirm the taxonomy and phylogeny of interesting species that were reported as new to science based on single collections. Even though the unique morphological features and multiple gene phylogenies were sufficient to confirm them as new species, finding and examining additional material is needed to better characterize their variation for a more reliable taxonomic system. Moreover, a monograph of mushrooms in Thailand is required.

5.5.2 The sequences of nuclear or mitochondrial protein-coding genes from holotype specimens are needed. Many studies have been based on only ITS and LSU sequences as molecular evidence, which in some cases could not effectively resolve phylogenetic relationships. The evidence to confirm the status of species by using morphology and sequences of more genes from holotype specimens is preferable.

5.5.3 Many mushrooms have not been well investigated for their secondary metabolite production. In the future those strains should be explored for their potential in biotechnological process and industrial application.

5.5.4 Evolutionary approach can be used as evidence for mushroom identification. Therefore, the preserved strains can be used for genomics studies.

5.5.5 OMICS techniques, bioinformatics, analytical chemistry and biotechnology could be used for discover new metabolites and to develop them further to find the candidates drugs, agrochemicals and other products for the life science industry.

5.6 Publications

As a result of this thesis and other activities during my PhD, I have published four papers as first author and one paper as co-first author in SCI journals. Furthermore, I have also co-authored 7 other SCI publications. Those are listed below and appended to the theses.

First author

Chuankid, B., Vadthanarat, S., Hyde, K. D., Thongklang, N., Zhao, R., Lumyong, S., & Raspé, O. (2019). Three new *Phylloporus* species from tropical China and Thailand. *Mycological Progress*, *18*(5), 603–614.

Chuankid, B., Schrey, H., Thongbai, B., Raspé, O., Arnold, N., Hyde, K. D., & Stadler, M. (2020). Secondary metabolites of *Phlebopus* species from Northern Thailand. *Mycological Progress*, *19*(12), 1525-1536.

Chuankid, B., Vadthanarat, S., Thongbai, B., Stadler, M., Lumyong, S., Hyde, K. D., & Raspé, O. (2021). *Retiboletus* (Boletaceae) in northem Thailand: one novel species and two first records. *Mycoscience*, *62*(5), 297–306.

Chuankid, B., Schrey, H., Stadler, M., Thongklang, N., Hyde, K. D. (2021). Cultivation and identification of blazeispirols of *Agaricus campestroides* and *A. flocculosipes*. *Fungal Biotec*, *1*(2), 101–117.

Chuankid, B., Hyde, K. D., & Raspé, O. (2022). New species of Xerocomoideae. In press

Co-author

He, M. Q., Chuankid, B., Hyde, K. D., Cheewangkoon, R., & Zhao, R. L. (2018). A new section and species of *Agaricus* subgenus *Pseudochitonia* from Thailand. *MycoKeys*, (40), 53.

Hyde, K. D., Xu, J., Rapior, S., Jeewon, R., Lumyong, S., Niego, A. G. T., ... & Stadler, M. (2019). The amazing potential of fungi: 50 ways we can exploit fungi industrially. *Fungal Diversity*, *97*(1), 1–136.

Jayawardena, R. S., Hyde, K. D., Chen, Y. J., Papp, V., Palla, B., Papp, D., ... & Wang, Y. (2020). One stop shop IV: taxonomic update with molecular phylogeny for important phytopathogenic genera: 76–100 (2020). *Fungal Diversity*, *103*(1), 87-218.

Chethana, K. W. T., Niranjan, M., Dong, W., Samarakoon, M. C., Bao, D. F., Calabon, M. S., ... & Hyde, K. D. (2021). AJOM new records and c ollections of fungi: 101–150. *Asian J Mycol*, *4*, 113-260.

Phonemany, M., Raspé, O., Sysouphanthong, P., Niego, A. G. T., Thongklang, N., Chuankid, B., & Hyde, K. D. (2021). Two *Pleurotus* Species (Pleurotaceae) From Lao People's Democratic Republic. *Chiang Mai Journal of Science*, *48*(5), 1224-1235.

Fifteen major decadal advances in fungal biology leading towards human well-being – New mushrooms from wild to table.

Mushrooms as the future food and nutraceutical: mushroom genomics.

CHAPTER 6

TAXONOMY AND PHYLOGENY OF OTHER AGARICOMYCETIDAE IN THE CONTRIBUTED PAPERS

6.1 *Agaricus* (*Pseudochitonia*) section *Cymbiformes* M.Q. He & R.L. Zhao, sect. nov.

Mycobank number: MB824147, *Faceoffungi number*: FoF04104

Etymology: In reference to the cymbiform basidiospores.

KOH reaction negative, **Schäffer's reaction** negative on dry specimens. No discolouration on touching, but discolouration reddish-brown on cutting. **Annulus** membranous. **Smell** strong iodoform. **Basidiospores** cymbiform and **cheilocystidia** narrow with variable shapes.

Type species: *Agaricus angusticystidiatus* M.Q. He, Desjardin., K.D. Hyde & R.L. Zhao.

Agaricus angusticystidiatus M.Q. He, Desjardin, K.D. Hyde & R.L. Zhao, **sp. nov.**, MycoKeys 40: 62 (2018)

Mycobank number: MB825177, *Faceoffungi number*: FoF04105

Etymology: refers to the narrow clavate cheilocystidia.

Holotype: ZRL2043 (HMAS279593)

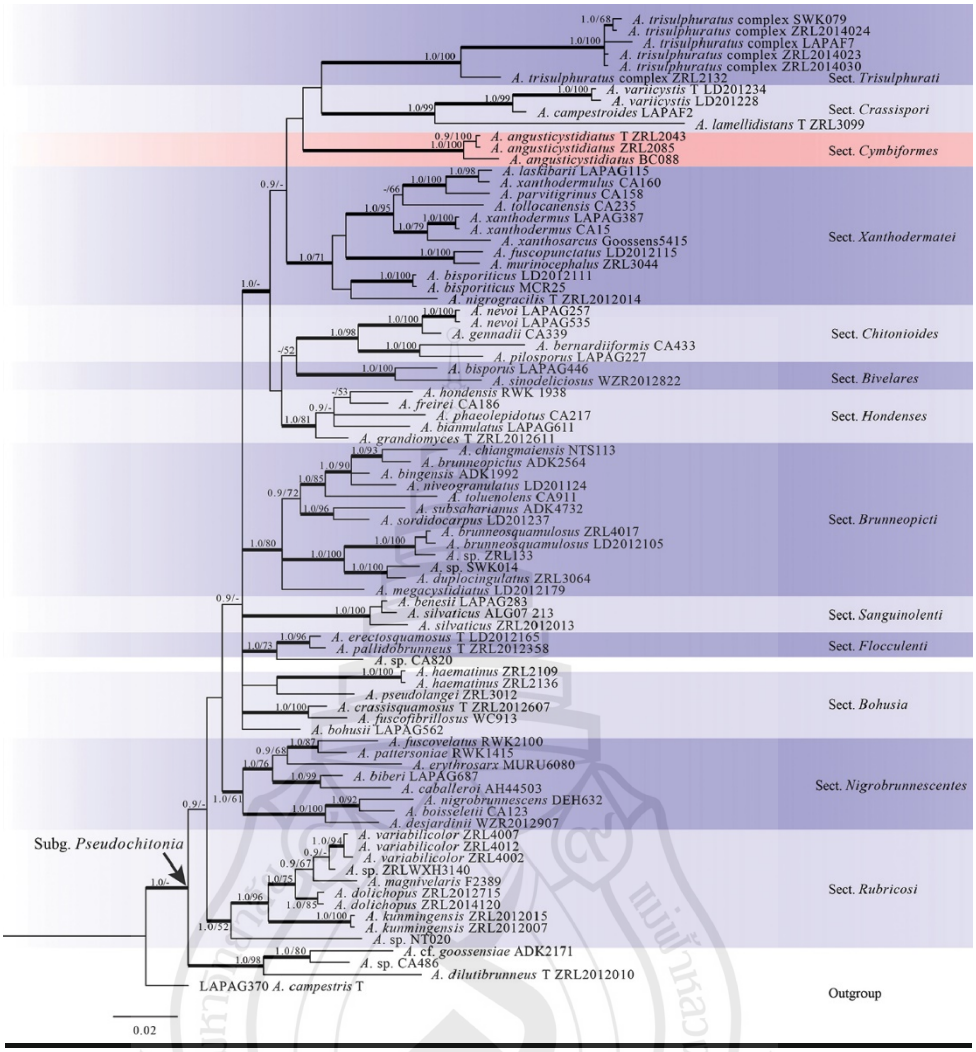
Pileus 40–80 mm diam., plano-convex, applanate, broadly umbonate; surface concentric squamulose with small skull-cup at disc, appressed, slightly fissured, light brown (6D8), brown (7E3), greyish-brown (5D5), dark brown (6D6) against the grey (8E3) background. Context 4–5 mm thick at disc, fragile, white to grey (8E3) in age. Lamellae free, crowded, lamellulae with 3–4 lengths, 3–4 mm broad, normal to slightly ventricose, brown (7E5) to dark brown (7F7-8), edge colour similar to the gill itself. ***Stipe*** 55–100 × 5–8 (base 8–15) mm, cylindrical bulbous, with rhizomorphs in most

cases, hollow, surface glabrous to silky, white to dark brown (6D6). Annulus pendent or percurrent; single; upper side membranous, white; lower side surface powdery, light yellow (4B2) grain-like dots in circulate; superior, persistent, edge entire, up to 5 mm broad. Smell of iodoform. No colour change on touching; light dull red, greyish brown (7D4) on cutting. ***KOH reaction***: negative. ***Schäffer's reaction***: negative on dry specimens.

Basidiospores 5–6.5 × 3–4 (–4.5) µm [X = 5.6 ± 0.5 × 3.8 ± 0.4, Q = 1.1–2.2, Q_m = 1.52 ± 0.7, n = 20], cymbiform, some endosporium, no germ pore, brown. ***Basidia*** 10–15 × 5.5–7 µm, clavate, hyaline, smooth, 4-spored. ***Pleurocystidia*** absent. ***Cheilocystidia*** 20–30 (–45) × 5–8 µm, occasionally one septum, narrowly clavate to clavate, some with elongated top, rarely subcapitate, hyaline, smooth. ***Pileipellis*** cutis consisting of 3–5 µm diam. hyphae, hyaline, smooth, non-constricted at septa. ***Annulus*** hyphae same as pileipellis.

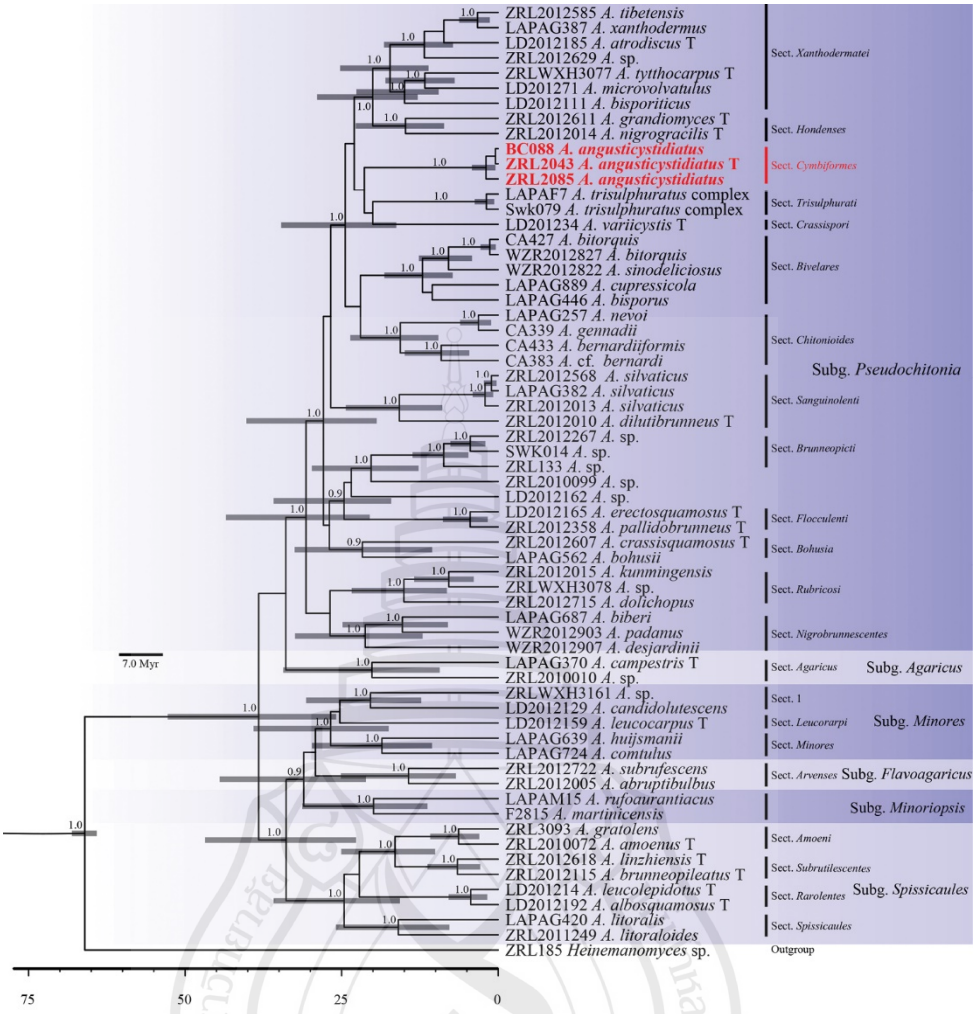
Materials examined: Thailand, Chiang Mai Province, Mae Taeng, Ban Mae Sae Village, on Hwy 1095 near 50 km marker, 19°14.599'N, 98°39.456'E, elev. ca. 960 m, 3 July 2004, collected by Thitiya Boonpratuang, ZRL2085 (HMAS279594, and SFSUZRL2085); Thailand, Chiang Mai Province, Mae Taeng, Mushrooms research center, 30 July 2014, collected by Boontiya Chuankid, BC088 (MFLU 14-0903).

Notes: This new species is morphologically distinguished from other *Agaricus* by its strong iodoform smell, context reddish-brown discolouration on cutting, cymbiform basidiospores and narrow cheilocystidia with variable shapes. Phylogenetic analyses confirmed it is a member of the subgenus *Pseudochitonia* with an isolated phylogenetic position in *Agaricus*. This new species is similar to *A. iodolens* Heinem. & Gooss.-Font. of section *Xanthodermatei*, because both have relatively slender basidiomes and odour of iodine (Thongklang et al., 2014). However, this new species has cymbiform basidiospores and a bulbous stipe, while those of *A. iodolens* are ellipsoid and an equal stipe (Zoberi, 1972). *Agaricus lamellidistans* R.L. Zhao and *A. variicystis* L.J. Chen, K. D. Hyde & R. L. Zhao of section *Crassispori* resemble this new species, because all have greyish-brown pilei and cymbiform basidiospores. These species lack discolouration on cutting, while those of *A. angusticystidiatus* have dull red discolouration on cutting (Zhao et al., 2016).



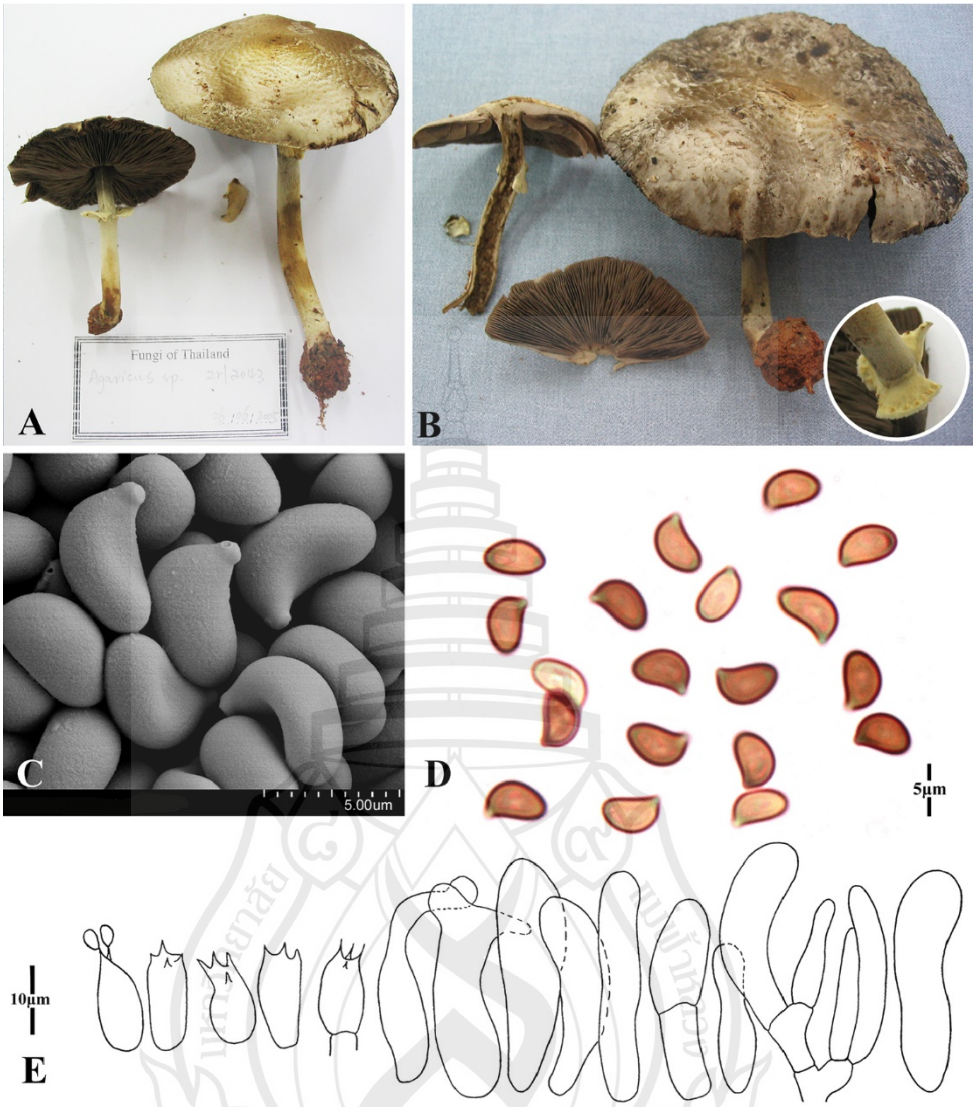
Note Phylogenetic tree of *Agaricus* subgenus *Pseudochitonia* generated from Bayesian analysis of ITS sequences, rooted with *A. campestris*. Bayesian posterior probability (PP) values ≥ 0.9 or Bootstrap support (BS) values ≥ 50% are indicated at the internodes (PP/BS). The branches in bold mean the related PP > 0.95, "T" refers to sequences from type specimen.

Figure 6.1 Phylogenetic tree of *Agaricus* subgenus *Pseudochitonia* generated from Bayesian analysis of ITS sequences



Note Maximium Clade Credibility tree of genus *Agaricus* based on ITS, LSU and *tef*1-α gene sequences with the outgroup *Heinemannomyces* sp. Posterior probability values equal or above 0.9 are annotated at the internodes. The 95% highest posterior density of divergence time estimation are marked by horizontal bars.

Figure 6.2 Maximium Clade Credibility tree of genus *Agaricus* based on ITS, LSU and *tef*1-α gene sequences with the outgroup *Heinemannomyces* sp.



Note Morphology of *Agaricus angusticystidiatus* A, B basidiomes C, D basidiospores E basidia and cheilocystidia.

Figure 6.3 Morphology of *Agaricus angusticystidiatus*

6.2 *Armillaria* (Fr.) Staude, Schwämme Mitteldeutschl. 28: xxviii, 130 (1857)

Classifcation—Basidiomycota, Agaricomycotina, Agaricomycetes, Agaricomycetidae, Agaricales, Physalacriaceae (He et al., 2019)

Disease symptoms—*Armillaria* root disease, shoestring root rot

Symptoms caused by this fungus can be categorized into two categories:

Crown symptoms—branch dieback, crown thinning, chlorosis, reddening of foliage or heavier than normal production of cones.

Basal symptoms—the fungus can grow up from the roots in the inner bark in some tree species and causes basal cankers above the infected roots. Resinosis (exudation of resin) can be observed in resinous conifers. In some plants, decayed roots or decay in the inner wood of stem bases can be observed. Species cause a white rot of wood. In white rot, wood often has a bleached, whitish appearance and are spongy or stringy, and maybe wet. Black lines called "zone lines" are usually seen in the decayed wood. These lines are curved planes in the wood, sometimes called "pseudosclerotial plates", composed of thickened, dark fungal cells. They may play a role in the protection of *Armillaria* from unfavourable conditions or other fungi that attempt to invade its territory, including other individuals of the same species. Actively decaying wood may be luminescent, producing a faint glow in the dark (Baumgartner & Rizzo 2002; Worrall, 2004; Klopfenstein, 2009).

There are three major signs of *Armillaria* root disease in the field.

Mycelia fans can always be seen in infected and recently killed trees. These are white mats of fungal mycelium between the inner bark and wood that are generally substantial and have a mushroom odour.

Rhizomorphs are commonly associated with infection and are often attached to infected roots, but they may also be attached to the surface of uninfected roots. Depending on the species these may be few, small, fragile, hard to find or abundant and robust. Rhizomorphs can be cylindrical in soil or fattened under bark, reddish-brown to black branched and have a cream-coloured tip when actively growing (Guillaumin & Legrand, 2013). Mushrooms that have honey-brown caps can be seen in clusters near or on the base of trees.

Type species—*Armillaria mellea* (Vahl) P. Kumm.

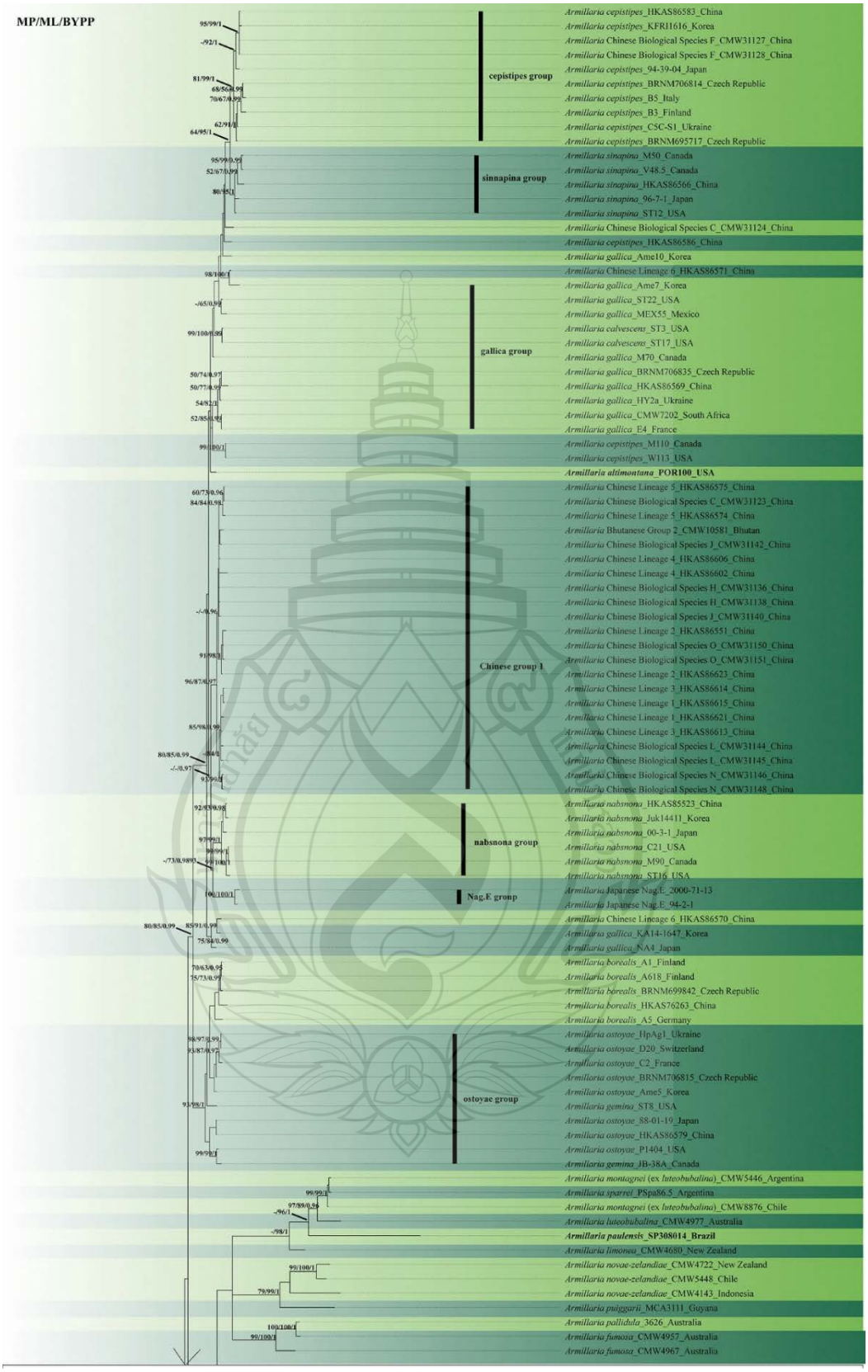
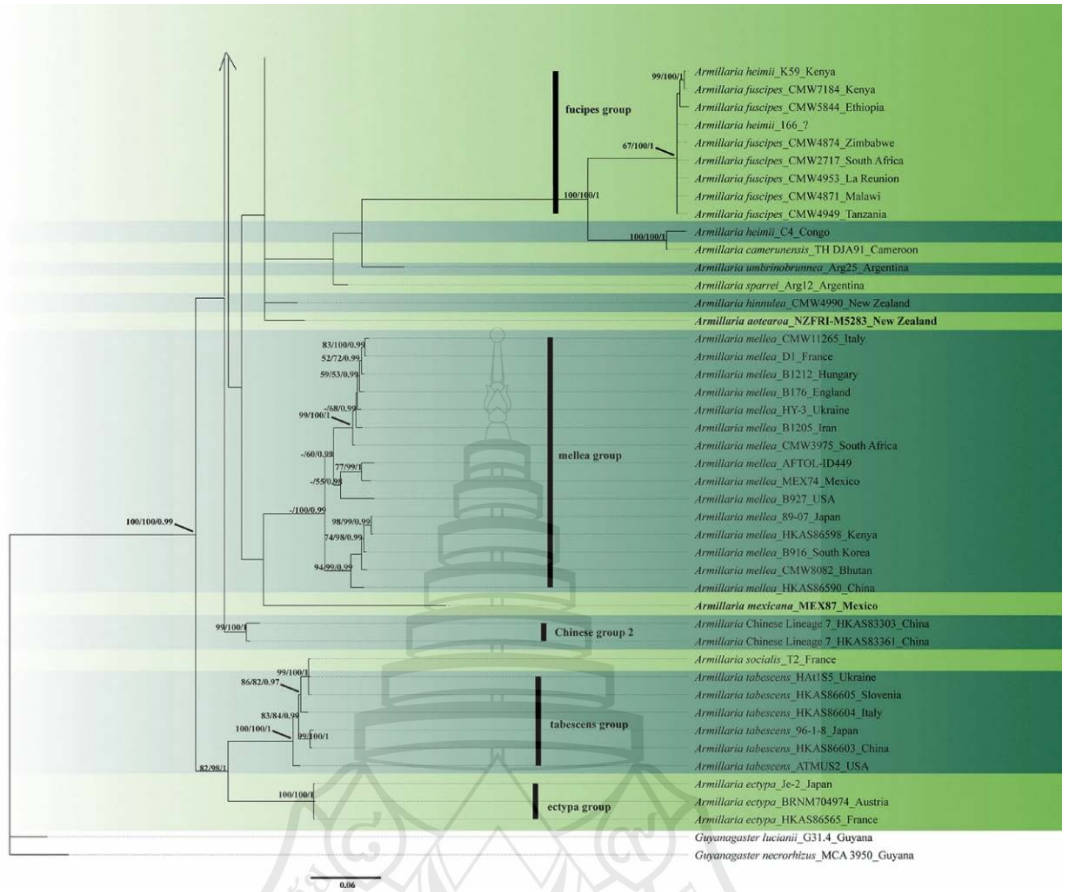


Figure 6.4 Phylogenetic tree generated by maximum likelihood analysis of combined ITS-IGS-*tef*1 sequence data of *Armillaria* species



Note Phylogenetic tree generated by maximum likelihood analysis of combined ITS-IGS-*tef*1 sequence data of *Armillaria* species. Related sequences were obtained from GenBank. One hundred and thirty-nine strains are included in the analyses, which comprise 4557 characters including gaps. The tree was rooted with *Guyanagaster lucianii* (G31.4) and *Guyanagaster necrorhizus* (MCA 3950). Single gene analyses were carried out to compare the topology of the tree and clade stability. Tree topology of the ML analysis was similar to the MP and BYPP. ML phylogenetic tree inference was performed using RAxML version 8.2.12 on the CIPRES web server, using a mixed-model analysis and the GTRCAT model of substitution. The four partitions were defined as ITS, IGS, *tef*1 exons and tef1 introns. The best scoring RAxML tree with a final likelihood value of − 25308.198187 is presented. The matrix had 1957 distinct alignment patterns, with 65.74% of undetermined characters or gaps. Estimated base frequencies of ITS were as follows: A=0.227071, C=0.203923, G=0.235701,

T=0.333305; substitution rates AC=0.628852, AG=3.751709, AT=1.365607, CG=1.467905, CT=2.788595, GT=1.000000. Estimated base frequencies of IGS were as follows: A=0.244624, C=0.196588, G=0.242370, T=0.316418; substitution rates AC=0.954911, AG=3.055115, AT=1.041498, CG=1.278095, CT= 3.421100, GT=1.000000. Estimated base frequencies of *tef1* exons were as follows: A=0.228587, C=0.301128, G=0.255865, T=0.214420; substitution rates AC=0.905728, AG=3.660986, AT=1.564184, CG=0.648739, CT= 28.048363, GT=1.000000. Estimated base frequencies of tef1 introns were as follows: A=0.215042, C=0.222693, G=0.185633, T=0.376631; substitution rates AC=1.170263, AG=5.878084, AT=0.847943, CG=1.087990, CT= 5.095797, GT=1.000000; gamma distribution shape parameter α =0.1000000000. The maximum parsimonious dataset consisted of 2908 constant, 1172 parsimony-informative and 477 parsimony-uninformative characters. The parsimony analysis: CI = 0.610, RI = 0.861, RC = 0.525, HI = 0.390 in the first tree. Bayesian posterior probability was performed using the Markov chain Monte Carlo (MCMC) method implemented in MrBayes 3.2.6 with a mixed-model partition identical to the ones defned in the ML analysis. The best-ft nucleotide substitution model was separately determined for each partition with jModeltest version 2.1.10 on CIPRES, using the Akaike Information Criterion. K80+I, K80+I, SYM+G and HKY+G were selected as best-fit models for ITS, IGS, *tef*1 exons and tef1 introns, respectively. At the end of the runs, the average deviation of split frequencies was 0.016675. MP and RAxML bootstrap support value≥ 50% and BYPP ≥ 0.95 are shown, respectively, near the nodes. Holotype or ex-type strains are in bold.

Table 6.1 DNA barcodes available for *Armillaria*

Species	Sources	Country	ITS	LSU	*tef1*	IGS1
Armillariaaffinis	JMCR.126	Central America?	-	AF261356	-	-
A. altimontana	**POR100***	USA	AY213579, AY213580	-	JN944606, JF313117	AY509181
A. aotearoa	**NZFRI-M5283***	New Zealand	NR_151846	-	KU295542	-
A. borealis	CMW31075	Belarus	-	-	KM205252	KM205305
	CMW31072	China	-	-	KM205251	KM205304
	HKAS 76263, Gt571	China	KT822294	-	KT822426	-
	BRNM 699842, MUAF 501	Czech Republic	EU257713	-	EU251402	EU257708
	CMW3172	Finland	-	DQ338540	DQ435623	-
	A1	Finland	JN657467	-	JN657494	JN657440
	A5	Germany	JN657468	-	JN657495	JN657441
	A618	Switzerland	JN657469	-	JN657496	JN657442
A. calvescens	ST3	USA	AY213559	JF895899	JF313138, JF895835	AY509163
	ST17	USA	AY213560, AY213561	JF895900	JF313130, JF895836	AY509164
	TH DJA 91/PUL F2895	Cameroon	KU170952	KU170942	KU289112	-
A. cepistipes	BRNM 706814, MUAF 516	Czech Republic	EU257715	-	EU251395	EU257709
	M110	Canada	AY213581	-	JF313121	AY509182

Table 6.1 (continued)

Species	Sources	Country	ITS	LSU	*tef1*	IGS1
	HKAS 86583, 01108/1	China	KT822290	-	KT822417	-
	B3	Finland	JN657445	-	JN657472	JN657418
	B5	Italy	JN657446	-	JN657473 KJ414321	JN657419, KJ414318
	94-39-04	Japan	AB510853	-	AB510786	AB510809
	SY1Ra	UK?	-	-	JF746917	JF288720
	C5C-S1	Ukraine	JN657450	-	JN657477	JN657423
	W113	USA	AY213583	-	JF313115	AY509184
	BRNM 695717	Czech Republic	EU257716	-	EU251396	EU257710
	HKAS 86586, 97033/1	China	KT822263	-	KT822416	-
	KFRI1616	Korea	MG543860	-	MG544785	-
A. ectypa	BRNM 704974	Austria	EU257720	-	EU251403	EU257712
	CMW15693	France	-	DQ338547	FJ875698	-
	HKAS 86565, 70011/13	France	KT822340	-	KT822438	-
	TFM27105, Je-2	Japan	AB559000	-	AB558992	-
A. fumosa	CMW4957, 123	Australia	AF329917	DQ338552	DQ435646	-
A. fuscipes	CBS 118122, CMW5844, WG1I	Ethiopia	AY882969	-	-	AY172032

Table 6.1 (continued)

Species	Sources	Country	ITS	LSU	*tef1*	IGS1
	CMW7184	Kenya	AY882973	-	-	AY882965
	CMW4953	La Reunion	AY882974	DQ338556	DQ435622	AY882963
	CMW4871	Malawi	AY882976	-	-	AY882959
	CMW2717	South Africa	AY882971	-	-	AF204821
	CMW4949	Tanzania	AY882978	-	-	AY882961
	CMW4874	Zimbabwe	AY882967	-	-	AF489481
A. gallica	M70	Canada	AY213568	-	JF313123	AY509171
	CMW31087	China	-	-	KM205260	KM205313
	HKAS 86569, 93421/1	China	KT822277	-	KT822414	-
	BRNM 706835, MUAF 575	Czech Republic	EU257718	-	EU251390	EU636240
	E4	France	JN657452	-	JN657479	JN657425
	86-016/3	Germany	-	-	KJ200952	KJ200946
	86-008/2	Iran	-	-	KJ200954	KJ200948
	NA4	Japan	AB510881	-	AB510761	AB510834
	MEX55	Mexico	JX281809	-	KC111014	JX281799
	CMW7202	South Africa	AY190247	-	-	AY190245
	HY2a	Ukraine	JN657455	-	JN657482	JN657428
	Aga235	USA	-	JF895911	JF895847	-

Table 6.1 (continued)

Species	Sources	Country	ITS	LSU	*tef1*	IGS1
	ST22, EL-1	USA	AY213569, AY213570	JF895912	JF313126, JF895848	AY509172
	Ame10	Korea	MG543850	-	MG544774	-
	KA14-1647	Korea	MG543859	-	MG544784	-
	Ame7	Korea	MG543852	-	MG544777	-
A. gemina	JB-38A	Canada	FJ664586	FJ618757	FJ618670	-
	ST8	USA	AY213555	-	JF313136	AY509158, AY509159
A. heimii	C4	Congo	AY333917	-	-	AY330630
	166	-	AY333913	-	-	AY330634
	K59	Kenya	AY333916	-	-	AY330627
A. hinnulea	CMW4980	Australia	-	DQ338555	DQ435648	AF445077
	CMW4990	New Zealand	AF329905	DQ338555	DQ435648	-
A. jezoensis	HUA9116	Japan	-	-	-	D89921
A. limonea	CMW4680	New Zealand	AF329930	DQ338560	DQ435655	AF445073
A. lutea	90-4 (Alut)	USA	-	-	-	AF243066
A. luteobubalina	CMW4977	Australia	AF329912	DQ338559	DQ435657	AF445069
A. mellea	AFTOL-ID449	USA	AY789081	AY700194	AY881023	-
	B176	England	AF163578	-	-	AF163602
	HKAS 86590, 00020/6	China	KT822251	-	KT822354	-
	D1	France	JN657464	-	JN657491	JN657437

Table 6.1 (continued)

Species	Sources	Country	ITS	LSU	*tef1*	IGS1
	B1212, CMW4615, 94056/1	Hungary	AF163581	-	-	AF163605
	B1205, CMW4613, 86009/1	Iran	AF163583	-	DQ435637	AF163606
	CBS122232, CMW11265, 426	Italy	FJ875692	FJ875694	DQ435636	-
	FFPRI420861, WD2588, 89-07	Japan	AB510852	-	AB510796	AB510808
	HKAS 86598, PFD84-103	Kenya	KT822248	-	KT822348	-
	MEX74	Mexico	JX281807	-	KC111011	JX281797
	CMW3975	South Africa	AF310329	-	-	AF310327
	B916, CMW4610, A-5	South Korea	AF163592	-	DQ435639	AF163612
	HY-3	Ukraine	JN657466	-	JN657493	JN657439
	Am115	USA	-	JF895920	JF895856	-
	B927	USA	AF163595	FJ875695	DQ435634	AF163608
	CMW31161	China	-	-	KM205267	KM205320
	CMW8082	Bhutan	AY554333	-	-	AY554335
	HUA93110	Japan	-	-	-	D89922

Table 6.1 (continued)

Species	Sources	Country	ITS	LSU	*tef1*	IGS1
A. mexicana	**MEX87***	Mexico	KR061310	-	KR061314	KR061306
A. montagnei (ex *luteobublina*)	CMW5446	Argentina	AF448422	DQ338562	DQ435650	AF445068
A. montagnei (ex *luteobublina*)	CMW8876	Chile	AF448423	-	DQ435658	AF445065
A. montagnei (Lineage II)	Arg309	Argentina	FJ660939	FJ711625	-	-
***A. montagnei* (Lineage II)**	**Arg270***	Argentina	FJ711609	-	-	-
A. nabsnona	ST16	USA	AY213574	-	JF313124	AY509178
	HKAS 85523, Gt798	China	KT822333	-	KT822411	-
	M90	Canada	AY213573	-	JF313122	AY509176, AY509177
	00-3-1	Japan	AB510899	-	AB510766	AB510850
	C21	USA	AY213572	-	JF313119	AY509174, AY509175
	CMW6905	USA	-	DQ338542	DQ435631	-
	Juk14411	Korea	MG543857	-	MG544782	-
A. novae-zelandiae	CMW4967	Australia	AF329921	-	DQ435651	-
	CMW5448	Chile	AF448417	DQ338554	DQ435653	-
	CMW4143	Indonesia	AF448421	DQ338564	DQ435654	-

Table 6.1 (continued)

Species	Sources	Country	ITS	LSU	*tef1*	IGS1
	CMW3951	Malaysia	AF448419	DQ338553	-	-
	CMW4722	New Zealand	AF329926	DQ338551	DQ435652	-
A. novae-zelandiae (Lineage I)	Arg49	Argentina	FJ660935	FJ711629	-	-
A. ostoyae	**SP308014***	Brazil	EF639348	-	-	-
	BRNM706815	Czech Republic	EU257717	-	EU251400	EU257711
	CMW31102	China	-	-	KM205272	KM205325
	HKAS 86579, 96043/11	China	KT822310	-	KT822428	-
	C2	France	JN657459	-	JN657486	JN657432
	88-01-19	Japan	AB510859	-	AB510784	AB510815
	D20	Switzerland	JN657463	-	JN657490	JN657436
	HpAg1	Ukraine	JN657462	-	JN657489	JN657435
	P1404	USA	AY213554	-	JF313140	AY509157
	Ame5	Korea	MG543851	-	MG544776	-
	3626	Australia	FJ664607	FJ618752	FJ618665	-
A. puiggarii	MCA 3111/PUL F2896/BRG 41295	Guyana	KU170954	KU254228	KU289104	-
A. sinapina	V48.5	Canada	FJ664609	FJ618763	FJ618676	-
	M50	Canada	AY213563, AY213564	-	JF313114	AY509167

Table 6.1 (continued)

Species	Sources	Country	ITS	LSU	*tef1*	IGS1
	CMW31112	China	-	-	KM205277	KM205330
	HKAS 86566, 96015/39	China	KT822323	-	KT822422	-
	96-7-1	Japan	AB510873	-	AB510774	AB510827
	P2-7	USA	-	JF895916	JF895850	-
	ST12	USA	AY213565	-	JF313132	AY509168
A. singula	**HUA9101***	Japan	-	-	-	D89926
A. socialis	T2	France	DQ784801	-	-	-
A. solidipes	MS2-11	USA	-	JF895918	JF895852	-
	CMW31107	Finland	-	-	KM205275	KM205328
A. sparrei	PSpa86.5	Argentina	FJ664612	FJ618750	-	-
	Arg12	Argentina	FJ660948	FJ711618	-	-
A. umbrinobrunnea	Arg25	Argentina	FJ660946	FJ711621	-	-
A. tabescens	CMW31118	China	-	-	KM205280	KM205333
	99122/13	China	KT822339	-	KT822441	-
	CMW3165	France	-	DQ338546	DQ435642	-
	CMW31119	Italy	-	-	KM205281	KM205334
	HKAS 86604, CT1097.3	Italy	KT822338	-	KT822440	-
	96-1-8	Japan	AB510867	-	AB510804	AB510823

Table 6.1 (continued)

Species	Sources	Country	ITS	LSU	*tef1*	IGS1
	HKAS 86605, 901582	Slovenia	KT822337	-	KT822439	-
	HAt1S5	Ukraine	HQ232292	-	HQ285906	HQ232284
	ATMUS2	USA	AY213588	-	JF313113	AY509189, AY509190
Bhutanese Group 2	CMW10581	Bhutan	AY554329	-	FJ875699	AY624365
Chinese Biological species C	CMW31123	China	-	-	KM205284	KM205337
	CMW31124	China	-	-	KM205285	KM205337
Chinese Biological species F	CMW31127	China	-	-	KM205286	KM205339
	CMW31128	China	-	-	KM205287	KM205340
Chinese Biological species H	CMW31136	China	-	-	KM205293	KM205346
	CMW31138	China	-	-	KM205294	KM205347
Chinese Biological species J	CMW31140	China	-	-	KM205296	KM205349
	CMW31142	China	-	-	KM205297	KM205350
Chinese Biological species L	CMW31144	China	-	-	KM205298	KM205351

Table 6.1 (continued)

Species	Sources	Country	ITS	LSU	*tef1*	IGS1
	CMW31145	China	-	-	KM205299	KM205352
Chinese Biological species N	CMW31146	China	-	-	KM205300	KM205353
	CMW31148	China	-	-	KM205301	KM205354
Chinese Biological species O	CMW31150	China	-	-	KM205302	KM205355
	CMW31151	China	-	-	KM205303	KM205356
Chinese Lineage 1	HKAS 86615	China	KT822315	-	KT822384	-
	HKAS 86621	China	KT822306	-	KT822386	-
Chinese Lineage 2	HKAS 86623	China	KT822318	-	KT822363	-
	HKAS 86551	China	KT822279	-	KT822367	-
Chinese Lineage 3	HKAS 86613	China	KT822319	-	KT822388	-
	HKAS 86614	China	KT822305	-	KT822391	-
Chinese Lineage 4	HKAS 86602	China	KT822308	-	KT822378	-
	HKAS 86606	China	KT822281	-	KT822359	-
Chinese Lineage 5	HKAS 86574	China	KT822324	-	KT822361	-
	HKAS 86574	China	KT822327	-	KT822364	-
Chinese Lineage 6	HKAS 86570	China	KT822320	-	KT822402	-
	HKAS 86571	China	KT822288	-	KT822404	-
Chinese Lineage 7	HKAS 83303	China	KU378047	-	KT822437	-

Table 6.1 (continued)

Species	Sources	Country	ITS	LSU	*tef1*	IGS1
	HKAS 83361	China	KU378048	-	KT822436	-
Japanese Nag. E	94-2-1	Japan	AB510888	-	AB510768	AB510840
	2000-71-13	Japan	AB510879	-	AB510773	AB510832

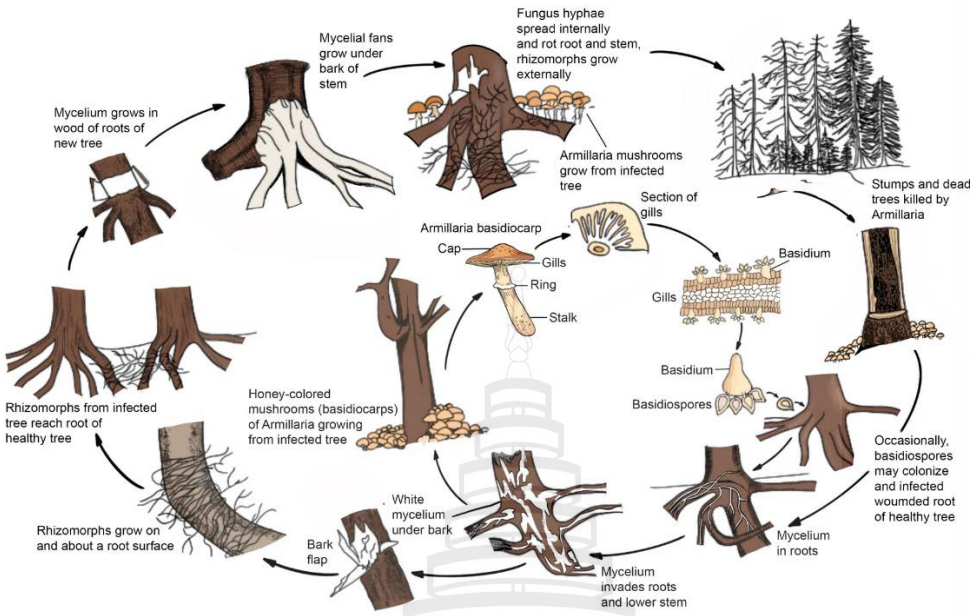


Figure 6.5 Disease cycle of *Armillaria mellea* (redrawn from Agrios, 2005)

6.3 *Phylloporus* Quél., Fl. mycol. France (Paris): 409 (1888)

Index Fungorum number: IF18275, *Facesoffungi number*: FoF 09166

Phylloporus is characterised by a gilled to somewhat poroid hymenophore and bacillate basidiospore ornamention, with few exceptions (Neves & Halling, 2010; Neves et al., 2012; Chuankid et al., 2019). The type species, *P. pelletieri* (Lév.) Quél., was described from Europe and approximately 90 species have been described from all over the world (He et al., 2019; Index Fungorum, 2020). *Phylloporus* species have been reported from tropical to subtropical as well as temperate areas (Corner, 1970). In Asia, they are found mostly in forests dominated by Fagaceae or Dipterocarpaceae (Neves et al., 2012; Zeng et al., 2013; Chuankid et al., 2019). An updated, three-gene phylogenetic tree of *Phylloporus* including the two first records for Thailand is presented here.

Phylloporus attenuatus Hosen, Mycologia 109: 279 (2017)

Index Fungorum number: IF803939, *Facesoffungi number*: FoF 09167

Basidiomata gregarious to caespitose, small to medium-sized. ***Pileus*** 11–62 mm in diam., convex to plano-convex, with age becoming applanate to slightly depressed at center; margin inflexed, uplifted in age; surface dry, even, becoming cracked with age, brown (7E7-8) or brownish orange (7C7–8) to brick red or burnt Sienna (7D7–8) when young, fading with age; context 7–24 mm thick at center, pale yellow (1A3), turning slightly blue when cut. ***Hymenophore*** lamellate, subdecurrent to deeply decurrent. ***Lamellae*** 11–36 × 3–5 mm, intervenose, sometimes forked, ventricose, subdistant; surface transvenose, smooth, yellow (2A6), rapidly and intensely staining blue when injured, then turning red with time; edge entire, concolorous; lamellulae common, in 1–3 tiers. ***Stipe*** 24–44 × 3–10 mm, central, straight or sometimes curved, tapering downwards, sometimes slightly radicant; surface dry, with yellow pruina at the top, then with fine reddish dots mostly down to the lower third, lower part off-white to light greyish yellow (2A4); context solid, pale yellow (1A3), staining slightly blue at upper part when cut or injured, lower part remaining unchanged. ***Basal mycelium*** little developed, tomentose, yellow. ***Odor and taste*** not distinctive.

Basidiospores [150/3/3] (6.5–)6.6–*7.6*–8.9(–9.7) × (4–)4–*4.4*–4.8(–4.9) µm, Q = (1.45–)1.58–*1.74*–2.19(–2.39), ovoid to ellipsoid, greyish yellow (1B2–4) when observed in H_2O and 5% KOH, smooth under light microscope. ***Basidia*** 23–36 × 7–10 µm, 4-spored, with sterigmata 3–6 µm long, narrowly clavate to clavate, hyaline to greyish yellow (1B3) in H_2O and 5% KOH. ***Hymenophoral trama*** 50–110 µm wide, bilateral, composed of cylindrical, hyaline hyphae 8–12 µm diam. ***Cheilo- and pleurocystidia*** 43–69 × 13–21 µm, narrowly clavate to clavate, sometime fusoid to narrowly fusoid, hyaline to greyish yellow (1B3) in H_2O and 5% KOH. ***Pileipellis*** a trichodermium, composed of cylindrical cells, more or less vertically arranged, slightly interwoven, hyaline to greyish yellow (1B3) in H_2O and KOH; terminal cells 19–47 × 7–17 µm, cylindrical, subclavate, sometimes attenuated toward the apex. ***Pileal trama*** made up of hyaline hyphae 6–14 diam. ***Stipitipellis*** an interrupted hymeniderm to trichoderm, hyphae 6–10 µm diam.; caulocystidia 28–54 × 11–19 µm, scattered, clavate, hyaline to greyish yellow (1B3), clay (5D5). ***Stipe trama*** composed of cylindrical, hyaline hyphae 6–13 µm diam. ***Clamp connections*** not seen in any tissue.

Material examined – Thailand. Chiang Mai Province, Mae On District, N18°51'55"–E99°17'23", 04/07/12, O. Raspé & K. Wisitrassameewong, OR0382 (MFLU12-0234); —, Muang District, N18°48'-E 98°56', 06/06/2013, O. Raspé & S. Vadthanarat, OR0536 (CMU-SDBR); —, Mae On District, N18°52'11"-E99°18'23", 29/06/2014, O. Raspé & B. Thongbai, OR0769 (MFLU14-0471); —, N18°51'57"-E99°17'23", 01/06/2015, O. Raspé & S. Vadthanarat, OR0914 (CMU-SDBR).

GenBank numbers – ATP6: MT861150 (OR0382), MT861151 (OR0536), MT861152 (OR0914); RPB2: MT861158 (OR0382), MT861159 (OR0536), MT861160 (OR0914); TEF1: MT861164 (OR0382), MT861165 (OR0536), MT861166 (OR0914).

Notes – *Phylloporus attenuatus* can be recognized by its brownish-red pileus, somewhat forking, strongly decurrent and intensely and quickly bluing lamellae, and tapering stipe. Macro- and micro-morphology of *P. attenuatus* specimens from Thailand are identical to the previous description of the specimens from Bangladesh (Hosen et al., 2017). In the mutli-gene tree, *P. attenuatus* from Thailand also groups with *P. attenuatus* (holotype, HKAS 76168) from Bangladesh with high support (BS=100% and PP=1). Both morphological and phylogenetic evidence indicate that the Thai specimens studied and the *P. attenuatus* specimens studied by Hosen et al. (2017) are conspecific.

Phylloporus gajari Hosen & Zhu L. Yang, Mycoscience 56: 585 (2015)

Index Fungorum number: IF803941, *Facesoffungi number*: FoF 09168

Basidiomata solitary or rarely caespitose, small to medium-sized. ***Pileus*** 21–47 mm in diam., plano-convex when young, becoming applanate in age, slightly depressed to depressed at center; surface dry, smooth when young, then becoming rough, finely areolate with age, mostly fox to English red (8D7–8), Sahara to caramel (6C5–6) around the edge when young, becoming yellowish brown or golden brown (5D7–8) to chamois (4C5–6) with age; margin straight to deflexed, usually uplifted when mature; context 4–8 mm thick at center, light yellow (1A4), slightly bluing when injured or cut. ***Hymenophore*** lamellate, deeply decurrent. ***Lamellae*** 15–26 × 2–8 mm, strongly intervenose to anastomosing, ventricose, subdistant, flexible; surface strongly transvenose, smooth, yellow (2A7) to pastel yellow (3A4), turning blue when injured;

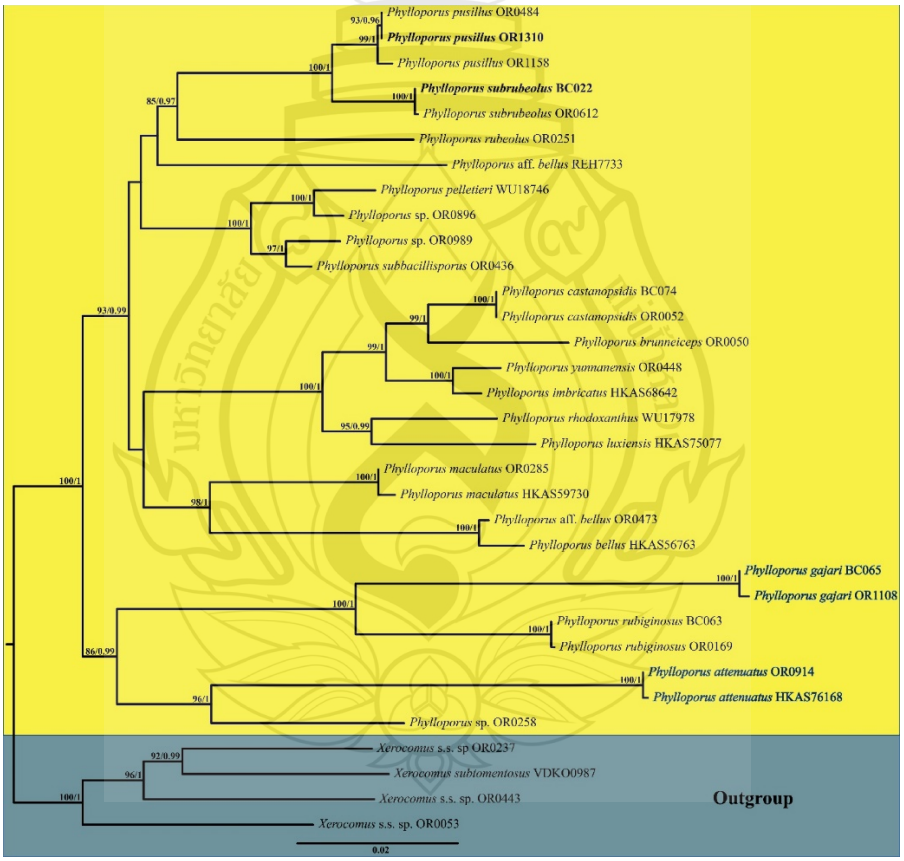
lamellulae common, in 1–2 tiers. ***Stipe*** 28–33 × 2–5 mm, central, straight to slightly curved, cylindrical; surface dry, fine yellow squamulose, fox to English red (8D7–8) when young, brownish orange (5C5–6) to brown (6E8); context solid, light yellow (1A4), slightly bluing then reddening with time in the upper part when cut or injured, but usually unchanging in the lower part. ***Basal mycelium*** well developed, tomentose, white. ***Odor and taste*** not distinctive.

Basidiospores [250/5/5] (9.2–)9.4–*11.6*–14.5(–14.9) × (4.4–)4.6–*5.1*–5.6(–5.8) µm, (1.76–)1.88–*2.25*–2.63(–2.9), ellipsoid to fusoid or subfusoid, light yellow (1A4) to greyish yellow (1B4) when observed in H_2O and 5% KOH, smooth under light microscope. ***Basidia*** 26–39 × 8–11 µm, 4-spored, with sterigmata 3–5 µm long, clavate, hyaline and light yellow (1A4) in H_2O and 5% KOH. ***Hymenophoral trama*** 100–140 µm wide, bilateral, composed of hyaline hyphae 5–10 µm wide, cylindrical. ***Cheilo- and pleurocystidia*** 42–72 × 10–17 µm, narrowly clavate to clavate, hyaline to light yellow (1A4) in H_2O and 5% KOH. ***Pileipellis*** a slightly interwoven trichoderm, composed of short chains of 4–5 cells, terminal cells 28–52 × 12–22 µm, cylindrical to somewhat slightly inflated, smooth, hyaline to yellowish white (1A2) in 5% H_2O and KOH. ***Pileal trama*** made up of hyaline hyphae 6–12 diam. ***Stipitipellis*** an interrupted hymeniderm, hyphae 6–13 µm diam; caulocystidia 22–46 × 13–21 µm, mostly clavate, sometimes mucronate, smooth, hyaline. ***Stipe trama*** composed of hyphae 8–11 µm wide, hyaline. ***Clamp connections*** not seen in any tissue.

Material examined – Thailand. Chiang Rai Province, Tha Sai District, Baan Hua Doi, 23/07/16, B. Chuankid, BC065 (MFLU16-2270); Chiang Mai Province, Muang District, N18°46'-E98°54', 15/10/2015, O. Raspé & S. Vadthanarat, OR1184 (CMU-SDBR); Ubon Ratchathani Province, Muang District, N15°18'-E104°48', 03/08/2015, O. Raspé & S. Vadthanarat, OR1104 and OR1110 (CMU-SDBR); —, N15°19'-E104°48', 03/08/2015, O. Raspé & S. Vadthanarat, OR1108 (CMU-SDBR).

GenBank numbers – ITS: MT880254 (OR1104); ATP6: MT861153 (BC065), MT861154 (OR1104), MT861155 (OR1108), MT861156 (OR1110), MT861157 (OR1184); RPB2: MT861161 (BC065), MT861162 (OR1108), MT861163 (OR1184); TEF1: MT861167 (BC065), MT861168 (OR1104), MT861169 (OR1108), MT861170 (OR1110), MT861171 (OR1184).

Notes – *Phylloporus gajari* is one of the most frequently collected species in forests dominated by *Shorea robusta* in Bangladesh. The pileus surface is pale red or reddish brown to yellowish brown or golden brown. The hymenophore is quickly staining blue when injured. The stipe is cylindrical, pale red to brownish orange or brown with white basal mycelium. The ITS sequences of the Thai specimen (OR1104) showed 100% similarity to *P. gajari* from Bangladesh (Hosen et al., 2015), which together with the morphological evidence, indicates that the studied specimens from Thailand belong in *P. gajari*. In the multi-gene phylogeny, the sequences from the Thai specimens clustered together with BS = 100%, PP = 1.0 and were clearly distinct from other *Phylloporus* species included in the analyses.



Note Phylogram generated from maximum likelihood analysis based on combined ATP6, RPB2 and TEF1-α sequence data for selected *Phylloporus*. Twenty-six strains are included in the combined analyses which comprised 1381 characters (774 characters for LSU, 607 characters for ITS) after alignment. The tree

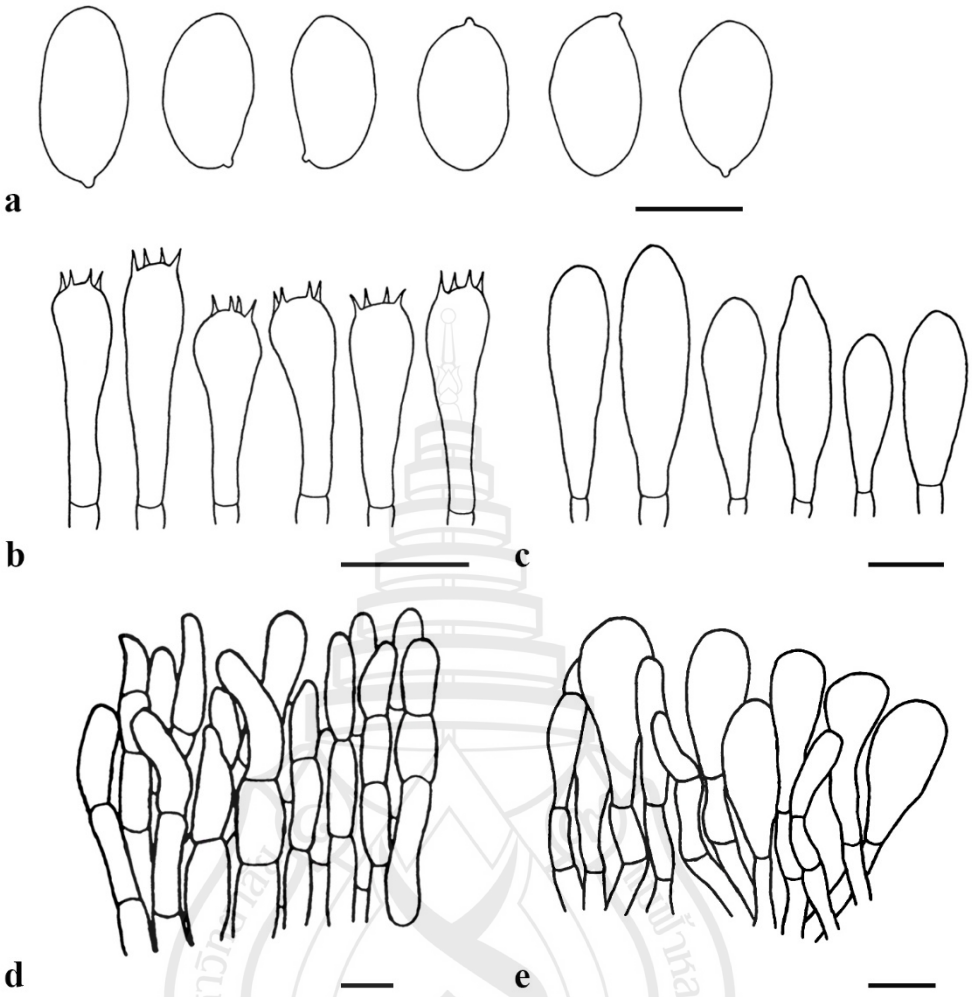
topology derived from the Bayesian analysis was similar to that derived from the maximum likelihood analysis. The best RaxML tree with a final likelihood value of -11227 is presented. The matrix has 766 distinct alignment patterns and 9.6% undetermined characters or gaps. For each gene, estimated base frequencies, substitution rates (relative to GT=1), and gamma distribution shape parameter α were as follows. *atp6*: A = 0.32, C = 0.12, G = 0.11, T = 0.45; AC = 0.64, AG = 1.36, AT = 1.12, CG = 0.24, CT = 1.23; α = 0.098; *ef1-α* exons: A = 0.23, C = 0.27, G = 0.25, T = 0.24; AC = 0.81, AG = 7.01, AT = 1.29, CG = 0.87, CT = 11.2; α = 0.206; *rpb2* exons: A = 0.28, C = 0.23, G = 0.25, T = 0.24; AC = 1.37, AG = 9.93, AT = 0.97, CG = 0.51, CT = 16.0; α = 0.187; *ef1-α* and *rpb2* introns: A = 0.25, C = 0.18, G = 0.23, T = 0.34; AC = 1.94, AG = 8.12, AT = 1.03, CG = 1.24, CT = 8.37; α = 0.677. Bootstrap frequencies greater than or equal to 70% and posterior probabilities greater than or equal to 0.95 are shown above supported branches. The tree is rooted with four *Xerocomus*. Holotypes are in bold. The newly generated sequences are indicated in yellow.

Figure 6.6 Phylogram generated from maximum likelihood analysis based on combined ATP6, RPB2 and TEF1-α sequence data for selected *Phylloporus*



Note Basidiomata of *Phylloporus attenuatus* in the field. a *P. attenuates* (OR0914). b *P. attenuatus* (OR0382). c *P. attenuatus* (OR0536). Scale bars: a–c = 2 cm.

Figure 6.7 Basidiomata of *Phylloporus attenuatus* in the field



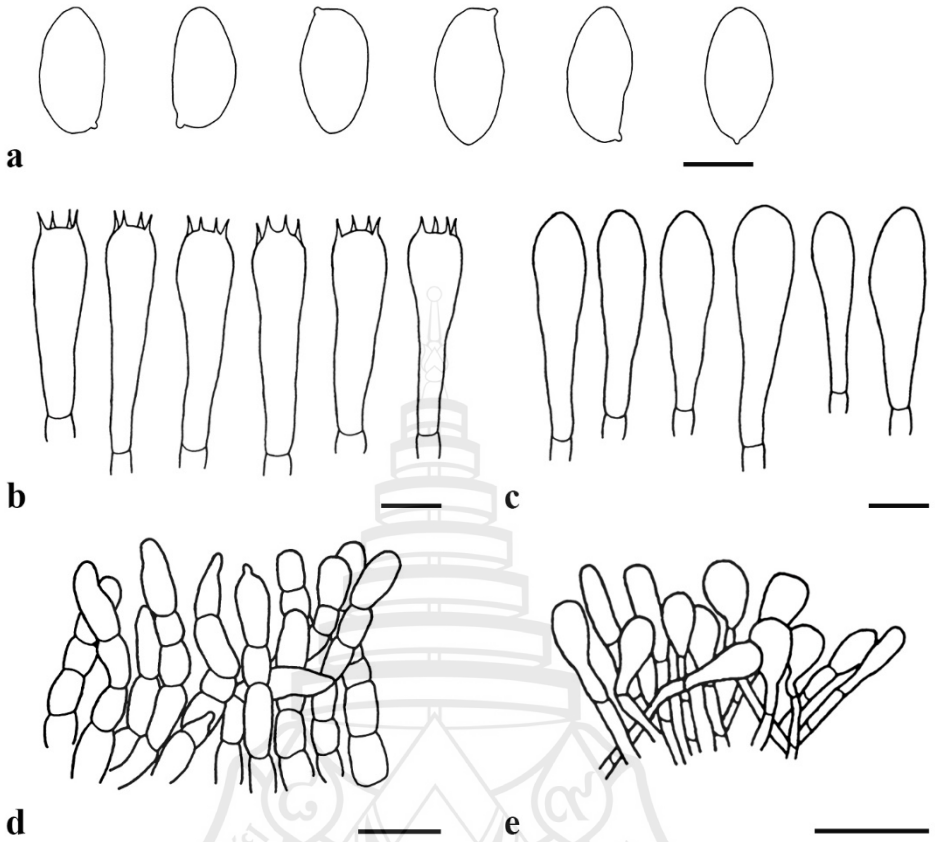
Note Microscopic characters of *Phylloporus attenuatus* (OR0914). a Basidiospores. b Basidia. c Cheilo- and pleurocystidia. d Pileipellis. e Stipitipellis. Scale bars: a = 5 µm, b–e = 20 µm.

Figure 6.8 Microscopic characters of *Phylloporus attenuatus* (OR0914)



Note Basidiomata of *Phylloporus gajari* in the field. a, b *P.* gajari (BC065). c *P.* gajari (OR1184). d, e *P.* gajari (OR1108). f Close up of the hymenophore. Scale bars: a–e = 2 cm, f = 1 cm.

Figure 6.9 Basidiomata of *Phylloporus gajari* in the field



Note Microscopic characters of *Phylloporus gajari* (BC065). a Basidiospores. b Basidia. c Cheilo- and pleurocystidia. d Pileipellis. e Stipitipellis. Scale bars: a = 5 µm, b = 10 µm, c =20 µm, d–e = 50 µm.

Figure 6.10 Microscopic characters of *Phylloporus gajari* (BC065)

REFERENCES

REFERENCES

Abdel-Lateff, A., Fisch, K., & Wright, A. D. (2009). Trichopyrone and other constituents from the marine sponge-derived fungus *Trichoderma* sp. *Zeitschrift fur Naturforschung. C, Journal of biosciences, 64*(3–4), 186–192.

Ahmed, Z., & Langer, P. (2005). Synthesis of natural pulvinic acids based on a '[3+2] cyclization–Suzuki cross-coupling' strategy. *Tetrahedron, 61,* 2055–2063.

Angeli, J. P. F., Ribeiro, L. R., Bellini, M. F., & Mantovani, M. S. (2009). β-glucan extracted from the medicinal mushroom Agaricus blazei prevents the genotoxic effects of benzo [a] pyrene in the human hepatoma cell line HepG2. *Archives of Toxicology, 83*(1), 81–86.

Antane, S. A., Caufield, C. E., Hu, W., Keeney, D., ... Yang, Y. (2006). Pulvinones as bacterial cell wall biosynthesis inhibitors. *Bioorganic & Medicinal Chemistry Letters, 73,* 176–180.

Aumann, D., Clooth, G., Steffan, B., & Steglich, W. (1989). Complexation of caesium-137 with the top pigment of maronenroehrlings (*Xerocomus badius*). *Angewandte Chemie, 101,* 495–496.

Badou, A. S., De Kesel, A., Raspé, O., Ryberg, M. K., Guelly, A. K., & Yorou, N. S. (2018). Two new African siblings of *Pulveroboletus ravenelii* (Boletaceae). *MycoKeys, 43,* 115–130.

Barrero, A. F., Oltra, J. E., Herrador, M. M., Cabrera, E., ... Reyes, J. F. (1993). Gibepyrones: α-pyrones from Gibberella fujikuroi. *Tetrahedron, 49,* 141–150.

Bas, C. (1991). *A short introduction to the ecology, taxonomy and nomenclature of the genus Agaricus* [Paper presentation].1st International Seminar on Mushroom Science, Wageningen, Netherlands.

Becker, K., Wessel, A. C., Luangsa-ard, J., & Stadler, M. (2020). Viridistratins A−C, antimicrobial and cytotoxic benzo[*j*]fluoranthenes from stromata of *Annulohypoxylon viridistratum* (Hypoxylaceae, Ascomycota). *Biomolecules, 10*, 805.

Beetz, A. E., & Greer, L. (1999). *Mushroom cultivation and marketing.* ATTRA.

Bengtsson-Palme, J., Ryberg, M., Hartmann, M., Branco, S., ... Nilsson, R. H. (2013). ITSx: Improved software detection and extraction of ITS1 and ITS2 from ribosomal ITS sequences of fungi and other eukaryotes for analysis of environmental sequencing data. *Methods in Ecology and Evolution, 4*, 914–919.

Berkeley, M. J., (1872). Notices of North American fungi. *Grevillea, 1*, 33–39.

Binder, M., & Bresinsky, A. (2002). *Retiboletus*, a new genus for a species-complex in the Boletaceae producing retipolides. *Feddes Repertorium, 113*, 30–40.

Braga, G. C., Montini, R. M. C., & Salibe, A. B. (2006). Parâmetros da produção de *Agaricus blazei* sob diferentes condições ambientais de cultivo. *Scientia Agraria Paranaensis, 5*, 47–56.

Bresinsky, A. (2014). *Ants, Plants and Fungi: A View on Some Patterns of Interaction and Diversity*. In: Lüttge, U., Beyschlag, W., Cushman, J. (eds), Progress in Botany. Progress in Botany: Vol. 75. (pp. 35–39). Springer, Berlin, Heidelberg.

Callac, P., & Chen, J. (2018). *Tropical species of Agaricus*. J. E. Sánchez, G. Mata, & D. J. Royse (Eds.), *Updates on tropical mushrooms* (pp. 25–38). Basic and applied research.

Cavalcante, J. L. R., Gomes, V. F. F., Kopytowski Filho, J., Minhoni, M. T. D. A. … de Andrade, M. C. N. (2008). Cultivation of *Agaricus blazei* in the environmental protection area of the Baturité region under three types of casing soils. *Acta Scientiarum. Agronomy, 30*, 513–517.

Chandrasrikul, A., Suwanarit, P., Sangwanit, U., Lumyong, S., Payapanon, A., Sanoamuang, N., . . . Klinhom, U. (2011). *Checklist of mushrooms (Basidiomycetes) in Thailand*. Office of Natural Resources and Environmental Policy and Planning.

Chandrasrikul, A., Suwanarit, P., Sangwanit, U., Morinaga, T., Nishizawa, Y., & Murakami, Y. (2008). *Diversity of mushrooms and macrofungi in Thailand*. Kasetsart University.

Chang, S. T. (2008). Overview of mushroom cultivation and utilization as functional foods. W, Mushrooms as functional foods (pp. 1–33). John Wiley & Sons.

Chang, S., & Miles, P. (1987). Historical record of the early cultivation of Lentinus in China. *Mushroom Journal of the Tropics, 7*, 31–37.

Chantorn, K., Pachinburavan, A., & Sanoamuang, N. (2007). Nine new records of boletes (Boletales, Hymenomycetes) from Nam Nao and Phu Rua National Parks, Thailand. *Khon Kaen University Research Journal, 12*(3), 257–264.

Chen, J., Zhao, R., Parra, L. A., Guelly, A. K., De Kesel, A., . . . Callac, P. (2015). *Agaricus* section *Brunneopicti*: A phylogenetic reconstruction with descriptions of four new taxa. *Phytotaxa, 192*(3), 145–168.

Chen, J., Zhao, R. L., Karunarathna, S. C., Callac, P., Raspé, O., Bahkali, A. H., & Hyde, K. D. (2012). *Agaricus megalosporus*: A new species in section *Minores*. *Cryptogamie Mycologie*, *33*(2), 145–155.

Chepkirui, C., Yuyama, K. T., Wanga, L. W., Decock, C., Matasyoh, J. C., Abraham, W. R., & Stadler, M. (2018). Microporenic acids A–G, biofilm inhibitors and antimicrobial agents from the basidiomycete *Microporus* species. *Journal of Natural Products, 81*, 778–784.

Chuankid, B., Vadthanarat, S., Hyde, K. D., Thongklang, N., Zhao, R., Lumyong, S., & Raspé, O. (2019). Three new *Phylloporus* species from tropical China and Thailand. *Mycological Progress, 18*, 603–614.

Clémençon, H., Emmett, V., & Emmett, E. (2004). Cytology and plectology of the Hymenomycetes. *Persoonia*, *18*, 3.

Colauto, N. B., da Silveira, A. R., da Eira, A. F., & Linde, G. A. (2010). Alternative to peat for *Agaricus brasiliensis* yield. *Bioresource Technology*, *101*, 712–716.

Corner, E. J. H. (1970). *Phylloporus* Quél. and *Paxillus* Fr. in Malaya and Borneo. *Nova Hedwigia*, *20*, 793–822.

Corner, E. J. H. (1972). *Boletus in Malaysia* (p. 263). Government Printer.

Corner, E. J. H. (1974). *Boletus* and *Phylloporus* in Malaysia: Further notes and descriptions. *Garden's Bull Singapore 27*, 1–16.

Darriba, D., Taboada, G. L., Doallo, R., & Posada, D. (2012). jModelTest 2: More models, new heuristics and parallel computing. *Nature Methods*, *9*, 772.

Davoodian, N., Bergemann, S., Hosaka, K., Raspé, O., Bougher, N. L., Fechner, N. A., . . . Halling, R. E. (2018). A global view of *Gyroporus*: Molecular phylogenetics, diversity patterns, and new species. *Mycologia*, *110*, 985–995.

Dejene, T., Oria-de-Rueda, J. A., & Martín-Pinto, P. (2017). Edible wild mushrooms of Ethiopia: Neglected non-timber forest products. *Revista Fitotecnia Mexicana*, *40*, 391–397.

Delgat, L., Dierickx, G., De Wilde, S., Angelini, C., ... Verbeken, A. (2019). Looks can be deceiving: The deceptive milkcaps (*Lactifluus*, Russulaceae) exhibit low morphological variance but harbor high genetic diversity. *IMA Fungus*, *10*, 14.

Dias, E. S. (2010). Mushroom cultivation in Brazil, challenges and potential for growth. *Science and Agrotechnology Lavras*, *34*, 795–803.

Dias, E. S., Abe, C., & Schwan, R. F. (2004). Truths and myths about the mushroom Agaricus blazei. *Scientia Agricola*, *61*(5), 545–549.

Doyle, J. J., & Doyle, J. L. (1990). Isolation of plant DNA from fresh tissue. *Focus, 12*, 13–15.

Duengkae, K. (2006). Monitoring on species diversity of macrofungi in Khek watershed, Phetchabun Province. *Songklanakarin Journal of Science and Technology, 28*, 293.

Edwards, R. L. (1977). Constituents of the higher fungi XVII. Methyl variegatate from the fungi *Hygrophoropsis aurantica* (Wulfen ex Fr.). *Journal of Chemical Research, Synopses 11*, 276.

Edwards, R. L., & Gill, M. (1973). 3',4'4-Trihydroxypulvinone, helephoric acid, and novel pyrandione and furanone pigments from *Suillus grevellei* (Klotsch) Sing Boletus elegans (Schum. Per Fries). *Journal of the Chemical Society, Perkin Transactions, 1*, 1921–1929.

Feng, B., Xu, J., Wu, G., Zeng, N. K., ... Yang, Z. L. (2012). DNA sequence analyses reveal abundant diversity, endemism and evidence for Asian origin of the porcini mushrooms. *PLoS ONE, 7*, e37567.

Firenzuoli, F., Gori, L., & Lombardo, G. (2008). The medicinal mushroom *Agaricus blazei* Murrill: Review of literature and pharmaco-toxicological problems. *Evidence-based Complementary and Alternative Medicine: eCAM, 5*(1), 3–15.

Gao, H., Guo, W., Wang, Q., Zhang, L., Zhu, M., Zhu, T., . . . Li, D. (2013). Aspulvinones from a mangrove rhizosphere soil-derived fungus *Aspergillus terreus* Gwq-48 with anti-influenza A viral (H1N1) activity. *Bioorganic & Medicinal Chemistry Letters, 23*, 1776–1778.

Gao, W. N., Wei, D. Q., Li, Y., Gao, H., Xu, W. R., Li, A. X., & Chou, K. C. (2007). Agaritine and its derivatives are potential inhibitors against HIV proteases. *Medicinal Chemistry, 3*(3), 221–226.

Gardes, M., & Bruns, T. D. (1993). ITS primers with enhanced specificity for basidiomycetes-application to the identification of mycorrhizae and rusts. *Molecular Ecology, 2*, 113–118

Georgiadis, D. (2013). *Tetronic Acids*. In T. Janecki (Ed.). *Natural Lactones and Lactams* (pp. 1–49). Wiley-VCH.

Geösel, A. (2011). Az Agaricus blazei (Murrill) termesztési lehetőségei és komplex összehasonlító vizsgálata= The cultivation opportunities and complex comparison survey of *Agaricus blazei* (Murrill) (Doctoral dissertation). Corvinus University of Budapest.

Gilbert, E. J. (1931). *Les bolets*. Librairie E. Le François.

Gill, M., & Kiefel, M. J. (1994). Pisoquinone, a new naphthalenoid pulvinic acid from the fungus *Pisolithus arhizus*. *Australian Journal of Chemistry, 47*, 1967–1977.

Gill, M., & Steglich, W. (1987). Pigments of fungi (Macromycetes). *Progress in the chemistry of organic natural products, 51*, 1–317.

Ginns, J., Reijnders, A., & Staplers, J. (1993). *The Development of the Hymenophoral Trama in the Aphyllophorales and the Agaricales.* In A. F. M. Reijnders & J. A. Staplers (pp. 718–719). JSTOR.

Gómez, L. D. (1996). Basidiomycetes de Costa Rica 9. *Xerocomus, Chalciporus, Pulveroboletus, Boletellus, Xanthoconium* (Agaricales, Boletaceae). In J. Carranza, G. M. Mueller (Eds.), *Fungi of Costa Rica: Selected Studies on Ecology and Biodiversity* (pp. 59–90) Revista de Biología Tropical.

Golding, B. T., & Rickards, R. W. (1975). New metabolites od *Aspergillus terreus*: 3 Hydroxy-2,5-bis-(p-hydroxyphenyl) penta-2,4-dien-4-olide and derivatives. *Journal of the Chemical Society, Perkin Transactions, 1*, 1961–1963.

Gonzaga, M. L. C., Bezerra, D. P., Alves, A. P. N. N., de Alencar, N. M. N., de Oliveira Mesquita, R., Lima, M. W., . . . Costa-Lotufo, L. V. (2009). In vivo

growth-inhibition of Sarcoma 180 by an α-(1→ 4)-glucan–β-(1→ 6)-glucan-protein complex polysaccharide obtained from *Agaricus blazei* Murill. *Journal of Natural Medicines, 63*(1), 32–40.

Gordon, C. P., Griffith, R., & Keller, P. A. (2007). Control of HIV through the inhibition of HIV-1 integrase: A medicinal chemistry perspective. *Medicinal Chemistry, 3*, 199–220.

Gottlieb, H. E., Kotlyar, V., & Nudelman, A. (1997). NMR chemical shifts of common laboratory solvents as trace impurities. *The Journal of Organic Chemistry, 62*, 7512–7515.

Gregori, A., Pahor, B., Glaser, R., & Pohleven, F. (2008). Influence of carbon dioxide, inoculum rate, amount and mixing of casing soil on *Agaricus blazei* fruiting bodies yield. *Acta Agriculturae Slovenica, 91*, 371–378.

Grothe, T., Stadler, M., Köpcke, B., Roemer, E., Bitzer, J., Wabnitz, P., & Küper, T. (2016). *Terpenoid Spiro Ketal Compounds with LXR Agonists Activity, Their Use and Formulations with Them*. US 9.453,016 B2.

Gruber, G., Kerschensteiner, L., & Steglich, W. (2014). New pulvinic acid and phenylalaninol derivatives from the mushrooms *Retiboletus griseus* and *R. nigerrimus*. *Journal for Nature Research, 69b*, 432–438.

Gruber, G., Kerschensteiner, L., Marumoto, R., & Steglich, W. (2013). New pulvinic acid and phenylalaninol derivatives from the mushrooms *Retiboletus griseus* and *R. nigerrimus. Journal for Nature Research, 68b*, 675–682.

Gui, Y., Zhu, G. S., Callac, P., Hyde, K. D., Parra, L. A., Chen, J., . . . Liu, Z. Y. (2015). *Agaricus* section *Arvenses*: Three new species in highland subtropical Southwest China. *Fungal biology, 119*(2), 79–94.

Halling, R., & Mueller, G. (2002). Agarics and boletes of neotropical oakwoods. *Tropical mycology, 1*, 1–10.

He, M. Q., Zhao, R. L., Hyde, K. D., Begerow, D., Kemler, M., Yurkov, A., . . . Kirk, P. K. (2019). Notes, outline and divergence times of Basidiomycota. *Fungal Diversity*, *99*, 105–367.

Heinemann, P. (1964). Boletineae du Katanga. *Bulletin du Jardin botanique de l'État a Bruxelles*, *34*, 425–478.

Heinemann, P., & Goossens-Fontana, M. (1954). Flore iconographique des champignons du Congo. Fascicle 3. Boletineae. *Brussels: Le Jardin botanique de l'Etat 3*, 51–78.

Heinemann, P. (1953). Etat actuel de la systématique de genre *Agaricus*. *Mushroom Science*, *2*, 8–11.

Heinemann, P. (1956a). Champignons recoltes au Congo Belge par Madame M. Goossens-Fontana II. Agaricus Fries ss. *Bulletin du Jardin botanique de l'Etat, Bruxelles/Bulletin van den Rijksplantentuin, Brussel 1956*, 1–127.

Heinemann, P. (1956b). Champignons récoltés au Congo Belge par Madame M. Goossens-Fontana II. Agaricus Fries ss: Note complementaire I. *Bulletin du Jardin botanique de l'Etat, Bruxelles/Bulletin van den Rijksplantentuin, Brussel 50*, 325–333.

Heinemann, P. (1957). Agaricus Robynsianus sp. nov. *Bulletin du Jardin botanique de l'Etat, Bruxelles/Bulletin van den Rijksplantentuin, Brussel 50*, 449–452.

Heinemann, P. (1961). Agarici Austro-Americani: I: Agaricus of Trinidad. *Kew Bulletin*, *15*(2), 231–248.

Heinemann, P. (1962). Agarici austro-americani: IV. Quatre Agaricus du Venezuela. *Bulletin du Jardin botanique de l'État a Bruxelles*, *32*(Fasc. 2), 155–161.

Heinemann, P. (1962a). Agarici Austro-Americani: II: Agaricus de Bolivie. *Bulletin du Jardin botanique de l'État a Bruxelles*, *32*(Fasc. 1), 1–21.

Heinemann, P. (1962b). Agarici Austro-Americani: III. Trois Agaricus de la Jamaïque. *Bulletin du Jardin botanique de l'Etat, Bruxelles/Bulletin van den Rijksplantentuin, Brussel 32*, 23–28.

Heinemann, P. (1962c). Agarici Austroamericani V. *Etude des types de C. Spegazzini. Extrait du Bulletin de l'Institut. agronomique et des Stations de Recherches de Gembloux, 30*, 273–282.

Heinemann, P. (1971). Quelques Psalliotes du Congo-Brazzaville. *Cahier Makobé, 9*, 5–10.

Heinemann, P. (1974). Agaricus kuehnerianus sp. nov., la Psalliote géante des Alpes de Haute Provence. *Bulletin Mensuel de la Société Linnéenne de Lyon No. sp*, 181–187.

Heinemann, P. (1978). Essai d'une clé de détermination des genres Agaricus et Micropsalliota. Sydowia.

Heinemann, P. (1980). Les genres Agaricus et Micropsalliota en Malaisie et en Indonésie. *Bulletin du Jardin botanique national de Belgique/Bulletin van de Nationale Plantentuin van Belgie 50*, 3–68.

Heinemann, P. (1982). Quelques Psalliotes de Nouvelle-Guinee (Papua New Guinea). *Bulletin du Jardin botanique national de Belgique/Bulletin van de Nationale Plantentuin van Belgie 52*, 405–413.

Heinemann, P. (1986). Agarici austroamericani VI. Apercu sur les Agaricus de Patagonie et de la terre de Feu. *Bulletin du Jardin botanique national de Belgique/Bulletin van de Nationale Plantentuin van Belgie 56*, 417–446.

Heinemann, P. (1987). Clave para la determinación de las especies de Agaricus (Agaricales) de la Patagonia y Tierra del Fuego. *Darwiniana 28*, 283–291.

Heinemann, P. (1990a). Agarici Austroamericani VII. Agariceae des zones tempérées de l'Argentine et du Chili. *Bulletin du Jardin botanique national de Belgique/Bulletin van de Nationale Plantentuin van Belgie 60*, 331–370.

Heinemann, P. (1990b). Agaricus singaporensis sp. nov. *Bulletin du Jardin botanique national de Belgique/Bulletin van de National Plantentuin van België, 60*(3/4), 417–419.

Heinemann, P., & Rammeloo, J. (1987). *Phylloporus (Boletineae)*. Jardin botanique national de Belgique.

Hellwig, V. (1998). *Isolierung, Strukturaufklärung und chemotaxonomische Untersuchungen von Sekundärmetaboliten aus Pilzen* (Doctoral dissertation). Universität München.

Hetland, G., Johnson, E., Lyberg, T., Bernardshaw, S., Tryggestad, A. M. A., & Grinde, B. (2008). Effects of the medicinal mushroom *Agaricus blazei* Murill on immunity, infection and cancer. *Scandinavian Journal of Immunology, 68*(4), 363–370.

Hibbett, D. S., Bauer, R., Binder, M., Giachini, A. J., Hosaka, K., Justo, A., . . . Thorn, R. G. (2014). 14 Agaricomycetes. In D. McLaughlin, J. Spatafora (Eds). *Systematics and Evolution* (pp. 373–429). Springer.

Hirotani, M., Hirotani, S., Takayanagi, H., & Yoshikawa, T. (1999). Blazeispirol A, an unprecedented skeleton from the cultured mycelia of the fungus *Agaricus blazei*. *Tetrahedron Letters, 40*, 329–332.

Hirotani, M., Hirotani, S., & Yoshikawa, T. (2000). Blazeispirol X and Y, two novel carbon skeletal sterols from the cultured mycelia of the fungus *Agaricus blazei*. *Tetrahedron Letters, 41*, 5107–5110.

Hirotani, M., Hirotani, S., & Yoshikawa, T. (2001). Blazeispirol D and Z, as the actual intermediates of blazeispirol A biosynthesis from the cultured mycelia of the fungus *Agaricus blazei*. *Tetrahedron Letters, 42*, 5261–5264.

Hirotani, M., Sai, K., Hirotani, S., & Yoshikawa, T. (2002). Blazeispirols B, C, E and F, des-*A*-ergostane-type compounds, from the cultured mycelia of the fungus *Agaricus blazei*. *Phytocheistry, 5*, 571–577.

Horak, E. (2011). *Revision of Malaysian species of Boletales s.l. (Basidiomycota) described by E.J.H. Corner (1972, 1974)*. Forest Research Institute Malaysia.

Hosen, I, & Li, T. H. (2017). Two new species of *Phylloporus* from Bangladesh, with morphological and molecular evidence. *Mycologia, 109*, 277–286.

Huang, Y. T., Onose, J. I., Abe, N., & Yoshikawa, K. (2009). In vitro inhibitory effects of pulvinic acid derivatives isolated from Chinese edible mushrooms, *Boletus calopus* and *Suillus bovinus*, on cytochrome P450 activity. *Bioscience, Biotechnology, and Biochemistry*, *16*, 855–860.

Hyde, K. D., Xu, J. C., Rapior, S., Jeewon, R., Lumyong, S., Niego, A. G. T., . . . Stadler, M. (2019). The amazing potential of fungi, 50 ways we can exploit fungi industrially. *Fungal Diversity, 97*, 1–136.

Hyde, K. D., Norphanphoun, C., Chen, J., Dissanayake, A. J., Doilom, M., Hongsanan, S., . . . Stadler, M. (2018). Thailand's amazing diversity – up to 96% of fungi in northern Thailand are novel. *Fungal Diversity, 93,* 215–239.

Irschik, H., Jansen, R., Höfle, G., Gerth, K., & Reichenbach, H. (1985). The corallopyronins, new inhibitors of bacterial RNA synthesis from Myxobacteria. *The Journal of Antibiotics, 38,* 145–152.

Itoh, H., Ito, H., & Hibasami, H. (2008). Blazein of a new steroid isolated from *Agaricus blazei* Murrill (himematsutake) induces cell death and morphological change indicative of apoptotic chromatin condensation in human lung cancer LU99 and stomach cancer KATO III cells. *Oncology Reports, 20*(6), 1359.

Iwade, I., & Mizuno, T. (1997). Cultivation of Kawariharatake (*Agaricus blazei* Murill). *Food Reviews International, 13,* 338–390.

Jatuwong, K., Kakumyan, P., Chamyuang, S., Chukeatirote, E., & Hyde, K. D. (2014). *Optimization condition for cultivation of Agaricus subrufescens hybrid strains; The 26th Annual meeting of the Thai Society for Biotechnology and International Conference* (pp. 244–251). Mae Fah Luang University, Chiang Rai, Thailand.

Jayasiri, S. C., Hyde, K. D., Ariyawansa, H. A., Bhat, D. J., Buyck, B., Cai, L., . . . Promputtha, I. (2015). The faces of Fungi database: Fungal names linked with morphology, phylogeny and human impacts. *Fungal Diversity*, *74*, 3–18.

Ji, K. P. (2016). *The first successful industrial-scale cultivation of Phlebopus portentosus in Yunnan Province, China.* WSMBMP Bulletin number 14. http://www.wsmbmp.org/Bol14/3.html.

Ji, K. P., Cao, Y., Zhang, C. X., He, M. X., Liu, J., Wang, W. B., & Wang, Y. (2011). Cultivation of *Phlebopus portentosus* in southern China. *Mycological Progress, 10*, 293–300.

Justus, K., Herrmann, R., Klamann, J. D., Gruber, G., Hellwig, V., Ingerl, A., . . . Steglich, W. (2007). Retipolides–unusual spiromacrolactones from the mushrooms *Retiboletus retipes* and *R. ornatipes*. *European Journal of Organic Chemistry*, *2007*, 5560–5572.

Kalač, P. (2009). Chemical composition and nutritional value of European species of wild growing mushrooms: A review. *Food chemistry, 113*(1), 9–16.

Karunarathna, S. C., Guinberteau, J., Chen, J., Vellinga, E. C., Zhao, R. L., Chukeatirote, E., . . . Callac, P. (2014). Two new species in Agaricus tropical clade I. *Chiang Mai Journal of Science, 41*, 771–780.

Karunarathna, S., Chen, J., Mortimer, P., Xu, J., Zhao, R. L., Callac, P., & Hyde, K. (2016). Mycosphere Essay 8: A review of genus *Agaricus* in tropical and humid subtropical regions of Asia. *Mycosphere, 7*(4), 417–439.

Katoh, K., & Standle, D. M. (2013). MAFFT multiple sequence alignment software version 7: Improvements in performance and usability. *Molecular Biology and Evolution, 30*, 772–780.

Kerrigan, R. W. (2005). *Agaricus subrufescens*, a cultivated edible and medicinal mushroom, and its synonyms. *Mycologia, 97*, 12–24.

Kerrigan, R. W., Callac, P., & Parra, L. A. (2008). New and rare taxa in Agaricus section Bivelares (Duploannulati). *Mycologia, 100*(6), 876–892.

Khmelnitsky, O., Davoodian, N., Singh, P., Raspé, O., Lee, S. M., Fechner, N., . . . Halling, R. E. (2019). *Ionosporus*: a new genus for *Boletus longipes* (Boletaceae), with a new species, *I. australis*, from Australia. *Mycological Progress, 18*, 439–451.

Kirk, P., Cannon, P., Minter, D., & Stalpers, J. (2008). *Ainsworth & Bisby's Dictionary of the Fungi* (10th ed.). CABI.

Kopytowski Filho, J., Minhoni, M. T. A., Andrade, M. C. N., Zied, D. (2008). Effect of compost supplementation (soybean meal and Champfood) at different phases (spawning and before casing) on productivity of *Agaricus blazei* ss. Heinemann (*A. brasiliensis*). *International Society for Mushroom Science, 17*, 260–270.

Kornerup, A., & Wanscher, J. (1978). *Methuen handbook of colour* (3rd ed.). Eyre.

Kretzer, A. M., & Bruns, T. D. (1999). Use of *atp*6 in fungal phylogenetics: An example from the Boletales. *Molecular Phylogenetics and Evolution, 13*, 483–492.

Kuhnert, E., Fournier, J., Peršoh, D., Luangsaard, J. J., & Stadler, M. (2014). New *Hypoxylon* species from Martinique and new evidence on the molecular phylogeny of *Hypoxylon* based on ITS rDNA and β-tubulin data. *Fungal Diversity, 64*, 181–203.

Kumla, J., Danell, E., & Lumyong, S. (2015). Improvement of yield for a tropical black bolete, *Phlebopus portentosus*, cultivation in northern Thailand. *Mycoscience, 56*, 114–117.

Kumla, J., Suwannarach, N., & Lumyong, S. (2020). A new report on edible tropical Bolete, *Phlebopus spongiosus* in Thailand and its fruiting body formation without the need for a host plant. *Mycobiology*, 263–275.

Ladurner, H., & Simonini, G. (2003). *Xerocomus* s. l. *Fungi Europaei. 8*, 527.

Largeteau, M. L., Llarena-Hernández, R. C., Regnault-Roger, C., & Savoie, J. M. (2011). The medicinal Agaricus mushroom cultivated in Brazil: Biology, cultivation and non-medicinal valorisation. *Applied Microbiology and Biotechnology, 92*(5), 897–907.

Le Thi, T. N., Phan, M. H., Tran, C. H., Bul, V. T., Pham Nguyen, D. H., & Duong, H. X. (2018). Cultivation media for incubation period and fruit body formation of *Phlebopus spongiosus*, an edible ectomycorrhizal mushroom in Vietnam. *Proceedings of the National Conference on Biotechnology* (pp. 1034–1038). Vietnam.

Lebel, T. (2013). Two new species of sequestrate Agaricus (section Minores) from Australia. *Mycological Progress, 12*(4), 699–707.

Lebel, T., & Syme, A. (2012). Sequestrate species of Agaricus and Macrolepiota from Australia: New species and combinations and their position in a calibrated phylogeny. *Mycologia, 104*(2), 496–520.

Linnaeus, C. (1753). *Species plantarum, exhibentes plantas rite cognitas ad genera relatas cum differentiis specificis, nominibus trivialibus, synonymis selectis, locis natalibus, secundum systema sexuale digestas* (Vol. 2). Sweden.

Liu, H. Y., Li, Y. C., & Bau, T. (2020). New species of *Retiboletus* (Boletales, Boletaceae) from China based on morphological and molecular data. *MycoKeys*, *67*, 33–44.

Liu, Y., Fukuwatari, Y., Okumura, K., Takeda, K., Ishibashi, K. I., Furukawa, M., . . . Motoi, M. (2008). Immunomodulating activity of *Agaricus brasiliensis* KA21 in mice and in human volunteers. *Evidence-Based Complementary and Alternative Medicine, 5*(2), 205–219.

Llarena-Hernández, C. R., Largeteau, M. L., Ferrer, N., Regnault-Roger, C., & Savoie, J. M. (2014). Optimization of the cultivation conditions for mushroom production with European wild strains of Agaricus subrufescens and Brazilian cultivars. *Journal of the Science of Food and Agriculture, 94*, 77–84.

Ma, L. Y., Liu, D. S., Li, D. G., Huang, Y. L., Kang, H. H., Wang, C. H., & Liu, W. Z. (2017). Pryran rings containing polyketides from *Penicillium raistrickii*. *Marine Drugs*, *15*, 2–8.

Madhosingh, C. (1966). Pigmented bacteriostatic substances and amino acids produced by *Phlebopus sulphureus* and *Phlebopus lignicola*. *Applied and Environmental Microbiology*, *14*, 331–336.

Mantovani, T. R. D., Linde, G. A., & Colauto, N. B. (2007). Effect of addition of nitrogen sources to cassava fiber and carbon-to-nitrogen ratios on *Agaricus brasiliensis* growth. *Canadian Journal of Microbiology, 53*, 139–143.

Matheny, P. B. (2005). Improving phylogenetic inference of mushrooms with RPB1 and RPB2 nucleotide sequences (Inocybe; Agaricales). *Molecular Phylogenetics and Evolution, 35*(1), 1–20.

McNabb, R. F. R. (1968). The Boletaceae of New Zealand. *New Zealand Journal of Botany*, *6*, 137–176.

Merdivan, S., Willke, C., & Lindequist, U. (2016). Development and validation of an LC-MS/MS method for the quantification of Agaritine in mushrooms. *International journal of medicinal mushrooms, 18*(1), pp. 13–21.

Miles, P. G., & Chang, S. T. (2004). *Mushrooms: Cultivation, nutritional value, medicinal effect, and environmental impact*. CRC Press.

Miller, M. A., Pfeiffer, W., & Schwartz, T. (2010). Creating the CIPRES Science Gateway for inference of large phylogenetic trees. Gateway Computing Environments Workshop (GCE). IEEE, pp 1–8.

Montoya, L., & Bandala, V. M. (1991). Studies on the genus Phylloporus in Mexico. I. Discussion of the known species and description of a new species and a new record. *Mycotaxon, 41*(2), 471–482.

Murr, M. D. E., Nowaczyk, S., Le Gall, T., & Mioskowski, C. (2006). Synthesis of pulvinic acid and norbadione A analogues by Suzuki–Miyaura cross-coupling of benzylated intermediates. *European Journal of Organic Chemistry,* 1489–1498.

Nelsen, S. F. (2010). Bluing components and other pigments of boletes. *Fungi ,3,* 11–14.

Neves, M. A. (2007). *Toward a revision of the genus Phylloporus (Boletaceae): Systematics and phylogeny of species from various parts of the world* (Doctoral dissertation), University of New York.

Neves, M. A., Binder, M., Halling, R. E., Hibbett, D., & Soytong, K. (2012). The phylogeny of selected *Phylloporus* species, inferred from NUC–LSU and ITS sequences, and descriptions of new species from the Old World. *Fungal Diversity, 55,* 109–123.

Neves, M. A., & Halling, R. E. (2010). Study on species of Phylloporus I: Neotropics and North America. *Mycologia, 102*(4), 923–943.

Neves, M. A., Binder, M., Halling, R., Hibbett, D., & Soytong, K. (2012). The phylogeny of selected Phylloporus species, inferred from NUC-LSU and ITS sequences, and descriptions of new species from the Old World. *Fungal Diversity, 55*(1), 109–123.

Newman, E., & Reddell, P. (1987). The distribution of mycorrhizas among families of vascular plants. *New Phytologist, 106*(4), 745–751.

Niu, Y., Liu, J., Zhao, X., & Wu, X. (2009). A low molecular weight polysaccharide isolated from Agaricus blazei suppresses tumor growth and angiogenesis in vivo. *Oncology Reports, 21*(1), 145–152.

Nuhn, M. E., Binder, M., Taylor, A. F., Halling, R. E., & Hibbett, D. S. (2013). Phylogenetic overview of the Boletineae. *Fungal Biology, 117*, 479–511.

Ojima, N., Takenaka, S., & Seto, S. (1973). New butenolides from *Aspergillus terreus*. *Phytochemistry, 12*, 2527–2529.

Ortiz-Santana, B., Lodge, D. J., Baroni, T. J., & Both, E. E. (2007). Boletes from Belize and the Dominican Republic. *Fungal Diversity, 27*, 247–416.

Pang, X., Zhao, J. Y., Fang, X. M., Zhang, T., Zhang, D. W., Liu, H. Y., . . . Yu, L. Y. (2017). Metabolites from the plant endophytic fungus *Aspergillus* sp. CPCC 400735 and their anti-HIV activities. *Journal of Natural Products, 80*, 2595–2601.

Park, J. S. (2001). *Characteristics and cultivation technology of Agaricus blazei*. MushWorld. http//www.mushworld.com.

Parmasto, E. (1986). On the origin of Hymenomycetes (What are corticioid fungi?). *Windahlia, 16*, 3–19.

Parra, L. (2013). *Fungi europaei, Volume 1A, Agaricus L. Allopsalliota, Nauta & Bas (Parte II)*. Candusso Edizioni.

Pham, N. D. H., Takahashi, H., Fukiharu, T., Shimizu, K., Le, B. D., & Suzuki, A. (2012). A *Phlebopus spongiosus* sp. nov. (Boletales, Boletinellaceae) with a sponge-like tissue. *Mycotaxon, 119*, 27–34.

Phukhamsakda, C., Macabeo, A. P. G., Huch, V., Cheng, T., Hyde, K. D., & Stadler, M. (2019). Sparticolins A–G, biologically active oxidized spirodioxynaphthalene derivatives from the ascomycete *Sparticola junci*. *Journal of Natural Products, 82*, 2878–2885.

Pokhrel, C. P., & Ohga, S. (2007). Cattle bedding waste used as a substrate in the cultivation of *Agaricus blazei* Murill. *Journal of the Faculty of Agriculture, Kyushu University, 52*, 295–298.

Quélet, L. (1888). *Flore mycologique de la France et des pays limitrophes*. O. Doin.

Rao, Y. S. (1975). Chemistry of lactones: A one step synthesis of α-phenyl-γ benzylidene-$\Delta^{\alpha,\beta}$-butenolide. *Tetrahedron Letters, 17*, 1457–1459.

Raspé, O., Vadthanarat, S., De Kesel, A., Degreef, J., Hyde, K. D., & Lumyong, S. (2016). *Pulveroboletus fragrans*, a new Boletaceae species from Northern Thailand, with a remarkable aromatic odor. *Mycological Progress, 15*, 38.

Rehner, S. A., & Buckley, E. (2005). A Beauveria phylogeny inferred from nuclear ITS and EF1-α sequences: Evidence for cryptic diversification and links to *Cordyceps* teleomorphs. *Mycologia*, *97*(1), 84–98.

Rinaldi, A., Comandini, O., & Kuyper, T. W. (2008). Ectomycorrhizal fungal diversity: seperating the wheat from the chaff. *Fungal Diversity, 33*, 1–45.

Ronquist, F., Teslenko, M., Van Der, M. P., Ayres, D. L., Darling, A., Höhna, S., . . . Huelsenbeck, J. P. (2012). MrBayes 3.2: Efficient Bayesian phylogenetic inference and model choice across a large model space. *Systematic Biology, 61*, 539–542.

Royse, D. J., & Beelman, R. B. (2016). *Six steps to mushroom farming*. https://extension.psu.edu/six-steps-to-mushroom-farming.

Royse, D. J. (2010). Effects of fragmentation, supplementation and the addition of phase II compost to 2nd break compost on mushroom (*Agaricus bisporus*) yield. *Bioresource Technology, 101*, 188–92.

Royse, D. J., & Beelman, R. B. (2007). *Six steps to mushroom farming*. http://mushroomspawn.cas.psu.edu/SixSteps.shtml.

Sandargo, B., Chepkirui, C., Cheng, T., Chaverra-Muñoz, L., Thongbai, B., Stadler, M., & Hüttel, S. (2019). Biological and chemical diversity go hand in hand: Basidomycota as source of new pharmaceuticals and agrochemicals. *Biotechnology Advances, 37*, 107344.

Sarakham, M, Et, R., Chaiyaphum, Y., Charoen, A. (2015). *The Climate of Thailand*. Thai Meteorological Department. https://www.tmd.go.th.

Schäberle, T. F. (2016). Biosynthesis of α-pyrones. *Beilstein Journal of Organic Chemistry, 12*, 571–588.

Singer, R. (1945). The Boletineae of Florida with notes on extralimital species. I. Strobilomycetaceae. *Farlowia, 2*, 97–141.

Singer, R., Garcia, J., & Gómez, P. L. (1991). The Boletineae of Mexico and Central America III. *Beihefte zur Nova Hedwigia, 102*, 1–99.

Singer, R., Ivory, M., & Araujo, I. (1983). The ectotrophically mycorrhizal fungi of the Neotropical lowlands, especially central Amazonia. *Beihefte zur Nova Hedwigia, 77*, 1–352.

Singer, R. (1986). *The Agaricales in modern taxonomy*. Sven Koeiltz Scientific Books. Koenigstein, Germany.

Singer, R., & Gómez-Pignataro, L. D. (1984). The basidiomycetes of Costa Rica. III. The genus *Phylloporus* (Boletaceae). Los basidiomicetos de Costa Rica. III. El género *Phylloporus* (Boletaceae). *Brenesia, 22*, 163–181.

Singer, R., Ovrebo, C. L., & Halling, R. E. (1990). New species of *Phylloporus* and *Tricholomopsis* from Colombia, with notes on *Phylloporus boletinoides*. *Mycologia*, 452–459.

Siqueira, F. G., Dias, E. S., Silva, R. D., Martos, E. T., & Rinker, D. L. (2009). Cultivation of *Agaricus blazei* ss. Heinemann using different soils as source of casing materials. *Scientia Agricola, 66*, 827–830.

Smith, A. H., & Thiers, H. D. (1971). *The boletes of Michigan*. University of Michigan Press.

Snell, W. H., & Dick, E. A. (1970). *The boleti of northeastern North America* (p. 115). Cramer.

Sorimachi, K., Akimoto, K., & Koge, T. (2008). Inhibitory effect of Agaricu blazeimurill components on abnormal collagen fiber formation in human hepatocarcinoma cells. *Bioscience, Biotechnology, and Biochemistry, 72*(2), 621–623.

Stadler, M., Hellwig, V., Mayer-Bartschmid, A., Denzer, D., Wiese, B., & Burkhardt, N. (2005). Novel analgesic triglycerides from cultures of *Agaricus macrosporus* and other basidiomycetes as selective inhibitors of neurolysin. *The Journal of Antibiotics, 58*, 775–786.

Stamatakis, A. (2014). RAxML version 8: A tool for phylogenetic analysis and post-analysis of large phylogenies. *Bioinformatics, 30*, 1312–1313.

Stamets, P. (2000). *Growing Gourmet and Medicinal Mushrooms* (p. 574). Ten Speed Press.

Steffan, B., & Steglich, W. (1984). Cap pigments from the chestnut bolete tubes (*Xerocomus badius*). *Angewandte Chemie, 96*, 435–437.

Steglich, W., Besl, H., & Zipfel, K. (1974). Structural determination of pulvinic acids by NMR spectroscopy. *Z. Naturforsch, 29b*, 96–98.

Steglich, W., Furtner, W., & Prox, A. (1970). Variegatorubin, an oxydation product of variegatic acid from *Suillus piperatus* and other Boletaceae. *Z Naturforsch, 25*, 557–558.

Stojković, D., Reis, F. S., Glamočlija, J., Ćirić, A., Barros, L., Van Griensven, L. J., . . . Soković, M. (2014). Cultivated strains of *Agaricus bisporus* and *A. brasiliensis*: Chemical characterization and evaluation of antioxidant and antimicrobial properties for the final healthy product–natural preservatives in yoghurt. *Food & Function, 5*(7), 1602–1612.

Sun, Z., Sun, Z., Zhu, N., Yang, J, Ma, G., & Xu, X. (2018). Pyrrole alkaloids from the edible mushroom *Phlebopus portentosus* with their bioactive activities. *Molecules, 23*, 1198–1205.

Šutara, J. (2008). *Xerocomus* s.l. in the light of the present state of knowledge. *Czech Mycology, 60*, 29–62.

Tauber, J. P., Gallegos-Monterrosa, R., Kovacs, A. T., Shelest, E., & Hoffmeister, D. (2018). Dissimilar pigment regulation in *Serpula lacrymans* and *Paxillus involutus* during inter-kingdominteractions. *Microbiology, 164*, 65–77.

Tedersoo, L., May, T. W., & Smith, M. E. (2010). Ectomycorrhizal lifestyle in fungi: Global diversity, distribution, and evolution of phylogenetic lineages. *Mycorrhiza, 20*(4), 217–263.

Thawthong, A., Karunarathna, S. C., Thongklang, N., Chukeatirote, E., Kakumyan, P., Chamyuang, S., . . . Hyde, K. D. (2014). Discovering and domesticating wild tropical cultivatable mushrooms. *Chiang Mai Journal of Science, 41*, 731–764.

Thongklang, N., Sysouphanthong, P., Callac, P., & Hyde, K. D. (2014). First cultivation of *Agaricus flocculosipes* and a novel Thai strain of *A. subrufescens*. *Mycosphere, 5*, 814–820.

Thongklang, N., Thongbai, B., Chamyuang, S., Callac, P., Chukeatirote, E., Hyde, K. D., . . . Stadler, M. (2017). Blazeispirol A, a chemotaxonomic marker from mycelia of the medicinal mushroom *Agaricus subrufescens*. *Chiang Mai Journal of Science, 44*, 298–308.

Thongklang, N., Chen, J., Bandara, A. R., Hyde, K. D., Raspé, O., Parra, L. A., & Callac, P. (2016). Studies on *Agaricus subtilipes*, a new cultivatable species from Thailand, incidentally reveal the presence of *Agaricus subrufescens* in Africa. *Mycoscience, 57*(4), 239–250.

Underwood, L. M. (1899). *Moulds, Mildews, and Mushrooms: A Guide to the Systematic Study of the Fungi and Mycetozoa and Their Literature*. H. Holt & Company.

Vadthanarat, S., Raspé, O., & Lumyong, S. (2018). Phylogenetic affinities of the sequestrate genus *Rhodactina* (Boletaceae), with a new species, *R. rostratispora* from Thailand. *MycoKeys*, *29*, 63–80.

Vadthanarat, S., Raspé, O., & Lumyong, S. (2022). *Rubinosporus auriporus* gen. et sp. nov. (Boletaceae: Xerocomoideae) from Tropical Forests of Thailand, Producing Unusual Dark Ruby Spore Deposits. *Journal of Fungi*, *8*(3), 278.

Velíšek, J., & Cejpek, K. (2011). Pigments of higher fungi: A review. *Czech J Food Sci, 29*, 87–102.

Wang, Q., Li, B. B., Li, H., & Han, J. R. (2010). Yield, dry matter and polysaccharides content of the mushroom *Agaricus blazei* produced on asparagus straw substrate. *Scientia Horticulturae, 125*, 16–18.

Wang, J. T., Wang, Q., & Han, J. R. (2013). Yield, polysaccharides content and antioxidant properties of the mushroom *Agaricus subrufescens*, produced on different substrates based on selected agricultural wastes. *Scientia Horticulturae, 157*, 84–89.

Wang, Y., & Xu, B. (2014). Distribution of antioxidant activities and total phenolic contents in acetone, ethanol, water and hot water extracts from 20 edible mushrooms via sequential extraction. *Austin Journal of Nutrition and Food Sciences, 2*(1), 5.

Wang, Y., Su, M. S., Jiang, S., Xue, R., Wu, L. L., Xie, H. J., . . . & Zeng, N. K. (2020). The genus *Hourangia* in China and a description of *Aureoboletus erythraeus* sp. nov. *Phytotaxa, 472*(2), 87–106.

Wang, Z. R., Parra, L. A., Callac, P., Zhou, J. L., Fu, W. J., Dui, S. H., . . . Zhao, R. L. (2015). Edible species of *Agaricus* (Agaricaceae) from Xinjiang Province (Western China). *Phytotaxa, 202*(3), 185–197.

Wani, B. A., Bodha, R. H., & Wani, A. H. (2010). Nutritional and medicinal importance of mushrooms. *Journal of Medicinal Plants Research, 24*, 2598–2604.

Wasser, S. P., Didukh, M. Y., de Amazonas, M. A. L., Nevo, E., & Amazonas, A. (2002). Is a widely cultivated culinary-medicinal royal sun *Agaricus* (the Himematsutake Mushroom) indeed *Agaricus blazei* Murrill?, *International Journal of Medicinal Mushrooms, 4*, 267–290.

Watling, R. (2008). *A manual and source book on the Boletales and their alles*. Fungiflora.

Westerdijk Fungal Biodiversity Institute Centre (continuously updated). *MycoBank*. Accessed at: http://www.mycobank.org/

White, T. J., Bruns, T., Lee, S., & Taylor, J. (1990). Amplification and direct sequencing of fungal ribosomal RNA genes for phylogenetics. *PCR Protocols: A guide to Methods and Applications, 18*, 315–322.

Winner, M., Giménez, A., Schmidt, H., Sontag, B., Steffan, B., & Steglich, W. (2004). Unusual pulvinic acid dimers from the common fungi *Scleroderma citrinum* (Common Earthball) and *Chalciporus piperatus* (Peppery Bolete). *Angewandte Chemie, 43*, 1883–1886.

Wisitrassameewong, K., Karunarathna, S. C., Thongklang, N., Zhao, R., Callac, P., Moukha, S., . . . Hyde, K. D. (2012b). *Agaricus subrufescens*: A review. *Saudi Journal of Biological Sciences, 19*(2), 131–146.

Wisitrassameewong, K., Karunarathna, S. C., Thongklang, N., Zhao, R. L., Callac, P., Chukeatirote, E., . . . Hyde, K. D. (2012). *Agaricus subrufescens*: new to Thailand. *Chiang Mai Journal of Science, 39*(2), 281–291.

Wu, G., Feng, B., Xu, J., Zhu, X. T., Li, Y. C., Zeng, N. K., . . . Yang, Z. L. (2014). Molecular phylogenetic analyses redefine seven major clades and reveal 22 new generic clades in the fungal family Boletaceae. *Fungal Diversity*, *69*(1), 93–115.

Wu, G., Li, Y. C., Zhu, X. T., Zhao, K., Han, L. H., Cui, Y. Y., . . . Yang, Z. L. (2016). One hundred noteworthy boletes from China. *Fungal Diversity*, *81*(1), 25–188.

Wuest, P. J., Royse, D. J., Duffy, M. D., & Service, N. C. E. (1979). *Six Steps to Mushroom Farming.* Pennsylvania State University, College of Agriculture, Extension Service.

Ye, L., Mortimer, P. E., Xu, J., Karunarathna, S. C., & Hyde, K. D. (2014). The genus Phylloporus (Boletaceae, Boletales), from Mekong River Basin (Yunnan Province, China). *Chiang Mai Journal of Science*, *41*(4), 798–810.

Zeng, N. K., Tang, L. P., & Yang, Z. L. (2011). Type studies on two species of *Phylloporus* (Boletaceae, Boletales) described from southwestern China. *Mycotaxon*, *117*, 19–28.

Zeng, N. K., Chai, H., Jiang, S., Xue, R., Wang, Y., Hong, D., & Liang, Z. Q. (2018). *Retiboletus nigrogriseus* and *Tengioboletus fujianensis*, two new boletes from the south of China. *Phytotaxa*, *367*, 45–54.

Zeng, N. K., Liang, Z. Q., Wu, G., Li, Y. C., & Yang, Z. L. (2016). The genus *Retiboletus* in China. *Mycologia*, *108*, 363–380.

Zeng, N. K., Tang, L. P., Li, Y. C., Tolgor, B., Zhu, X. T., Zhao, Q., & Yang, Z. L. (2013). The genus *Phylloporus* (Boletaceae, Boletales) from China: Morphological and multilocus DNA sequence analyses. *Fungal Diversity, 58*(1), 73–101.

Zhang, C., He, M., Liu, J., Xu, X., Cao, Y., Gao, F., . . . Wang, Y. (2017). Brief introduction to a unique edible Bolete - *Phlebopus portentosus* in Southern China. *Journal of Agricultural Science and Technology, 7*, 386–394.

Zhao, K., Zeng, N. K., Han, L. H., Gao, X. Y., Liu, J., Wang, S., & Gu, B. (2018). *Phylloporus pruinatus*, a new lamellate bolete from subtropical China. *Phytotaxa*, *372*, 212–220.

Zhao, R. L., Desjardin, D. E., Callac, P., Parra, L. A., Guinberteau, J., Soytong, K., . . . Hyde, K. D. (2013). Two species of *Agaricus* sect. *Xanthodermatei* from Thailand. *Mycotaxon, 122*(1), 187–195.

Zhao, R. L., Hyde, K. D., Karunarathna, S. C., Desjardin, D. E., Raspé, O., Soytong, K., . . . Callac, P. (2012). *Agaricus flocculosipes* sp. nov., a new potentially cultivatable species from the palaeotropics. *Mycoscience, 53*(4), 300–311.

Zhao, R. L., Zhou, J. L., Chen, J., Margaritescu, S., Sánchez-Ramírez, S., Hyde, K. D., . . . Moncalvo, J. M. (2016). Towards standardizing taxonomic ranks using divergence times–a case study for reconstruction of the *Agaricus* taxonomic system. *Fungal Diversity, 78*(1), 239–292.

Zhao, R., Karunarathna, S., Raspé, O., Parra, L. A., Guinberteau, J., Moinard, M., . . . & Callac, P. (2011). Major clades in tropical *Agaricus*. *Fungal Diversity, 51*(1), 279–296.

Zhou, Q., Tang, X., Huang, Z., Song, P., & Zhou, J. J. (2010). Novel method for cultivating *Agaricus blazei*. *Acta Edulis Fungi, 17*, 39–42. http://www.syjxb.com/EN/Y2010/V17/I02/43.

Zhu, X. T., Wu, G., Zhao, K., Halling, R. E., & Yang, Z. L. (2015). *Hourangia*, a new genus of Boletaceae to accommodate *Xerocomus cheoi* and its allied species. *Mycological Progress, 14*(6), 37.

Zied, D. C., Minhoni, M. T. A., Kopytowski-Filho, J., & Andrade, M. C. N. (2010). Production of *Agaricus blazei* ss. Heinemann (*A. brasiliensis*) on different casing layers and environments. *World Journal of Microbiology and Biotechnology, 26,* 1857–1863.

Zied, D. C, Minhoni, M. T. A., Kopytowski-Filho, J., Barbosa, L., & Andrade, M. C. N. (2011a). Medicinal mushroom growth as affected by non-axenic casing soil. *Pedosphere, 21,* 146–153.

Zied, D. C., Pardo-Gime´nez, A., Savoie, J. M., Pardo-Gonzalez, J. E., & Callac, P. (2011b). Indoor method of composting and genetic breeding of the strains to improve yield and quality of the almond mushroom *Agaricus subrufescens*. In *Proceedings of the seventh International Conference on Mushroom Biology and Mushroom Products (ICMBMP7)* (pp. 419–427). France.

APPENDICES

APPENDIX A

CHEMICAL REAGENTS AND MEDIA

Table A1 List of media

Medium	Ingredients	Amount (/L)
BAF	Glucose	10 g
	Maltose	20 g
	Soya peptone	2 g
	Yeast extract	0.2 g
	KH_2PO_4	1 g
	$MgSO_4 \times 7H_2O$	0.5 g
	$FeCl_3$ (10 µM)	1 mL
	$ZnSO_4$ (1.78 g/L)	1 mL
	$CaCl_2$ (0.1 M)	1 mL
	After autoclave	
	Thiaminiumchlorid	50 µg
	Biotin	1 µg
	Folate	100 µg
	myo-Inosit	50 µg

Table A1 (continued)

Medium	Ingredients	Amount (/L)
MGP	Glucose	10 g
	Maltose	20 g
	Soya peptone	2 g
	Yeast extract	1 g
	KH_2PO_4	1 g
	$MgSO_4 \times 7H_2O$	0.5 g
	$FeCl_3$ (10 µM)	1 mL
	$ZnSO_4$ (1.78 g/L)	1 mL
	$CaCl_2$ (0.1 M)	1 mL
MMK	Mannitol	40 g
	Yeast extract	5 g
	Murashige & Skoog Salts	4.3 g
Potato dextrose agar (PDA)	Potato extract	4 g
	Dextrose	20 g
	Agar	15 g
Cottonseed flour medium (Q6 ½)	D-Glucose	2.5 g
	Glycerin	10 g
	Cotton seed flour	5 g
Yeast Malt medium (YM)	Glucose	4 g
	Malt extract	10 g
	Yeast extract	4 g
Malt extract agar (MEA)	Malt extract	30g
	Mycological peptone	5 g
	Agar	15 g

Table A1 (continued)

Medium	Ingredients	Amount (/L)
Sugar malt medium (ZM ½)	Molasses	5 g
	Oatmeal	5 g
	Sucrose	4 g
	Mannitol	4 g
	D-Glucose	1.5 g
	$CaCO_3$	0.5 g
	Edamin $(NH_4)_2SO_4$	0.5 g

Chemical reagents

1. Ammoniacal solution

Add 66 mL of concentrated ammonium hydroxide (28% NH_4OH) to 500 mL of purified water and dilute to 1 L.

2. Ammonical congo red solution

Add 1:1 volume of ammoniacal solution and congo red.

3. Congo red stain, 100 ml

Add 1 g of congo red in 99 ml 5% potassium hydroxide (KOH) and filter the excess dye.

4. Melzer's reagent

Potassium iodide	5 g
Iodine	1.5 g
Chloral hydrate	100 g
Distilled water	100 ml

Add 1.5 g iodine crystals, 5 g of potassium iodide, and 100 ml of chloral hydrate to 100 ml of water.

5. Potassium hydroxide (5% KOH)

Add 0.50 g of KOH and adjust the volume to 100 ml of KOH then mix the solution until it is clear.

APPENDIX B

HPLC-ESI-MS AND NMR DATA

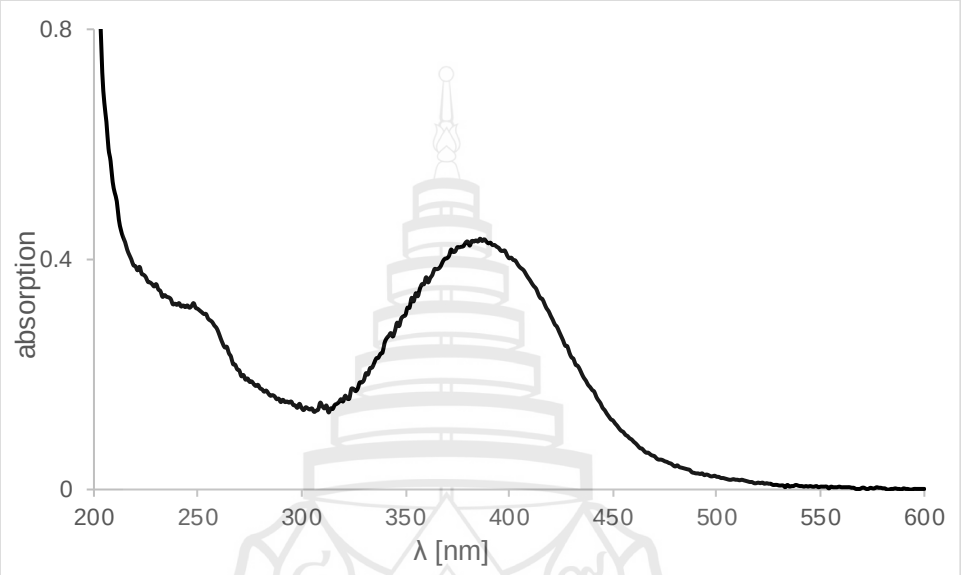
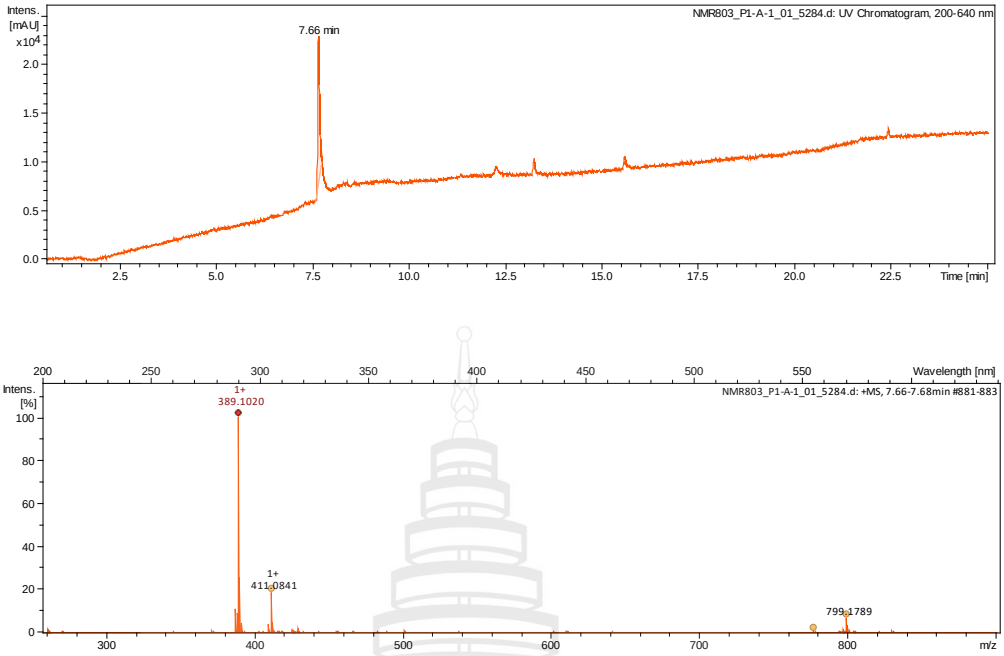
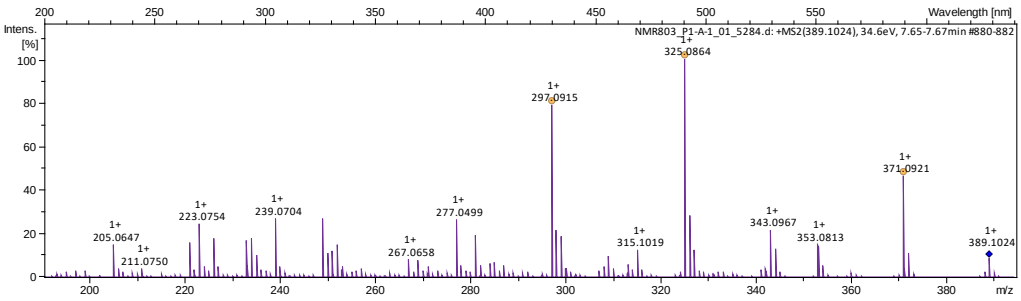


Figure B1 UV/Vis spectrum of 9’-hydroxyphenyl pulvinone (1)



Meas. *m/z*	Ion Formula	*m/z*	err [ppm]
389.101966	$C_{23}H_{17}O_6$	389.101965	-0.0
411.084105	$C_{23}H_{16}NaO_6$	411.083909	-0.5
777.197295	$C_{46}H_{33}O_{12}$	777.196653	-0.8
799.178900	$C_{46}H_{32}NaO_{12}$	799.178597	-0.4

Figure B2 Chromatogram and HR-LC-ESI(+)-MS of 9'-hydroxyphenyl pulvinone (1)



Meas. *m/z*	Ion Formula	*m/z*	err [ppm]
297.091457	$C_{21}H_{13}O_2$	297.091006	-1.5
325.086383	$C_{22}H_{13}O_3$	325.085921	-1.4
371.092093	$C_{23}H_{15}O_5$	371.091400	-1.9

Figure B3 HR-ESI(+)-MS/MS of 9'-hydroxyphenyl pulvinone (**1**) (precursor ion 389.1024, 34.6 eV)

^{1}H NMR (700 MHz, METHANOL-d_4) δ ppm 5.97 (s, 1 H) 6.64 (d, *J*=8.2 Hz, 1 H) 6.77 (d, *J*=8.4 Hz, 3 H) 6.77 (d, *J*=8.6 Hz, 3 H) 6.87 (d, *J*=8.4 Hz, 2 H) 6.91 (d, *J*=2.2 Hz, 1 H) 7.16 (d, *J*=8.6 Hz, 2 H) 7.62 (d, *J*=8.8 Hz, 2 H)

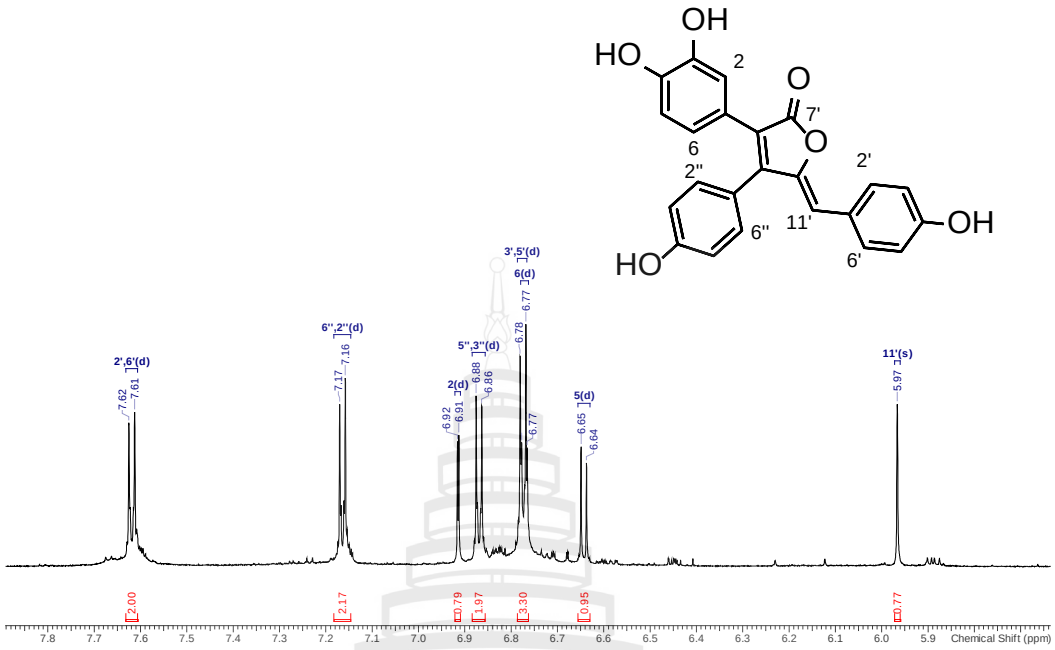


Figure B4 ^{1}H NMR spectrum (700 MHz, CD_3OD, 300 K) of 9'-hydroxyphenyl pulvinone (1)

^{13}C NMR (176 MHz, METHANOL-d_4) δ ppm 114.65 (s, 1 C) 116.24 (s, 1 C) 117.17 (s, 1 C) 117.52 (s, 1 C) 117.78 (s, 1 C) 122.44 (s, 1 C) 122.55 (s, 1 C) 122.61 (s, 1 C) 123.18 (s, 1 C) 125.64 (s, 1 C) 132.02 (s, 1 C) 133.74 (s, 1 C) 146.74 (s, 1 C) 147.81 (s, 1 C) 148.31 (s, 1 C) 150.99 (s, 1 C) 161.65 (s, 1 C) 162.39 (s, 1 C) 171.76 (s, 1 C)

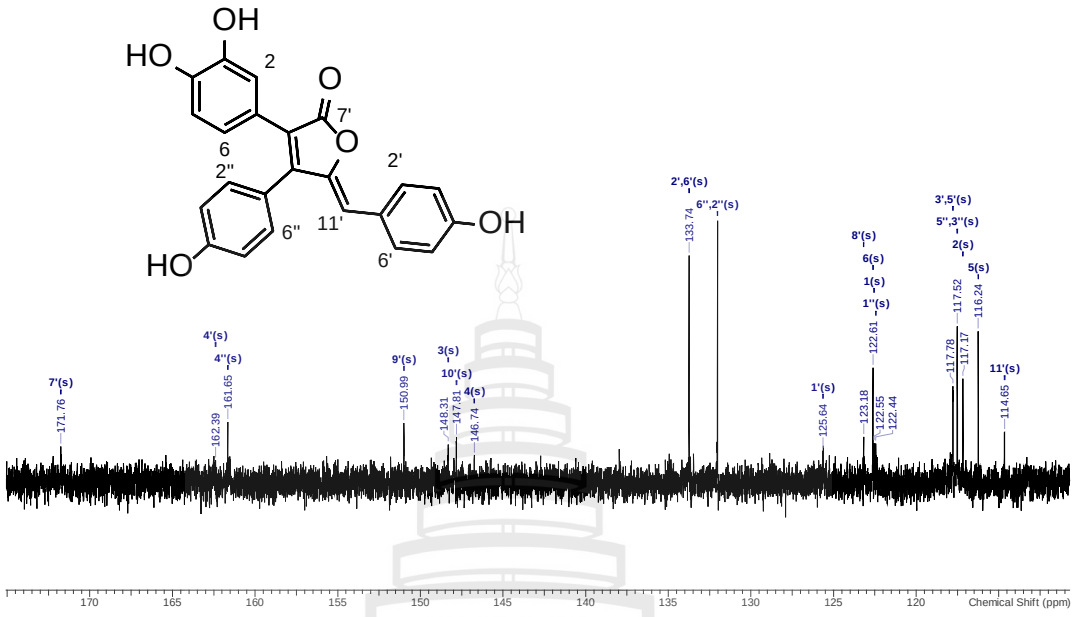


Figure B5 ^{13}C NMR spectrum (176 MHz, CD_3OD, 300 K) of 9'-hydroxyphenyl pulvinone (1)

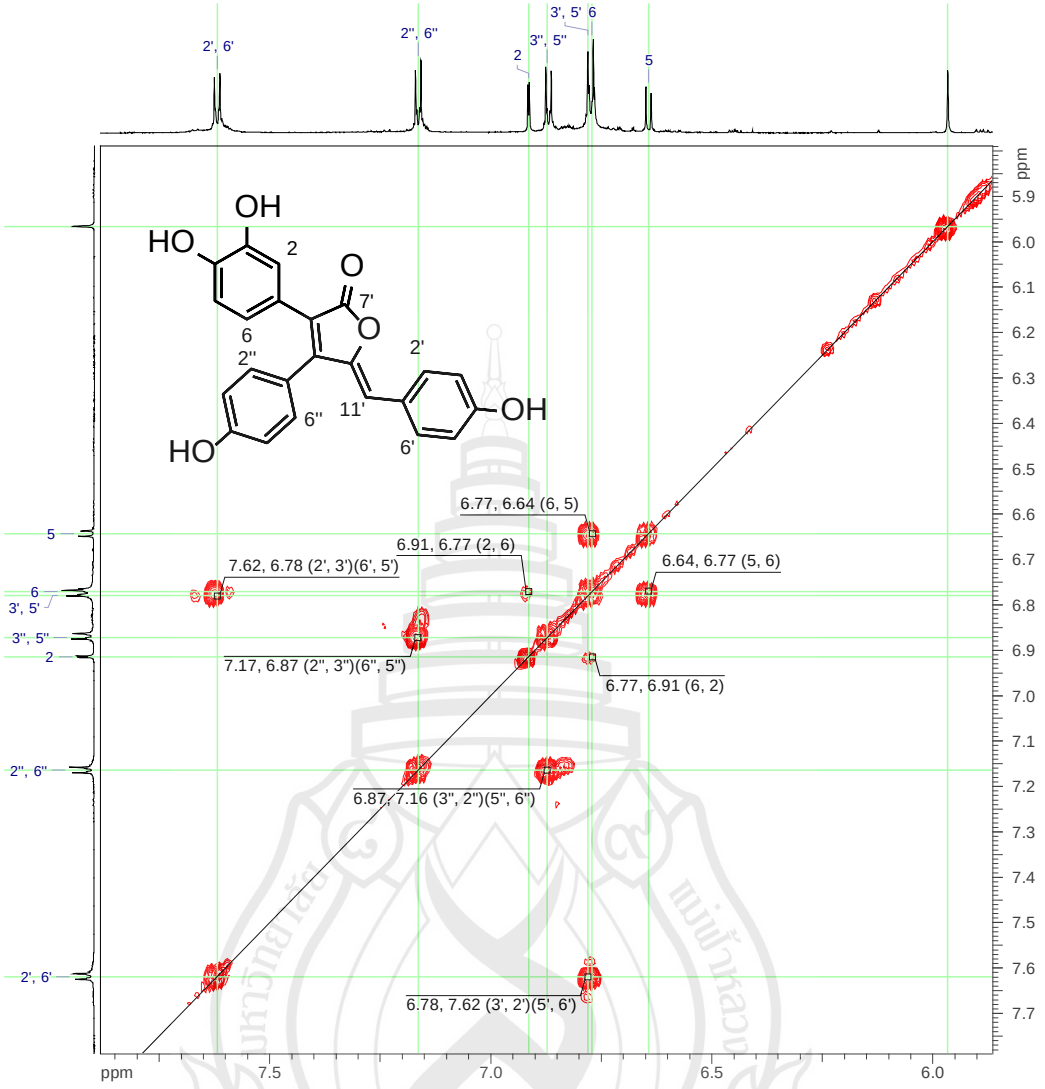


Figure B6 $^{1}H,^{1}H$ COSY spectrum (700 MHz, CD_3OD, 300 K) of 9'-hydroxyphenyl pulvinone (1)

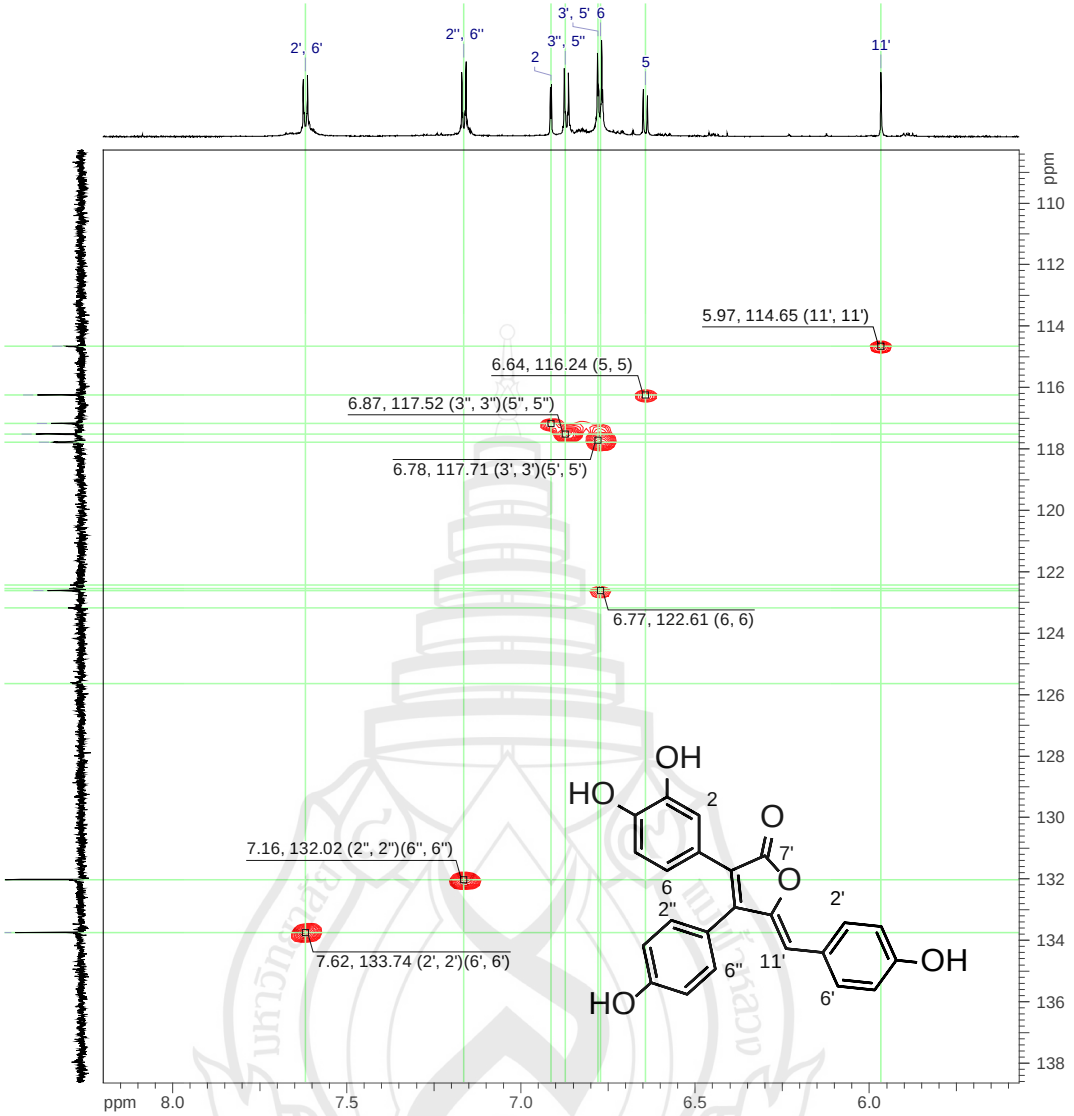


Figure B7 $^{1}H, ^{13}C$ HSQC spectrum (700 MHz, CD_3OD, 300 K) of 9'-hydroxyphenyl pulvinone (1)

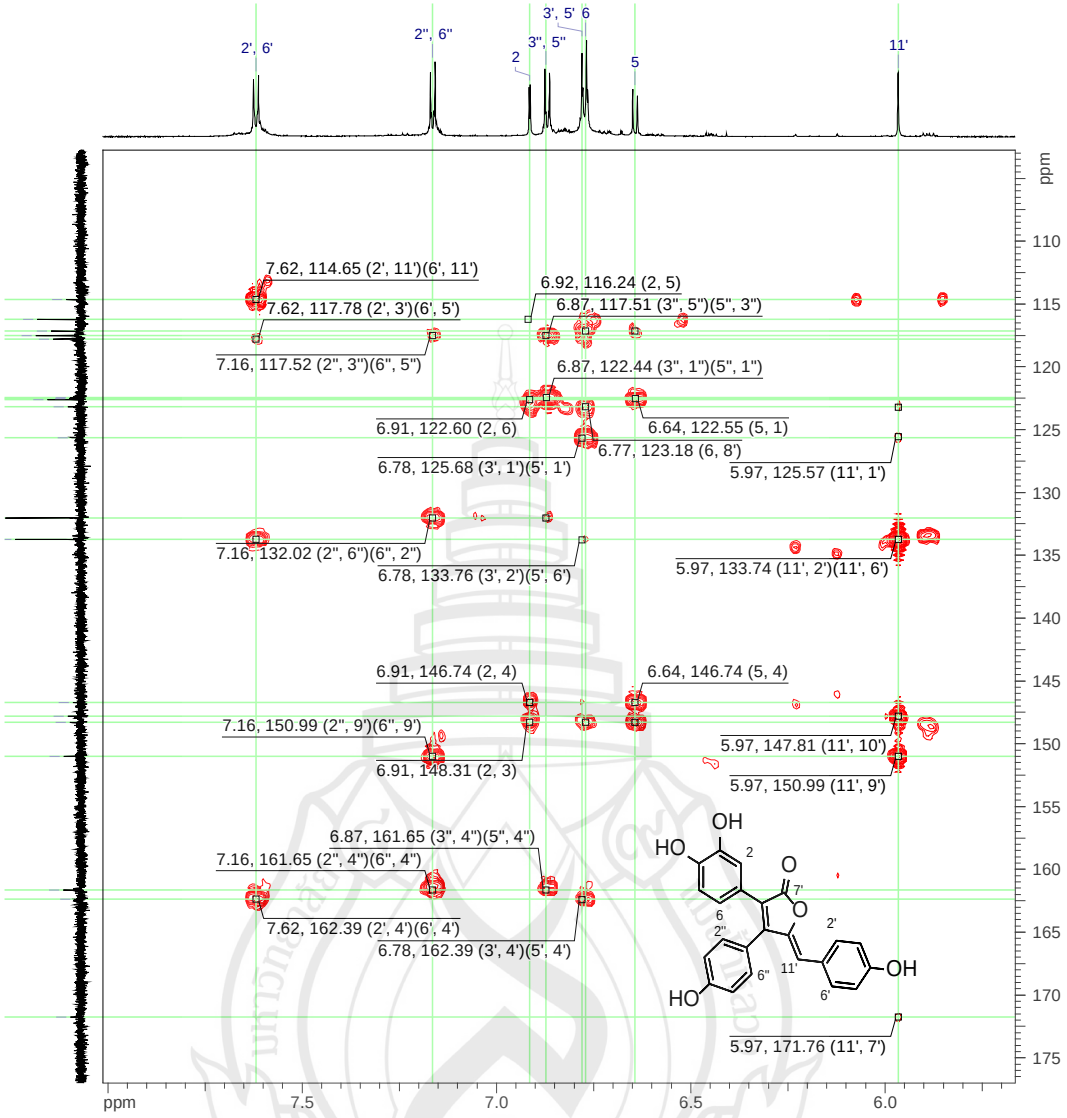


Figure B8 $^{1}H,^{13}C$ HMBC spectrum (700 MHz, CD_3OD, 300 K) of 9'-hydroxyphenyl pulvinone (1)

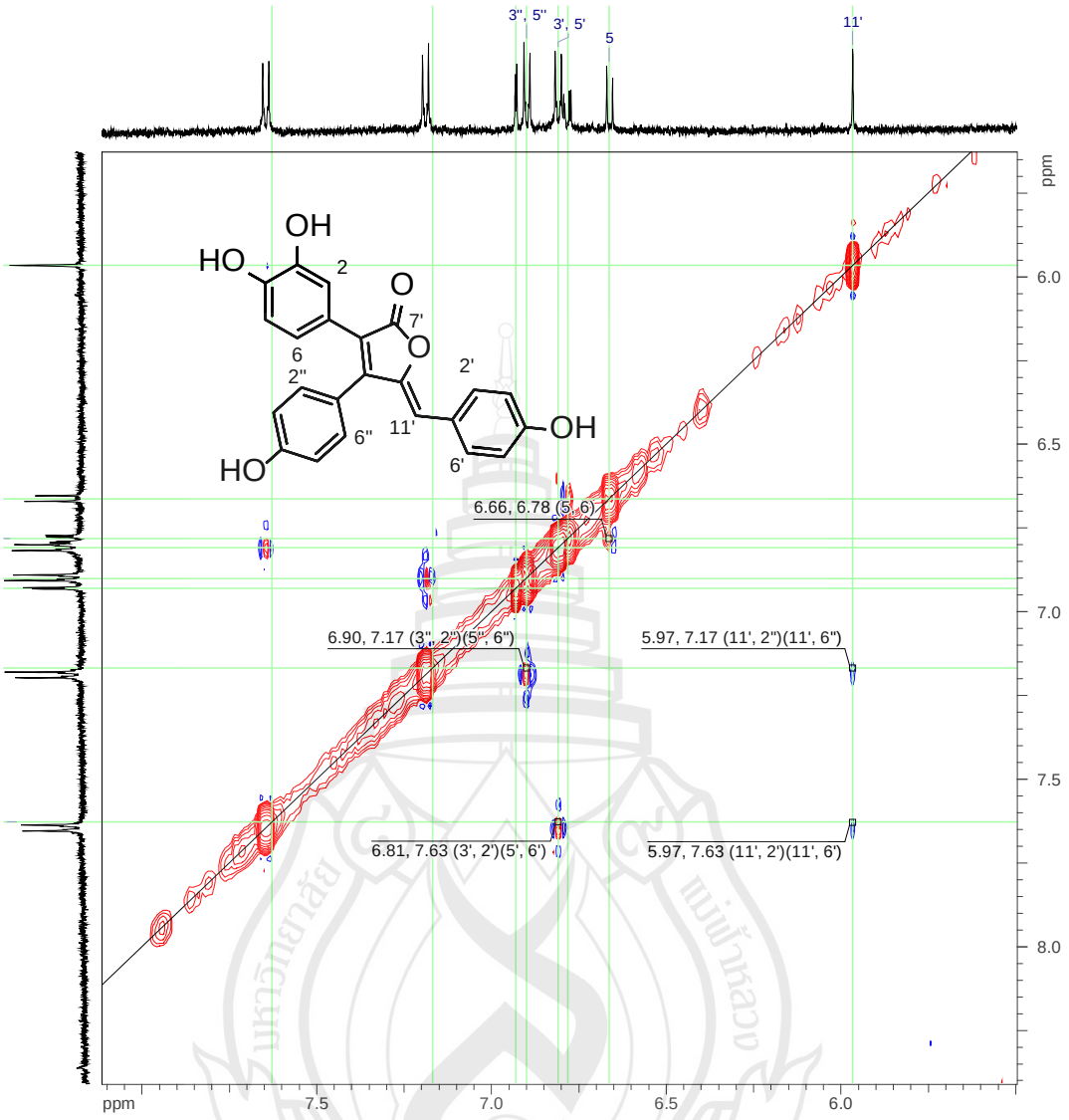


Figure B9 $^{1}H,^{1}H$ NOESY spectrum (500 MHz, CD_3CN, 300 K) of 9'-hydroxyphenyl pulvinone (1)

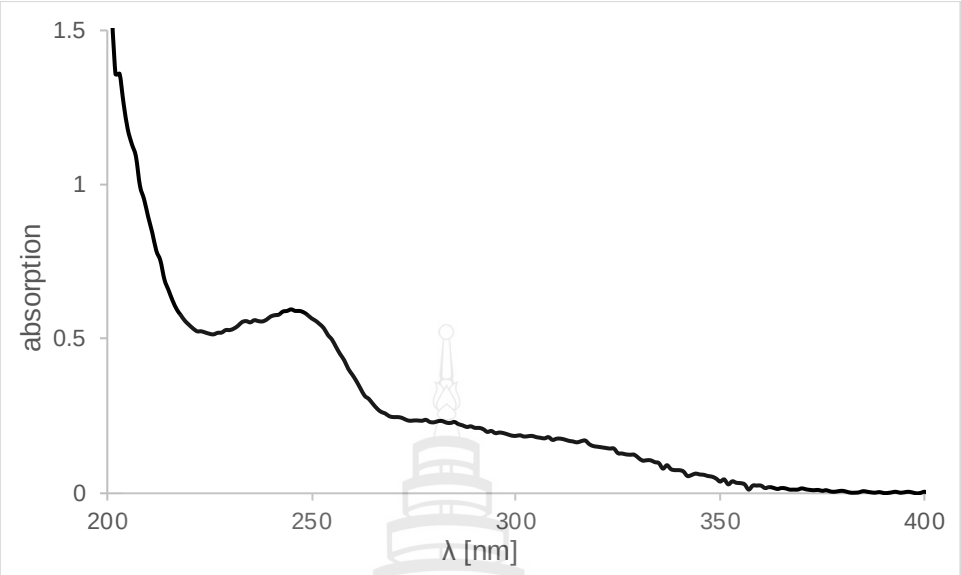
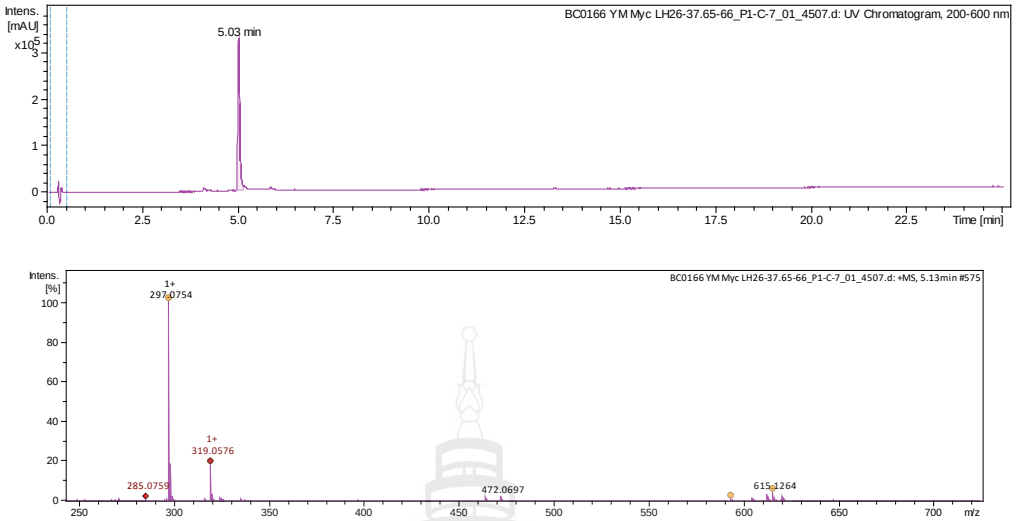
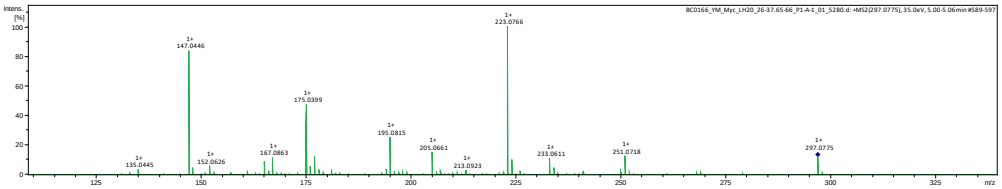


Figure B10 UV/Vis spectrum of phlebopyron (2)



Meas. *m/z*	Ion Formula	*m/z*	err [ppm]
297.075440	$C_{17}H_{13}O_5$	297.075750	1.0
319.057562	$C_{17}H_{12}NaO_5$	319.057694	0.4
593.143960	$C_{34}H_{25}O_{10}$	593.144223	0.4
615.126422	$C_{34}H_{24}NaO_{10}$	615.126168	-0.4

Figure B11 Chromatogram and HR-LC-ESI(+)-MS of phlebopyron (2)



Meas. m/z	Ion Formula	*m/z*	err [ppm]
147.044556	$C_9H_7O_2$	147.044056	-3.4
175.039868	$C_{10}H_7O_3$	175.038971	-5.1
223.076627	$C_{15}H_{11}O_2$	223.075356	-5.7
251.071767	$C_{16}H_{11}O_3$	251.070271	-6.0

Figure B12 HR-ESI(+)-MS/MS of phlebopyron (**2**) (precursor ion 297.0775, 35.0 eV)

^{1}H NMR (700 MHz, ACETONITRILE-d_3) δ ppm 6.89 (d, *J*=8.6 Hz, 2 H) 6.91 (d, *J*=8.7 Hz, 2 H) 7.25 (d, *J*=8.7 Hz, 2 H) 7.29 (d, *J*=8.7 Hz, 2 H) 7.48 (s, 1 H)

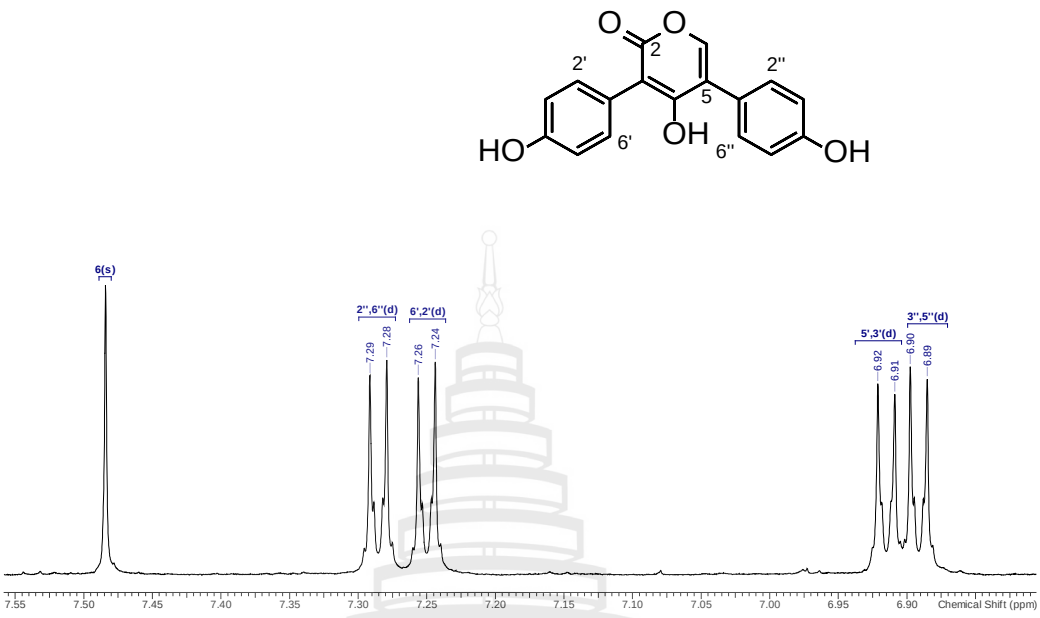


Figure B13 ^{1}H NMR spectrum (700 MHz, CD_3CN, 300 K) of phlebopyron (2)

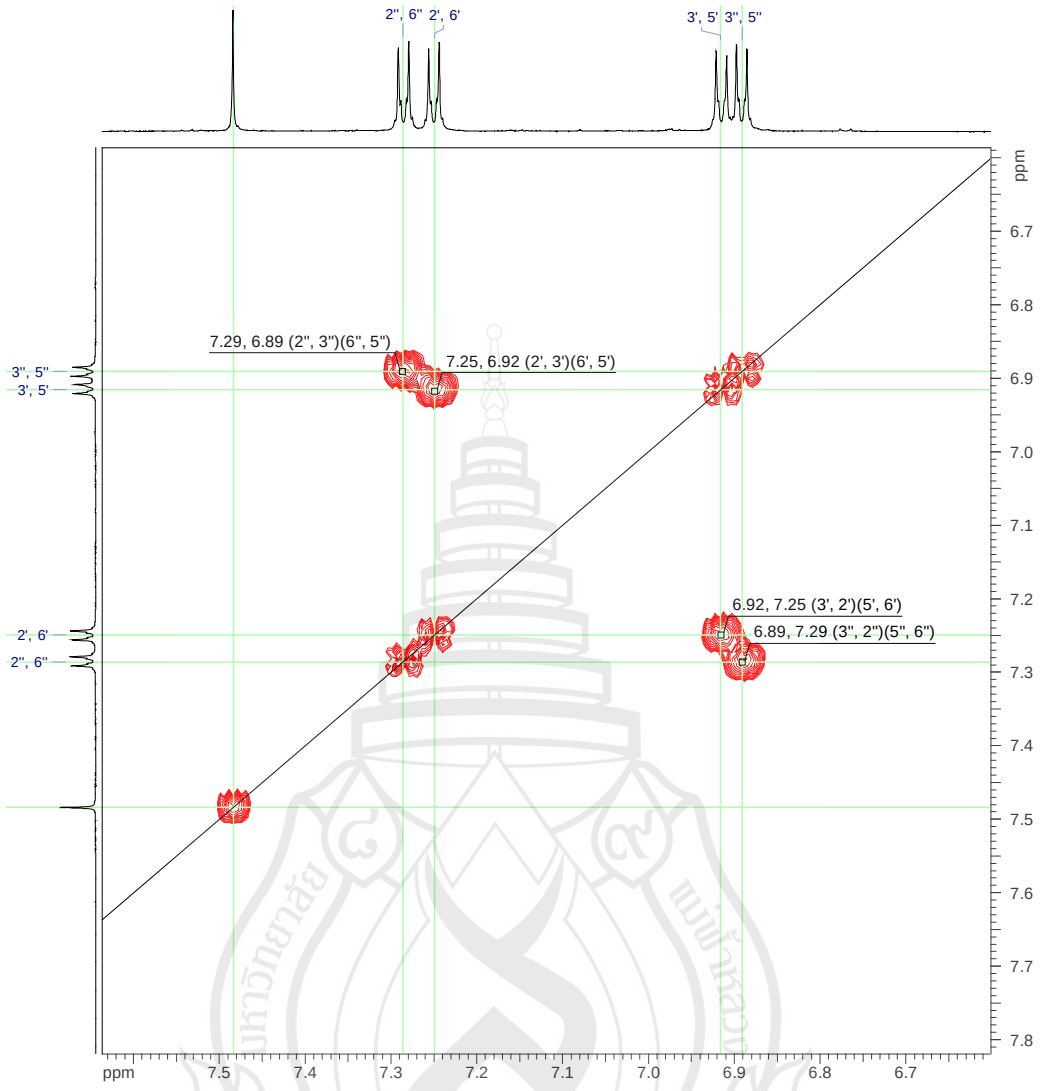


Figure B14 $^{1}H,^{1}H$ COSY spectrum (700 MHz, CD_3CN, 300 K) of phlebopyron (2)

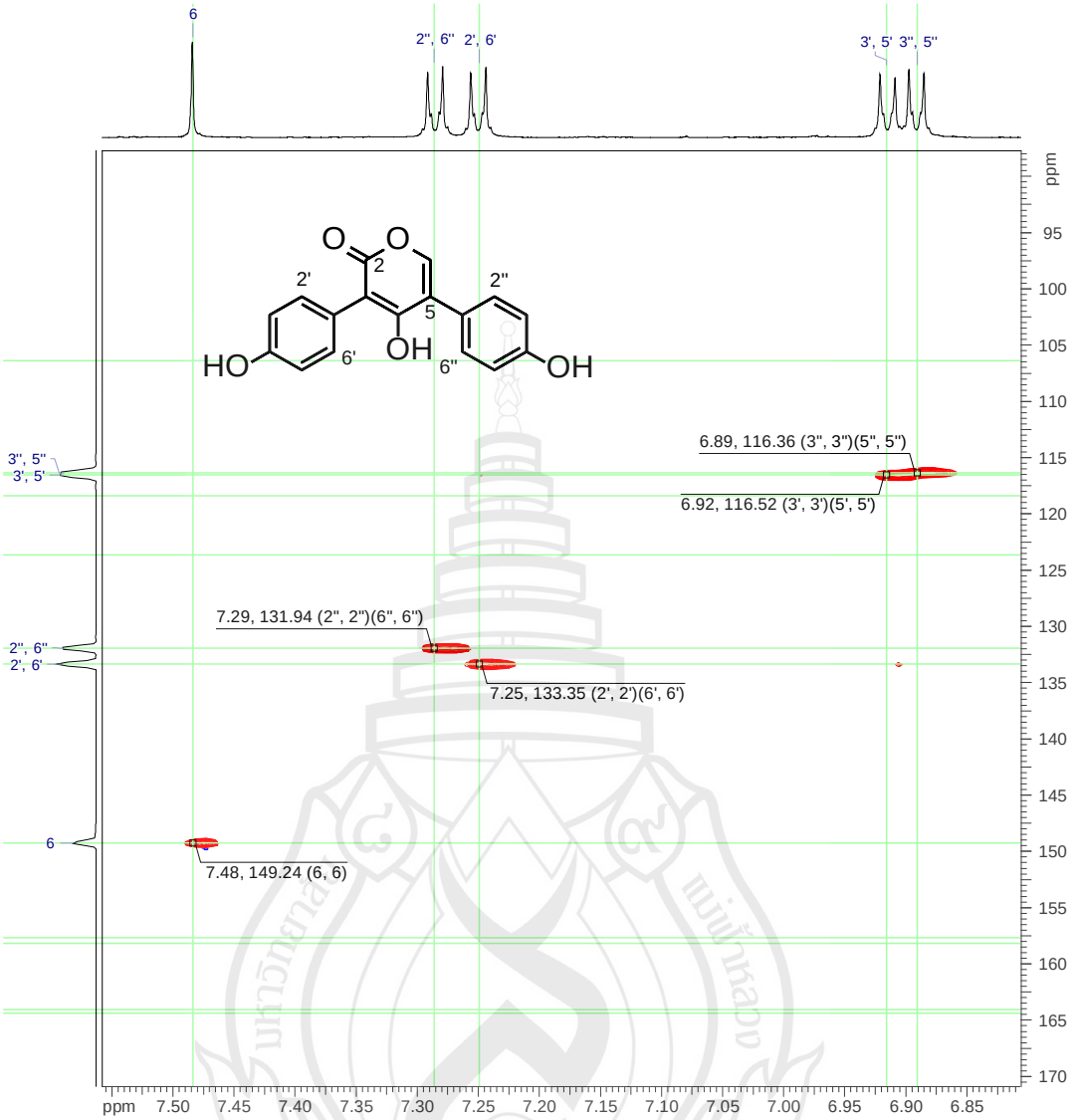


Figure B15 $^{1}H,^{13}C$ HSQC spectrum (700 MHz, CD_3CN, 300 K) of phlebopyron (2)

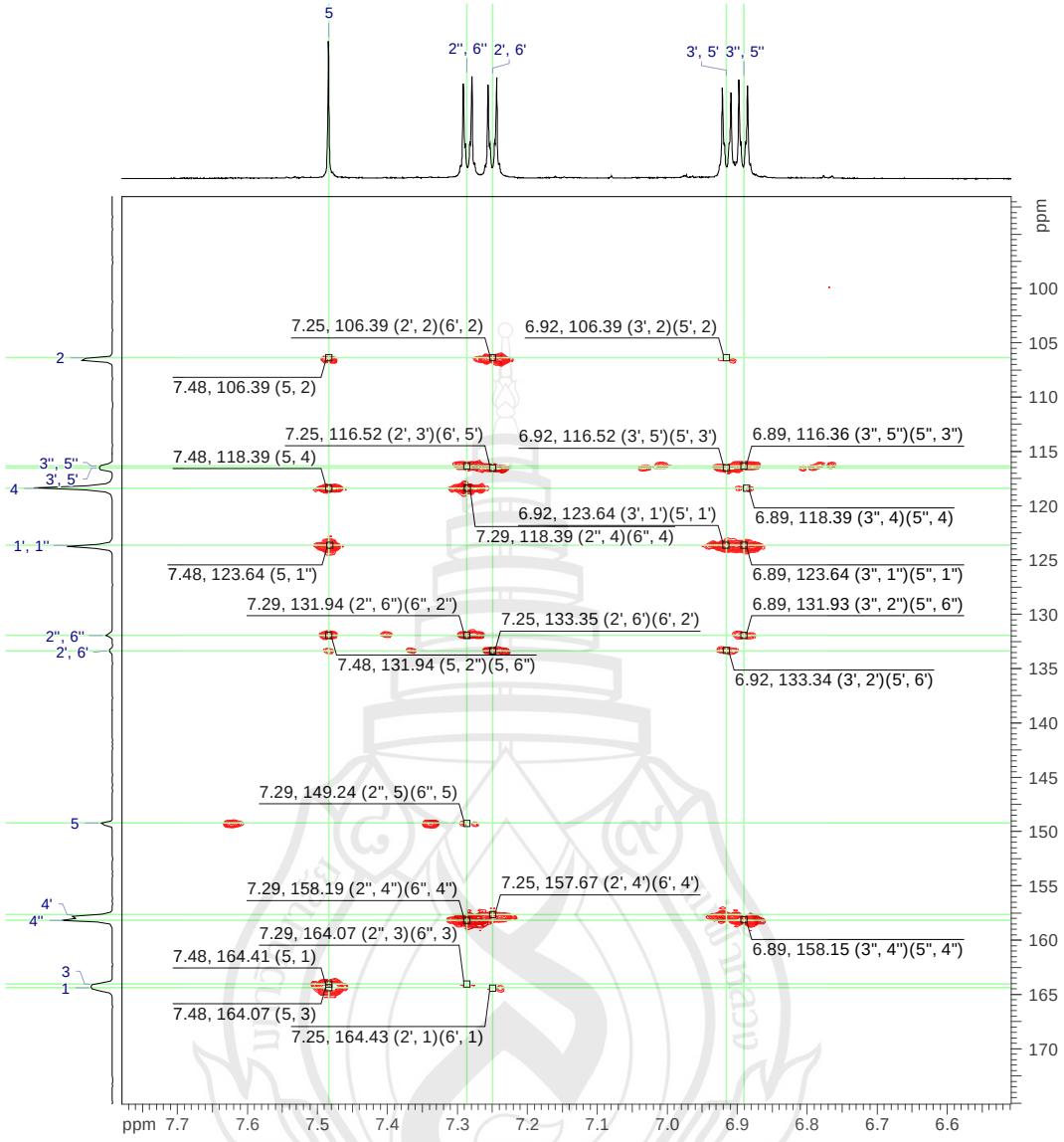


Figure B16 $^{1}H,^{13}C$ HMBC spectrum (700 MHz, CD_3CN, 300 K) of phlebopyron (2)

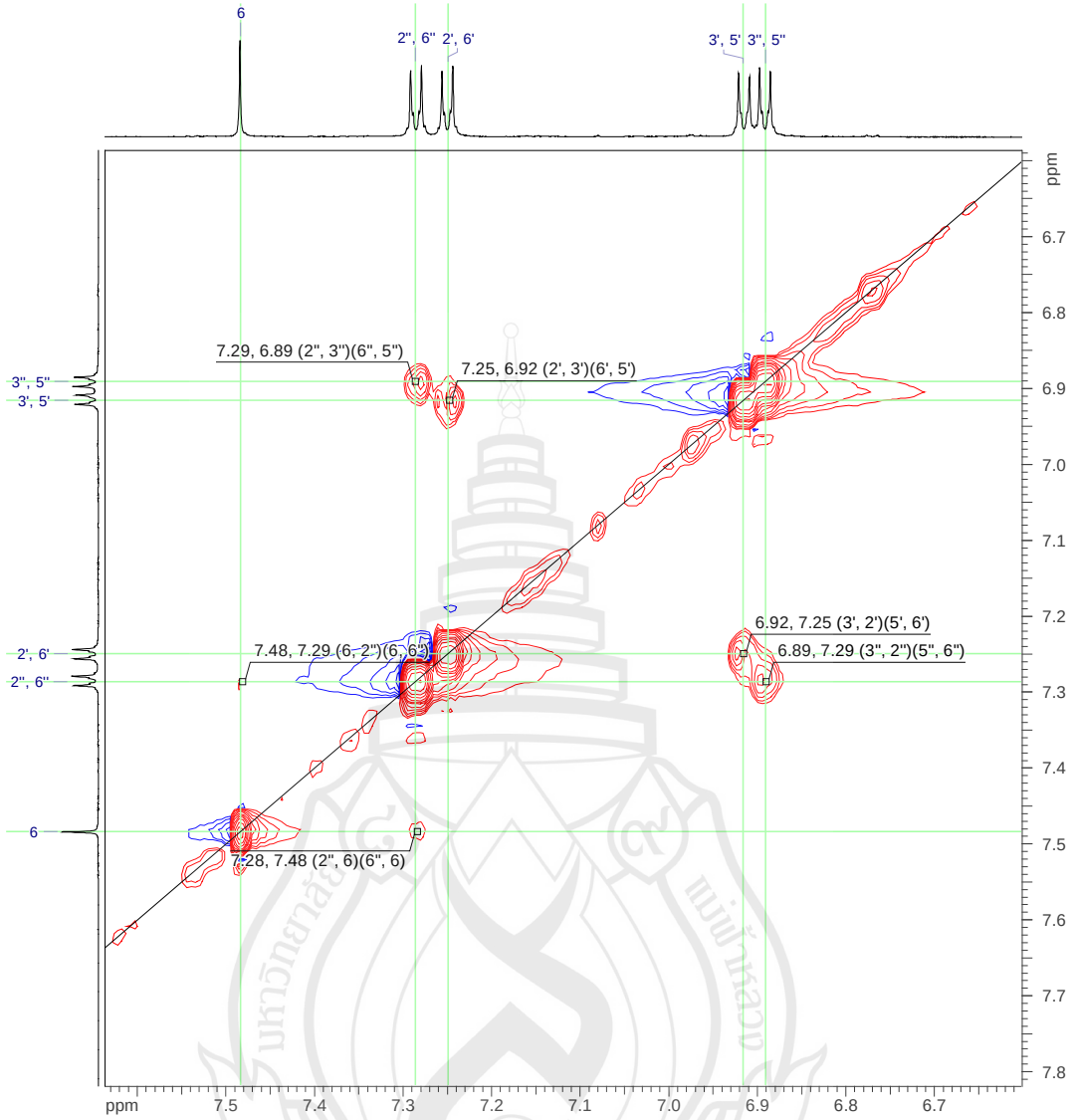


Figure B17 ^{1}H,^{1}H NOESY spectrum (700 MHz, CD_3CN, 300 K) of phlebopyron (2)

Atromentic acid (3): R_f (TLC) = 0.60 (acetone : dichloromethane, 11 : 9, 6/6); UV/Vis (MeOH): λ_{max} (log ε) = 257 (4.33), 385 (3.99) nm; analytical HPLC (t_R) = 5.40 min; HR-ESI(+)-MS: *m/z* (%) = 703.1062 (8) $[2M+Na]^+$ ($C_{36}H_{24}NaO_{14}$ cald. for 703.1058), 681.1241 (2) $[2M+H]^+$ ($C_{36}H_{25}O_{14}$ cald. for 681.1239), 363.0479 (7) $[M+Na]^+$ ($C_{18}H_{12}NaO_7$ cald. for 363.0475), 341.0568 (100) $[M+H]^+$ ($C_{18}H_{13}O_7$ cald. for 341.0656); HR-ESI(+)-MS/MS (precursor ion *m/z* 341.0697): *m/z* (%) = 323.0558 (6) $[M+H–H_2O]^+$ ($C_{18}H_{11}O_6$ cald. for 323.0550), 295.0611 (100) $[M+H–CH_2O_2]^+$ ($C_{17}H_{11}O_5$ cald. for 295.0611), 267.0660 (13) $[M+H–CH_2O_2–CO]^+$ ($C_{16}H_{11}O_4$ cald. for 267.0660), 239.0711 (12) $[M+H–CH_2O_2–CO–CO]^+$ ($C_{15}H_{11}O_3$ cald. for 239.0703); ^{1}H

NMR (700 MHz, CD_3CN, 300 K): δ = 7.96 (2 H, d, J = 9.0 Hz, H-2/6), 7.17 (2 H, d, J = 8.7 Hz, H-2'/6'), 6.88 (2 H, d, J = 9.0 Hz, H-3/5), 6.86 (2 H, d, J = 8.7 Hz, H-3'/5'); ^{13}C NMR (176 MHz, CD_3CN, 300 K): δ = 173.9 (C-12'), 167.7, 161.2, 158.1 (C-4'), 157.8 (C-4), 132.6 (C-2'/6'), 130.0 (C-2/6), 125.9 (C-1'), 123.5 (C-1), 117.0 (C-11'), 116.3 (C-3/5), 115.7 (C-3'/5'), 104.5 (C-8').

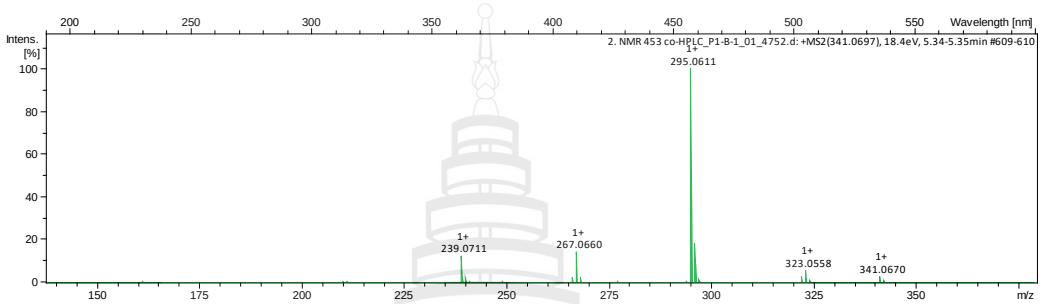


Figure B18 HR-ESI(+)-MS/MS of atromentic acid (**3**) (precursor ion *m/z* 341.0697, 18.4 eV)

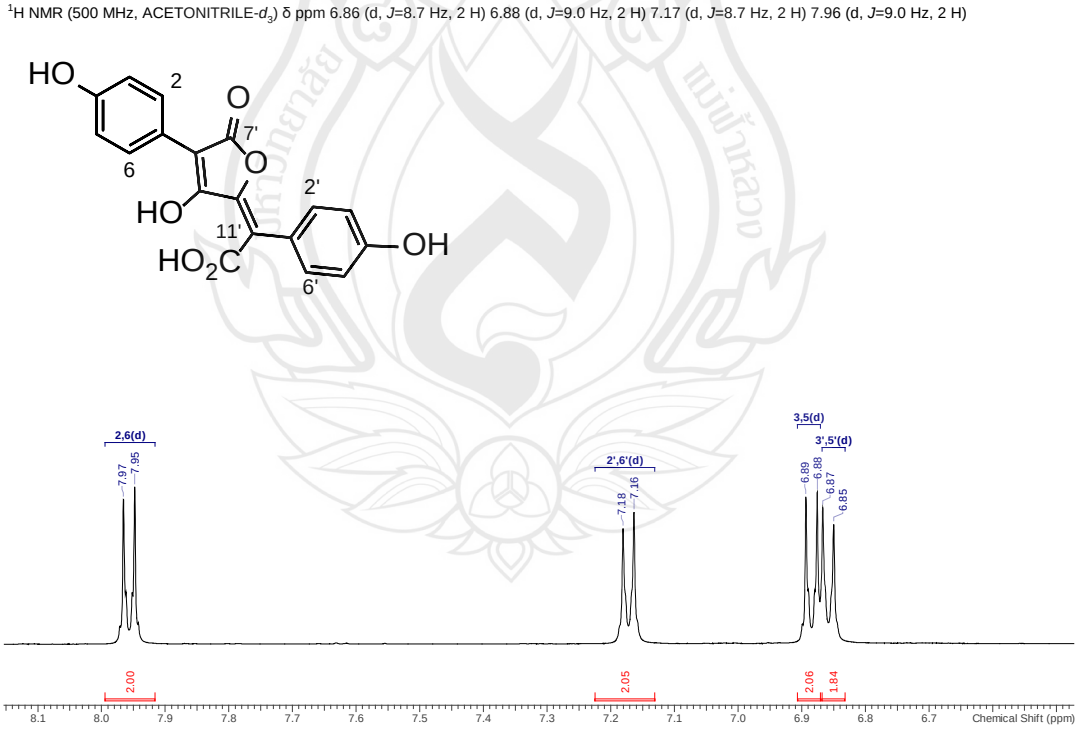


Figure B19 ^{1}H NMR (700 MHz, CD_3CN, 300 K) of atromentic acid (3)

Xerocomic acid (4): R_f (TLC) = 0.80 (dichloromethane : methanol, 6 : 4, (6/6); UV/Vis (MeOH): λ_{max} (log ε) = 261 (4.18), 394 (3.84) nm; analytical HPLC (t_R) = 4.76 min; HR-ESI(+)-MS: *m/z* (%) = 735.0956 (5) $[2M+Na]^+$ ($C_{36}H_{24}NaO_{16}$ cald. for 735.0957), 713.1136 (3) $[2M+H]^+$ ($C_{36}H_{25}O_{16}$ cald. for $C_{36}H_{25}O_{16}$), 379.0428 (7) $[M+Na]^+$ ($C_{18}H_{12}NaO_8$ cald. for 379.0424), 357.0607 (100) $[M+H]^+$ ($C_{18}H_{13}O_8$ cald. for 357.0605); HR-ESI(+)-MS/MS (precursor ion *m/z* 357.0633): *m/z* (%) = 339.0497 (4) $[M+H–H_2O]^+$ ($C_{18}H_{11}O_7$ cald. for 339.0499), 311.0556 (100) $[M+H–CH_2O_2]^+$ ($C_{17}H_{11}O_6$ cald. for 311.0550), 283.0607 (15) $[M+H–CH_2O_2–CO]^+$ ($C_{16}H_{11}O_5$ cald. for 283.0601), 255.0657 (4) $[M+H–CH_2O_2–CO–CO]^+$ ($C_{15}H_{11}O_4$ cald. for 255.0652); ^{1}H NMR (500 MHz; CD_3OD, 300 K): δ = 7.73 (1 H, d, *J* = 2.1 Hz, H-2), 7.59 (1 H, dd, *J* = 8,4 Hz; 2.1 Hz, H-6), 7.28 (2 H, d, *J* = 8.5 Hz, H-2'/H-6'), 6.89 (3 H, d, *J* = 8.5 Hz; 8.4 Hz, H-5'/H-3'; H-5); ^{13}C NMR (126 MHz, CD_3OD, 300 K): δ = 173.8 (C-12'), 166.4, 159.5, 157.8 (C-4'), 154.9 (C-10'), 145.8 (C-4), 145.0 (C-3), 132.0 (C-2'/C6'), 124.7 (C-1'), 121.9 (C-1), 120.6 (C-6), 116.2 (C-11'), 115.5 (C-5), 115.0 (C-2), 114.9 (C-5'/C-3'), 104.2 (C-8').

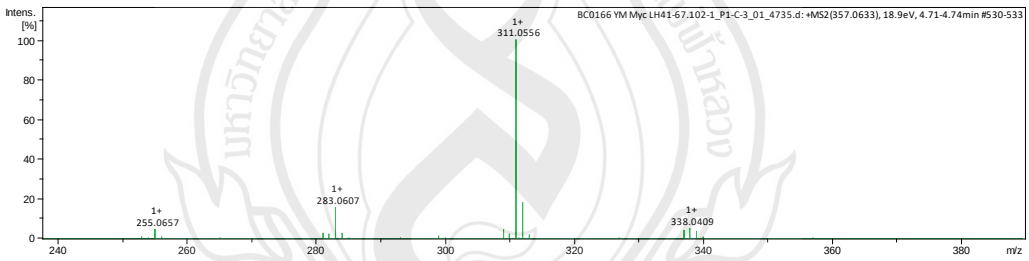


Figure B20 HR-ESI(+)-MS/MS of xerocomic acid (4) (precursor ion *m/z* 357.0633, 18.9 eV)

^{1}H NMR (500 MHz, acetone) δ ppm 6.89 (d, *J*=8.5 Hz, 3 H) 7.28 (d, *J*=8.5 Hz, 2 H) 7.59 (dd, *J*=8.4, 2.1 Hz, 1 H) 7.73 (d, *J*=2.1 Hz, 1 H)

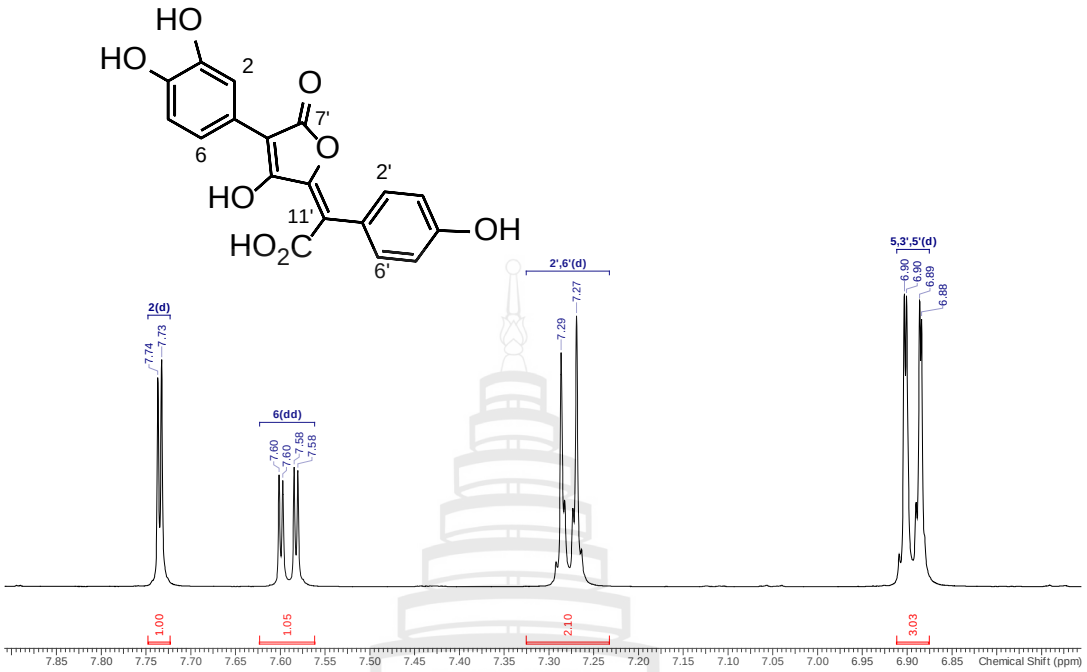


Figure B21 ^{1}H NMR (500 MHz, $(CD_3)_2CO$, 300 K) of xerocomic acid (4)

Variegatic acid (5): R_f (TLC) = 0.43 (toluene : ethyl acetate : formic acid, 10 : 5 : 3, 4/4/4); UV/Vis (MeOH): λ_{max} (log ε) = 265 (3.96), 380 (3.39) nm; analytical HPLC (t_R) = 4.32 min; HR-ESI(+)-MS: *m/z* (%) = 767.0847 (3) $[2M+Na]^+$ ($C_{36}H_{24}NaO_{18}$ cald. for 767.0855), 745.1035 (4) $[2M+H]^+$ ($C_{36}H_{25}O_{18}$), 395.03711 (7) $[M+Na]^+$ ($C_{18}H_{12}NaO_9$ cald. for 395.0374), 373.0551 (100) $[M+H]^+$ ($C_{18}H_{13}O_9$ cald. for 373.0554); HR-ESI(+)-MS/MS (precursor ion *m/z* 373.0554): *m/z* (%) = 327.0502 (100) $[M+H–CH_2O_2]^+$ ($C_{17}H_{11}O_7$ cald. for 327.0499), 299.0552 (12) $[M+H–CH_2O_2–CO]^+$ ($C_{16}H_{11}O_6$ cald. for 299.0550), 271.0602 (3) $[M+H–CH_2O_2–CO–CO]^+$; ^{1}H NMR (500 MHz, CD_3CN, 300 K): δ = 7.80 (1 H, d, *J* = 2.2 Hz, H-2), 7.61 (1 H, dd, *J* = 8.2; 2.0 Hz, H-6), 6.78 (2 H, d, *J* = 8.2 Hz, H-5/5'), 6.72 (1 H, d, *J* = 2.2 Hz, H-2'), 6.61 (1 H, dd, *J* = 8.2; 2.0 Hz, H-6'); ^{13}C NMR (126 MHz, CD_3CN, 300 K): δ = 171.1, 170.5, 169.3, 153.9, 144.9 (C-3), 144.8 (C-3'), 144.4 (C-4'), 143.4 (C-4), 129.9 (C-1), 126.5 (C-1'), 123.6 (C-6'), 119.3 (C-6), 118.84 (C-11'), 118.75 (C-2'), 115.9 (C-5'), 115.1 (C-5), 114.0 (C-2), 96.6 (C-8').

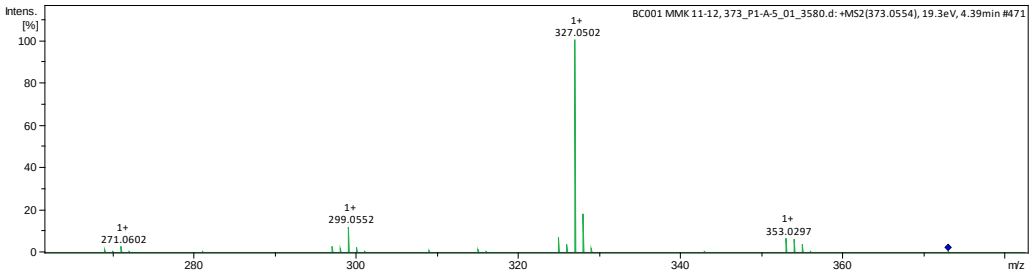


Figure B22 HR-ESI(+)-MS/MS of variegatic acid (**5**) (precursor ion 373.0554, 19.3 eV).

^{1}H NMR (700 MHz, ACETONITRILE-d_3) δ ppm 6.61 (dd, *J*=8.1, 2.0 Hz, 1 H) 6.72 (d, *J*=2.2 Hz, 1 H) 6.78 (d, *J*=8.2 Hz, 2 H) 7.61 (dd, *J*=8.3, 2.0 Hz, 1 H) 7.80 (d, *J*=2.2 Hz, 1 H)

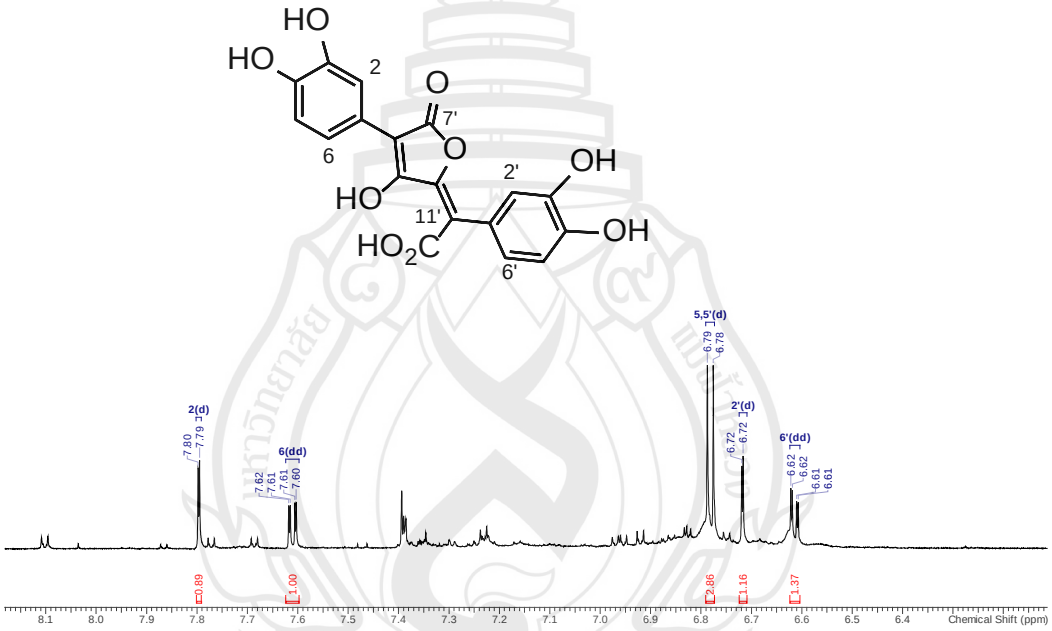


Figure B23 ^{1}H NMR (500 MHz, CD_3CN, 300 K) of variegatic acid (5)

Methyl atromentate (6): R_f (TLC) = 0.14 (pentane : ethyl acetate, 1 : 1, 6/6); UV/Vis (MeOH): λ_{max} (log ε) = 231 (4.13), 256 (4.05), 314 (4.11), 386 (3.77) nm; analytical HPLC (t_R) = 8.34 min; HR-ESI(+)-MS: *m*/*z* (%) = 731.1369 (14) $[2M+Na]^+$ ($C_{38}H_{28}NaO_{14}$ cald. for 731.1371), 709.1548 (1) $[2M+H]^+$ ($C_{38}H_{29}O_{14}$ cald. for 709.1552), 377.0631 (24) $[M+Na]^+$ ($C_{19}H_{14}NaO_7$ cald. for 377.0632), 355.0811 (100) $[M+H]^+$ ($C_{19}H_{15}O_7$ cald. for 355.0812); HR-ESI(+)-MS/MS (precursor ion *m*/*z* 355.0824): *m*/*z* (%) = 323.0553 (15) $[M+H–CH_4O]^+$ ($C_{18}H_{11}O_6$ cald. for 323.0550), 295.0607 (100) $[M+H–C_2H_4O_2]^+$ ($C_{17}H_{11}O_5$ cald. for 295.0601), 267.0655 (7) [M+H–

$C_2H_4O_2$–CO]$^+$ ($C_{16}H_{11}O_4$ cald. for 267.0652), 239.0706 (4) [M+H–$C_2H_4O_2$–CO–CO]$^+$ ($C_{15}H_{11}O_3$ cald. for 239.0703); ^{1}H NMR (700 MHz, $(CD_3)_2CO$, 300 K): δ = 8.28 (2 H, d, *J* = 8.7 Hz, H-2/H-6), 7.55 (2 H, d, *J* = 8.8 Hz, H-2'/H-6'), 6.83 (2 H, d, *J* = 8.8 Hz, H-3'/H-5'), 6.67 (2 H, d, *J* = 8.7 Hz, H-3/H-5), 3.79 (3 H, s, H-13');^{1}H NMR (700 MHz, CD_3OD, 300 K): δ = 7.92 (2 H, d, *J* = 8.9 Hz, H-2/H-6), 7.51 (2 H, d, *J* = 8.8 Hz, H-2'/H-6'), 6.79 (2 H, d, *J* = 8.8 Hz, H-3'/H-5'), 6.73 (2 H, d, *J* = 8.9 Hz, H-3/H-5), 3.89 (3 H, s, H-13'); ^{13}C NMR (176 MHz, CD_3OD, 300 K): δ = 171.4 (C-12'), 158.4 (C-4'), 154.8 (C-4), 130.8 (C-2'/C-6'), 127.6 (C-2/C-6), 126.5 (C-1), 125.2 (C-1'), 116.0 (C-'/C-6'), 115.2 (C-3/C-5), 111.4 (C-11'), 94.0 (C-8'), 52.6 (C-13').

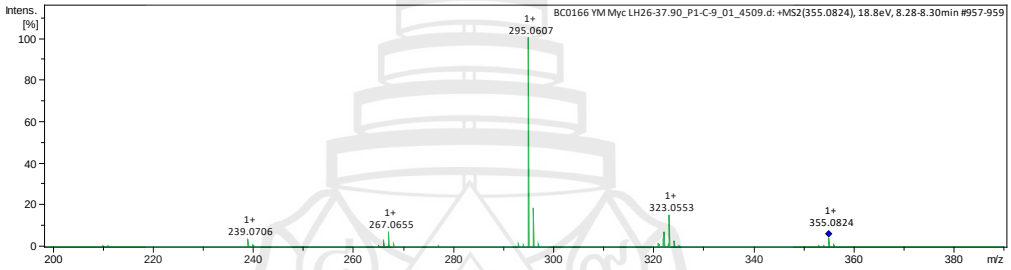


Figure B24 HR-ESI(+)-MS/MS of methyl atromentate (**6**) (precursor ion 355.0824, 18.8 eV)

^{1}H NMR (700 MHz, acetone) δ ppm 3.79 (s, 3 H) 6.67 (d, *J*=8.8 Hz, 2 H) 6.83 (d, *J*=8.8 Hz, 2 H) 7.55 (d, *J*=8.8 Hz, 2 H) 8.28 (d, *J*=8.6 Hz, 2 H)

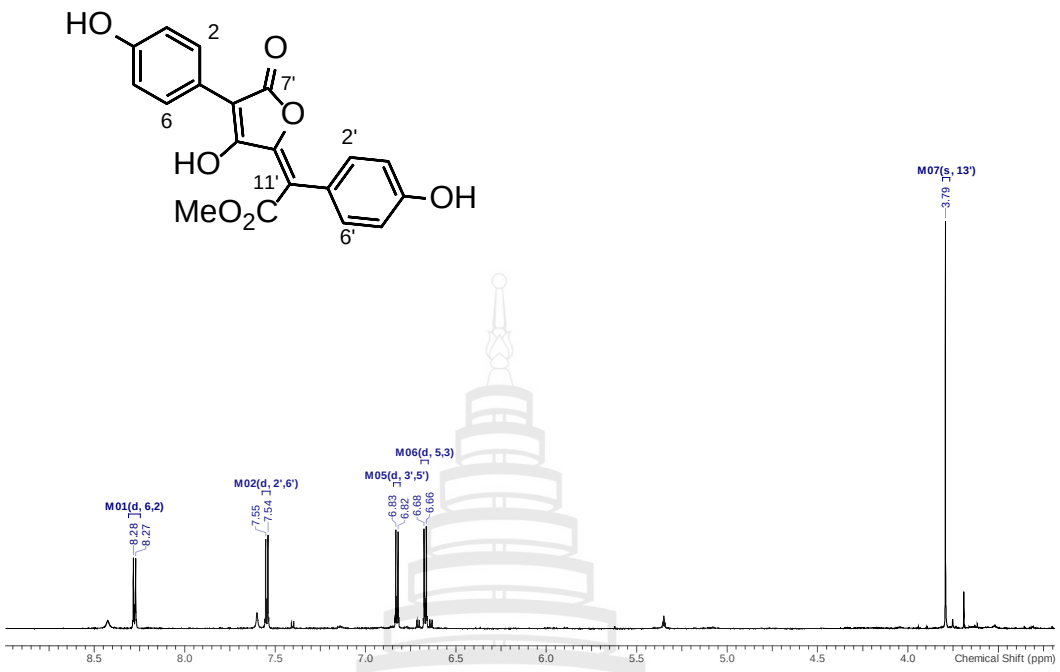


Figure B25 ^{1}H NMR (700 MHz, $(CD_3)_2CO$, 300 K) of methyl atromentate (6)

Methyl isoxerocomate (7): R_f (TLC) = 0.45 (dichloromethane : methanol, 6 : 4, 6/6); UV/Vis (MeOH): λ_{max} (log ε) = 259 (4.32), 344 (4.15), 389 (4.16) nm; analytical HPLC (t_R) = 7.35 min; HR-ESI(+)-MS: *m*/*z* (%) = 763.1244 (0.7) $[2M+Na]^+$ ($C_{38}H_{28}NaO_{16}$ cald. for 763.1270), 393.0581 (30) $[M+Na]^+$ ($C_{19}H_{14}NaO_8$), 371.0761 (100) $[M+H]^+$ ($C_{19}H_{15}O_8$ cald. for 371.0761); HR-ESI(+)-MS/MS (precursor ion *m*/*z* 371.0766): *m*/*z* (%) = 339.0499 (15) $[M+H–CH_4O]^+$ ($C_{18}H_{11}O_7$ cald. for 339.0499), 311.055473 (100) $[M+H–C_2H_4O_2]^+$ ($C_{17}H_{11}O_6$ cald. for 311.0550), 299.0556 (4) $[M+H–C_2H_4O_2–CO]^+$, 283.0602 (10) $[M+H–C_2H_4O_2–CO–CO]^+$ ($C_{15}H_{11}O_5$ cald. for 283.0601); ^{1}H NMR (500 MHz, $(CD_3)_2CO$, 300 K): δ = 8.00 (2 H, d, *J* = 9.0 Hz, H-6/H-2), 6.92 (2 H, d, *J* = 9.0 Hz, H-5/H-3), 6.90 (1 H, d, *J* = 2.0 Hz, H-2'), 6.87 (1 H, d, *J* = 8.2 Hz, H-2'), 6.75 (1 H, dd, *J* = 8.2, 2.0 Hz, H-6'), 3.90 (3 H, s, H-13'); ^{13}C NMR (126 MHz, $(CD_3)_2CO$, 300 K): δ = 173.1 (C-13'), 167.0, 159.7, 158.5 (C-4), 154.6, 146.5 (C-4'), 145.4 (C-3'), 130.2 (C-2/C-6), 125.1 (C-1'), 123.2 (C-6'), 121.8 (C-1), 118.5 (C-2'), 116.3 (C-3/C-5), 115.7 (C-5'), 105.3 (C-8'), 54.8 (C-13').

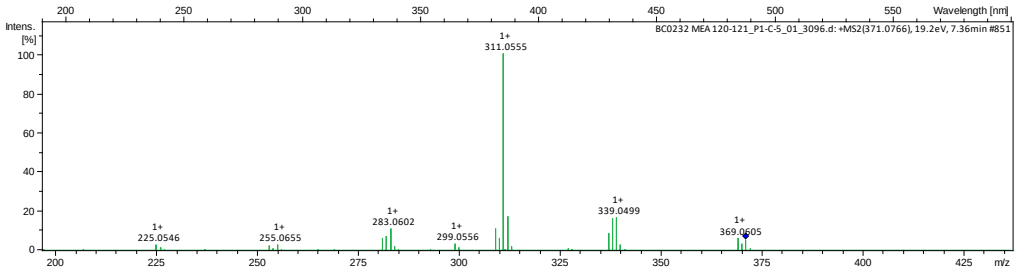


Figure B26 HR-ESI(+)-MS/MS of methyl isoxerocomate (**7**) (precursor ion *m/z* 371.0766, 19.2 eV)

^{1}H NMR (500 MHz, acetone) δ ppm 3.90 (s, 3 H) 6.75 (dd, *J*=8.2, 2.2 Hz, 1 H) 6.87 (d, *J*=8.2 Hz, 1 H) 6.90 (d, *J*=2.0 Hz, 1 H) 6.92 (d, *J*=9.1 Hz, 2 H) 8.00 (d, *J*=8.9 Hz, 2 H)

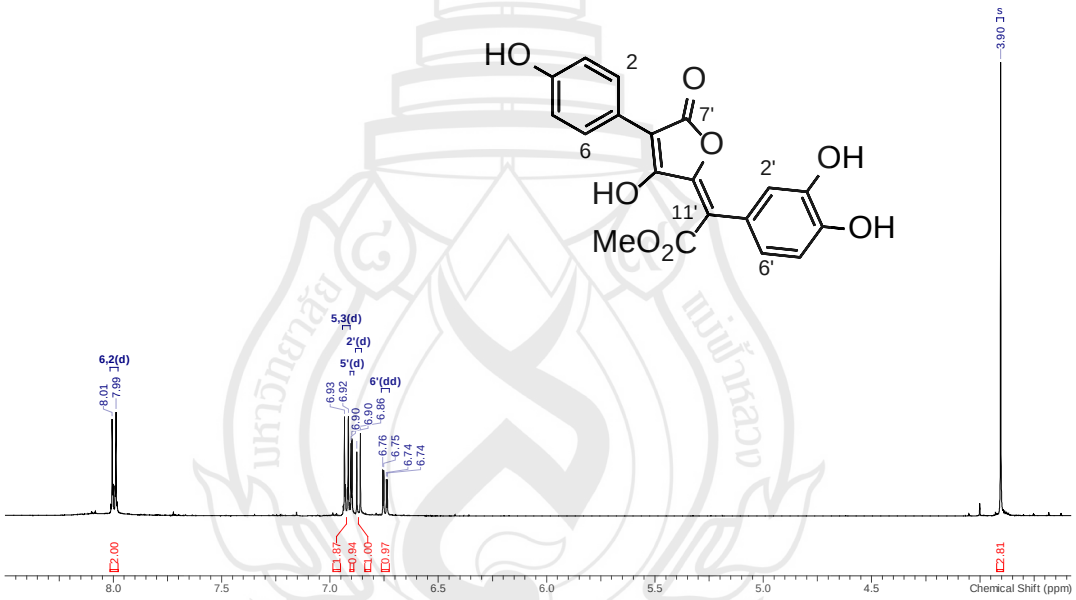


Figure B27 ^{1}H NMR (500 MHz, $(CD_3)_2CO$, 300 K) of methyl isoxerocomate (7)

Methyl variegatate (8): R_f (TLC) = 0.25 (dichloromethane-methanol, 6 : 4); UV/Vis (MeOH): λ_{max} (log ε) = 257 (3.80), 326 (3.69), 387 (3.48) nm; analytical HPLC (t_R) = 6.42 min; HR-ESI(+)-MS: *m/z* (%) = 795.1166 (4) $[2M+Na]^+$ ($C_{38}H_{28}NaO_{18}$ cald. for 795.1168), 773.1349 (8) $[2M+H]^+$ ($C_{38}H_{29}O_{18}$ cald. for 773.1348), 409.1527 (13) $[M+Na]^+$ ($C_{19}H_{14}NaO_9$ cald. for 409.0530), 387.0708 (100) $[M+H]^+$ ($C_{19}H_{15}O_9$ cald. for 387.0711); HR-ESI(+)-MS/MS (precursor ion *m/z* 387.0722): *m/z* (%) = 355.0453 (16) $[M+H–CH_4O]^+$ ($C_{18}H_{11}O_8$ cald. for 355.0448), 327.0508 (100) $[M+H–C_2H_4O_2]^+$ ($C_{17}H_{11}O_7$ cald. for 327.0499), 299.0555 (20) $[M+H–C_2H_4O_2–CO]^+$ ($C_{19}H_{11}O_6$ cald. for

299.0550), 271.0606 (4) $[M+H-C_2H_4O_2-CO-CO]^+$; ^1H NMR (500 MHz, CD_3CN, 300K): δ = 7.64 (1 H, d, *J* = 2.1 Hz, H-2), 7.53 (1 H, dd, *J* = 8.5, 2.1 Hz, H-6), 6.89 (1 H, d, *J* = 8.5 Hz, H-5), 6.87 (1 H, d, *J* = 8.1 Hz, H-5'), 6.80 (1 H, d, *J* = 2.0 Hz, H-2'), 6.70 (1 H, d, *J*=8.2; 2.1 Hz, H-6'), 3.85 (3 H, s, H-13'); ^{13}C NMR (126 MHz, CD_3CN, 300 K): δ = 173.1 (C-13'), 167.4, 160.1, 155.0, 146.1 (C-4), 146.0 (C-4'), 145.4 (C-3), 145.1 (C-3'), 125.6 (C-6), 123.5 (C-6'), 122.5 (C-1), 118.4 (C-2'), 116.7 (C-11'), 116.3 (C-5), 115.8 (C-5'), 115.6 (C-2), 105.5 (C-8'), 55.2 (C-13').

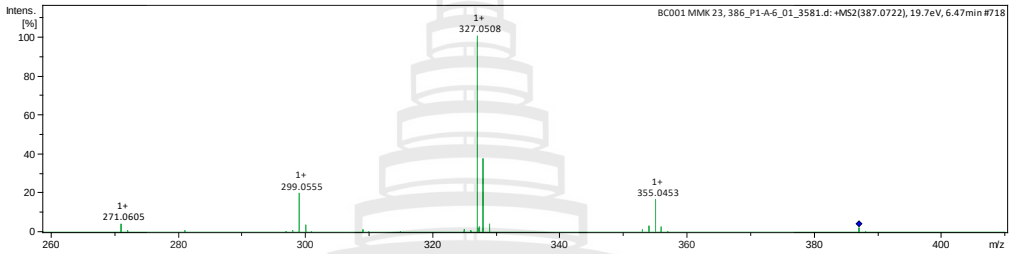


Figure B28 HR-ESI(+)-MS/MS of methyl variegatate (**8**) (precursor ion 387.0722, 19.7 eV)

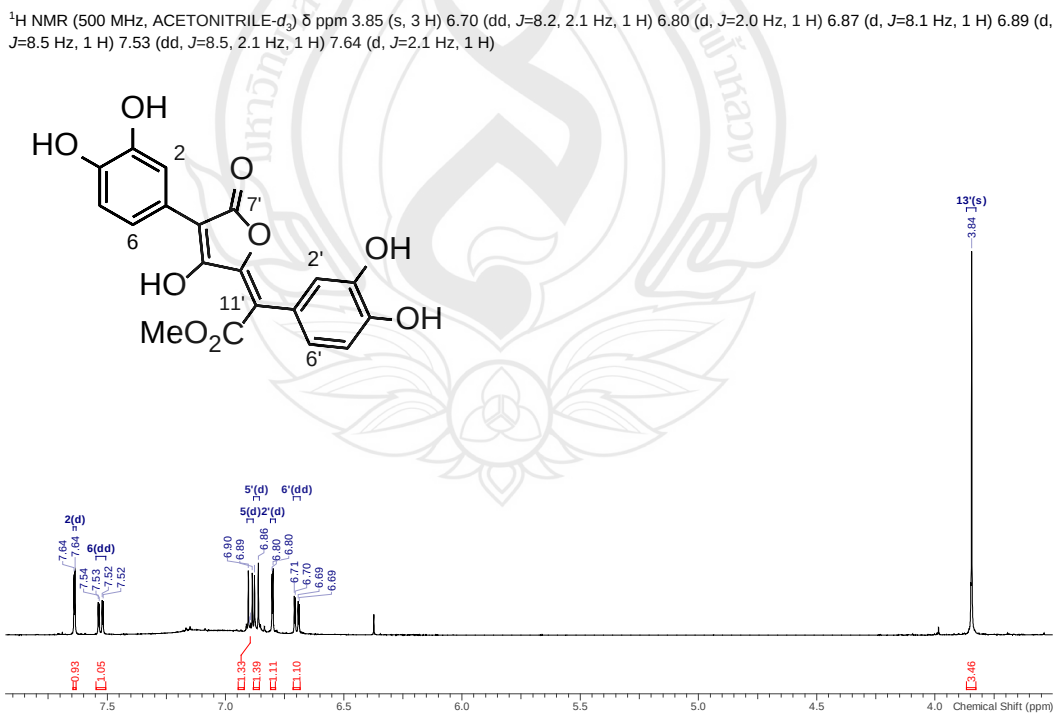


Figure B29 ^1H NMR (500 MHz, CD_3CN, 300 K) of methyl variegatate (8)

Variegatorubin (9): UV/Vis$_{qual}$ (H_2O + 0.1% FA : ACN + 0.1% FA, 62 : 38): λ_{max} = 354, 520 nm; analytical HPLC (t_R) = 7.70 min; HR-ESI(+)-MS: *m/z* (%) = 393.0199 (1) $[M+Na]^+$ ($C_{18}H_{10}NaO_9$ cald. for 393.0217), 371.0389 (100) $[M+H]^+$ ($C_{18}H_{11}O_9$ cald. for 371.0398); HR-ESI(+)-MS/MS (precursor ion *m/z* 371.0399, 25 eV): *m/z* (%) = 281.0444 (32) ($C_{16}H_9O_5$ cald. for 281.0445), 193.0123 (100) $[M+H–C_9H_6O_4]^+$ ($C_9H_5O_5$ cald. for 193.0132), 177.0173 (15) $[M+H–C_9H_6O_5]^+$ ($C_9H_5O_4$ cald. for 177.0182).

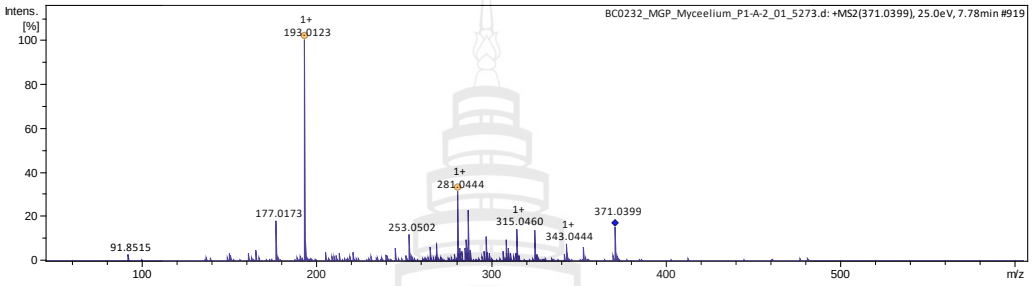


Figure B30 HR-ESI(+)-MS/MS of variegatorubin (**9**) (precursor ion 371.0399, 25.0 eV)

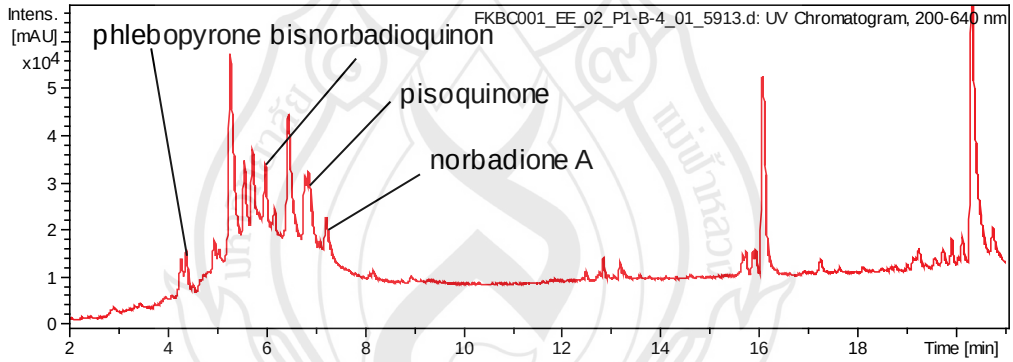
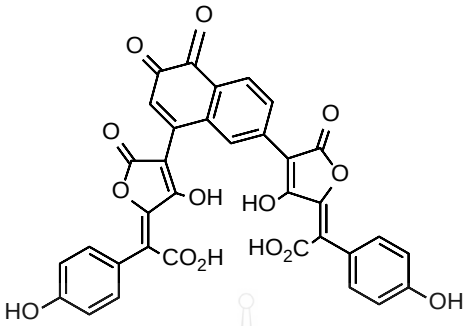
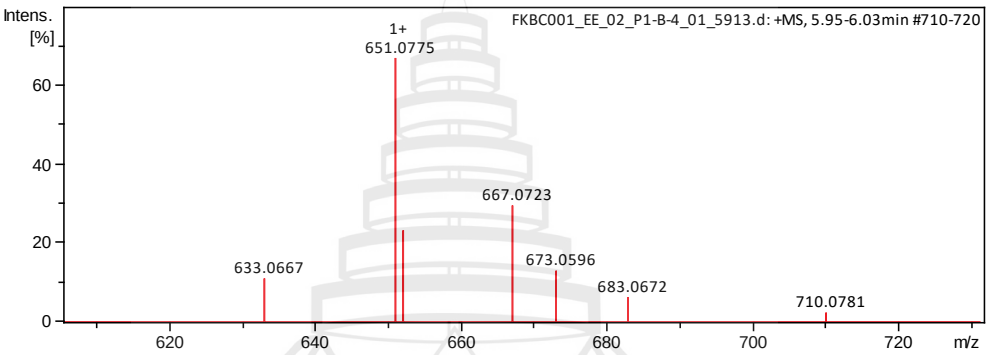


Figure B31 Chromatogram of the crude extract from dried basidiomata of *P. portentosus*

Dried fruiting bodies (1.3 g) of *P. portentosus* (MFLUCC-T19-0088) were homogenized and extracted with acetone (3 x 50 mL) and small amounts of acid (2 ml HCl, 1 N). The resulting residue was evaporated to dryness, redissolved with H_2O (50 mL) and extracted with ethyl acetate (2 x 50 mL). The yellow organic layers were combined, dried over Na_2SO_4 and evaporated to dryness. The resulting crude extract (37.8 mg) was redissolved in acetone (2.0 mL) and subjected to HR-LC-ESI(+)-MS analysis using gradient A.



bisnorbadiochinone A



Meas. *m/z*	Ion Formula	*m/z*	err [ppm]
651.077468	$C_{34}H_{19}O_{14}$	651.076932	-0.8
673.059609	$C_{34}H_{18}NaO_{14}$	673.058876	-1.1

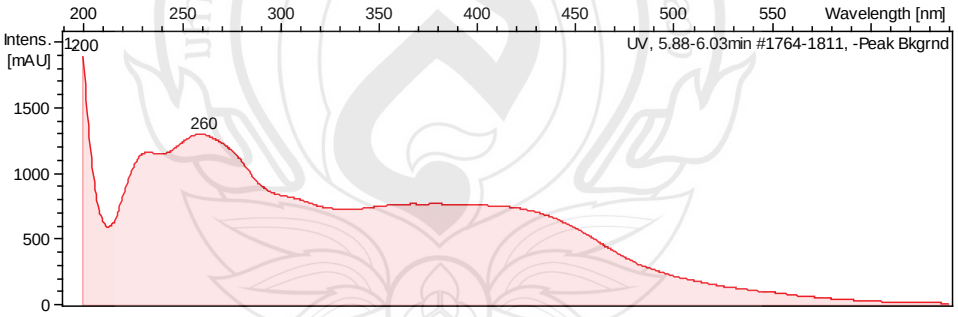
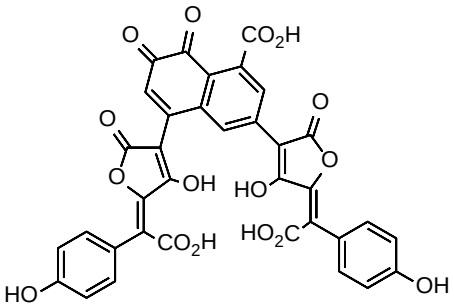
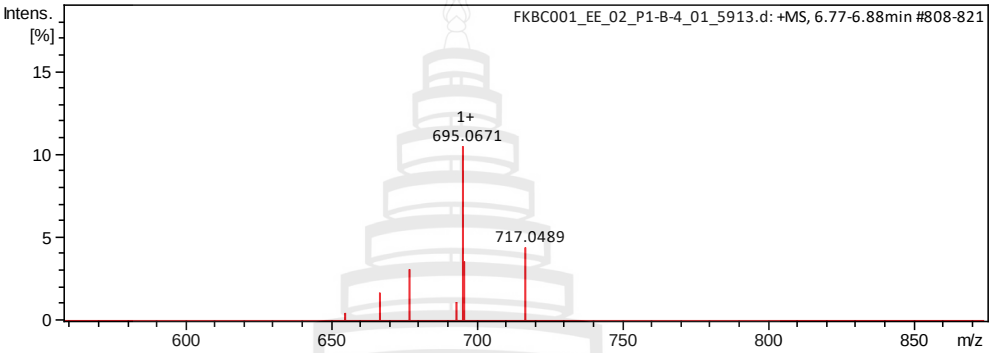


Figure B32 HR-LC-ESI(+)-MS and UV/Vis spectra pointing to the presence of bisnorbadiochinone A from *P. portentosus*



pisoquinone



Meas. *m/z*	Ion Formula	*m/z*	err [ppm]
695.067094	$C_{35}H_{19}O_{16}$	695.066761	-0.5
717.048857	$C_{35}H_{18}NaO_{16}$	717.048705	-0.2

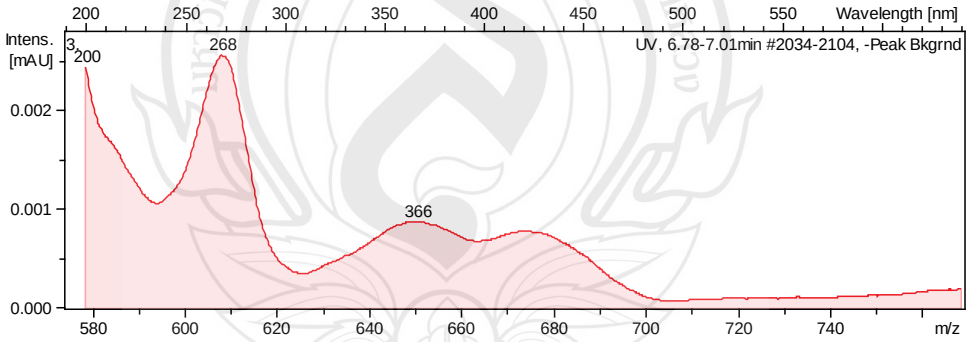
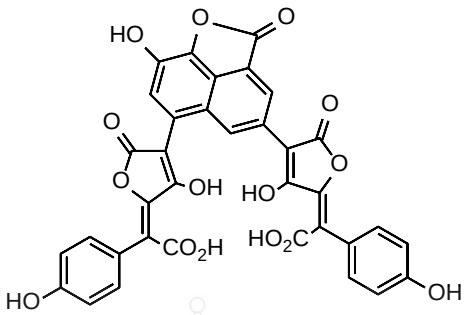
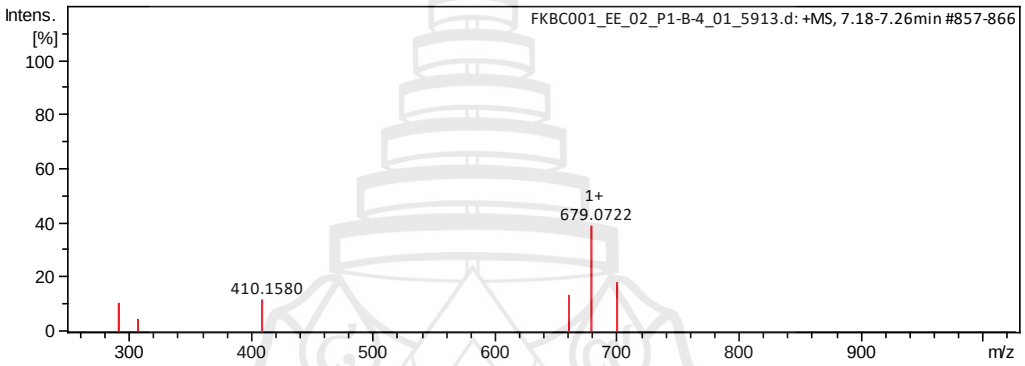


Figure B33 HR-LC-ESI(+)-MS and UV/Vis spectra pointing to the presence of pisoquinone from *P. portentosus*



norbadion A



Meas. *m/z*	Ion Formula	*m/z*	err [ppm]
679.072195	$C_{35}H_{19}O_{15}$	679.071846	-0.5
701.054260	$C_{35}H_{18}NaO_{15}$	701.053791	-0.7

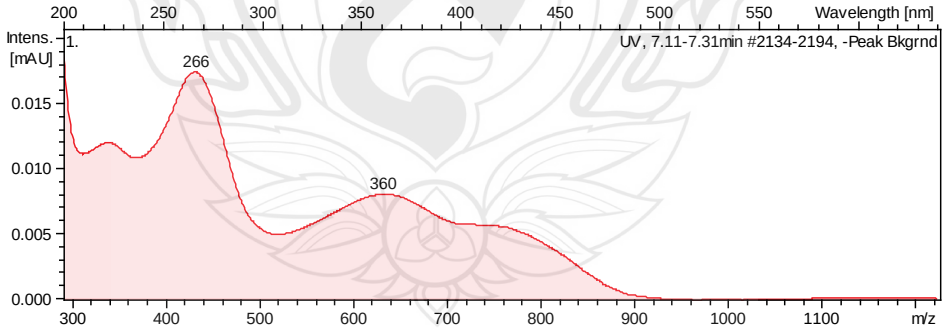


Figure B34 HR-LC-ESI(+)-MS and UV/Vis spectra pointing to the presence of norbadione A from *P. portentosus*

Dried fruiting bodies (0.3 g) of *P. spongiosus* (MFLUCC-T19-0091) were homogenized and extracted with acetone (3 x 20 mL) and small amounts of acid (1 mL HCl, 1 N). The resulting residue was evaporated to dryness, redissolved in H_2O (20 mL) and extracted with ethyl acetate (2 x 20 mL). The yellow organic layers were combined, dried over Na_2SO_4 and evaporated to dryness. The resulting crude extract (10.8 mg) was redissolved in acetone (0.5 mL) and subjected to HR-LC-ESI(+)-MS analysis using gradient A.

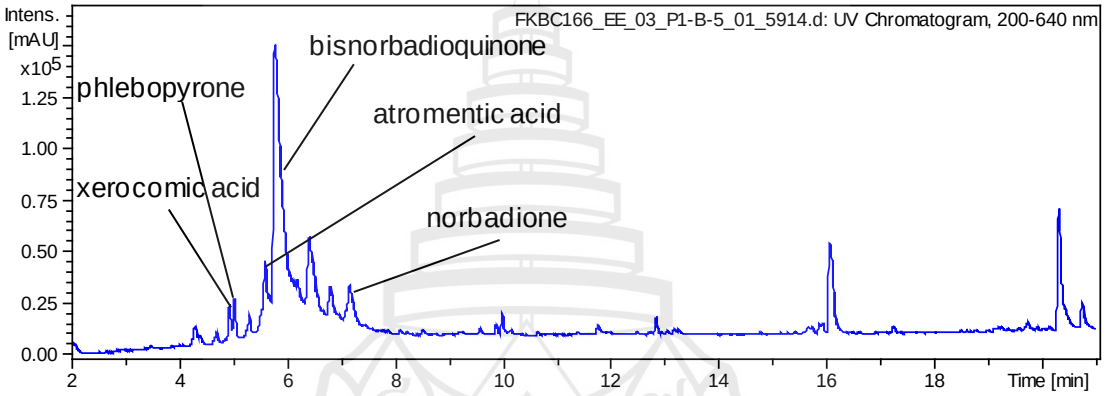
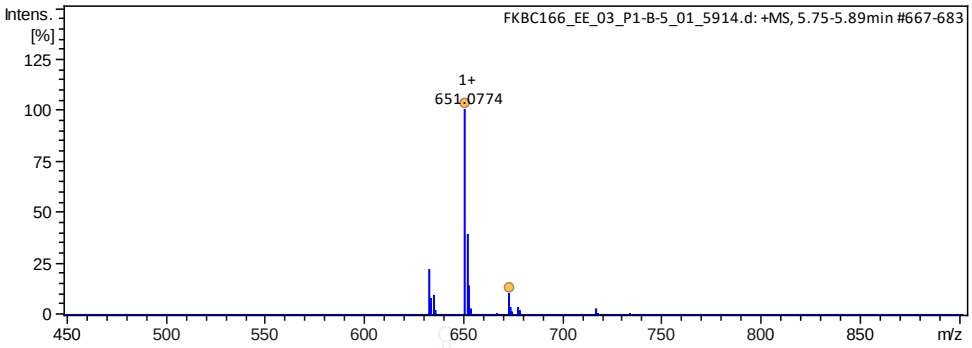


Figure B35 Chromatogram of the crude extract from dried basidiomata of *P. spongiosus*



Meas. *m/z*	Ion Formula	*m/z*	err [ppm]
651.077370	$C_{34}H_{19}O_{14}$	651.076932	-0.7
673.059536	$C_{34}H_{18}NaO_{14}$	673.058876	-1.0

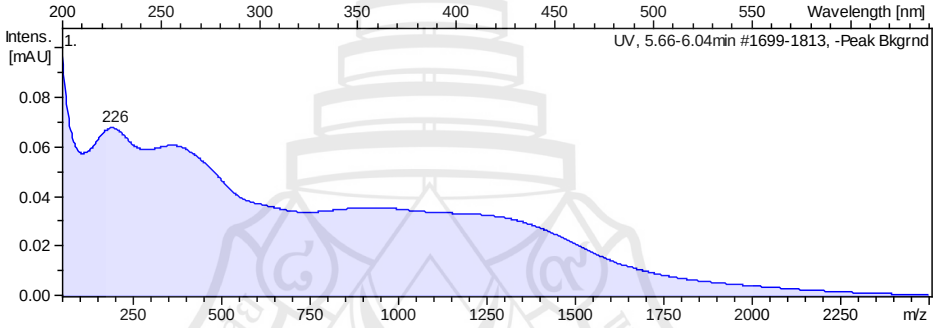
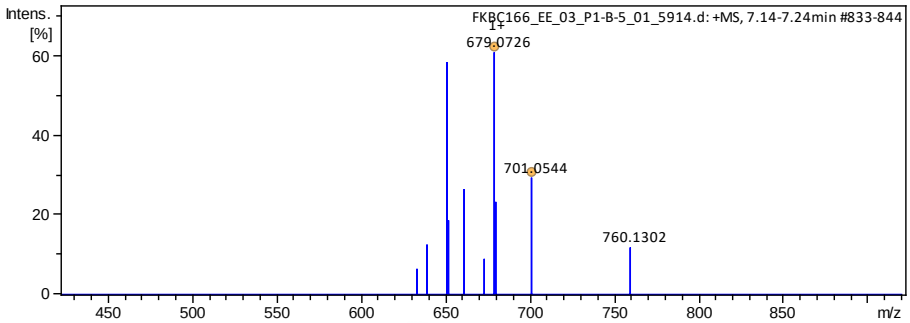


Figure B36 HR-LC-ESI(+)-MS and UV/Vis spectra pointing to the presence of bisnorbadiochinone A from *P. spongiosus*



Meas. *m/z*	Ion Formula	*m/z*	err [ppm]
679.072616	$C_{35}H_{19}O_{15}$	679.071846	-1.1
701.054434	$C_{35}H_{18}NaO_{15}$	701.05379	-0.9

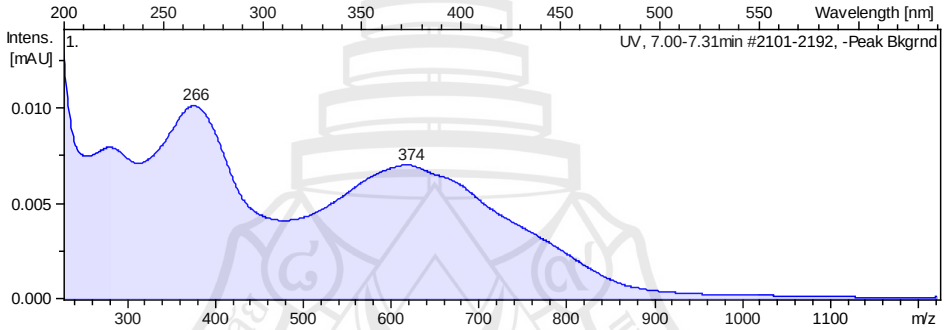
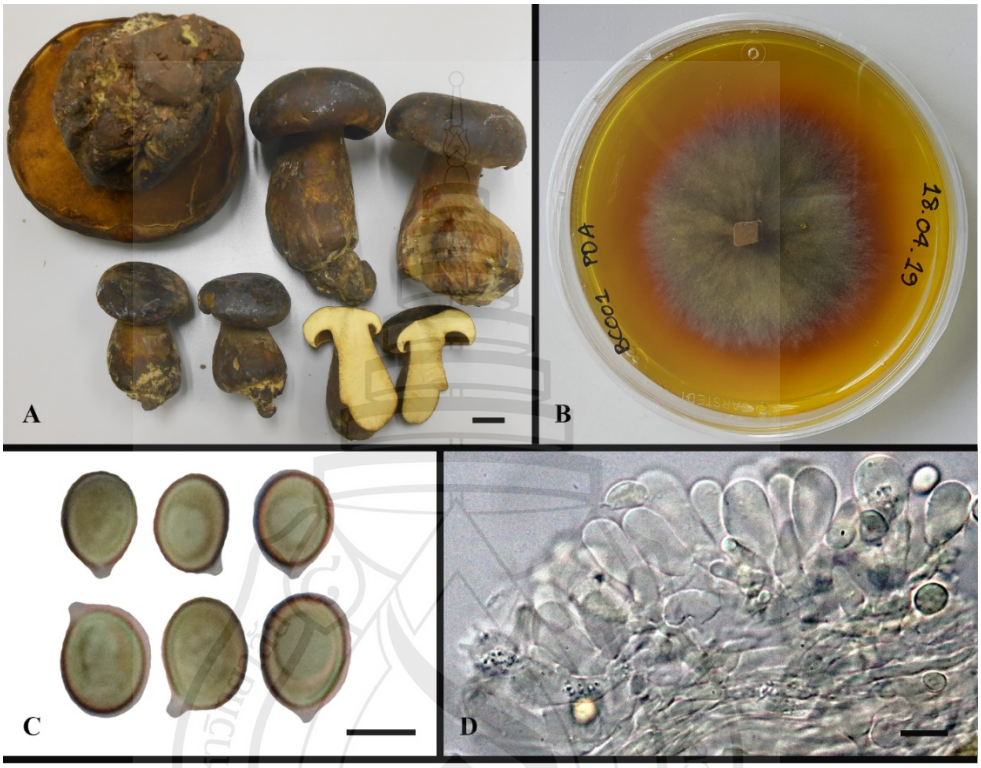


Figure B37 HR-LC-ESI(+)-MS and UV/Vis spectra pointing to the presence of norbadione A from *P. spongiosus*

APPENDIX C

IDENTIFICATION OF *PHLEBOPUS*



Note A Basidiomata. B Culture mycelium on PDA (MFLUCC-T19-0088). C Basidiospores in 5% KOH. D Basidia and subhymenium in 5% KOH. Scale bar: A = 2 cm, C = 5 µm, D = 10 µm.

Figure C1 Morphological analysis of *Phlebopus portentosus* (Berk. And Broome) Boedijn

Basidiomata medium to large-sized. *Pileus* 50–160 mm in diameter, hemispherical when young, plano-convex to convex when mature; surface dry, smooth, subtomentose, olive brown to raw umber (4D8 to 5F8), becoming darker where handled; margin involute when young, then becoming inflexed when aged; context 25–43 mm thick at the center of pileus, soft, light yellow (3A4), slightly bluing when exposed. *Hymenophore* poroid, depressed around the stipe; tubes 3–10 mm long, at first

stuffed with butter yellow to maize (4A5-6) ; pores small, angular to subcircular, more elongated around the stipe, oak brown (5D6). *Stipe* 79–140 × 30–50 mm, central, subclavate to clavate, somewhat enlarged at the base, solid; surface dry, subtomentose, honey yellow (4D6) to dark brown (6F7), becoming darker where handled; context light yellow (3A4), slightly bluing when exposed. *Basal mycelium* sulphur yellow (1A5). *Spore print* not observed. *Odour* like muddy or earthy. *Spores* yellowish brown, oval to subglobose, with large central guttule, 7.85–9.52 × 6.05–6.96 µm. *Basidia* club-shaped, 4-spored. *Pleurocystidia* absent.



Note A Basidiomata. B Culture mycelium on MEA. (MFLUCC-T19-0091). C Section of the hymenophore in dried specimens showing the sponge-like tissues enclosing and stuffing the immature pores (arrow). Scale bar: A = 1 cm, C = 0.5 mm.

Figure C2 Morphological analysis of *Phlebopus spongiosus* Pham & Har. Takah

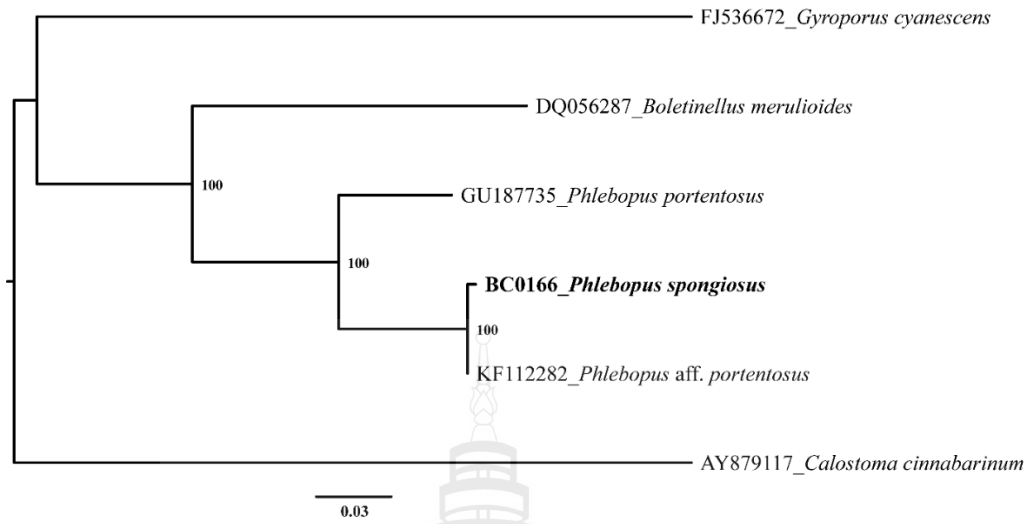
Basidiomata (observed from young basidiom) small sized. *Pileus* 27 mm in diameter, hemispherical to convex; surface dry, subtomentose; brown to olive brown

(4D8), tinged with olive (3F4-5) when injured; margin; inflexed; context 9 mm thick at the center of pileus, soft, pale yellow to light yellow (1A3-4), no colour change when cut or bruised. *Hymenophore* poroid, depressed around the stipe; tubes ≤ 2 mm, vertically arranged, greenish yellow (1B8), sponge-like tissues with hollow spaces in the tubes of dried specimen; pores small, angular to subcircular, more elongated around the stipe, thin membrane of dissepiments enclosing the pores in dried specimen, olive brown (4E8). *Stipe* 53 × 13 mm, central, subclavate or somewhat enlarged at the base, solid; surface dry, subtomentose to tomentose, olive to olive brown (3F5 to 4F5), golden brown (5D7) at base, becoming darker where handled; context pale yellow to light yellow (1A3-4)), no colour change when cut or bruised. *Basal mycelium* light yellow (3A4). *Spore print* not observed. *Odour* like muddy or earthy.

According to these features, the mushrooms BC001 and BC0166 were identified as a member of the genus *Phlebopus*.

These findings were corroborated by molecular data (The DNA sequence data and GenBank accession number in Table S1.): A nucleotide BLAST search[1] of BC001 ATP6 sequence indeed revealed that all the most homologous sequence data belonged to members of the genus *Phlebopus*. The BLAST search, however, did not provide an exact match. The ATP6 sequence data of *Phlebopus portentosus* BC001 showed 99% homology to *Phlebopus portentosus* MK571437 and 96% homology to *Phlebopus portentosus* AF114453. The latter sequence was obtained from a specimen (HD Thiers 42534) collected in Australia, which was likely misidentified. The comparison of the morphology of the specimen BC001(Fig. S38) with that reported in the literature[2] also suggested that specimen BC001 belongs in *Phlebopus portentosus*.

For BC0166, the LSU sequences was 100% identical to the holotype of *Phlebopus spongiosus* CBM FB-38014 (NG_060059). The sponge-like tissues with hollow spaces in the tubes and thin membrane of dissepiments enclosing the pores in dried specimen (Fig. S39, C) also resemble to the previously descried characters of *P. spongiosus*.[3] The phylogenetic analysis of elongation factor 1-alpha gene also reveal that BC0166 is distinct from *P. portentosus*.



Note Bootstrap frequencies are shown above supported branches.

Figure C40 Maximum likelihood phylogenetic tree inferred from the elongation factor 1-alpha gene (*tef1*), including *Phlebopus spongiosus* and the related species

Table C1 List of specimens and reference sequences used for molecular identification

Species	Strain no.	Origin	GenBank accession			References
			LSU	ATP6	EF1-α	
Boletinellus merulioides	MB 02-199	---	---	---	DQ056287	Matheny et al. (2007)[4]
Calostoma cinnabarinum	AW 136	---	---	---	AY879117	Matheny et al. (2005)[5]
Gyroporus cyanescens	MB 05-001	---	---	---	FJ536672	Wilson et al. (2012)[6]
Phlebopus aff. *portentosus*	HKAS 52855	---	---	---	KF112282	Wu et al. (2014)[7]
P. portentosus	Php1	---	---	---	GU187735	Binder et al. (2010)[8]
P. portentosus	BC001	Thailand	---	MT755373	---	This study
P. spongiosus (T)	CBM FB-38014	Viet Nam	NG_060059	---	---	Pham et al. (2012)[3]

Table C1 (continued)

Species	Strain no.	Origin	GenBank accession			References
			LSU	ATP6	EF1-α	
P. spongiosus	BC0166	Thailand	MT757956	---	MT769252	This study

Note Type strains are indicated by (T)

Table C2 GenBank BLAST search results of *Phlebopus* species from this study against GenBank database

Species	Voucher, GB accession no.	Most similar sequences in GenBank	Species name	Voucher	Origin	Reference
Phlebopus portentosus	BC001, MT755373	MK571437, I = 99.85%, QC = 100%	*Phlebopus portentosus*	---	---	Jiang et al. (2017)[9]
		AF114453, I = 96.70%, QC = 92%	*P. portentosus*	HDT-42534	---	Kretzer and Thomas (1999)[10]
P. spongiosus	BC0166, MT757956	AF114453, I = 100%, QC = 99%	*P. spongiosus*	CBM FB-38014	Viet Nam	Pham et al. (2012)[3]

Note I = Identity and QC = Query Cover

Table C3 Log-likelihhod of the best tree and values of the parameters of the GTR+G model of sequence evolution from RAxML analysis of EF1-α sequences

Alignment	**EF1-α**
ln(L)	-3692.764206
α-value	0.259310
Tree length	0.895735
Substitution rates:	
A ↔ C	1.072052
A ↔ G	2.963902
A ↔ T	1.547267
C ↔ G	0.587532
C ↔ T	7.440752
G ↔ T	1.000000
Base frequencies:	
$f\pi$(A)	0.232042
$f\pi$(C)	0.274419
$f\pi$(G)	0.250616
$f\pi$(T)	0.242922

References

(1) http://blast.ncbi.nlm.nih.gov/Blast.cgi

(2) S38 Boedijn KB (1951) Some mycological notes. Sydowia 5:211–229

(3) S39 Pham NDH, Takahashi H, Fukiharu T, Shimizu K, Le BD, Suzuki A (2012) *Phlebopus spongiosus* sp. nov. (Boletales, Boletinellaceae) with a sponge-like tissue. Mycotaxon 119:27–34

(4) Matheny PB, Wang Z, Binder M, Curtis JM, Lim YW, Nilsson RH, Hughes KW, Hofstetter V, Ammirati JF, Schoch CL, Langer E, Langer G, McLaughlin DJ, Wilson AW, Frøslev T, Ge ZW, Kerrigan RW, Slot JC, Yang ZL, Baroni TJ, Fischer M, Hosaka K, Matsuura K, Seidl MT, Vauras J, Hibbett DS (2007) Contributions of rpb2 and tef1 to the phylogeny of mushrooms and allies (Basidiomycota, Fungi). Mol Phylogenet Evol 43:430–451. https://doi.org/10.1016/j.ympev.2006.08.024

(5) Wilson AW, Binder M, Hibbett DS (2011) Effects of gasteroid fruiting body morphology on diversification rates in three independent clades of fungi estimated using binary state speciation and extinction analysis. Evolution 65:1305–22

(6) Wilson AW, Binder M, Hibbett DS (2012) Diversity and evolution of ectomycorrhizal host associations in the Sclerodermatineae (Boletales, Basidiomycota). New Phytol 194:1079–1095. https://doi.org/10.1111/j.1469-8137.2012.04109.x

(7) Wu G, Feng B, Xu J, Zhu XT, Li YC, Zeng NK, Hosen MI, Yang ZL (2014) Molecular phylogenetic analyses redefine seven major clades and reveal 22 new generic clades in the fungal family Boletaceae. Fungal Divers 69:93–115. https://doi.org/10.1007/s13225-014-0283-8

(8) Binder M, Larsson KH, Matheny PB, Hibbett DS (2010) Amylocorticiales ord. nov. and Jaapiales ord. nov.: early diverging clades of agaricomycetidae dominated by corticioid forms. Mycologia 102:865–880. https://doi.org/10.3852/09-288

(9) Jiang L, Yang D, Cao Y, Wang P, Zhang Y, Zhang KQ, Xu J, Zhang Y (2017) The complete mitochondrial genome of the edible Basidiomycete mushroom *Phlebopus Portentosus*. Mitochondrial DNA Part B 2:696–697. https://doi.org/10.1080/23802359.2017.1383195

(10) Kretzer AM, Bruns TD (1999) Use of atp6 in fungal phylogenetics: an example from the Boletales. Mol Phylogenet Evol 13:483–492. https://doi.org/10.1006/mpev.1999.0680

APPENDIX D

GROWTH CONDITION AND YIELD FOR SMALL SCALE LIQUID CULTIVATION OF *PHLEBOPUS*

Table D1 *Phlebopus portentosus*

Media	Times (Days)	Mycelium (mg)	Supernatant (mg)
BAF	30	96.7	47.6
MGP	30	151.9	40.7
MMK	40	93.6	9.5
YM 5.5	35	3.5	2.3
ZM ½	Not grow	-	-

Table D2 *Phlebopus spongiosus*

Media	Times (Days)	Mycelium (mg)	Supernatant (mg)
BAF	30	133.4	83.5
MGP	30	140.8	146.3
MMK	40	39.9	16.9
YM 5.5	23	13.9	18.0
ZM ½	Not grow	-	-

APPENDIX E

ANTIMICROBIAL ACTIVITY AND CYTOTOXICITY ASSAYS OF *PHLEBOPUS*

Table E1 Antimicrobial activity of compounds 1–8

Tested organisms	**Strain No.**	**Minimum inhibitory concentration (MIC) [µg/mL]**								
		Compounds								**Positive control* [µg/mL]**
		1	**2**	**3**	**4**	**5**	**6**	**7**	**8**	
Bacteria										
Bacillus subtilis	DSM 10	-	-	-	-	nt	-	-	-	8.3[a]
Chromobacterium violaceum	DSM 30191	-	-	-	-	nt	nt	-	-	0.8[a]
Escherichia coli	DSM 1116	-	-	-	-	nt	-	-	-	6.7[a]
Micrococcus luteus	DSM 1790	-	-	-	-	nt	-	-	33.3	0.8[a]
Mycobacterium smegmatis	ATCC 700084	-	-	-	-	nt	nt	-	-	1.7[b]
Pseudomonas aeruginosa	PA14	-	-	-	-	nt	-	-	-	0.4[c]
Staphylococcus aureus	DSM 346	66.7	-	-	-	nt	-	66.7	66.7	0.8[a]

Table E1 (continued)

Fungal										
Mucor hiemalis	DSM 2656	-	-	-	-	nt	-	66.7	66.7	33.3[d]
Pichia anomala	DSM 6766	-	-	-	-	nt	-	66.7	66.7	16.7[d]
Rhodoturula glutinis	DSM 10134	-	-	-	-	nt	nt	-	-	8.3[d]
Yeast										
Candida albicans	DSM 1665	-	-	-	-	nt	-	-	-	66.7[d]
Schizosaccharomyces pombe	DSM 70572	-	-	-	-	nt	-	66.7	66.7	8.3[d]

Note * Positive controls: [a] oxytetracycline hydrochloride, [b] kanamycin, [c] gentamicin, [d] nystatin. Negative control = MeOH. (-) = no inhibition. (nt)=not tested.

Table E2 Cytotoxic activity of compounds 1–8

Cell Lines	**(IC_{50}) µM Compounds [µg/mL]**								**Positive control***
	1	**2**	**3**	**4**	**5**	**6**	**7**	**8**	
Epidermoid carcinoma A431	nt	nt	nt	9.0	nt	nt	nt	16.8	0.000028
Adenocarcinomic human alveolar basal epithelial A549	nt	nt	nt	8.7	nt	nt	nt	16.0	0.000019
HeLa KB3.1	18.5	-	-	17.4	nt	-	-	17.6	0.000024
Fibroblasts L929	-	-	-	16.5	nt	-	-	17.8	0.00061
MCF-7	46.4	nt	nt	3.9	nt	nt	nt	6.5	0.000025
Human prostate cancer PC-3	nt	nt	nt	-	nt	nt	nt	-	0.000028
Ovarian cancer SKOV-3	nt	nt	nt	25.6	nt	nt	nt	49.2	0.00009

Note * Positive control: Epothilone B. Negative control = MeOH. Results were expressed as IC_{50}: half maximal inhibitory concentration (µM). (-) = no inhibition. (nt) = not tested.

Table E3 Biofilm inhibition and nematicidal activities of compounds 3 and 4

Tested organisms	**Strain No.**	**Biofilm inhibition %**								
		Compounds								**Positive control* %**
		1	**2**	**3**	**4**	**5**	**6**	**7**	**8**	
Bacteria										
Staphylococcus aureus	DSM 1104	nt	nt	-	-	nt	nt	nt	nt	88% (250 μg/mL) M
Nematode		**Nematode assay LD_{50} [μg/mL]**								
Caenorhabditis elegans	AB1	nt	nt	100	100	nt	nt	nt	nt	(1.0 μg/mL) I

Note * Positive control: M = microporenic acid A,[22] I = ivermectin. Negative control = MeOH. (-) = no inhibition. (nt) = not tested.

APPENDIX F

LISTS OF CULTURES AND HERBARIUM

Table F1 Lists of herbarium

MFLU	Original Code	Species Name	Collector	Collection Site	Sequences
14-0834	DSK-32B/BC067	*Agaricus megalosporus*	Boontiya Chuankid	Doi Sa Ket, Chiang Mai, Thailand	/
14-0835	DSK-33B	*Agrocybe* sp.	Boontiya Chuankid	Doi Sa Ket, Chiang Mai, Thailand	-
14-0836	MFU-8Ak	*Agrocybe* sp.	Kritsana Jatuwong	Mae Fah Luang University, Ching Rai, Thailand	-
14-0837	MFU-9S	*Agaricus* sp.	Samantha Chandranath Karunarathna	Mae Fah Luang University, Ching Rai, Thailand	-
14-0838	MRC-20	*Chlorophyllum* sp.	Boontiya Chuankid	MRC, Chiang Mai, Thailand	/

Table F1 (continued)

MFLU	Original Code	Species Name	Collector	Collection Site	Sequences
14-0839	MRC-29/BC097	*Agaricus sp.*	Boontiya Chuankid	MRC, Chiang Mai, Thailand	/
14-0840	DSK-2B/BC069	*Agaricus* sp.	Boontiya Chuankid	Doi Sa Ket, Chiang Mai, Thailand	/
14-0841	DSK-3B/BC070	*Agaricus* sp.	Boontiya Chuankid	Doi Sa Ket, Chiang Mai, Thailand	/
14-0842	DSK-5B/BC071	*Micropsalliota furfuracea*	Boontiya Chuankid	Doi Sa Ket, Chiang Mai, Thailand	/
14-0843	DSK-6B/BC072	*Micropsalliota globocystis*	Boontiya Chuankid	Doi Sa Ket, Chiang Mai, Thailand	/
14-0844	DSK-7B	*Ganoderma* sp.	Boontiya Chuankid	Doi Sa Ket, Chiang Mai, Thailand	-
14-0845	DSK-8B/BC073	*Boletus* sp.	Boontiya Chuankid	Doi Sa Ket, Chiang Mai, Thailand	/
14-0846	DSK-9B/BC074	*Phylloporus* sp.	Boontiya Chuankid	Doi Sa Ket, Chiang Mai, Thailand	/
14-0847	DSK-10B/BC075	*Boletellus emodensis*	Boontiya Chuankid	Doi Sa Ket, Chiang Mai, Thailand	/

Table F1 (continued)

MFLU	Original Code	Species Name	Collector	Collection Site	Sequences
14-0848	DSK-11B	*Lactarius* sp.	Boontiya Chuankid	Doi Sa Ket, Chiang Mai, Thailand	-
14-0849	DSK-14B	Unidentified	Boontiya Chuankid	Doi Sa Ket, Chiang Mai, Thailand	-
14-0850	DSK-15B	Unidentified	Boontiya Chuankid	Doi Sa Ket, Chiang Mai, Thailand	-
14-0851	DSK-16B	*Micropsalliota* sp.	Boontiya Chuankid	Doi Sa Ket, Chiang Mai, Thailand	-
14-0852	DSK-21B	*Marasmius* sp.	Boontiya Chuankid	Doi Sa Ket, Chiang Mai, Thailand	-
14-0853	DSK-22B	*Filoboletus* sp.	Boontiya Chuankid	Doi Sa Ket, Chiang Mai, Thailand	-
14-0854	DSK-23B	Unidentified	Boontiya Chuankid	Baan Mae-kampong, Chiang Mai, Thailand	-
14-0855	DSK-24B	Unidentified	Boontiya Chuankid	Baan Mae-kampong, Chiang Mai, Thailand	-
14-0856	DSK-25B	*Clavulina* sp.	Boontiya Chuankid	Baan Mae-kampong, Chiang Mai, Thailand	-

Table F1 (continued)

MFLU	Original Code	Species Name	Collector	Collection Site	Sequences
14-0857	DSK-26B	*Inocybe sp.*	Boontiya Chuankid	Baan Mae-kampong, Chiang Mai, Thailand	-
14-0858	DSK-27B	Unidentified	Boontiya Chuankid	Baan Mae-kampong, Chiang Mai, Thailand	-
14-0859	DSK-28B	Unidentified	Boontiya Chuankid	Baan Mae-kampong, Chiang Mai, Thailand	-
14-0860	DSK-29B	Unidentified	Boontiya Chuankid	Baan Mae-kampong, Chiang Mai, Thailand	-
14-0861	DSK-30B	Unidentified	Boontiya Chuankid	Baan Mae-kampong, Chiang Mai, Thailand	-
14-0862	DSK-31B	Unidentified	Boontiya Chuankid	Baan Mae-kampong, Chiang Mai, Thailand	-
14-0863	DSK-34B	Unidentified	Boontiya Chuankid	Baan Mae-kampong, Chiang Mai, Thailand	-
14-0864	DSK-35B	Unidentified	Boontiya Chuankid	Baan Mae-kampong, Chiang Mai, Thailand	-
14-0865	DSK-36B	Unidentified	Boontiya Chuankid	Baan Mae-kampong, Chiang Mai, Thailand	-

Table F1 (continued)

MFLU	Original Code	Species Name	Collector	Collection Site	Sequences
14-0866	DSK-37B/BC076	*Agaricus megalosporus*	Boontiya Chuankid	Baan Mae-kampong, Chiang Mai, Thailand	/
14-0867	DSK-38B/BC077	*Agaricus* sp.	Boontiya Chuankid	Baan Mae-kampong, Chiang Mai, Thailand	/
14-0868	MFU-1B	*Lepiota* sp.	Boontiya Chuankid	Mae Fah Luang University, Chiang Rai, Thailand	-
14-0869	MFU-2B	*Lepiota* sp.	Boontiya Chuankid	Mae Fah Luang University, Chiang Rai, Thailand	-
14-0870	MFU-3B	*Agaricus* sp.	Boontiya Chuankid	Mae Fah Luang University, Chiang Rai, Thailand	-
14-0871	MFU-4B/BC078	*Lepiota* sp.	Boontiya Chuankid	Mae Fah Luang University, Chiang Rai, Thailand	/

Table F1 (continued)

MFLU	Original Code	Species Name	Collector	Collection Site	Sequences
14-0872	MFU-5B/BC079	*Agaricus campestroides*	Boontiya Chuankid	Mae Fah Luang University, Chiang Rai, Thailand	/
14-0873	MFU-6B/BC080	*Agaricus variicystis*	Boontiya Chuankid	Mae Fah Luang University, Chiang Rai, Thailand	/
14-0874	MFU-7B/BC081	*Agaricus flocculosipes*	Boontiya Chuankid	Mae Fah Luang University, Chiang Rai, Thailand	/
14-0876	MFU-10S/BC082	*Agaricus flocculosipes*	Samantha Chandranath Karunarathna	Mae Fah Luang University, Chiang Rai, Thailand	/
14-0877	MFU-11B/BC083	*Agaricus gratolens*	Boontiya Chuankid	Mae Fah Luang University, Chiang Rai, Thailand	/
14-0878	MFU-12B	*Micropsalliota* sp.	Boontiya Chuankid	Mae Fah Luang University, Chiang Rai, Thailand	-

Table F1 (continued)

MFLU	Original Code	Species Name	Collector	Collection Site	Sequences
14-0879	MFU-13B	*Micropsalliota* sp.	Boontiya Chuankid	Mae Fah Luang University, Chiang Rai, Thailand	-
14-0880	MFU-14B	*Micropsalliota* sp.	Boontiya Chuankid	Mae Fah Luang University, Chiang Rai, Thailand	-
14-0881	MFU-15B/BC084	*Agaricus gratolens*	Boontiya Chuankid	Mae Fah Luang University, Chiang Rai, Thailand	/
14-0882	MFU-16B	*Micropsalliota* sp.	Boontiya Chuankid	Mae Fah Luang University, Chiang Rai, Thailand	-
14-0883	DH-1B	*Agaricus* sp.	Boontiya Chuankid	Baan Du, Chiang Rai, Thailand	-
14-0884	DH-2L	*Agaricus* sp.	Leea Rizal Maya	Baan Du, Chiang Rai, Thailand	-
14-0885	DH-3K	*Agaricus* sp.	Anan Thawthong	Baan Du, Chiang Rai, Thailand	-

Table F1 (continued)

MFLU	Original Code	Species Name	Collector	Collection Site	Sequences
14-0886	DH-4K	*Agaricus* sp.	Anan Thawthong	Baan Du, Chiang Rai, Thailand	-
14-0887	MRC-1B	*Micropsalliota* sp.	Boontiya Chuankid	MRC, Chiang Mai, Thailand	-
14-0888	MRC-2B	Unidentified	Boontiya Chuankid	MRC, Chiang Mai, Thailand	-
14-0889	MRC-3B	Unidentified	Boontiya Chuankid	MRC, Chiang Mai, Thailand	-
14-0890	MRC-4B/BC085	*Boletus* sp.	Boontiya Chuankid	MRC, Chiang Mai, Thailand	/
14-0891	MRC-5B	*Russula* sp.	Boontiya Chuankid	MRC, Chiang Mai, Thailand	-
14-0892	MRC-6B/BC086	*Boletus* sp.	Boontiya Chuankid	MRC, Chiang Mai, Thailand	/
14-0893	MRC-7B	*Xerula* sp.	Boontiya Chuankid	MRC, Chiang Mai, Thailand	-
14-0894	MRC-8B/BC087	*Agaricus* sp.	Boontiya Chuankid	Doi Pha Deang temple, Chiang Mai, Thailand	/

Table F1 (continued)

MFLU	Original Code	Species Name	Collector	Collection Site	Sequences
14-0895	MRC-9B	*Amanita* sp.	Boontiya Chuankid	Doi Pha Deang temple, Chiang Mai, Thailand	-
14-0896	MRC-10B	*Xerula* sp.	Boontiya Chuankid	Doi Pha Deang temple, Chiang Mai, Thailand	-
14-0897	MRC-11B	*Termitomyces* sp.	Boontiya Chuankid	Doi Pha Deang temple, Chiang Mai, Thailand	-
14-0898	MRC-12B	*Amanita* sp.	Boontiya Chuankid	Doi Pha Deang temple, Chiang Mai, Thailand	-
14-0899	MRC-13B	*Micropsalliota* sp.	Boontiya Chuankid	Doi Pha Deang temple, Chiang Mai, Thailand	-
14-0900	MRC-14B	*Amanita* sp.	Boontiya Chuankid	Doi Pha Deang temple, Chiang Mai, Thailand	-
14-0901	MRC-15B	*Ganoderma* sp.	Boontiya Chuankid	Doi Pha Deang temple, Chiang Mai, Thailand	-
14-0902	MRC-16B	*Ganoderma* sp.	Boontiya Chuankid	Doi Pha Deang temple, Chiang Mai, Thailand	-

Table F1 (continued)

MFLU	Original Code	Species Name	Collector	Collection Site	Sequences
14-0903	MRC-17B/BC088	*Agaricus angusticystidiata*	Boontiya Chuankid	Pang Sa Det water management, Chiang Mai, Thailand	/
14-0904	MRC-18B/BC089	*Micropsalliota* sp.	Boontiya Chuankid	Pang Sa Det water management, Chiang Mai, Thailand	/
14-0905	MRC-19B/BC090	*Agaricus* sp.	Boontiya Chuankid	Pang Sa Det water management, Chiang Mai, Thailand	/
14-0906	MRC-21B	*Ganoderma* sp.	Boontiya Chuankid	Pang Sa Det water management, Chiang Mai, Thailand	-
14-0907	MRC-22B	*Ganoderma* sp.	Boontiya Chuankid	Pang Sa Det water management, Chiang Mai, Thailand	-
14-0908	MRC-23B/BC091	*Agaricus* sp.	Boontiya Chuankid	Mae Tang water research station, Chiang Mai,Thailand	/

Table F1 (continued)

MFLU	Original Code	Species Name	Collector	Collection Site	Sequences
14-0909	MRC-24B/BC092	*Agaricus trisulphuratus*	Boontiya Chuankid	Mae Tang water research station, Chiang Mai, Thailand	/
14-0910	MRC-25B/BC093	*Agaricus gratolens*	Boontiya Chuankid	Mae Tang water research station, Chiang Mai, Thailand	/
14-0911	MRC-26B/BC094	*Agaricus gratolens*	Boontiya Chuankid	Mae Tang water research station, Chiang Mai, Thailand	/
14-0912	MRC-27B/BC095	*Agaricus* sp.	Boontiya Chuankid	Mae Tang water research station, Chiang Mai, Thailand	/
14-0913	MRC-28B/BC096	*Agaricus* sp.	Boontiya Chuankid	Mae Tang water research station, Chiang Mai, Thailand	/
14-0914	MRC-30B	*Agaricus* sp.	Boontiya Chuankid	Mae Tang water research station, Chiang Mai, Thailand	-

Table F1 (continued)

MFLU	Original Code	Species Name	Collector	Collection Site	Sequences
14-0915	MRC-31B/BC098	*Agaricus* sp.	Boontiya Chuankid	Mae Tang water research station, Chiang Mai, Thailand	/
14-0916	MRC-32B	*Micropsalliota* sp.	Boontiya Chuankid	Mae Tang water research station, Chiang Mai, Thailand	-
14-0917	MRC-33B	*Amanita* sp.	Boontiya Chuankid	Mae Tang water research station, Chiang Mai, Thailand	-
14-0918	MRC-34B	*Xerula* sp.	Boontiya Chuankid	Mae Tang water research station, Chiang Mai, Thailand	-
14-0919	MRC-35B	*Agrocybe* sp.	Boontiya Chuankid	Mae Tang water research station, Chiang Mai, Thailand	-
14-0920	MRC-36B	*Agaricus* sp.	Boontiya Chuankid	Mae Tang water research station, Chiang Mai, Thailand	-

Table F1 (continued)

MFLU	Original Code	Species Name	Collector	Collection Site	Sequences
14-0921	MRC-37B	*Hebeloma* sp.	Boontiya Chuankid	Mae Tang water research station, Chiang Mai, Thailand	-
14-0922	MRC-38B/BC099	*Agaricus gratolens*	Boontiya Chuankid	Mae Tang water research station, Chiang Mai, Thailand	/
14-0923	MRC-39B/BC100	*Agaricus* sp.	Boontiya Chuankid	Pang Sa Det water management, Chiang Mai, Thailand	/
14-0924	MRC-40B/BC101	*Agaricus* sp.	Boontiya Chuankid	Pang Sa Det water management, Chiang Mai, Thailand	/
14-0925	MRC-41B/BC102	*Agaricus* sp.	Boontiya Chuankid	Pang Sa Det water management, Chiang Mai, Thailand	/
14-0926	MRC-42B/BC103	*Agaricus* sp.	Boontiya Chuankid	Pang Sa Det water management, Chiang Mai, Thailand	/

Table F1 (continued)

MFLU	Original Code	Species Name	Collector	Collection Site	Sequences
14-0927	MRC-43B/BC104	*Agaricus flocculosipes*	Boontiya Chuankid	Pang Sa Det water management, Chiang Mai,Thailand	/
16-2170	CB001/BC105	*Agaricus subrufescens*	Boontiya Chuankid	Mae Fah Luang University	/
16-2171	CB002/BC106	*Agaricus subrufescens*	Boontiya Chuankid	Mae Fah Luang University	/
16-2172	CB003/BC107	*Agaricus subrufescens*	Boontiya Chuankid	Mae Fah Luang University	/
16-2173	CB004/BC108	*Agaricus subrufescens*	Boontiya Chuankid	Mae Fah Luang University	/
16-2174	CB005/BC109	*Agaricus subrufescens*	Boontiya Chuankid	Mae Fah Luang University	/
16-2175	CB006/BC110	*Agaricus bisporiticus*	Boontiya Chuankid	Mae Fah Luang University	/
16-2176	CB007/BC111	*Agaricus bisporiticus*	Boontiya Chuankid	Mae Fah Luang University	/

Table F1 (continued)

MFLU	Original Code	Species Name	Collector	Collection Site	Sequences
16-2177	CB008/BC112	*Agaricus bisporiticus*	Boontiya Chuankid	Mae Fah Luang University	/
16-2178	CB009/BC113	*Agaricus gratolens*	Boontiya Chuankid	Mae Fah Luang University	/
16-2179	CB010/BC114	*Agaricus gratolens*	Boontiya Chuankid	Mae Fah Luang University	/
16-2180	CB011	*Micropsalliota* sp.	Boontiya Chuankid	Mae Fah Luang University	-
16-2181	CB012	*Micropsalliota* sp.	Boontiya Chuankid	Mae Fah Luang University	-
16-2182	CB013/BC115	*Agaricus gratolens*	Boontiya Chuankid	Mae Fah Luang University	/
16-2183	CB014/BC116	*Agaricus trisulphuratus*	Boontiya Chuankid	Mae Fah Luang University	/
16-2184	CB015/BC117	*Agaricus subrufescens*	Boontiya Chuankid	Mae Fah Luang University	/
16-2185	CB016	*Agaricus* sp.	Boontiya Chuankid	Nan	-
16-2186	CB017	*Agaricus* sp.	Boontiya Chuankid	Nan	-

Table F1 (continued)

MFLU	Original Code	Species Name	Collector	Collection Site	Sequences
16-2187	CB018	*Agaricus* sp.	Boontiya Chuankid	Nan	-
16-2188	CB019/BC118	*Agaricus subrufescens*	Jie Chen	Mae Fah Luang University	/
16-2189	CB020/BC119	*Agaricus subrufescens*	Jie Chen	Mae Fah Luang University	/
16-2190	CB021/BC120	*Agaricus subrufescens*	Jie Chen	Mae Fah Luang University	/
16-2191	CB022/BC121	*Agaricus subrufescens*	Jie Chen	Mae Fah Luang University	/
16-2192	CB023/BC122	*Agaricus floculosipes*	Jie Chen	Mae Fah Luang University	/
16-2193	CB024/BC123	*Agaricus floculosipes*	Jie Chen	Mae Fah Luang University	/
16-2194	CB025/BC124	*Agaricus* sp.	Jie Chen	Mae Fah Luang University	/
16-2195	CB026	*Agaricus* sp.	Jie Chen	Mae Fah Luang University	-

Table F1 (continued)

MFLU	Original Code	Species Name	Collector	Collection Site	Sequences
16-2196	CB027/BC125	*Agaricus floculosipes*	Jie Chen	Mae Fah Luang University	/
16-2197	CB028	*Agaricus* sp.	Jie Chen	Mae Fah Luang University	-
16-2198	CB029	*Calvatia* sp.	Jie Chen	Mae Fah Luang University	-
16-2199	CB030	*Agaricus* sp.	Jie Chen	Mae Fah Luang University	-
16-2200	CB034/BC126	*Micropsalliota megarubescens*	Jie Chen	Mae Fah Luang University	/
16-2201	CB035/BC127	*Agaricus subrufescens*	Boontiya Chuankid	Mae Fah Luang University	/
16-2202	CB036/BC128	*Agaricus subrufescens*	Boontiya Chuankid	Mae Fah Luang University	/
16-2203	CB037/BC129	*Agaricus subrufescens*	Boontiya Chuankid	Mae Fah Luang University	/
16-2204	CB040	*Agaricus* sp.	Boontiya Chuankid	Mae-on, Chiang Mai, Thailand	-

Table F1 (continued)

MFLU	Original Code	Species Name	Collector	Collection Site	Sequences
16-2205	CB042	*Agaricus* sp.	Anan Thawthong	Mae Suay, Chiang Rai, Thailand	-
16-2206	CB043	*Agaricus* sp.	Anan Thawthong	Mae Suay, Chiang Rai, Thailand	-
16-2207	CB045	*Agaricus* sp.	Anan Thawthong	Doi Sa Ket, Chiang Mai, Thailand	-
16-2208	BC001	*Phlebopus portentosus*	Boontiya Chuankid	Pa Daet Market	/
16-2209	BC002	*Boletellus* sp.	Boontiya Chuankid	MRC, Chiang Mai, Thailand	/
16-2210	BC003	*Boletellus* sp.	Boontiya Chuankid	MRC, Chiang Mai, Thailand	/
16-2211	BC004	*Agaricus* sp.	Boontiya Chuankid	MRC, Chiang Mai, Thailand	/
16-2212	BC005	*Tylopilus* sp.	Boontiya Chuankid	MRC, Chiang Mai, Thailand	/
16-2213	BC006	*Boletus* sp.	Boontiya Chuankid	MRC, Chiang Mai, Thailand	/

Table F1 (continued)

MFLU	Original Code	Species Name	Collector	Collection Site	Sequences
16-2214	BC007	*Agaricus floculosipes*	Boontiya Chuankid	Mae Fah Luang University	/
16-2215	BC008	*Agaricus* sp.	Boontiya Chuankid	Mae Fah Luang University	/
16-2216	BC009	*Phlebopus spongiosus*	Boontiya Chuankid	Hua Doi Market	/
16-2217	BC010	*Tylopilus* sp.	Boontiya Chuankid	Hua Doi Market	/
16-2218	BC011	*Tylopilus* sp.	Boontiya Chuankid	Hua Doi Market	/
16-2219	BC012	*Boletus* sp.	Boontiya Chuankid	Hua Doi Market	/
16-2220	BC013	*Boletus* sp.	Boontiya Chuankid	Hua Doi Market	/
16-2221	BC014	*Tylopilus* sp.	Boontiya Chuankid	Hua Doi Market	/
16-2222	BC015	*Boletellus emodensis*	Boontiya Chuankid	Hua Doi Market	/
16-2223	BC016	*Boletellus emodensis*	Boontiya Chuankid	Mae-on, Chiang Mai, Thailand	/
16-2224	BC017	*Tylopilus* sp.	Boontiya Chuankid	Mae-on, Chiang Mai, Thailand	/
16-2225	BC018	*Tylopilus* sp.	Boontiya Chuankid	Mae-on, Chiang Mai, Thailand	/

Table F1 (continued)

MFLU	Original Code	Species Name	Collector	Collection Site	Sequences
16-2226	BC019	*Agaricus* sp.	Boontiya Chuankid	Mae-on, Chiang Mai, Thailand	/
16-2227	BC020	*Micropsalliota* sp.	Boontiya Chuankid	Mae-on, Chiang Mai, Thailand	/
16-2228	BC021	*Tylopilus* sp.	Boontiya Chuankid	Ban Mae Kampong, Chiang Mai, Thailand	/
16-2229	BC022	*Phylloporus subrubeolus*	Boontiya Chuankid	Ban Mae Kampong, Chiang Mai, Thailand	/
16-2230	BC023	*Boletus* sp.	Boontiya Chuankid	Ban Mae Kampong, Chiang Mai, Thailand	/
16-2231	BC024	*Phylloporus* sp.	Boontiya Chuankid	Ban Mae Kampong, Chiang Mai, Thailand	/
16-2232	BC025	*Tylopilus* sp.	Boontiya Chuankid	Ban Mae Kampong, Chiang Mai, Thailand	/
16-2233	BC026	*Tylopilus* sp.	Boontiya Chuankid	Ban Mae Kampong, Chiang Mai, Thailand	/
16-2234	BC027	*Tylopilus* sp.	Boontiya Chuankid	Ban Mae Kampong, Chiang Mai, Thailand	/

Table F1 (continued)

MFLU	Original Code	Species Name	Collector	Collection Site	Sequences
16-2235	BC028	*Boletus* sp.	Boontiya Chuankid	Ban Mae Kampong, Chiang Mai, Thailand	/
16-2236	BC029	*Boletus* sp.	Boontiya Chuankid	Mae-on, Chiang Mai, Thailand	/
16-2237	BC030	*Boletus* sp.	Boontiya Chuankid	Mae-on, Chiang Mai, Thailand	/
16-2238	BC032	*Boletus* sp.	Boontiya Chuankid	Ban Mae Kampong, Chiang Mai, Thailand	/
16-2239	BC033	*Phylloporus rubiginosus*	Boontiya Chuankid	Ban Mae Kampong, Chiang Mai, Thailand	/
16-2240	BC034	*Boletellus emodensis*	Boontiya Chuankid	Ban Mae Kampong, Chiang Mai, Thailand	/
16-2241	BC035	*Boletellus emodensis*	Boontiya Chuankid	Mae-on, Chiang Mai, Thailand	/
16-2242	BC036	*Agaricus erectosquamosus*	Boontiya Chuankid	Mae-on, Chiang Mai, Thailand	/
16-2243	BC037	*Tylopilus* sp.	Boontiya Chuankid	Mae-on, Chiang Mai, Thailand	/

Table F1 (continued)

MFLU	Original Code	Species Name	Collector	Collection Site	Sequences
16-2244	BC038	*Strobilomyces* sp.	Boontiya Chuankid	Mae-on, Chiang Mai, Thailand	/
16-2245	BC039	*Boletellus emodensis*	Boontiya Chuankid	Mae-on, Chiang Mai, Thailand	/
16-2246	BC040	*Agaricus trisulphuratus*	Boontiya Chuankid	Mae-on, Chiang Mai, Thailand	/
16-2247	BC041	*Boletellus emodensis*	Boontiya Chuankid	Mae-on, Chiang Mai, Thailand	/
16-2248	BC042	*Boletellus emodensis*	Boontiya Chuankid	Mae-on, Chiang Mai, Thailand	/
16-2249	BC043	*Tylopilus* sp.	Boontiya Chuankid	Mae-on, Chiang Mai, Thailand	/
16-2250	BC044	*Tylopilus* sp.	Boontiya Chuankid	Mae Taeng, Chiang Mai, Thailand	/
16-2251	BC045	*Heimiella* sp.	Boontiya Chuankid	Mae Taeng, Chiang Mai, Thailand	/
16-2252	BC046	*Tylopilus* sp.	Boontiya Chuankid	Mae Taeng, Chiang Mai, Thailand	/

Table F1 (continued)

MFLU	Original Code	Species Name	Collector	Collection Site	Sequences
16-2253	BC047	*Tylopilus* sp.	Boontiya Chuankid	Mae Taeng, Chiang Mai, Thailand	/
16-2254	BC048	*Tylopilus* sp.	Boontiya Chuankid	Mae Taeng, Chiang Mai, Thailand	/
16-2255	BC049	*Agaricus megacystidiatus*	Boontiya Chuankid	Mae Taeng, Chiang Mai, Thailand	/
16-2256	BC050	*Boletellus* sp.	Boontiya Chuankid	Mae Taeng, Chiang Mai, Thailand	/
16-2257	BC051	*Agaricus_bisporiticus*	Boontiya Chuankid	Mae Taeng, Chiang Mai, Thailand	/
16-2258	BC053	Polypore	Boontiya Chuankid	Pa Pae, Chiang Mai, Thailand	-
16-2259	BC054	*Tylopilus* sp.	Boontiya Chuankid	Mae Faek, Chiang Mai, Thailand	/
16-2260	BC055	*Tylopilus* sp.	Boontiya Chuankid	Mae Faek, Chiang Mai, Thailand	/
16-2261	BC056	*Boletus* sp.	Boontiya Chuankid	Mae Faek, Chiang Mai, Thailand	/

Table F1 (continued)

MFLU	Original Code	Species Name	Collector	Collection Site	Sequences
16-2262	BC057	*Agaricus* sp.	Boontiya Chuankid	Mae Faek, Chiang Mai, Thailand	/
16-2263	BC058	*Agaricus* sp.	Boontiya Chuankid	Mae Faek, Chiang Mai, Thailand	/
16-2264	BC059	*Agaricus* sp.	Boontiya Chuankid	Mae Faek, Chiang Mai, Thailand	/
16-2265	BC060	*Agaricus brunneopileatus*	Boontiya Chuankid	Doi Pui, Chiang Rai, Thailand	/
16-2266	BC061	*Strobilomyces* sp.	Boontiya Chuankid	Doi Pui, Chiang Rai, Thailand	/
16-2267	BC062	*Boletus* sp.	Boontiya Chuankid	Doi Pui, Chiang Rai, Thailand	/
16-2268	BC063	*Phylloporus rubiginosus*	Boontiya Chuankid	Doi Pui, Chiang Rai, Thailand	/
16-2269	BC064	*Boletus* sp.	Boontiya Chuankid	Doi Pui, Chiang Rai, Thailand	/
16-2270	BC065	*Phylloporus gajari*	Boontiya Chuankid	Doi Pui, Chiang Rai, Thailand	/

Table F1 (continued)

MFLU	Original Code	Species Name	Collector	Collection Site	Sequences
16-2271	BC066	*Strobilomyces* sp.	Boontiya Chuankid	Doi Pui, Chiang Rai, Thailand	/
18-1726	BC130	*Scleroderma* sp.	Boontiya Chuankid	Tha Sai, Mueang Chiang Rai District, Chiang Rai, Thailand	-
18-1727	BC131	*Phylloporus* sp.	Boontiya Chuankid	Tha Sai, Mueang Chiang Rai District, Chiang Rai, Thailand	/
18-1728	BC132	*Phylloporus* sp.	Boontiya Chuankid	Tha Sai, Mueang Chiang Rai District, Chiang Rai, Thailand	/
18-1729	BC133	*Phylloporus* sp.	Boontiya Chuankid	Tha Sai, Mueang Chiang Rai District, Chiang Rai, Thailand	/
18-1730	BC134	*Phylloporus* sp.	Boontiya Chuankid	Tha Sai, Mueang Chiang Rai District, Chiang Rai, Thailand	/

Table F1 (continued)

MFLU	Original Code	Species Name	Collector	Collection Site	Sequences
18-1731	BC135	*Phylloporus* sp.	Boontiya Chuankid	Tha Sai, Mueang Chiang Rai District, Chiang Rai, Thailand	/
18-1732	BC136	*Boletus* sp.	Boontiya Chuankid	Tha Sai, Mueang Chiang Rai District, Chiang Rai, Thailand	/
18-1733	BC137	*Phylloporus rubiginosus*	Boontiya Chuankid	Mae Fa Luang, Mae Fa Luang District, Chiang Rai,Thailand	/
18-1734	BC138	*Tylopilus* sp.	Boontiya Chuankid	Mae Fa Luang, Mae Fa Luang District, Chiang Rai,Thailand	/
18-1735	BC139	*Tylopilus* sp.	Boontiya Chuankid	Mae Fa Luang, Mae Fa Luang District, Chiang Rai,Thailand	/
18-1736	BC140	*Phylloporus* sp.	Boontiya Chuankid	Mae Fa Luang, Mae Fa Luang District, Chiang Rai,Thailand	/

Table F1 (continued)

MFLU	Original Code	Species Name	Collector	Collection Site	Sequences
18-1737	BC142	*Tylopilus* sp.	Boontiya Chuankid	Pa Pae, Mae Taeng, Chiang Mai, Thailand	/
18-1738	BC143	*Hortiboletus* sp.	Boontiya Chuankid	Pa Pae, Mae Taeng, Chiang Mai, Thailand	/
18-1739	BC144	*Phylloporus rubiginosus*	Boontiya Chuankid	Pa Pae, Mae Taeng, Chiang Mai, Thailand	/
18-1740	BC145	*Phylloporus* sp.	Boontiya Chuankid	Pa Pae, Mae Taeng, Chiang Mai, Thailand	/
18-1741	BC146	*Hourangia* sp.	Boontiya Chuankid	Pa Pae, Mae Taeng, Chiang Mai, Thailand	/
18-1742	BC147	*Agaricus* sp.	Boontiya Chuankid	Pa Pae, Mae Taeng, Chiang Mai, Thailand	/
18-1743	BC148	*Phylloporus* sp.	Boontiya Chuankid	Tha Sai, Mueang Chiang Rai District, Chiang Rai, Thailand	/
18-1744	BC149	*Phylloporus* sp.	Boontiya Chuankid	Tha Sai, Mueang Chiang Rai District, Chiang Rai, Thailand	/

Table F1 (continued)

MFLU	Original Code	Species Name	Collector	Collection Site	Sequences
18-1745	BC150	*Agaricus* sp.	Benjarong Thongbai	MFU	/
18-1746	BC151	*Xerocomus* sp.	Boontiya Chuankid	Huai Kaeo, Mae On, Chiang Mai, Thailand	/
18-1747	BC152	*Micropsalliota megarubescens*	Boontiya Chuankid	Huai Kaeo, Mae On, Chiang Mai, Thailand	/
18-1748	BC153	*Phylloporus* sp.	Boontiya Chuankid	Baan Pox, Huai Kaeo, Mae On, Chiang Mai, Thailand	/
18-1749	BC154	*Phylloporus* sp.	Boontiya Chuankid	Baan Pox, Huai Kaeo, Mae On, Chiang Mai, Thailand	/
18-1750	BC155	*Xerocomus* sp.	Boontiya Chuankid	Baan Pox, Huai Kaeo, Mae On, Chiang Mai, Thailand	/
18-1751	BC156	*Pholiota multicingulata*	Boontiya Chuankid	Baan Pox, Huai Kaeo, Mae On, Chiang Mai, Thailand	/

Table F1 (continued)

MFLU	Original Code	Species Name	Collector	Collection Site	Sequences
18-1752	BC157	*Agaricus* sp.	Boontiya Chuankid	Baan Pox, Huai Kaeo, Mae On, Chiang Mai, Thailand	/
18-1753	BC158	*Agaricus* sp.	Boontiya Chuankid	Baan Pox, Huai Kaeo, Mae On, Chiang Mai, Thailand	/
18-1754	BC160	*Phylloporus rubiginosus*	Boontiya Chuankid	Huai Kaeo, Mae On, Chiang Mai, Thailand	/
18-1755	BC161	*Strobilomyces* sp.	Boontiya Chuankid	Huai Kaeo, Mae On, Chiang Mai, Thailand	/
18-1756	BC162	*Inocybe* sp.	Boontiya Chuankid	Huai Kaeo, Mae On, Chiang Mai, Thailand	/
18-1757	BC163	*Inocybe* sp.	Boontiya Chuankid	Huai Kaeo, Mae On, Chiang Mai, Thailand	/
18-1758	BC164	*Hourangia* sp.	Boontiya Chuankid	Chae Son, Mueang Pan, Lampang, Thailand	/
18-1759	BC165	*Phlebopus spongiosus*	Boontiya Chuankid	San Makhet, Phan, Chiang Rai, Thailand.	/

Table F1 (continued)

MFLU	Original Code	Species Name	Collector	Collection Site	Sequences
18-1760	BC166	*Phlebopus spongiosus*	Boontiya Chuankid	Nang Lae, Mueang Chiang Rai, Chiang Rai, Thailand	/
18-1761	BC167	*Agaricus microvolvatulus*	Boontiya Chuankid	MRC, Mae Taeng, Chiamg Mai, Thailand	/
18-1762	BC168	*Hourangia* sp.	Boontiya Chuankid	MRC, Mae Taeng, Chiamg Mai, Thailand	/
18-1763	BC169	*Phylloporus rubiginosus*	Boontiya Chuankid	MRC, Mae Taeng, Chiamg Mai, Thailand	/
18-1764	BC170	*Hourangia* sp.	Boontiya Chuankid	MRC, Mae Taeng, Chiamg Mai, Thailand	/
18-1765	BC171	*Tylopilus* sp.	Boontiya Chuankid	MRC, Mae Taeng, Chiamg Mai, Thailand	/
18-1766	BC172	*Boletus* sp.	Boontiya Chuankid	MRC, Mae Taeng, Chiamg Mai, Thailand	/
18-1767	BC173	*Phylloporus* sp.	Boontiya Chuankid	MRC, Mae Taeng, Chiamg Mai, Thailand	/

Table F1 (continued)

MFLU	Original Code	Species Name	Collector	Collection Site	Sequences
18-1768	BC174	*Phylloporus* sp.	Boontiya Chuankid	MRC, Mae Taeng, Chiamg Mai, Thailand	/
18-1769	BC175	*Phylloporus* sp.	Boontiya Chuankid	MRC, Mae Taeng, Chiamg Mai, Thailand	/
18-1770	BC176	*Phylloporus* sp.	Boontiya Chuankid	MRC, Mae Taeng, Chiamg Mai, Thailand	/
18-1771	BC177	*Phylloporus* sp.	Boontiya Chuankid	MRC, Mae Taeng, Chiamg Mai, Thailand	/
18-1772	BC178	*Retiboletus nigrogriseus*	Boontiya Chuankid	MRC, Mae Taeng, Chiamg Mai, Thailand	/
18-1773	BC179	*Retiboletus nigrogriseus*	Boontiya Chuankid	MRC, Mae Taeng, Chiamg Mai, Thailand	/
18-1774	BC180	*Hourangia* sp.	Boontiya Chuankid	MRC, Mae Taeng, Chiamg Mai, Thailand	/
18-1775	BC181	*Phylloporus castanopsidis*	Boontiya Chuankid	Pa Pae, Mae Taeng, Chiang Mai, Thailand	/
18-1776	BC182	*Phylloporus castanopsidis*	Boontiya Chuankid	Pa Pae, Mae Taeng, Chiang Mai, Thailand	/

Table F1 (continued)

MFLU	Original Code	Species Name	Collector	Collection Site	Sequences
18-1777	BC183	*Phylloporus rubiginosus*	Boontiya Chuankid	Pa Pae, Mae Taeng, Chiang Mai, Thailand	/
18-1778	BC184	*Phylloporus rubiginosus*	Boontiya Chuankid	Pa Pae, Mae Taeng, Chiang Mai, Thailand	/
18-1779	BC185	*Phylloporus rubiginosus*	Boontiya Chuankid	Pa Pae, Mae Taeng, Chiang Mai, Thailand	/
18-1780	BC186	*Phylloporus rubiginosus*	Boontiya Chuankid	Pa Pae, Mae Taeng, Chiang Mai, Thailand	/
18-1781	BC187	*Phylloporus rubiginosus*	Boontiya Chuankid	Pa Pae, Mae Taeng, Chiang Mai, Thailand	/
18-1782	BC188	*Phylloporus castanopsidis*	Boontiya Chuankid	Baan Pox, Huai Kaeo, Mae On, Chiang Mai, Thailand	/
18-1783	BC189	*Phylloporus* sp.	Boontiya Chuankid	Baan Pox, Huai Kaeo, Mae On, Chiang Mai, Thailand	/

Table F1 (continued)

MFLU	Original Code	Species Name	Collector	Collection Site	Sequences
18-1784	BC190	*Phylloporus castanopsidis*	Boontiya Chuankid	Baan Pox, Huai Kaeo, Mae On, Chiang Mai, Thailand	/
18-1785	BC191	*Retiboletus* sp.	Boontiya Chuankid	Baan Pox, Huai Kaeo, Mae On, Chiang Mai, Thailand	/
18-1786	BC195	*Phylloporus* aff. *bellus*	Boontiya Chuankid	Huai Kaeo, Mae On, Chiang Mai, Thailand	/
18-1787	BC196	*Phylloporus* aff. *bellus*	Boontiya Chuankid	Huai Kaeo, Mae On, Chiang Mai, Thailand	/
18-1788	BC197	*Phylloporus* aff. *bellus*	Boontiya Chuankid	Huai Kaeo, Mae On, Chiang Mai, Thailand	/
18-1789	BC198	*Phylloporus* aff. *bellus*	Boontiya Chuankid	Huai Kaeo, Mae On, Chiang Mai, Thailand	/
18-1790	BC199	*Phylloporus* sp.	Boontiya Chuankid	Huai Kaeo, Mae On, Chiang Mai, Thailand	/
18-1791	BC200	*Thelephora* sp.	Boontiya Chuankid	Huai Kaeo, Mae On, Chiang Mai, Thailand	/

Table F1 (continued)

MFLU	Original Code	Species Name	Collector	Collection Site	Sequences
18-1792	BC201	*Thelephora* sp.	Boontiya Chuankid	Huai Kaeo, Mae On, Chiang Mai, Thailand	/
18-1793	BC206	*Hortiboletus* sp.	Boontiya Chuankid	Huai Kaeo, Mae On, Chiang Mai, Thailand	/
18-1794	BC207	*Boletus* sp.	Boontiya Chuankid	Huai Kaeo, Mae On, Chiang Mai, Thailand	/
18-1795	BC216	*Phylloporus* sp.	Boontiya Chuankid	Huai Kaeo, Mae On, Chiang Mai, Thailand	/
18-1796	BC221	*Hourangia* sp.	Boontiya Chuankid	Huai Kaeo, Mae On, Chiang Mai, Thailand	/
18-1797	BC222	*Hourangia* sp.	Boontiya Chuankid	Huai Kaeo, Mae On, Chiang Mai, Thailand	/
18-1798	BC226	*Borofutus* sp.	Boontiya Chuankid	Mae Loi, Thoeng, Chiang Rai, Thailand	/
18-1799	BC227	*Phylloporus parvisporus*	Boontiya Chuankid	Mae Loi, Thoeng, Chiang Rai, Thailand	/
18-1800	BC228	*Pulveroboletus* sp.	Boontiya Chuankid	Mae Loi, Thoeng, Chiang Rai, Thailand	/

Table F2 Lists of cultures

MFLUCC	Original Code	Species Name	Collection Site	Collector
14-1019	Ak-1	*Agaricus* sp.	MFU	Kritsana Jatuwong
14-1020	DSK-6B	*Micropsalliota globocystis*	Doi Sa Ket	Boontiya Chuankid
14-1021	DSK-32B	*Agaricus subrutilescens*	Doi Sa Ket	Boontiya Chuankid
14-1022	DSK-33B	*Agrocybe* sp.	Doi Sa Ket	Boontiya Chuankid
14-1023	MFU-4B	*Micropsalliota* sp.	MFU	Boontiya Chuankid
14-1024	MFU-5B	*Agaricus campestroides*	MFU	Boontiya Chuankid
14-1025	MFU-6B	*Agaricus variicystis*	MFU	Boontiya Chuankid
14-1026	MFU-7A	*Agaricus floculosipes*	MFU	Asanka Ranjana Bandara
14-1027	MFU-8Ak	*Agrocybe* sp.	MFU	Kritsana Jatuwong
14-1028	MFU-9S	*Agaricus* sp.	MFU	Samantha Chandranath Karunarathna
14-1029	MFU-10S	*Agaricus floculosipes*	MFU	Samantha Chandranath Karunarathna
14-1030	MFU-14B	*Agaricus* sp.	MFU	Boontiya Chuankid
14-1031	MFU-19B	*Agaricus* sp.	MFU	Boontiya Chuankid

Table F2 (continued)

MFLUCC	Original Code	Species Name	Collection Site	Collector
14-1032	DH-1B	*Agaricus* sp.	Baan Pong Prabaht	Boontiya Chuankid
14-1033	DH-2L	*Agaricus* sp.	Baan Pong Prabaht	Leela Rizal
14-1034	DH-3K	*Agaricus* sp.	Baan Pong Prabaht	Anan Thawthong
14-1035	DH-4K	*Agaricus* sp.	Baan Pong Prabaht	Anan Thawthong
14-1036	MRC-23B	*Agaricus* sp.	Mae Tang water research station	Boontiya Chuankid
14-1037	MRC-24B	*Agaricus trisulphuratus*	Mae Tang water research station	Boontiya Chuankid
14-1038	MRC-25B	*Agaricus gratolens*	Mae Tang water research station	Boontiya Chuankid
14-1039	MRC-27B	*Agaricus* sp.	Mae Tang water research station	Boontiya Chuankid
14-1040	MRC-29B	*Agaricus subrufescens*	Mae Tang water research station	Boontiya Chuankid
14-1041	MRC-38B	*Agaricus gratolens*	Mae Tang water research station	Boontiya Chuankid
14-1042	MRC-39B	*Agaricus* sp.	Pang Sa Det water management	Boontiya Chuankid
14-1043	MRC-40B	*Agaricus* sp.	Pang Sa Det water management	Boontiya Chuankid

Table F2 (continued)

MFLUCC	Original Code	Species Name	Collection Site	Collector
14-1044	MRC-42B	*Agaricus* sp.	Pang Sa Det water management	Boontiya Chuankid
14-1045	MRC-43B	*Agaricus floculosipes*	Pang Sa Det water management	Boontiya Chuankid
T19-0088	BC001	*Phlebopus portentosus*	Pa Daet Market	Boontiya Chuankid
T19-0089	BC009	*Phlebopus spongiosus*	Hua Doi Market	Boontiya Chuankid
T19-0090	BC165	*Phlebopus spongiosus*	San Makhet, Phan, Chiang Rai, Thailand	Boontiya Chuankid
T19-0091	BC166	*Phlebopus spongiosus*	Nang Lae, Mueang Chiang Rai, Chiang Rai, Thailand	Boontiya Chuankid
T19-0092	BC231	*Phlebopus portentosus*	Pa Daet Market	Boontiya Chuankid
T19-0093	BC232	*Phlebopus portentosus*	Pa Daet Market	Boontiya Chuankid

APPENDIX G

ABSTRACT OF PUBLICATIONS

MycoKeys 40: 53–67 (2018)
doi: 10.3897/mycokeys.40.26918
http://mycokeys.pensoft.net

RESEARCH ARTICLE

A peer-reviewed open-access journal
MycoKeys
Launched to accelerate biodiversity research

A new section and species of *Agaricus* subgenus *Pseudochitonia* from Thailand

Mao-Qiang He[1,2,3], Boontiya Chuankid[3], Kevin D. Hyde[3], Ratchadawan Cheewangkoon[1], Rui-Lin Zhao[2,4]

1 *Department of Entomology and Plant Pathology, Faculty of Agriculture, Chiang Mai University, Chiang Mai, 50200, Thailand* **2** *State key laboratory of Mycology, Institute of Microbiology, Chinese Academy of Sciences, Beijing, 100101, China* **3** *Center of Excellence in Fungal Research, Mae Fah Luang University, Chiang Rai, 57100, Thailand* **4** *College of Life Sciences, University of Chinese Academy of Sciences, Huairou District, Beijing, 100408, China*

Corresponding authors: *R. Cheewangkoon* (ratchadawan.c@cmu.ac.th); *R.-L. Zhao* (zhaorl@im.ac.cn)

Academic editor: *Zai-Wei Ge* | Received 29 June 2018 | Accepted 7 September 2018 | Published 20 September 2018

Citation: He M-Q, Chuankid B, Hyde KD, Cheewangkoon R, Zhao R-L (2018) A new section and species of *Agaricus* subgenus *Pseudochitonia* from Thailand. MycoKeys 40: 53–67. https://doi.org/10.3897/mycokeys.40.26918

Abstract

A large species diversity has recently been discovered in the genus *Agaricus*. Six subgenera and 23 sections are now recognised. In this study, three specimens collected from Thailand, formed a monophyletic clade in subgenus *Pseudochitonia*, based on analyses of ITS sequence data. Further analyses, based on multi-gene sequence data (ITS, LSU, tef1-α), using BEAST, revealed that this clade originated 26.7 Ma. According to their distinct morphological characteristics, phylogenetic position and relatively old divergence time, a new section *Cymbiformes* is proposed and this section is represented by a new species *A. angusticystidiatus*. This new section is characterised by the strong iodoform odour of basidiomes and cymbiform basidiospores. Descriptions, colour photographs and illustrations are presented.

Keywords

New taxa, Agaricaceae, Phylogeny, Taxonomy

Mycological Progress (2019) 18:603–614
https://doi.org/10.1007/s11557-019-01474-6

DGfM

ORIGINAL ARTICLE

CrossMark

Three new *Phylloporus* species from tropical China and Thailand

Boontiya Chuankid[1] · Santhiti Vadthanarat[2] · Kevin D. Hyde[1] · Naritsada Thongklang[1] · Ruilin Zhao[3] · Saisamorn Lumyong[2,4] · Olivier Raspé[5,6]

Received: 28 August 2018 / Revised: 15 January 2019 / Accepted: 21 January 2019
© German Mycological Society and Springer-Verlag GmbH Germany, part of Springer Nature 2019

Abstract
We introduce three new *Phylloporus* species, *P. pusillus*, *P. subbacillisporus* and *P. subrubeolus*, from southwestern China and northern Thailand with macro- and micro-descriptions and illustrations. They are found mostly in forests dominated by Fagaceae or Dipterocarpaceae trees. A three-gene phylogenetic analysis of the new *Phylloporus* species along with other selected *Phylloporus* species confirmed that all new *Phylloporus* species are related to previously described *Phylloporus* species. *Phylloporus pusillus* and *P. subrubeolus* are morphologically similar, but the former can be separated by very small basidiomata, lamellae becoming deeper yellow to reddish with age and less densely encrusted walls of pileipellis hyphae. *Phylloporus subbacillisporus* can be easily distinguished from other species by shallowly intervenose lamellae and subbacilliform basidiospores.

Keywords *atp6* · *Boletaceae* · *rpb2* · Asia · Taxonomy · *tef1* · *Xerocomoideae* · 3 new species

Fungal Diversity (2019) 97:1–136
https://doi.org/10.1007/s13225-019-00430-9

REVIEW

The amazing potential of fungi: 50 ways we can exploit fungi industrially

Kevin D. Hyde[1,2,3,4,5,9] · Jianchu Xu[1,10,21] · Sylvie Rapior[22] · Rajesh Jeewon[18] · Saisamorn Lumyong[9,13] · Allen Grace T. Niego[2,3,20] · Pranami D. Abeywickrama[2,3,7] · Janith V. S. Aluthmuhandiram[2,3,7] · Rashika S. Brahamanage[2,3,7] · Siraprapa Brooks[3] · Amornrat Chaiyasen[28] · K. W. Thilini Chethana[2,3,7] · Putarak Chomnunti[2,3] · Clara Chepkirui[12] · Boontiya Chuankid[2,3] · Nimali I. de Silva[1,2,4,13] · Mingkwan Doilom[1,4,13] · Craig Faulds[6] · Eleni Gentekaki[3] · Venkat Gopalan[14] · Pattana Kakumyan[2,3] · Dulanjalee Harishchandra[2,3,7] · Hridya Hemachandran[24] · Sinang Hongsanan[26,27] · Anuruddha Karunarathna[2,17] · Samantha C. Karunarathna[1] · Sehroon Khan[10] · Jaturong Kumla[13,9] · Ruvishika S. Jayawardena[2,3] · Jian-Kui Liu[11] · Ningguo Liu[2,3] · Thatsanee Luangharn[1,21,22,29] · Allan Patrick G. Macabeo[12,23] · Diana S. Marasinghe[2,5] · Dan Meeks[19] · Peter E. Mortimer[1,10] · Peter Mueller[19] · Sadia Nadir[18,15,21] · Karaba N. Nataraja[16] · Sureeporn Nontachaiyapoom[3] · Meghan O'Brien[19] · Watsana Penkhrue[9,13] · Chayanard Phukhamsakda[2,3] · Uma Shaanker Ramanan[16,25] · Achala R. Rathnayaka[2,3] · Resurreccion B. Sadaba[29] · Birthe Sandargo[12] · Binu C. Samarakoon[2,3] · Danushka S. Tennakoon[2,3] · Ramamoorthy Siva[24] · Wasan Sriprom[9,13] · T. S. Suryanarayanan[30] · Kanaporn Sujarit[9,13] · Nakarin Suwannarach[9,13] · Thitipone Suwunwong[3,8] · Benjarong Thongbai[12] · Naritsada Thongklang[2] · Deping Wei[1,2,3,17] · S. Nuwanthika Wijesinghe[2,3] · Jake Winiski[19] · Jiye Yan[7] · Erandi Yasanthika[2,3] · Marc Stadler[12]

Received: 5 April 2019 / Accepted: 20 May 2019 / Published online: 3 July 2019
© The Author(s) 2019

Abstract
Fungi are an understudied, biotechnologically valuable group of organisms. Due to the immense range of habitats that fungi inhabit, and the consequent need to compete against a diverse array of other fungi, bacteria, and animals, fungi have developed numerous survival mechanisms. The unique attributes of fungi thus herald great promise for their application in biotechnology and industry. Moreover, fungi can be grown with relative ease, making production at scale viable. The search for fungal biodiversity, and the construction of a living fungi collection, both have incredible economic potential in locating organisms with novel industrial uses that will lead to novel products. This manuscript reviews fifty ways in which fungi can potentially be utilized as biotechnology. We provide notes and examples for each potential exploitation and give examples from our own work and the work of other notable researchers. We also provide a flow chart that can be used to convince funding bodies of the importance of fungi for biotechnological research and as potential products. Fungi have provided the world with penicillin, lovastatin, and other globally significant medicines, and they remain an untapped resource with enormous industrial potential.

Keywords Biocontrol · Biodiversity · Biotechnology · Food · Fungi · Mushrooms

Fungal Diversity (2020) 103:87–218
https://doi.org/10.1007/s13225-020-00460-8

One stop shop IV: taxonomic update with molecular phylogeny for important phytopathogenic genera: 76–100 (2020)

Ruvishika S. Jayawardena[1,2,7] · Kevin D. Hyde[1,2,3,18] · Yi Jyun Chen[2,7] · Viktor Papp[4] · Balázs Palla[4] · Dávid Papp[5,6] · Chitrabhanu S. Bhunjun[2,7] · Vedprakash G. Hurdeal[2,7] · Chanokned Senwanna[2,8] · Ishara S. Manawasinghe[2,9,18] · Dulanjalee L. Harischandra[2,7,9] · Ajay Kumar Gautam[10] · Shubhi Avasthi[11] · Boontiya Chuankid[2,7] · Ishani D. Goonasekara[2,7] · Sinang Hongsanan[12] · XiangYu Zeng[2,7,19] · Kapila K. Liyanage[2,17,20] · NingGuo Liu[2] · Anuruddha Karunarathna[2,8] · Kalani K. Hapuarachchi[2] · Thatsanee Luangharn[2,3] · Olivier Raspé[2,7] · Rashika Brahmanage[2,7,9] · Mingkwan Doilom[3,16,17] · Hyang B. Lee[13] · Liu Mei[9] · Rajesh Jeewon[14] · Naruemon Huanraluek[2] · Napalai Chaiwan[2,7] · Marc Stadler[15] · Yong Wang[1]

Received: 20 May 2020 / Accepted: 7 August 2020 / Published online: 24 September 2020
© The Author(s) 2020

Abstract
This is a continuation of a series focused on providing a stable platform for the taxonomy of phytopathogenic fungi and fungus-like organisms. This paper focuses on one family: *Erysiphaceae* and 24 phytopathogenic genera: *Armillaria, Barriopsis*, *Cercospora*, *Cladosporium*, *Clinoconidium*, *Colletotrichum*, *Cylindrocladiella*, *Dothidotthia*,, *Fomitopsis*, *Ganoderma*, *Golovinomyces*, *Heterobasidium*, *Meliola*, *Mucor*, *Neoerysiphe*, *Nothophoma*, *Phellinus*, *Phytophthora*, *Pseudoseptoria*, *Pythium*, *Rhizopus*, *Stemphylium*, *Thyrostroma* and *Wojnowiciella*. Each genus is provided with a taxonomic background, distribution, hosts, disease symptoms, and updated backbone trees. Species confirmed with pathogenicity studies are denoted when data are available. Six of the genera are updated from previous entries as many new species have been described.

Keywords Disease · Plant pathology · Phylogeny · Taxonomy · Symptoms

Contents and contributors (main contributors underlined)

Newly discussed genera and family

76. ***Armillaria*** – B Chuankid, M Stadler
77. ***Barriopsis*** – IS Manawasinghe, RS Jayawardena
78. ***Cercospora*** – ID Goonasekara
79. ***Clinoconidium*** – AK Gautam, S Avasthi
80. ***Cylindrocladiella*** – D Harischandra, RS Jayawardena
81. ***Dothidotthia*** – C Senwanna
82. ***Erysiphaceae*** – KK Liyanage, RS Jayawardena, KD Hyde
83. ***Fomitopsis*** – V Papp, B Palla, D Papp
84. ***Ganoderma*** – KK Hapuarachchi, T Luangharn, O Raspe
85. ***Golovinomyces*** – RS Jayawardena
86. ***Heterobasidium*** – V Papp, B Palla, D Papp
87. ***Meliola*** – S Hongsanan, XY Zeng
88. ***Neoerysiphe*** – RS Jayawardena
89. ***Nothophoma*** – IS Manawasinghe, RS Jayawardena
90. ***Phellinus*** – V Papp, B Palla, D Papp
91. ***Pseudoseptoria*** – A Karunarathna, RS Jayawardena
92. ***Stemphylium*** – RS Jayawardena, KD Hyde
93. ***Thyrostroma*** – C Senwanna, KD Hyde
94. ***Wojnowiciella*** – D Harischandra, RS Jayawardena

Updated genera

95. ***Cladosporium*** – NG Liu, RS Jayawardena
96. ***Colletotrichum*** – RS Jayawardena, KD Hyde
97. ***Mucor*** – VG Hurdeal, HB Lee
98. ***Phytophthora*** – CS Bhunjun, RS Jayawardena
99. ***Pythium*** – CS Bhunjun, RS Jayawardena
100. ***Rhizopus*** – VG Hurdeal, HB Lee

✉ Yong Wang
yongwangbis@aliyun.com
Extended author information available on the last page of the article

Mycological Progress (2020) 19:1525–1536
https://doi.org/10.1007/s11557-020-01643-y

DGfM

ORIGINAL ARTICLE

Secondary metabolites of *Phlebopus* species from Northern Thailand

Boontiya Chuankid[1,2] · Hedda Schrey[2] · Benjarong Thongbai[2] · Olivier Raspé[1] · Norbert Arnold[3] · Kevin David Hyde[1] · Marc Stadler[2]

Received: 11 September 2020 / Revised: 20 October 2020 / Accepted: 22 October 2020
© The Author(s) 2020

Abstract
Submerged cultures of the edible mushrooms *Phlebopus portentosus* and *Phlebopus spongiosus* were screened for their secondary metabolites by HPLC-UV/Vis and HR-LC-ESI-MS. Two new compounds, 9′-hydroxyphenyl pulvinone (**1**), containing an unusual pulvinone structure, and phlebopyron (**2**), together with the seven known pigments, atromentic acid (**3**), xerocomic acid (**4**), variegatic acid (**5**), methyl atromentate (**6**), methyl isoxerocomate (**7**), methyl variegatate (**8**), and variegatorubin (**9**) were isolated from the cultures. Their structures were assigned on the basis of extensive 1D/2D NMR spectroscopic analyses, as well as HR-ESI-MS, and HR-ESI-MS/MS measurements. Furthermore, the isolated compounds were evaluated for their antimicrobial and cytotoxic properties. 9′-hydroxyphenyl pulvinone (**1**), xerocomic acid (**4**), and methyl variegatate (**8**) exhibited weak to moderate cytotoxic activities against several tumor cell lines. The present paper provides a comprehensive characterization of pigments from the class of pulvinic acids that are present in the basidiomes of many edible bolete species.

Keywords Boletales · Basidiomycota · Edible mushrooms · Pulvinic acid derivatives · Secondary metabolites · Structure elucidation

Asian Journal of Mycology 4(1): 113–260 (2021) ISSN 2651-1339
www.asianjournalofmycology.org Article
Doi 10.5943/ajom/4/1/8

AJOM new records and collections of fungi: 101-150

Chethana KWT[1,2], Niranjan M[3,4], Dong W[1,5,15], Samarakoon MC[1,7,8], Bao DF[1,9], Calabon MS[1,2], Chaiwan N[1,2], Chuankid B[1], Dayarathne MC[10], de Silva NI[1,6,8,11], Devadatha B[3], Dissanayake AJ[7], Goonasekara ID[1,2,5,6,11], Huanraluek N[1], Jayawardena RS[1,2], Karunarathna A[1,5,9,11], Luo ZL[12], Marasinghe DS[1,2,5,13], Ma XY[1,2], Norphanphoun C[1,2,5,13,14], Pem D[1,2], Perera RH[1,2,5,14], Rathnayaka AR[1,2,13], Raspé O[1,2], Samarakoon BC[1,2], Senwanna C[1,5,6,9], Sun YR[1,2,10], Tang X[1], Thiyagaraja V[1,5,6,9], Tennakoon DS[1,2,5,13], Zeng M[1,2,6], Zeng XY[1], Zhang JY[1], Zhang SN[1,7,9], Bulgakov TS[16], Camporesi E[18,19], Sarma VV[3], Wang Y[10], Bhat DJ[17] and Hyde KD[1,2,5,8,11,15,*]

[1]*Center of Excellence in Fungal Research, Mae Fah Luang University, Chiang Rai 57100, Thailand*
[2]*School of Science, Mae Fah Luang University, Chiang Rai 57100, Thailand*
[3]*Fungal Biotechnology Laboratory, Department of Biotechnology, School of Life Sciences, Pondicherry University, Kalapet, Pondicherry 605014, India*
[4]*Department of Botany, Rajiv Gandhi University, Rono Hills, Doimukh, Papum Pare, Itanagaar, Arunachal Pradesh 791112, India*
[5]*Mushroom Research Foundation, 128 M.3 Ban Pa Deng T. Pa Pae, A. Mae Taeng, Chiang Mai 50150, Thailand*
[6]*Key Laboratory for Plant Biodiversity and Biogeography of East Asia (KLPB), Kunming Institute of Botany, Chinese Academy of Science, Kunming 650201, Yunnan, People's Republic of China*
[7]*School of Life Science and Technology, University of Electronic Science and Technology of China, Chengdu 611731, People's Republic of China*
[8]*Department of Biology, Faculty of Science, Chiang Mai University, Chiang Mai, 50200, Thailand*
[9]*Department of Entomology and Plant Pathology, Faculty of Agriculture, Chiang Mai University, Chiang Mai 50200, Thailand*
[10]*Department of Plant Pathology, Agriculture College, Guizhou University, Guiyang, 550025 Guizhou People's Republic of China*
[11]*World Agroforestry Centre (ICRAF), East and Central Asia Regional Office, Kunming 650201, Yunnan, People's Republic of China*
[12]*College of Agriculture and Biological Sciences, Dali University, Dali 671003, Yunnan province, People's Republic of China*
[13]*Department of Plant Medicine, National Chiayi University, 300 Syuefu Road, Chiayi City 60004, Taiwan*
[14]*Guizhou Key Laboratory of Agricultural Biotechnology, Guizhou Academy of Agricultural Sciences, Guiyang 550006, People's Republic of China*
[15]*Institute of Plant Health, Zhongkai University of Agriculture and Engineering, Haizhu District, Guangzhou 510225, People's Republic of China*
[16]*Department of Plant Protection, Federal Research Centre the Subtropical Scientific Centre of the Russian Academy of Sciences, Sochi 354002, Krasnodar region, Russia*
[17] *No. 128/1-J, Co-Op Azad Housing Society, Curca, Goa Velha, India*
[18] *A.M.B. Circolo Micologico "Giovanni Carini", C.P. 314, Brescia, Italy*
[19] *A.M.B. Gruppo, Micologico Forlivese "Antonio Cicognani", Via Roma 18, Forlì, Italy*

Chethana KWT, Niranjan M, Dong W, Samarakoon MC, Bao DF, Calabon MS, Chaiwan N, Chuankid B, Dayarathne MC, de Silva NI, Devadatha B, Dissanayake AJ, Goonasekara ID, Huanraluek N, Jayawardena RS, Karunarathna A, Luo ZL, Marasinghe DS, Ma XY, Norphanphoun C, Pem D, Perera RH, Rathnayaka AR, Raspé O, Samarakoon BC, Senwanna C, Sun YR, Tang X, Thiyagaraja V, Tennakoon DS, Zeng M, Zeng XY, Zhang JY, Zhang SN,

Submitted 1 November 2020, Accepted 15 March 2021, Published 27 May 2021
Corresponding Author: K. D. Hyde – e-mail – kdhyde1@gmail.com

Bulgakov TS, Camporesi E, Sarma VV, Wang Y, Bhat DJ, Hyde KD 2021 – AJOM new records and collections of fungi: 101-150. Asian Journal of Mycology 4(1), 113–260, Doi 10.5943/ajom/4/1/8

Abstract

This article is the second in the Asian Journal of Mycology Notes series, wherein we report 50 new fungal collections distributed in two phyla, six classes, 23 orders and 38 families. The present study provides descriptions and illustrations for three new species (*Acolium yunnanense*, *Muyocopron cinnamomi* and *Thyrostroma ulmeum*), 44 new host records and new geographical distributions and three new reference collections. All these introductions are supported by morphological data as well as the multi-gene phylogenetic analyses. This article provides a venue to publish fungal collections with new sequence data, which is important for future studies. An accurate and timely report of new fungus-host or fungus-county records are essential for diagnostics, identification and management of economically significant fungal groups, especially the phytopathogens.

Key words – 3 new taxa – 44 new records – Ascomycota – Basidomycota – Dothideomycetes – Molecular phylogeny – Sordariomycetes – Taxonomy

Chiang Mai J. Sci. 2021; 48(5) : 1224-1235
http://epg.science.cmu.ac.th/ejournal/
Contributed Paper

Two *Pleurotus* Species (Pleurotaceae) From Lao People's Democratic Republic

Monthien Phonemany [a,b], Olivier Raspé [a,b], Phongeun Sysouphanthong [a,c], Allen Grace T. Niego [a,b,d], Naritsada Thongklang [a,b], Boontiya Chuankid [a,b] and Kevin D. Hyde*[a,b]

[a] Center of Excellence in Fungal Research, Mae Fah Luang University, 333 Moo 1 Thasud, Mueang, Chiang Rai, Thailand.

[b] School of Science, Mae Fah Luang University, 333 Moo 1 Thasud, Mueang, Chiang Rai 57100, Thailand.

[c] Biotechnology and Ecology Institute, Ministry of Agriculture and Forestry, P.O.Box: 811, Vientiane Capital, Lao PDR.

[d] Iloilo Science and Technology University, Burgos St. Lapaz, Iloilo, 5000, Philippines.

*Author for correspondence; e-mail: kdhyde3@gmail.com

Received: 14 October 2020
Revised: 15 March 2021
Accepted: 18 March 2021

ABSTRACT

Pleurotus is widely distributed and the most commonly cultivated edible mushroom genus worldwide. In addition to being widely consumed, some species have medical, biotechnological and environmental applications owing to their bioactivities. In this study, we report two *Pleurotus* species from Laos. *Pleurotus djamor* is reported for the first time from Laos, while *P. giganteus* a common species in Laos is also reported. Molecular phylogenetic analyses of the nuclear ribosomal internal transcribed spacer region (nrITS) were performed in addition to the morphological analysis to confirm their identification. Full descriptions, color photo plates, micrographs, and taxonomic comparisons are provided.

Keywords: basidiomycota, distribution, diversity, southeast Asia, taxonomy

Mycoscience
An open access journal for general mycology
The Mycological Society of Japan

Full paper

Retiboletus (*Boletaceae*) in northern Thailand: one novel species and two first records

Boontiya Chuankid[a,b,e], Santhiti Vadthanarat[c,d], Benjarong Thongbai[e], Marc Stadler[e], Saisamorn Lumyong[c,d,h], Kevin David Hyde[a,b], Olivier Raspé[a,b,f,g,*]

[a] *Center of Excellence in Fungal Research, Mae Fah Luang University, Chiang Rai, Thailand*
[b] *School of Science, Mae Fah Luang University, Chiang Rai, Thailand*
[c] *Department of Biology, Faculty of Science, Chiang Mai University, Chiang Mai, Thailand*
[d] *Research Center of Microbial Diversity and Sustainable Utilization, Chiang Mai University, Chiang Mai, Thailand*
[e] *Department Microbial Drugs, Helmholtz Centre for Infection Research, and German Centre for Infection Research (DZIF), partner site Hannover-Braunschweig, Braunschweig, Germany*
[f] *Meise Botanic Garden, Nieuwelaan 38, Meise, Belgium*
[g] *Fédération Wallonie-Bruxelles, Service général de l'Enseignement universitaire et de la Recherche scientifique, Rue A. Lavallée 1, Bruxelles, Belgium*
[h] *Academy of Science, The Royal Society of Thailand, Bangkok, Thailand*

ABSTRACT

Morphological characters and multi-gene phylogenetic analyses were used to identify *Retiboletus* specimens collected in northern Thailand. *Retiboletus brevibasidiatus* is described as new to science, whereas *R. fuscus* and *R. nigrogriseus* are reported for the first time from Thailand. *Retiboletus brevibasidiatus* produces medium-sized basidiomes, with a dark blonde to clay pileus and densely reticulate stipe mostly on the upper part with pale yellow to chrome yellow basal mycelium. It is difficult to separate *R. brevibasidiatus* from other closely related species on the basis of macroscopic characters. However, the new species can be distinguished by microscopic characters, mostly the shorter basidia. The macro- and micro-morphology of the *R. fuscus* and *R. nigrogriseus* collections from Thailand fit well with the previous descriptions of materials from China and Japan. Detailed descriptions, molecular phylogeny, and illustrations of the three species are provided.

Keywords: 1 new species, *atp6*, *Leccinoideae*, *rpb2*, *tef1*

Fungal Biotec 1(2): 101–117 (2021) ISSN 2774-0323

www.fungalbiotec.org

Article – special issue
Doi 10.5943/FunBiotec/1/2/7

Cultivation and identification of blazeispirols of *Agaricus campestroides* and *A. flocculosipes*

Chuankid B[1,2,3,5], Schrey H[3,4], Stadler M[3,4], Thongklang N[1,2], Hyde KD[1,2*]

[1] *Center of Excellence in Fungal Research, Mae Fah Luang University, Chiang Rai 57100, Thailand*
[2] *School of Science, Mae Fah Luang University, Chiang Rai 57100, Thailand*
[3] *Department of Microbial Drugs, Helmholtz Centre for Infection Research, Inhoffenstraße 7, 38124 Braunschweig, Germany*
[4] *Technische Universität Braunschweig, Institute for Microbiology, 38106 Braunschweig, Germany*
[5] *Rak Ruay Mushroom Farm, Phetchabun 67160, Thailand*

Chuankid B, Schrey H, Stadler M, Thongklang N, Hyde KD 2021 – Cultivation and identification of blazeispirols of *Agaricus campestroides* and *A. flocculosipes*. Fungal Biotec 1(2), 101–117, Doi 10.5943/FunBiotec/1/2/7

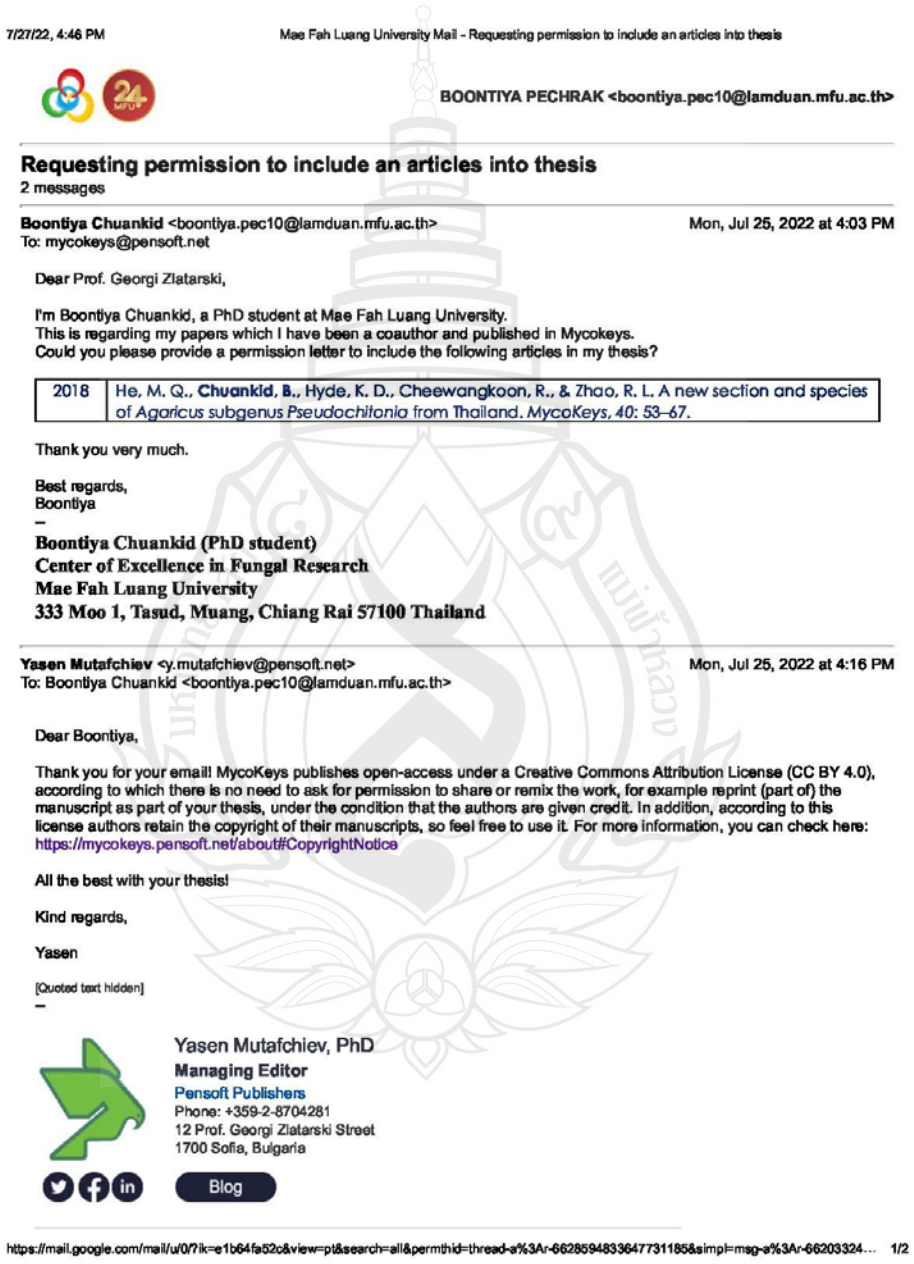
Abstract

The genus *Agaricus* contains many edible and medicinal mushrooms; and some of them are used for commercial purposes. Most *Agaricus* species have been described from temperate geographic areas, but their occurrence in the tropics is still underexplored. The present study describes the successful cultivation of two wild strains from Thailand, *A. flocculopsipes* and *A. campestroides* for the first time. The optimal conditions for mycelial growth have been evaluated for both strains, formation of basidiomata on compost could only be observed for *A. campestroides*. In the present study, mycelial growth and mushroom production conditions were optimized. The temperature range of 25–30 °C with 80–90% humidity was assessed as preferred conditions for primordia and basidiomata formation in a compost rice straw medium with sandy-soil casing layer. Blazeispirols (blazeispirol A and D), a family of triterpenoids that is known to act as selective agonists of Liver X receptor alpha with beneficial effects in vivo in a murine model, were detected in crude extracts from submerged cultures of *A. campestroides* and *A. flocculosipes*.

Keywords – Bioactive compounds – edible mushroom – mushroom farming – Thailand

APPENDIX H

PERMISSION TO INCLUDE AN ARTICLES INTO THESIS



7/27/22, 4:46 PM Mae Fah Luang University Mail - Requesting permission to include an articles into thesis

BOONTIYA PECHRAK <boontiya.pec10@lamduan.mfu.ac.th>

Requesting permission to include an articles into thesis
2 messages

Boontiya Chuankid <boontiya.pec10@lamduan.mfu.ac.th> Mon, Jul 25, 2022 at 4:03 PM
To: mycokeys@pensoft.net

Dear Prof. Georgi Zlatarski,

I'm Boontiya Chuankid, a PhD student at Mae Fah Luang University.
This is regarding my papers which I have been a coauthor and published in Mycokeys.
Could you please provide a permission letter to include the following articles in my thesis?

2018	He, M. Q., **Chuankid, B.**, Hyde, K. D., Cheewangkoon, R., & Zhao, R. L. A new section and species of *Agaricus* subgenus *Pseudochitonia* from Thailand. *MycoKeys*, *40*: 53–67.

Thank you very much.

Best regards,
Boontiya
–
Boontiya Chuankid (PhD student)
Center of Excellence in Fungal Research
Mae Fah Luang University
333 Moo 1, Tasud, Muang, Chiang Rai 57100 Thailand

Yasen Mutafchiev <y.mutafchiev@pensoft.net> Mon, Jul 25, 2022 at 4:16 PM
To: Boontiya Chuankid <boontiya.pec10@lamduan.mfu.ac.th>

Dear Boontiya,

Thank you for your email! MycoKeys publishes open-access under a Creative Commons Attribution License (CC BY 4.0), according to which there is no need to ask for permission to share or remix the work, for example reprint (part of) the manuscript as part of your thesis, under the condition that the authors are given credit. In addition, according to this license authors retain the copyright of their manuscripts, so feel free to use it. For more information, you can check here: https://mycokeys.pensoft.net/about#CopyrightNotice

All the best with your thesis!

Kind regards,

Yasen

[Quoted text hidden]
–

Yasen Mutafchiev, PhD
Managing Editor
Pensoft Publishers
Phone: +359-2-8704281
12 Prof. Georgi Zlatarski Street
1700 Sofia, Bulgaria

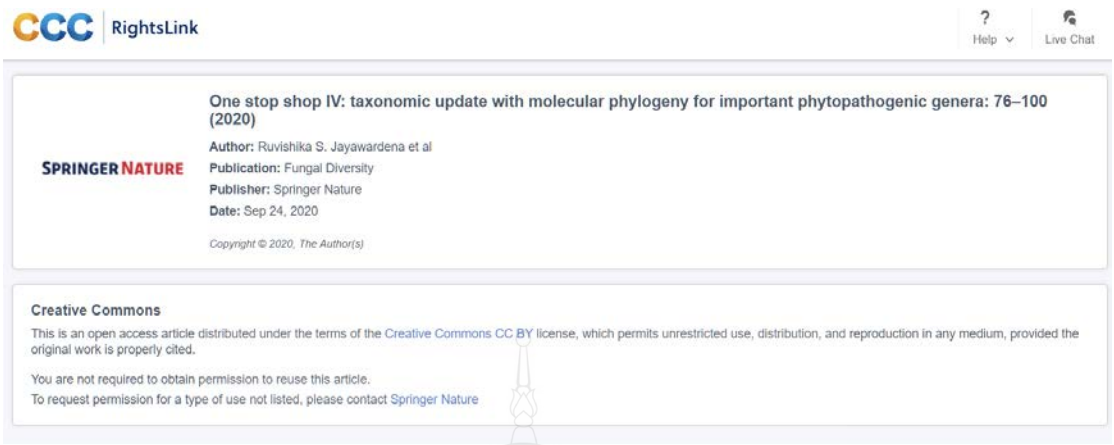
Blog

https://mail.google.com/mail/u/0/?ik=e1b64fa52c&view=pt&search=all&permthid=thread-a%3Ar-6628594833647731185&simpl=msg-a%3Ar-66203324… 1/2

SPRINGER NATURE ORDER DETAILS
Jul 27, 2022

This Agreement between Boontiya Chuankid ("You") and Springer Nature ("Springer Nature") consists of your order details and the terms and conditions provided by Springer Nature and Copyright Clearance Center.

Order Number	501748742
Order date	Jul 27, 2022
Licensed Content Publisher	Springer Nature
Licensed Content Publication	Mycological Progress
Licensed Content Title	Three new Phylloporus species from tropical China and Thailand
Licensed Content Author	Boontiya Chuankid et al
Licensed Content Date	Apr 15, 2019
Type of Use	Thesis/Dissertation
Requestor type	academic/university or research institute
Format	electronic
Portion	full article/chapter
Will you be translating?	no
Circulation/distribution	1000 - 1999
Author of this Springer Nature content	yes
Title	TAXONOMY, PHYLOGENY, CULTIVATION, AND BIOLOGICALLY ACTIVE COMPOUNDS OF SELECTED AGARICUS AND BOLETALES GENERA FROM NORTHERN THAILAND
Institution name	Mae Fah Luang University
Expected presentation date	Aug 2022
Requestor Location	Ms. Boontiya Chuankid Phahonyothin Tha-sud/Muang/Chiang Rai, Thailand 57100 Thailand Attn: Mae Fah Luang University/Center of excellence in fungal research
Billing Type	Invoice
Billing Address	Ms. Boontiya Chuankid Phahonyothin Tha-sud/Muang/Chiang Rai, Thailand 57100



CCC RightsLink

Help Live Chat

SPRINGER NATURE

One stop shop IV: taxonomic update with molecular phylogeny for important phytopathogenic genera: 76–100 (2020)

Author: Ruvishika S. Jayawardena et al
Publication: Fungal Diversity
Publisher: Springer Nature
Date: Sep 24, 2020

Copyright © 2020, The Author(s)

Creative Commons

This is an open access article distributed under the terms of the Creative Commons CC BY license, which permits unrestricted use, distribution, and reproduction in any medium, provided the original work is properly cited.

You are not required to obtain permission to reuse this article.
To request permission for a type of use not listed, please contact Springer Nature



CCC RightsLink

Help Email Support

SPRINGER NATURE

Secondary metabolites of Phlebopus species from Northern Thailand

Author: Boontiya Chuankid et al
Publication: Mycological Progress
Publisher: Springer Nature
Date: Dec 5, 2020

Copyright © 2020, The Author(s)

Creative Commons

This is an open access article distributed under the terms of the Creative Commons CC BY license, which permits unrestricted use, distribution, and reproduction in any medium, provided the original work is properly cited.

You are not required to obtain permission to reuse this article.
To request permission for a type of use not listed, please contact Springer Nature

Dr K. W. Thilini Chethana
Editor in Chief

https://asianjournalofmycology.org/
ISSN 2651 1339

27. 07. 2022

To whom it may concern,

Ref: Testimonial of publication in Asian Journal of Mycology

This is to certify that the paper entitled: *"AJOM new records and collections of fungi: 101–150"* has been published in Asian Journal of Mycology journal in 2021. Details are as follows:

Chethana, K.W.T., Niranjan, M., Dong, W., Samarakoon, M.C., Bao, D.F., Calabon, M.S., Chaiwan, N., Chuankid, B., Dayarathne, M.C., de Silva, N.I. & Devadatha, B. *"AJOM new records and collections of fungi: 101–150". Asian Journal of Mycology*, *4*, 113–260.

Paper submission date: 1 November 2020. Accepted: 15 March 2021. Published online: 27 May 2021

DOI number is 10.5943/ajom/4/1/8

Asian Journal of Mycology is an international peer-reviewed journal in mycological aspects with no page or article processing charges and all articles are made available freely to the scientific community.

Should you have any queries, plese feel free to email: asianjournalofmycology@gmail.com

With kind regards,

Dr K. W. Thilini Chethana, PhD
Editor in Chief,
Asian Journal of Mycology
Mae Fah Luang University,
Thailand.

THE MYCOLOGICAL SOCIETY OF JAPAN
http://www.mycology-jp.org/~msj7/WL_English_site/index_e.html

July 26, 2022

Boontiya Chuankid (PhD student)
Center of Excellence in Fungal Research
Mae Fah Luang University
333 Moo 1, Tasud, Muang, Chiang Rai 57100 Thailand
boontiya.pec10@lamduan.mfu.ac.th

PERMISSION FOR USAGE OF ARTICLE INTO THESIS

Dear Boontiya Chuankid,

I thank you for your inquiry.
We grant permission for the use of the article in the Mycoscience that you requested as follows,

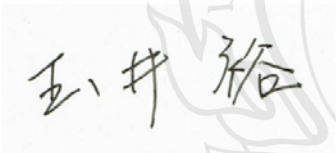
Authors: Chuankid, B., Vadthanarat, S., Thongbai, B., Stadler, M., Lumyong, S., Hyde, K. D., & Raspé, O.

Title of the paper: *Retiboletus* (*Boletaceae*) in northern Thailand: one novel species and two first records.

Journal, Volume, Pages and Year: Mycoscience 62(5):297-306. (2021).

Purpose: To include in PhD thesis

Sincerely yours,



Yutaka TAMAI, Dr. Agr.
Editor-in-Chief, Mycoscience
Research Faculty of Agriculture
Hokkaido University
N9-W9, Kita-ku, Sapporo 060-8589 JAPAN
Phone: +81-11-706-2509; E-mail: ytamai@for.agr.hokudai.ac.jp

Fungal Biotec
A journal of the Jilin Agricultural University

26 July, 2022

Boontiya Chuankid (PhD student)
Center of Excellence in Fungal Research
Mae Fah Luang University
333 Moo 1, Tasud, Muang, Chiang Rai 57100 Thailand
boontiya.pec10@lamduan.mfu.ac.th

PERMISSION FOR USAGE OF ARTICLE INTO THESIS

Dear Boontiya Chuankid,

This letter is to confirm that we grant permission for the use of the article in the Fungal Biotec that you requested as follows,

Authors: Chuankid B, Schrey H, Stadler M, Thongklang N, Hyde KD

Title of the paper: Cultivation and identification of blazeispirols of *Agaricus campestroides* and *A. flocculosipes*.

Journal, Volume, Pages and Year: Fungal Biotec 1(2), 101–117, Doi 10.5943/FunBiotec/1/2/7 (2021)

Purpose: To include in PhD thesis

Sincerely yours,

Yu Li, Professor, Academician, President,
Editor-in-Chief, Fungal Biotec
Jilin Agricultural University
Changchun District, Jilin, 130118, P.R. China
E-mail: yuli966@126.com